GEOLOGICA ULTRAIECTINA

Mededelingen van de
Faculteit Aardwetenschappen der
Rijksuniversiteit te Utrecht

No. 87

DYNAMIC BEHAVIOUR OF ^{210}PB, ^{210}PO AND ^{137}CS IN COASTAL AND SHELF ENVIRONMENTS

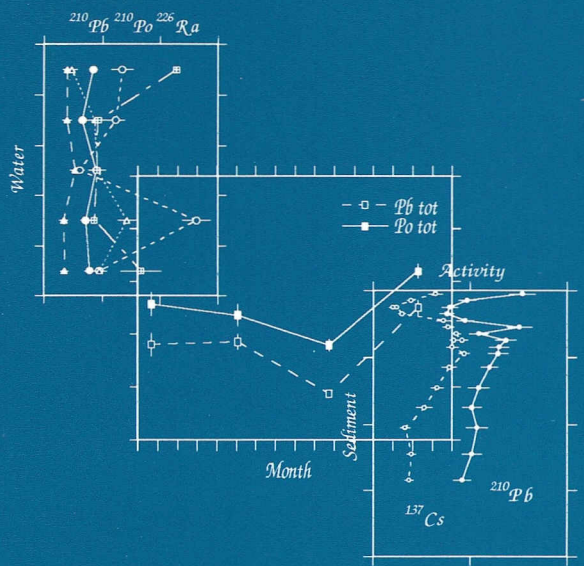

ZHIZHENG ZUO

GEOLOGICA ULTRAIECTINA

Mededelingen van de
Faculteit Aardwetenschappen der
Rijksuniversiteit te Utrecht

No. 87

DYNAMIC BEHAVIOUR OF ^{210}PB, ^{210}PO AND ^{137}CS IN COASTAL AND SHELF ENVIRONMENTS

DYNAMISCH GEDRAG VAN ^{210}PB, ^{210}PO EN ^{137}CS IN KUST EN SHELF GEBIEDEN

ZHIZHENG ZUO

CIP-GEGEVENS KONINKLIJKE BIBLIOTHEEK, DEN HAAG

Zuo, Zhizheng

Dynamic behaviour of ^{210}Pb, ^{210}Po and ^{137}Cs in coastal and shelf environments / Zhizheng Zuo.- [Utrecht: Faculteit Aardwetenschappen der Rijksuniversiteit Utrecht].-
(Geologica Ultraiectina, ISSN 0072-1026; no. 87)
Thesis Rijksuniversiteit Utrecht. - with summary in Dutch.
ISBN 90-71577-42-2
Subject heading: sedimentology / isotope Geochemistry.

DYNAMIC BEHAVIOUR OF ^{210}PB, ^{210}PO AND ^{137}CS IN COASTAL AND SHELF ENVIRONMENTS

DYNAMISCH GEDRAG VAN ^{210}PB, ^{210}PO EN ^{137}CS IN KUST EN SHELF GEBIEDEN

(MET EEN SAMENVATTING IN HET NEDERLANDS)

PROEFSCHIFT

TER VERKRIJGING VAN DE GRAAD VAN DOCTOR
AAN DE RIJKSUNIVERSITEIT TE UTRECHT
OP GEZAG VAN DE RECTOR MAGNIFICUS, PROF. DR. J. A. GINKEL
INGEVOLGE HET BESLUIT VAN HET COLLEGE VAN DEKANEN
IN HET OPENBAAR TE VERDEDIGEN
OP DINSDAG 8 SEPTEMBER 1992 TE 10.30 UUR

DOOR

ZHIZHENG ZUO

GEBOREN TE NANJING, CHINA

PROMOTORES: PROF. DR. D. EISMA
PROF. DR. W. G. MOOK

To my parents
and
Fangzhou

I write as I walk because I want to get somewhere, and I write as straight as I can, just as I walk as straight as I can, because is the best way to get there.

H. G. Wells

CONTENTS

ACKNOWLEDGEMENTS

I wish to thank the Foundation for Sea Research (SOZ) and the Netherlands Organization for Scientific Research (NWO) for their financing of this study. The research described here was carried out in the Netherlands Institute for Sea Research (NIOZ). I also wish to thank the European Community (EC) for their support for part of this work within the EROS-2000 programme (contract number: MAST-0016-C (EBD)).

I am deeply grateful to my promotor Prof. D. Eisma for his continuous support, encouragement and enthusiasm for this research work for the last four years. Had he not realized the importance and argued for radioactive isotope geochemistry and geochronology as potential key roles in studying coastal and shelf environments, the project would never have started. He critically read and significantly improved all my manuscripts.

I am equally grateful to my co-promotor Prof. W. G. Mook for his strong support and concern for this work. He was always there whenever I had a problem.

I am also grateful to Prof. P. A. W. J. de Wilde, Prof. H. J. W. de Baar, Dr. G. C. Cadée, Dr. J. H. F. Jansen, Dr. H. van Aken, Dr. A. J. van Bennekom, Dr. L. Otto (NIOZ) who have provided valuable discussions on many aspects of this work. Thanks are given to Mr. G. W. Berger, the person who introduced me into the isotope laboratory of the Institute.

I wish to express my sincere gratitude to Dr. A. G. M. Driedonks and Dr. J. W. Schaap (KNMI) who kindly allowed me setting the rain-collector in their experimental field and provided the meteorological data. Mr. Q. Liu (KNMI) helped with the rain collection in De Bilt for over a year, his assistance is deeply acknowledged.

I furthermore wish to thank Dr. J. van der Plicht and Dr. H. Heijnis (CIO, RUG) who helped in measuring of some water samples and provided a large set of rain samples, their kindness is unforgettable.

I am much indebted to many persons in the Institute (NIOZ) who have provided lots of technical assistance and/or practical help. Mr. R. Groenewegen and his group

helped with the CTD data collection; Mr. J. P. Beks, Mr. C. Fisher, Mrs. R. Gieles, Mr. J. Kalf, Miss E. Okkels and Mrs. N. Schogt provided the laboratory assistance and/or the shipboard sample collection; Miss C. J. de Boer and Mr. T. F. de Bruin learned me a lot about softwares and physics; Dr. W. Helder and Dr. R. F. Nolting kindly allowed me to use their atomic absorption spectrophotometer and Mr. J. T. M. de Jong was very helpful on the machine uses; Dr. B. R. Kuipers and Mr. H. Witte kindly let me use their water box; Mr. H. J. Boekel and his group made the rain collectors and provided lots of technical help. Mr. R. Dapper, Mr. F. Eijgenraam and Mr. G. M. Manshanden are thanked for their help on computer techniques. Mr. B. Verschuur, Mr. R. P. D. Aggenbach and Mr. R. Nichols are acknowledged for their help with some of the drawings and figures. Thanks are also due to Mr. A. Ran and Mr. S. Porto for their efficient supply which kept my work going smoothly. I also thank Mr. J. P. Beks and Dr. A. J. van Bennekom who helped with the translation of the summary for this study.

I wish to thank all people of the administrative department and the reception for their help during the last four years. I would also like to thank Mr. and Mrs. Steenhuizen who made my stay in the Potvis more pleasant. I will always remember those nice times I had by being with my fellow colleagues, which gave me much warmth and strength that made my being-away-from-home even bearable.

I am very grateful to the captains and all crew members of the R. V. *Aurelia*, the R. V. *Discovery* and the R. V. *Navicula* for their pleasant cooperation during the cruises.

Special thanks are to be given to Dr. M. P. Bacon (WHOI), Dr. J. K. Cochran (Marine Science Research Center, Stony Brook State University), Dr. R. Anderson and Dr. J. Crusius (Lamont Doherty Geological Survey) who provided fruitful and constructive discussions and comments on the work, which resulted in considerable improvement of the manuscript.

Finally, my deepest appreciations are to be given to my parents and my family as well as my friends, Michel, Henriette, Qing Liu and XiuLi, who with much patience, provided encouragement, energy and belief whenever I needed it.

SUMMARY

The continental margins of the southern North Sea and the northwestern Mediterranean Sea were chosen as the main subject areas for the study of some of the key processes operating in water and in sediment: chemical scavenging, particle transport, sediment resuspension and deposition. The dynamic behaviour of the radioactive tracers, ^{210}Pb, ^{210}Po and ^{137}Cs, was examined in the study areas to identify mechanisms and time scales of those key processes, in order to predict the fate and impact of the particle-reactive chemical pollutants in the coastal and shelf systems of the North Sea and the Mediterranean Sea.

Determination of sediment accumulation and mixing based on the ^{210}Pb and ^{137}Cs profiles gave an estimate of annual deposition flux (0.12 $g/cm^2/yr$) in the Oyster Ground, an organic-rich fine grained deposition area in the southern North Sea. A similar study was also carried out in the Gulf of Lions area (northwestern Mediterranean Sea), which showed that the intensive sediment reworking is restricted to the uppermost sediment column and most of the sediment supplied by the Rhône river is deposited close to the river mouth with only a small amount being transported towards the nearby deep basin of the Mediterranean Sea.

The spatial distribution of ^{210}Pb and ^{137}Cs and the mixing rates of the bottom sediment in the southern North Sea were studied. Profiles of the two radioactive nuclides show intensive sediment mixing and subsurface maxima of ^{210}Pb in most sediment cores down to 40 cm depth in the sediments. Diffusion model calculations revealed that sediment mixing in this area could not be described by diffusive processes. Applying a single event subsurface egestion model gave good agreement between model curves and measured profiles. It is concluded that the subsurface maxima of excess ^{210}Pb are related to the non-diffusive biogenic mixing and that this kind of mixing plays an important role in determining the fate of the sediment in the coastal and shelf environments of the study area.

A study of the disequilibrium and distribution of ^{210}Pb and ^{210}Po showed the importance of scavenging processes in the southern North Sea. The observed low concentrations of total ^{210}Pb in the study area were related to a high concentration of suspended matter, high resuspension rates and low atmospheric input. An excess of ^{210}Po, both in dissolved and particulate form, indicated an additional flux

of ^{210}Po from the coastal and shelf sediments because of high resuspension rates. Mass balance calculations from a box model revealed a shorter residence time and higher uptake rate for dissolved ^{210}Po than for dissolved ^{210}Pb, which indicates a high recycling efficiency. Comparison of data on the ^{210}Pb concentrations in water and sediment showed that a regular excess of ^{210}Po as observed in the water column is balanced by a small deficit of ^{210}Po in the sediments.

Special attention was also given to possible seasonal influces on distributions of ^{210}Pb and ^{210}Po in the water column of the Dutch coastal zone. Measurements of water samples revealed that the concentrations of dissolved ^{210}Pb and ^{210}Po were low during the summer, whereas the particulate ^{210}Pb and ^{210}Po were relatively high during the spring and winter. The observed seasonal variation in the distribution of the two radionuclides was considered to be the result of high effective scavenging in summer and enhanced resuspension in winter. A one-dimensional seasonal model was developed to account for the observed seasonal variation. The derived time-variation of the total ^{210}Pb and ^{210}Po is in close agreement with the field data. It is concluded that ^{210}Pb deposition from the atmosphere at the sea surface plays a key role in controlling the distribution of ^{210}Pb and ^{210}Po in the study area, but is not sufficient to account for all ^{210}Pb and ^{210}Po that is present. About 10-25% of the total amount of ^{210}Pb and ^{210}Po is supplied by lateral advection.

In order to assess the accuracy of the mass budget of particle transport and deposition, the flux of atmospheric deposition of ^{210}Pb in the Netherlands was studied. The observed total ^{210}Pb deposition shows strong variation on a short time scale as well as regional variations. There is a good correlation between the daily ^{210}Pb deposition and the precipitation, which indicates the presence of a strong seasonal effect during the year: the deposition flux is higher in the summer than in the winter. The dry fallout flux, estimated from the relation of ^{210}Pb flux with precipitation, is about 16-38% of the total deposition of ^{210}Pb. Although strong seasonal variations were observed in the daily total ^{210}Pb flux, the annual deposition rate of ^{210}Pb did not differ significantly from year to year. For a good representation of the flux, however, measurements on a longer time scale are required to overcome the influence of strong seasonal variation and regional variability.

SAMENVATTING

De shelf zeeën in het zuiden van de Noordzee en in het noordwesten van de Middellandse Zee zijn gekozen als de belangrijkste onderzoeksgebieden om enkele sleutelprocessen te bestuderen die in water en sediment optreden: chemische verwijdering (scavenging), deeltjes transport, resuspensie en depositie van sediment. Het dynamische gedrag van de radioactieve tracers ^{210}Pb, ^{210}Po, en ^{137}Cs, is bestudeerd in de onderzoeksgebieden, om de bestemming en het effect te voorspellen van deeltjes-gebonden chemische verontreinigingen in de kust- en shelf systemen van de Noordzee en de Middellandse Zee.

De bepaling van sediment accumulatie en menging uit de ^{210}Pb en ^{137}Cs profielen leverde een geschatte jaarlijkse sedimentatie flux (0.12 $g/cm^2/yr$) op de Oestergronden, een fijnkorrelig sedimentatie gebied in het zuiden van de Noordzee, rijk aan organisch materiaal. Een soortgelijke studie, uitgevoerd in de Golf van Lyon, toonde aan dat intensieve verstoring van het sediment beperkt blijft tot de toplaag, en dat het grootste deel van het materiaal dat de Rhône aanvoert dicht bij de monding van de rivier wordt afgezet, en slechts een klein deel wordt getransporteerd naar de nabij gelegen diepe bekkens van de Middellandse Zee.

De ruimtelijke verspreiding van ^{210}Pb en ^{137}Cs en de menging in het sediment zijn in het zuidelijk deel van de Noordzee bestudeerd. Profielen van de twee (radioactieve) isotopen tonen intensieve menging van het sediment en maxima van ^{210}Pb onder het oppervlak in de meeste kernen tot 40 cm diep. Diffusie model berekeningen toonden dat de verstoring van het sediment in dit gebied niet beschreven kan worden met diffusie processen. Toepassing van een "single event subsurface egestion model" gaf een goede overeenkomst tussen model curves en gemeten profielen. Geconcludeerd werd dat maxima van "excess" ^{210}Pb onder het oppervlak gerelateerd zijn aan niet-diffusieve biologische menging en dat dit soort verstoring een belangrijke rol speelt in het bepalen van de bestemming van het sediment in het kust en shelf milieu van het onderzoeksgebied.

Een studie naar het verstoorde evenwicht en de verspreiding van ^{210}Pb en ^{210}Po toonde het grote belang van scavenging processen in het zuidelijk deel van de Noordzee. De gevonden lage concentraties van totaal ^{210}Pb in het onderzoeksgebied waren gekoppeld aan een hoge concentratie gesuspendeerd materiaal, hoge

resuspensie waarden en een lage atmosferische bijdrage. Een ^{210}Po "excess" zowel in opgeloste vorm als in de vorm van deeltjes, duidde op een extra ^{210}Po flux van de kust en shelf sedimenten vanwege de hoge resupensie waarden. Massa balans berekeningen met een box model toonden een kortere verblijftijd en een hogere absorptie voor opgelost ^{210}Po dan voor opgelost ^{210}Pb, wat duidt op een efficiente recycling. Vergelijking van gegevens over ^{210}Pb concentraties in water en sediment toonde dat er een regelmatige ^{210}Po "excess", zoals waargenomen in de waterkolom, in evenwicht wordt gehouden door een klein tekort aan ^{210}Po in het sediment.

Ook werd aandacht besteed aan mogelijke seizoensinvloeden. Metingen aan watermonsters toonden dat de concentraties opgelost ^{210}Pb en ^{210}Po relatief laag waren in de zomer, terwijl de gesuspendeerd ^{210}Pb en ^{210}Po relatief hoog waren in lente en winter. De waargenomen seizoensvariatie in de verspreiding van de twee isotopen werd beschouwd als het resultaat van effectieve verwijdering in de zomer en verhoogde resuspensie in de winter. Een een-dimensionaal seizoens model werd ontwikkeld om de waargenomen seizoensvariatie te verklaren. De hieruit afgeleide tijdvariatie van totaal ^{210}Pb en ^{210}Po komt goed overeen met de veldgegevens. Geconcludeerd werd dat de ^{210}Pb depositie uit de atmosfeer op het zee oppervlak een sleutelrol speelt in de regulering van de verspreiding van ^{210}Pb en ^{210}Po in het onderzoeksgebied, maar dat deze te klein is om al het aanwezige ^{210}Pb en ^{210}Po te verklaren. Ongeveer 10-25% van de totale hoeveelheid ^{210}Pb en ^{210}Po wordt aangevoerd door laterale advectie.

Om de betrouwbaarheid te schatten van de massabalans van deeltjestransport en sedimentatie is de atmosferische depositie van ^{210}Pb in Nederland bestudeerd. De waargenomen totaal ^{210}Pb depositie vertoont een sterke variatie op korte tijdschaal en tevens ruimtelijke variaties. Er is een goede correlatie tussen dagelijkse ^{210}Pb depositie en neerslag, wat duidt op de aanwezigheid van een sterk seizoens effect over het jaar: de depositie flux is groter in de zomer dan in de winter. De droge "fallout" flux, geschat aan de hand van de relatie van de ^{210}Pb flux met de neerslag, is 16-38% van de totaal ^{210}Pb depositie. Hoewel een sterk seizoens effect is waargenomen in de dagelijkse totaal ^{210}Pb flux, verschilt de jaarlijkse depositie snelheid van ^{210}Pb niet significant van jaar tot jaar. Voor een juist beeld van de flux zijn echter metingen op een langere tijdschaal nodig om de invloed van een grote seizoens variatie en ruimtelijke variatie te ondervangen.

CHAPTER 1

INTRODUCTION

Particle-reactive chemical species introduced into rivers and seas are removed from the water column to the sediment by scavenging processes. The chemical adsorption onto particulate matter, with subsequent transport over vast distances to the sea-floor by the flux of sedimenting particles, is widely recognized as a major factor in the control of the concentration of many pollutants in seawater (Turekian, 1977). The continental margin is a potential barrier for the transfer of material from the land to the ocean basins, especially for those reactive species (suspended solids, trace metals, nutrient elements, etc.), which are likely to settle on the shelf or change their speciation in mixing zone between fresh and salt water.

To quantify the fluxes of the chemical species by direct methods is not yet possible. However, by using diagnostic natural and anthropogenic radionuclides, it is possible to identify mechanisms and time scales of the processes operating in the water and in the sediment, in order to predict the fate of these particle-reactive chemical substances.

Departure from secular equilibrium among members of the natural radioactive decay series occurs in the oceans because of differences in geochemical behaviour between parent and daughter radionuclides. When daughter activity differs measurable from parent activity in seawater, studies of radioactive disequilibrium can yield valuable information on the rates, mechanisms and removal processes in the coastal waters (Bacon et al., 1978). Members of the uranium decay series, particularly ^{210}Pb (half life 22.3 yr) and ^{210}Po (half life 138 d) have proven to be useful in this pursuit because of their suitable half-lives and because their sources are well known (Koide et al., 1973; Guinasso and Schink, 1975; Carpenter and Beasley, 1981; DeMaster and Cochran, 1982; Cochran, 1985; Buesseler et al., 1985/1986).

Two principal modes of supply of ^{210}Pb to the coastal and shelf waters should be considered: deposition from the atmosphere and production within the water column following decay of ^{226}Ra. Supply of ^{210}Pb by rivers is thought to be unimportant because of rapid scavenging of ^{210}Pb by riverine sediment particles and efficient trapping of the sediment in estuaries and nearshore waters (Benninger et al., 1975). ^{210}Po, on the other hand, is almost entirely supplied by in-situ decay of ^{210}Pb in the water column. The radioactive disequilibrium between ^{210}Po-^{210}Pb and

^{210}Pb-^{226}Ra serves suitably as a well-established tool for the study of scavenging rates, transport rates and particle mixing rates in coastal waters and bottom sediments: under steady state conditions, the distribution of radionuclides can be modelled by a function of radioactive decay, production rate from their parents and transport processes. Furthermore, ^{210}Pb decays significantly within the sediments and its activity at the sediment surface is the interplay between sedimentation, bioturbation, resuspension, adsorption / desorption and radioactive decay which determine to what extent particle exchange between the sediments and the overlying water column takes place (Turekian et al., 1980; Benninger and Krishnaswami, 1981).

^{137}Cs (half life 30 yr), an anthropogenic radionuclide, has been initially introduced into the environment as stratospheric fallout resulting from atmospheric nuclear weapons testing. It could also be added into the environment by waste discharges from the nuclear fuel reprocessing plants. It is a very recent injection into the environment (about 40 years) which makes it a suitable tracer of transport mechanisms.

By measuring the concentration of these nuclides in the water column and their inventories in the underlying sediment one can build up box models for mass balance calculations, hence being able to quantify the rates of chemical scavenging, particle deposition, boundary flux exchange and sediment resuspension, and eventually determine the fates and effects of organic and inorganic pollutants in coastal and shelf environments.

The North Sea, as a continental shelf sea, has a great variety in water depth from very shallow to a maximum of 50 metres in the southern part, to 100 metres in the Central North Sea and to over 200 metres in the northern part and the Norwegian Channel. Strong gradients in water temperature, salinity and tidal as well as wind-driven mixing make this area very versatile in nature. This results in a dynamic system with the deeper areas becoming stratified during the summer and shallower areas being continuously vertically mixed throughout the year. Sedimentation, resuspension, scavenging and particle transport are some of the key processes in determining the fate and impact of particle-reactive chemical substances in this area.

The northwestern Mediterranean Sea, similarly, is another type of a continental shelf sea. The deposition of sediment in this area is governed not only by the intricate topography of the sea bed but also by the terrigenous input and water circulation. The Rhône river is the dominant (80%) source of sediment for

this continental margin area (Martin and Thomas, 1991; Zuo et al., 1991). Also supply of material from the other small coastal rivers, atmospheric deposition and biogenic production play significant roles in the particle transport and deposition systems of the northwestern Mediterranean Sea.

The subject of this thesis is to study those key processes by examing the dynamic behaviour of radioactive tracers, ^{210}Pb, ^{210}Po and ^{137}Cs, in the coastal and shelf environments of the North Sea as well as of the northwest Mediterranean Sea.

REFERENCES

Bacon M. P., D. W. Spencer and P. G. Brewer (1978) Lead-210 and Polonium-210 as Marine geochemical tracers: review and discussion of results from the Labrador Sea. In: *Nature radiation environment III*, T. F. Gesell and W. F. Lowder, eds., Proceedings of a symposium held at Houston, Texas, U. S. A. No. 1, pp. 473-501.

Benninger L. K., D. M. Lewis and K. K. Turekian (1975) The use of natural Pb-210 as a heavy metal tracer in the river-estuarine system. In: *Marine chemistry in the coastal environment*, T. M. Church, editor, ACS Symposium Series, No. 18, pp. 202-210.

Benninger L. K. and S. Krishnaswami. (1981). Sedimentary processes in the inner New York Bight: evidence from excess ^{210}Pb and $^{239,240}Pu$. *Earth Planet. Sci. Lett.*, **53**, 158-174.

Buesseler K. O., H. D. Livingston and E. R. Sholkovitz. (1985/86). $^{239,240}Pu$ and excess ^{210}Pb inventories along the shelf and slope of the northeast U.S.A. *Earth Planet. Sci. Lett.*, **76**, 10-22.

Carpenter R. and T. M. Beasley. (1981) Plutonium and americium in anoxic marine sediments: Evidence against remobilization. *Geochim. Cosmochim. Acta*, **45**, 1917-1930.

Cochran J.K. (1985) Particle mixing rates in sediments of the eastern equatorial Pacific: Evidence from ^{210}Pb, $^{239+240}Pu$ and ^{137}Cs distributions at MANOP sites. *Geochim. Cosmochim. Acta*, **49**, 1195-1210.

DeMaster D.J. and J.K. Cochran (1982) Particle mixing rates in deep-sea sediments determined from excess ^{210}Pb and ^{32}Si profiles. *Earth Planet. Sci. Lett.*, **61**, 257-261.

Guinasso N. L., Jr. and D. R. Schink (1975) Quantitative estimates of biological mixing rates in abyssal sediments. *J. Geophys. Res.*, **80**, 3032-3043.

Koide M., K. W. Bruland and E. D. Goldberg (1973) Th-228/Th-232 and Pb-210 geochronologies in marine and lake sediments. *Geochim. Cosmochim. Acta*, **37**, 1171-1187.

Martin J.-M. and A. J. Thomas (1991) Origins, concentrations and distributions of artificial radionuclides discharged by the Rhône river to the Mediterranean Sea. *J. Envir. Radioactivity*, **11**, 105-139.

Turekian K. K. (1977) The fate of metals in the oceans. *Geochim. Cosmochim. Acta*, **41**, 1139-1144.

Turekian K. K., J. K. Cochran, L. K. Benninger and R. C. Aller (1980) The sources and sinks of nuclides in Long Island Sound. *Advan. Geophys.*, **22**, 129-164.

Zuo Z., D. Eisma and G. W. Berger (1991) Determination of sediment accumulation and mixing rates in the Gulf of Lions, the Mediterranean Sea. *Oceanol., Acta*, **14**, 253-262.

CHAPTER 2

RECENT SEDIMENT DEPOSITION RATYES IN THE OYSTER GROUND, NORTH SEA

ABSTRACT

Recent sediment accumulation rates were calculated from downcore ^{210}Pb-excess activity profiles obtained from box cores taken in the Oyster Ground, North Sea. The rates ranged from 0.04 to 0.94 cm·yr^{-1} with an average of 0.39 cm·yr^{-1}. In the top sediment layer the activities were rather low, the highest being only 1.15 dpm·g^{-1}, and the average value 0.92 dpm·g^{-1}.

As shown by X-ray radiographs, downcore variations in texture were small: most samples being homogeneous and lacking primary sedimentary structures. Burrowing was evident in all cores, and most of them had a surface mixed layer of at least 5 cm, below which the ^{210}Pb activity rapidly dropped to background value.

Downcore deviations from the logarithmic decrease in ^{210}Pb with depth could generally be attributed to biological disturbance or physical processes causing reworking of the sediment. Only in one core did the ^{210}Pb activity decrease regularly with depth. The activities of ^{137}Cs in this core and another demonstrated recent accumulation rates of 0.44 and 0.88 cm·yr^{-1}, respectively, which are in good agreement with the rates obtained from the ^{210}Pb method in the same cores (*viz.* 0.37 and 0.94 cm·yr^{-1}). From these sedimentation rates the total amount of mud yearly deposited in the muddy part of the Oyster Ground is estimated to be in the order of 2x10^{9} kg·yr^{-1}, which is 4 to 5% of the total amount of mud yearly deposited in the North Sea.

1. INTRODUCTION

The Oyster Ground, a large depression in the southern North Sea, roughly forms a circle with a radius of 80 km and its centre at 54°30'N and 4°30'E (Fig. 1). The depth at its edges is ~40 m and increases to more than 50 m at the centre. It is the most southern part of the North Sea that becomes stratified in spring (TIJSSEN & WETSTEIJN, 1984). Water masses coming from the south from the Channel and from the north along the English east coast converge in this area. It is an important spawning-ground for codfish and plaice.

Little is known about the origin of the sediment and the amounts deposited in the Oyster Ground area. The fine-grained sediments that form the sea floor in this area are largely reworked tidal flat deposits dating from ~8000 B.P. They contain a typical reworked tidal flat mollusc fauna (CADÉE, 1984). Recent data of BEHRE *et al.* (1984), CREUTZBERG *et al.* (1984) and CREUTZBERG (1985), however, indicate the presence of a narrow zone of muddy deposits without reworked tidal flat molluscs. According to BEHRE *et al.* (1984) these deposits have high contents of pollutants (trace metals). They describe a core from this zone showing deposition of 1.80 m of mud above the older tidal-flat sediments with an increase of Zn and Pb above background levels in the surface sediment starting from ~100 cm below the sediment surface. They correlate this level with the beginning of anthropogenic pollution, which they date around 1880. This would give an accumulation rate of ~1 cm·yr^{-1} for the upper 100 cm.

This paper discusses quantitative analyses of the deposition rate, using the ^{210}Pb dating method and fall-out isotope measurements, in 13 box cores collected in the zone of muddy deposits.

Acknowledgements.—We are indebted to the crew of R.V. 'Aurelia' for their efficient and pleasant cooperation during the coring cruise. We also wish to thank J. Kalf, S. Jansen and M.H.C. Stoll for their kind help during the preparation of the samples and of this paper.

2. MATERIAL AND METHODS

2.1. SAMPLING AND SEDIMENT DESCRIPTION

In 1987, 23 box cores were collected with R.V. 'Aurelia' of the Netherlands Institute for Sea Research. The location of the box cores is indicated in Fig. 2. The cores were collected along 3 transects crossing the area where fine-grained sediment could be expected.

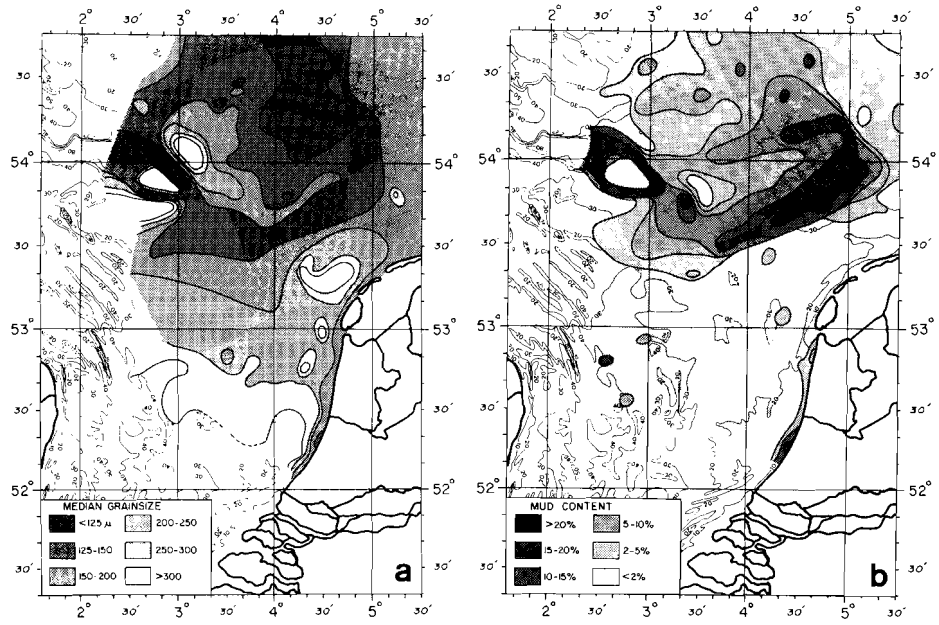

Fig. 1. Distribution of (a) median grain size (in μm) and (b) mud content (particles <50 μm) (in %) of bottom sediments in the southern North Sea (from CREUTZBERG *et al.*, 1984; CREUTZBERG, 1985).

The cores were taken by a box corer with a 25x40 cm box, subsampled with PVC pipe of 6 cm diameter and stored upright to avoid mixing of the soft top layer.

In the laboratory the subsamples were split and one half was used for X-ray and ^{210}Pb sampling. The other half was stored, except for the second halves of cores -9 and -23, which were used for gamma activity analysis. X-ray radiographs were made to examine the cores for bioturbation, structural and textural discontinuities, and evidence of disturbance during the coring operation or transport.

The cores, as shown by X-ray radiographs, were of different types of sediment ranging from sand to clay with little downcore variations in texture. Most cores were homogeneous and lacked primary sedimentary structures, but contained some layers of mollusc shells or shell fragments. Burrowing was evident in all cores, and most of them had surface mixed layers of at least 5 cm which showed some degree of bioturbation or physical mixing. For ^{210}Pb and ^{137}Cs subsamples were selected only from the cores that contained mud (*viz.* cores -6, -7, -8, -9, -12, -13, -14, -15, -16, -17, -21, -22, -23).

2.2. METHODS

^{210}Pb, a member of the ^{238}U series with a half-life of 22.3 years, has been used as a powerful tool for studying recent sedimentation processes in the Wadden Sea and the Skagerrak (BERGER *et al.*, 1987; EISMA *et al.*, 1989; HEIJNIS *et al.*, 1987; VAN WEERING *et al.*, 1987). The ^{210}Pb activity was determined by measuring its granddaughter ^{210}Po, which is assumed to be in secular equilibrium with ^{210}Pb. For ^{210}Pb analysis the samples taken along the vertical profiles in the subsamples were selected on the basis of X-ray radiographs in such a way that clay-silt sediment samples were taken from undisturbed layers, *i.e.* without bioturbation, at approximately 5-cm intervals in the cores. Samples of 2 g (dry weight) were spiked with ^{208}Po as a yield tracer and digested on an electrical hotplate with a 1:1 mixture of concentrated HNO_3:HCl and 70% $HClO_4$. After evaporation, the ^{210}Po isotopes were plated on silver discs at 85°C after reduction of Fe^{3+} with ascorbic acid, and analysed by α-spectroscopy. Calculations were made according to the constant-initial-concentration

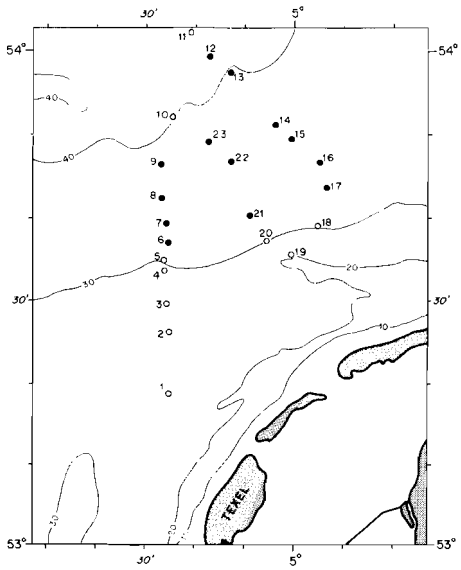

Fig. 2. Position of 23 box cores collected in 1987 in the Oyster Ground area, North Sea. Cores containing silty clay and clay denoted by full symbol; those containing silt and sand with <5 % mud by open symbol.

method (ROBBINS & EDGINGTON, 1975; GOLDBERG *et al.*, 1977) with the formula:

$$T_i = {}^1/\lambda \; I_n \, (A_o \, / A_i)$$

where: A_o = unsupported ^{210}Pb activity at the sediment surface in dpm·g^{-1} dry sediment;
A_i = unsupported ^{210}Pb activity at depth i in dpm·g^{-1} dry sediment;
λ = decay constant of ^{210}Pb (= 0.03114 yr^{-1});
T_i = difference in age of surface sediment and sediment at depth i in years.

The sedimentation rate was determined from the slope of the least-square fit for ^{210}Pb excess values plotted versus depth. The calculation assumed biological and physical mixing to be restricted to the surface mixed layer (SML). Except in cores-6 and -12, which were completely mixed, this seems reasonable. The accuracy of the ^{210}Pb activity measurements was 5% or better, based on counting error alone. The chemical yield was 90% or more.

Since the early 1950s, environmental radioactivity has increased considerably, primarily because of nuclear weapon tests conducted in the atmosphere. The variations in time of some artificial radionuclides in the sources are expected to be recorded and preserved in a continuously accumulating, undisturbed sediment, so it is possible to derive sediment accumulation rates for the past two decades by correlating the distribution pattern of these nuclides in sediments with their delivery pattern from the atmosphere. ^{137}Cs is the most extensively used nuclide for such studies. It has a half-life of ~30 years and was first introduced into the atmosphere in the early 1950s. It reached its peak value in 1963,

TABLE 1

Surface mixed layer depths and estimates of recent deposition rates of 13 cores. Completely mixed cores indicated by xx. The average deposition rate has been calculated from 11 cores omitting the 2 completely mixed cores, and using the mean if 2 values were available for 1 core.

core number	*box core length (cm)*	*surface mixed layer (cm)*	*deposition rate (cm·yr^{-1})*
NZ87-6	33	xx	
-7	37	6	0.30
-8	39	10	0.26
-9	41	5	0.94 (5-21 cm) 0.23 (>21 cm)
-12	31	xx	
-13	40	11	0.70
-14	38	10	0.40
-15	38	10	0.41
-16	40	6	0.75 (6-12 cm) 0.34 (>21 cm)
-17	33	16	0.13
-21	44	10	0.72 (10-26 cm) 0.04 (>26 cm)
-22	39	10	0.37 (10-26 cm) 0.08 (>26 cm)
			average 0.39

the year of the heaviest global fall-out. From then on the values of ^{137}Cs have kept decreasing, interrupted by a small peak in 1980 and another (even smaller one) in 1986, found only in areas affected by fall-out from the USSR nuclear power station in Chernobyl. Thus ^{137}Cs can be used for dating rapidly accumulating sediments. In the laboratory, the concentrations of ^{137}Cs were determined non-destructively in a high resolution Ge detector. About 25 to 50 g (dry weight) of sediment were placed in a plastic box. The activity of ^{137}Cs was determined by integrating the counts under the peak at 662 KeV.

3. RESULTS AND DISCUSSION

Table 1 lists station depths, SML depths and all estimates of accumulation rate. Some typical ^{210}Pb-excess activity profiles are shown in Fig. 3. The downcore ^{210}Pb-excess activity profiles indicate a 5 to 16 cm thick SML at all stations and unusual ^{210}Pb-decay behaviour at depth beneath the SML in all cores except core-23. Near the sediment-water interface the ^{210}Pb activities were rather low, the highest being only 1.15 dpm·g^{-1}, and the average value 0.92 dpm·g^{-1}. The values of ^{210}Pb background ranged from 0.46 to 0.80 dpm·g^{-1} with an average value of 0.61 dpm·g^{-1}. These variations were probably caused by porosity variations reflecting grain-size differences.

Least square fits for exponential decrease of excess ^{210}Pb yielded sedimentation rates as shown in Table 1. The rates ranged from 0.04 to 0.94 cm·yr^{-1}, the highest occurring in core-9, while in the deeper part of the sediments the rates were lowest (0.04-0.34 cm·yr^{-1}, Fig. 3). Downcore deviations from the exponential decrease with depth could generally be attributed to biological disturbance or physical processes causing erosion and/or redeposition associated with sediment transport. Only in core-23 did the ^{210}Pb activity decrease regularly to the background value with depth.

The average of the estimated accumulation rates was only 0.39 cm·yr^{-1}. This is a low figure, indicating that although CREUTZBERG & POSTMA (1979) demonstrated experimentally that fine-grained sediments may settle in the Oyster Ground area, apparently there is little lasting sediment deposition (EISMA, 1981; CREUTZBERG *et al.*, 1984). CADÉE (1984) also concluded that there is little sedimentation in the Oyster Ground because remains of a ~ 9000 yr-old tidal-flat fauna were still present at or near the sediment surface.

From inspection of the X-ray radiographs, it can be concluded that reworking of sediments near or at the

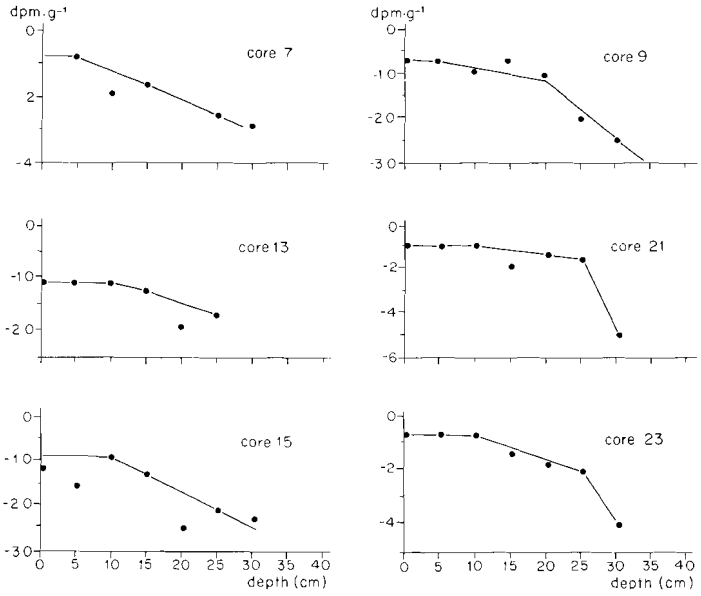

Fig. 3. Example of typical decay profiles of excess ^{210}Pb activities (6 different cores, collected in 1987, indicated by their number, compare Fig. 2).

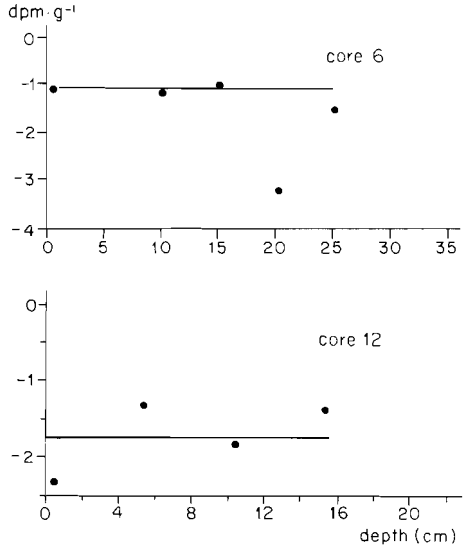

Fig. 4. Unusual distribution of excess ^{210}Pb activities in cores-6 and -12.

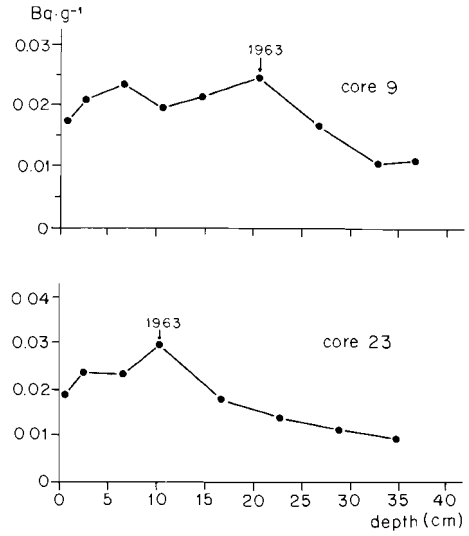

Fig. 5. The decay profiles of ^{137}Cs activities in cores-9 and -23.

sediment-water interface is a universal phenomenon in the Oyster Ground caused not only by bioturbation but also by strong tidal currents and high wave activity (McCAVE, 1971). From the ^{210}Pb-activity distribution in cores-6 and -12 (Fig. 4) it was not possible to estimate a rate of deposition because of sediment mixing over the entire depth of the core and, probably, irregular alternation of erosion and deposition. However, the sedimentation rates calculated from ^{210}Pb profiles below the SML can certainly reflect true rates of deposition (NITTROUER *et al.*, 1984; SMITH & SCHÄFER, 1984). Cores-7, -13, and -15 had an SML of at least 6 cm; below this layer the deposition rates ranged from 0.13 to 0.70 cm.yr^{-1} (Fig. 3). In some cores, for instance cores-9, -21 and -23, two depositional periods below the SML appear to be present (Fig. 3), which reflects a change in depositional conditions. Core-9 had a sedimentation rate of 0.94 cm·yr^{-1} at 5 to 21 cm depth in the core, and below 21 cm depth a rate of only 0.23 cm·yr^{-1}. Core-23 had a deposition rate of 0.37 cm·yr^{-1} at 10 to 26 cm depth below the SML, while in the deeper part the rate was lower (0.08 cm·yr^{-1}). In core-21, in the upper layer below the SML, the rate was 0.72 cm·yr^{-1}, and at the deeper layer only 0.04 cm·yr^{-1}. This demonstrates that above a depth of ~25 cm below the sediment-water interface there has been a period with high deposition rate at least in some parts of the Oyster Ground area. Biological and physical activities occurring near the sediment-water interface will have resulted in lateral and vertical redistribution and displacement of sediment.

The concentrations of ^{137}Cs in cores-9 and -23 are given in Table 2. The concentration of ^{137}Cs (orginating both from dry and wet fall-out) ranged from 0.01 to 0.029 Bq·g^{-1}, with an average of 0.018 Bq·g^{-1}. The profile of core-23 showed a single peak at a depth of ~10.5 cm in the core with a concentration of 0.029 Bq·g^{-1} (Fig. 5). Core-9 seems to have two peaks (Fig. 5): the first peak at 21 cm depth and the second at 7 cm depth. The peak values were 0.024 and 0.023 Bq·g^{-1}, respectively. The estimate of the sedimentation rate is based on the depth at which the ^{137}Cs activity reached its peak value. This is assumed to be 1963, the year of maximum global fall-out. So in core-9, by using the first peak depth, an accumulation rate of 0.88 cm·yr^{-1} is estimated,

TABLE 2

Observed ^{137}Cs activities and estimated deposition rates.

station	^{137}Cs concentration (Bq·g^{-1}) range	average	peak value	peak depth (cm)	deposition rate (cm·yr^{-1})
NZ87-9	0.010-0.024	0.018	0.024 0.023	21 7	0.88
NZ87-23	0.011-0.029	0.018	0.029	10.5	0.44

which is in good agreement with ^{210}Pb accumulation at the station (0.94 cm·yr^{-1}). The second peak value was lower than the first, and it is probably caused by a few nuclear weapon tests conducted during the 1970s. In core-23, the deposition rate calculated by the depth of ^{137}Cs peak value amounted to 0.44 cm·yr^{-1}, which is in agreement with the rate of 0.37 cm·yr^{-1} (in the upper 26 cm, see Table 1) derived from ^{210}Pb data. It is important to emphasize that the ^{210}Pb method gives an average accumulation rate for the past 100 yr, while ^{137}Cs is applicable for the past 20 yr only. Moreover, the profiles of ^{137}Cs activity also display bioturbation in the upper sediments of the cores.

4. CONCLUSIONS

The downcore excess ^{210}Pb profiles from the Oyster Ground allowed a number of determinations of mass accumulation rate. ^{210}Pb analyses demonstrated the presence of upper layers of reworked sediment and an average deposition rate of 0.39 cm·yr^{-1} in sediments which were not or only little reworked. Taking this rate as a base and estimating the area to be 840 km^2, with a mud content (<50 μm) of 25% (CREUTZBERG *et al.*, 1984) and a water content of the sediment of ~25%, and taking 2.65 g·cm^{-3} as the density of the sediment particles, the total amount of mud yearly deposited in this principally muddy area (including some mud deposited outside this area) amounts to the order of 2 x 10^9 kg·yr^{-1}. This is 4 to 5% of the total amount of mud yearly deposited in the North Sea (EISMA & IRION, 1988).

The estimated accumulation rate of 0.37 cm·yr^{-1} in core-23 is in good agreement with the rate derived from the ^{137}Cs activity. A fair agreement between the sedimentation rates determined by ^{210}Pb and ^{137}Cs methods is also observed in core-9. This suggests that the average rate of 0.39 cm·yr^{-1} represents a real sedimentation in the last 100 yr of ~40 cm of sediment in this part of the Oyster Ground. This is less than the 100 cm of deposition inferred by BEHRE *et al.* (1984) from the presence of pollutants at that depth in the sediment. The sampling station of BEHRE *et al.* (1984) was located close to the location of our core-9 with an estimated rate of 0.94 cm·yr^{-1} (^{210}Pb) or 0.88 cm·yr^{-1} (^{137}Cs) in the top 21 cm but with an estimated rate of only ~0.23 cm·yr^{-1} at greater depth in the core down to the end of the core at 41 cm, where the sediment has an estimated age of 109 yr (1878 AD). Extrapolating this rate to 1 m depth would give an age of 365 yr (1622 AD), which is much too early for pollution to appear in North Sea sediments (BEHRE *et al.*, 1984). This points to the possibility that in the core studied by BEHRE *et al.* (1984) pollutants have reached this depth in the sediment by reworking (resuspension mixing with polluted mud and redeposition) or downward diffusion through the pore water. Outside the mud area we found sandy sediments with reworked Early Holocene tidal flat mollusc shells, as expected from the maps (Fig. 1) given by CREUTZBERG *et al.* (1984) and CREUTZBERG (1985) and the data given by CADÉE (1984). Therefore we assume these sediments to be principally reworked tidal deposits. The ^{210}Pb activities of mud in the mud area are rather low compared to the activities of recent mud in the Wadden Sea and the Skagerrak (EISMA *et al.*, 1989; VAN WEERING *et al.*, 1987), including places where no reworked old shells are present. This indicates a possible admixture of nearby reworked old mud in recent mud deposits (EISMA *et al.*, 1989).

5. REFERENCES

BERGER, G.W., D. EISMA & A.J. VAN BENNEKOM, 1987. ^{210}Pb derived sedimentation rate in the Vlieter, a recently filled-in tidal channel in the Wadden Sea.—Neth. J. Sea Res. **21**: 287-294.

BEHRE, K., J. DÖRJES & G. IRION, 1984. Ein datierter Sedimentkern aus dem Holozän der südlichen Nordsee, Probleme der Küstenforschung im südlichen Nordseegebiet. Verlag August Lax, Hildesheim. **15:** 135-148.

CADÉE, G.C., 1984. Macrobenthos and macrobenthic remains on the Oyster Ground, North Sea.—Neth. J. Sea Res. **18:** 160-178.

CREUTZBERG, F., 1985. A persistent chlorophyll a maximum coinciding with an enriched benthic zone. In: P.E. GIBBS. Proceedings of the 19th European Marine Biology Symposium. Cambridge University Press: 97-108.

CREUTZBERG, F. & H. POSTMA, 1979. An experimental approach to the distribution of mud in the southern North Sea.—Neth. J. Sea Res. **13:** 99-116.

CREUTZBERG, F., P. WAPENAAR, G. DUINEVELD & N. LOPEZ LOPEZ, 1984. Distribution and density of the benthic fauna in the southern North Sea in relation to bottom characteristics and hydrographic conditions.—Rapp. P.-v. Cons. perm. int. Explor. Mer **183:** 101-110.

EISMA, D., 1981. Supply and deposition of suspended matter in the North Sea.—Spec. Publs int. Ass. Sedim. **5:** 229-237.

EISMA, D. & G. IRION, 1988. Suspended matter and sediment transport. In: W. SALOMONS, B.L. BAYNE, E.K. DUURSMA & U. FÖRSTNER. Pollution of the North Sea, an Assessment. Springer Verlag, Heidelberg: 20-35.

EISMA, D., G.W. BERGER, W.Y. CHEN & J. SHEN, 1989. ^{210}Pb as a tracer for sediment transport and deposition in the Dutch-German Waddensea. Proc. KNGMG Symp. Coastal Lowlands. Den Haag, 1987, 237-253.

GOLDBERG, E.D., E. GAMBLE, J.J. GRIFFIN & M. KOIDE, 1977. Pollution history of Narragansett Bay as recorded in its sediments.—Estuar. coast. mar. Sci. **5:** 549-561.

HEIJNIS, H., G.W. BERGER & D. EISMA, 1987. Accumulation

rates of estuarine sediment in the Dollard area: comparison of ^{210}Pb and pollen influx methods.—Neth. J. Sea Res. **21:** 295-301.

MCCAVE, I. N., 1971. Wave effectiveness at the sea bed and its relationship to bedforms and deposition of mud.—J. Sedim. Petrol. **41:** 89-96.

NITTROUER, C.A., D.J. DE MASTER, B.A. MCKEE, N.H. CUTSHALL & I.L. LARSEN, 1984. The effect of sediment mixing on ^{210}Pb accumulation rates for the Washington continental shelf.—Mar. Geol. **54:** 201-221.

ROBBINS, J. & D.N. EDGINGTON, 1975. Determination of recent sedimentation rates in Lake Michigan using ^{210}Pb and ^{137}Cs.—Geochim. cosmochim. Acta **39:** 285-301.

SMITH, J.N. & C.T. SCHÄFER, 1984. Bioturbation processes in continental slope and rise sediments delineated by ^{210}Pb, microfossil and textural indicators.—J. mar. Res. **42:** 1117-1145.

TIJSSEN, S. B. & F. J. WETSTEYN, 1984. Hydrographic observations near a subsurface drifter in the Oyster Ground, North Sea.—Neth. J. Sea Res. **18:** 1-12.

WEERING, T.C.E. VAN, G.W. BERGER & J. KALF, 1987. Recent sediment accumulation in the Skagerrak, Northeastern North Sea.—Neth. J. Sea Res. **21:** 177-189.

(received 13 October 1988; revised 1 March 1989)

CHAPTER 3

SPATIAL DISTRIBUTIONS OF ^{210}PB AND ^{137}CS AND MIXING RATES IN SEDIMENTS OF THE SOUTHERN NORTH SEA

ABSTRACT--**^{210}Pb and ^{137}Cs were used as tracers to examine particle mixing and sediment deposition in the southern North Sea. The profiles of these two radioactive nuclides in the sediments show the presence of intense sediment mixing. Subsurface ^{210}Pb maxima were commonly found. Results from the calculation of the conventional diffusion model suggest that sediment mixing in the study area cannot be described by diffusive processes. However, applying a single event subsurface egestion model to our data gives good agreement between the model curves and the measured profiles. It is concluded that the subsurface maxima of excess ^{210}Pb are related to the non-diffusive biogenic mixing, and that this kind of biological mixing plays an important role in determining the fate of the sediment in the coastal and shelf environments of the southern North Sea.**

1. INTRODUCTION

Sediment mixing produced by the feeding and burrowing activities of benthic fauna leads to the modification of both the physical and the geochemical properties of sediments (Rhoads, 1974; Guinasso and Schink, 1975; Smith et al., 1986/1987; Gerino, 1990). The physical and chemical properties of sediment, as controlled by biological processes, may have a major effect on sedimentation, particle transport, nutrient regeneration and the fates and historical records of radiochemical species and pollutants. The characteristics of sediment mixing are probably best determined by using radionuclide tracers, which are delivered to the sediments in association with particles settling through the water column, to estimate the rate and depth of particle mixing. Many such estimates have been obtained from investigations of the near-surface distributions of various natural and fallout radioactive tracers such as long-lived radionuclides like ^{230}Th and ^{14}C (Goldberg and Koide, 1962; Nozaki et al. 1977; Anderson et al., 1983; Shimmield et al., 1986; Thomson et al., 1988) and short-lived radionuclides ^{234}Th and ^{210}Pb (Benninger et al., 1979; Carpenter et al., 1981, DeMaster and Cochran, 1982; Aller and DeMaster, 1984; Cochran, 1985; Gardner et al., 1987; Alexander et al., 1991) as well as the bomb-produced artificial radionuclides ^{239,240}Pu and ^{137}Cs (Guinasso and Schink, 1975; Carpenter and Beasley, 1981; Stordal and Johnson, 1982; Santschi et al., 1983; Druffel et al., 1984). In many cases the complex mechanisms of sediment

reworking process are conveniently modelled by analogy with diffusive processes (Goldberg and Koide, 1962; Guinasso and Schink, 1975; DeMaster and Cochran, 1982). However, it has been increasingly evident that many organisms do not transport particles in a random manner over short distances as required by the diffusive analogue model. Some organisms, such as surface deposit feeders or head-down deposit feeders, ingest sediment at depth and excrete it at the surface in a 'conveyor belt' fashion and generate bioadvective processes in sediment (Robbins et al., 1979; Rice, 1986; Gerino, 1990). The non-local component of the mixing process is characterized by the appearance of distinct subsurface maxima in the radionuclide distributions which have been commonly observed in a wide range of depositional regimes. For example, Smith et al. (1986/1987) examined $^{239,240}Pu$ and ^{210}Pb distributions in northeast Atlantic sediments and proposed that the subsurface tracer maxima observed in their study were generated by the feeding and defecation activities of a specific infaunal organism and that similar non-local transport processes may affect many other marine and aquatic depositional regimes.

The effects of sediment mixing are clearly delineated in the present study of distribution of radioactive tracers ^{210}Pb and ^{137}Cs in southern North Sea sediments, in order to understand the dynamics of sediment depositional/post-depositional processes in this continental shelf sea. The use of a multiple tracer approach is important in providing a check on the reliability of mixing rates calculated from a single tracer and may help assess the validity of mixing models applied in the study. Comparison of ^{210}Pb with ^{137}Cs is of interest because the former is a naturally-occurring isotope with a suitable half-life (22.3 years) and is assumed to be added to the sediments continuously, which often allows a presumed steady-state distribution, whereas the latter has been input in sediments as a fission product (half-life = 30 years) only over the past 25-35 years and is not at steady-state.

2. SAMPLING AND STUDY AREA

In April 25-26 of 1988, 22 boxcores were collected with R.V. *Aurelia* in the southern North Sea. The location of the sampling stations is shown in Figure 1. Among the 22 boxcores, 12 (Cores 8810-8821) were taken from the Outer Silver Pit and its southeast adjacent areas such as Markhams Hole, Botney Ground and New Zealand Ground whereas the remainder (Cores 8822-8831) were obtained from the German Bight (Elbe Rinne; Fig. 1).

Boxcores were subsampled with a PVC-pipe (inside-diameter 6 cm) immediately after the recovery of the boxcorer. Care was taken to minimize the

coring disturbance to the sediment during the sampling procedure and transportation.

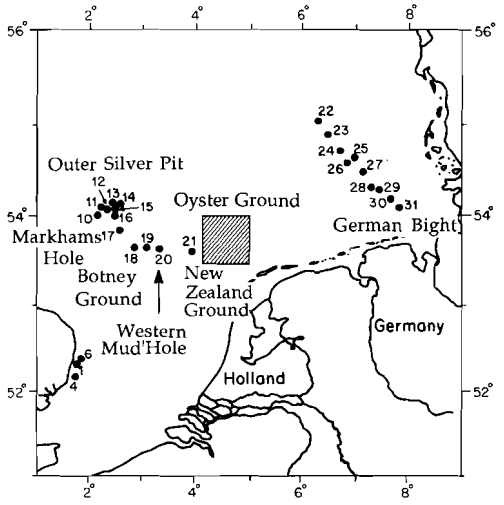

Fig. 1 *The location of bottom sediment sampling stations in the southern North Sea. The shaded area is a previous work area (Oyster Ground; Zuo et al., 1989). The core number prefix (88) is removed for clarity.*

Water depth in the study area gradually increases northward from 20 to 80 m, with an average depth of 70 m for the Outer Silver Pit, 40 m for the southeast area of the Outer Silver Pit and 40 m for the German Bight. Water masses are controlled by the presence of relatively fresh coastal water and Channel water as well as North Atlantic water, which all generally circulate in a counter-clockwise direction. The character of the bottom, the composition of the sediment, and the deposition or resuspension of inorganic and organic particles are strongly influenced by the water flow, of which the most important component is the tidal current (velocities in the order of 10 - 40 cm/sec, the strongest tidal currents being more than 1 m/sec; Eisma, 1987). Waves also play an important role in erosion of fine-grained sediments. The effectiveness of waves - even of storm waves - generated in the southern North Sea is, however, supposed to be small below a

depth of 30 m (McCave, 1971). There is little recent fine-grained deposition in most of the study area as the circulation pattern in the southern North Sea tends to concentrate suspended matter in the nearshore areas because residual currents carry bottom water shoreward (Eisma, 1981). However, local deposition has been reported, based on a study of radionuclides, at the Oyster Ground area (mean sedimentation rate 0.39 cm/yr, Zuo et al., 1989) and in the German Bight (sedimentation rate 0.6 - 1.8 cm/yr, Dominik et al. 1978).

3. SEDIMENTS

In the laboratory, the sediment cores were split, X-rayed and sectioned into 1-cm increments to 10 cm and 2-cm (sometimes 3-cm) increments thereafter, in order to obtain a high resolution for the top layer in which sediment is usually intensively mixed. Water content of sediments was determined by weight loss of wet sediment on drying (at 105^0C) for each core.

The observations and X-ray radiographs show that most sediments consist of fine sand, silt and some silty clay and have homogeneous and mottled structure with a much disturbed upper layer (5-10 cm). Many burrows and tubes are evident on the radiographs. Cores taken from the Outer Silver Pit (Sta.8810-8816, Fig. 1), except Sta. 8810, show an uppermost finely bedded layer from 0-5 cm which was penetrated later by some worm tubes and burrow holes. For example, core 8813 has a layered top zone of 4 cm with a tube (diameter 0.4 cm) cutting through the bedding zone and down to 11 cm depth. We believe that this type of structure was formed by bioturbation following a storm event. The size of burrows and tubes varies from 0.2 to 0.5 cm diameter, and in some case the deep burrowing can be seen clearly like the one in core 8811 at 20 cm depth.

Sediment cores collected from the adjacent area of the Outer Silver Pit, such as the Botney Ground and the Western Mud Hole (Sta. 8817-8821, Fig. 1), have somewhat different profiles with uniform structure. No obvious burrowing was seen in most cores but an erosion boundary was found in core 8818 at a depth of 6-7 cm.

In cores 8822-8831, obtained from the German Bight (Fig.1), mottled structures with many shells and shell fragments were observed. The X-ray photographs exhibit faint bedding in cores 8830 and 8831. A thin layered zone at the top of the sediment column (0-2 cm) was found again in cores 8826 and 8828, which is possibly related to storm effects. The depth limit for evident biological disturbance in the whole sampling area is commonly a few centimetres to 15 cm,

but sometimes can be 20 cm or even deeper, suggesting that sediment mixing due to the bioturbation must play an important role in distribution of particle-reactive isotopes such as ^{210}Pb and ^{137}Cs.

4. RADIOCHEMICAL METHODS

^{210}Pb and ^{137}Cs activities were determined by alpha-spectrometry and a high resolution Germanium detector interfaced with a 4096 multi-channel analyzer, respectively, using standard procedures (Zuo et al, 1991). The one sigma counting errors quoted were calculated from counting statistics only. Replicate analyses of well homogenized sediments revealed an analytical precision of 3-5%. Reagent blanks were measured periodically and showed negligible contribution. Selected samples were reanalyzed over two years after collection. The agreement with the first analyses indicated that ^{210}Po and ^{210}Pb were in equilibrium and ^{210}Pb activity measured via ^{210}Po ingrowth is therefore reliable.

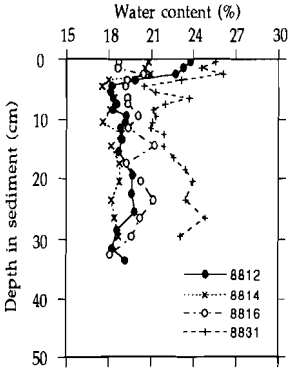

Fig. 2 *The plot of water content (%) against depth (cm) in sediments.*

5. THE DISTRIBUTION OF ^{210}PB AND ^{137}CS

The activities of ^{210}Pb, excess ^{210}Pb ($^{210}Pb_{xs}$) and ^{137}Cs, together with the data for water content, porosity and dry bulk density for 22 sediment cores, are listed in Appendix A. The ^{210}Pb activities in deeper sections of the sediments have been taken as an index of ^{226}Ra for the calculation of $^{210}Pb_{xs}$. For cores from the Outer Silver Pit and the adjacent areas (cores 8810-8821), a value of 1.07 ± 0.17 dpm/g (n=24, at depth ≥ 15 cm) was taken as the mean activity of ^{226}Ra and for cores from the German Bight (cores 8822-8831) the mean value of ^{226}Ra was assumed to be 0.83

± 0.17 dpm/g (n=28, at depth ≥ 15 cm). The profiles of water content in the sediment (Fig. 2) show a similar trend in all cores: being about 27% at the water-sediment interface, it rapidly drops down to about 18% at around 5 cm depth and then remains nearly constant below that depth.

^{210}Pb distribution

The distribution of total ^{210}Pb and ^{137}Cs in the 22 cores are shown in Figure 3. It is obvious that most of the cores have a pronounced concentration increase to a maximum below the surface layer, then the ^{210}Pb activity decreases exponentially with depth and eventually levels off at a rather constant value deeper in the cores (Fig. 3), which indicates the ^{226}Ra content of the sediment. In cores 8812 and 8813 (Fig. 3c, d), more than one activity peak was found. This type of distribution is commonly observed in sediments and is interpreted to indicate rapid mixing of top layer sediment either by biological or physical processes. The homogeneous or mottled sediment structure in a much disturbed upper layer with many burrow and tubes (as is evident from the X-ray radiographs) strongly indicates biogenic sediment mixing in this part of the core. The distribution of ^{210}Pb in cores 8816, 8818 and 8821 (Fig. 3g, i, l) shows little gradients without obvious subsurface peak values throughout the sediment column.

A number of explanations have been proposed for the ^{210}Pb subsurface maximum peaks. Koide et al. (1973) made similar observations on their sediment cores from Baja California and the Santa Barbara basin. Their interpretation was that ^{210}Pb was initially deposited under oxidizing conditions and was distributed between the solid phase and the interstitial water in proportions determined by those conditions. At some depth below the surface, in the anoxic, sulfate-reducing zone, most of the dissolved ^{210}Pb was removed as an insoluble sulphide. This resulted in a gradient in the interstitial water which fueled diffusion of ^{210}Pb away from the surface, creating a subsurface maximum in the solid-phase ^{210}Pb concentration. The study of early diagenesis of lead in Laurentian Trough sediment done by Gobeil and Silverberg (1989) also demonstrated that Pb is subject to remobilization and has undergone post-depositional chemical transformations during early diagenesis. However, several other studies have contended that ^{210}Pb is immobile (Appleby et al., 1979; Crusius and Anderson, 1990; 1991). Crusius and Anderson (1991) concluded that, based on a fine-scaled ^{210}Pb study in Black Sea sediments, ^{210}Pb showed no indication of mobility under anoxic, moderately

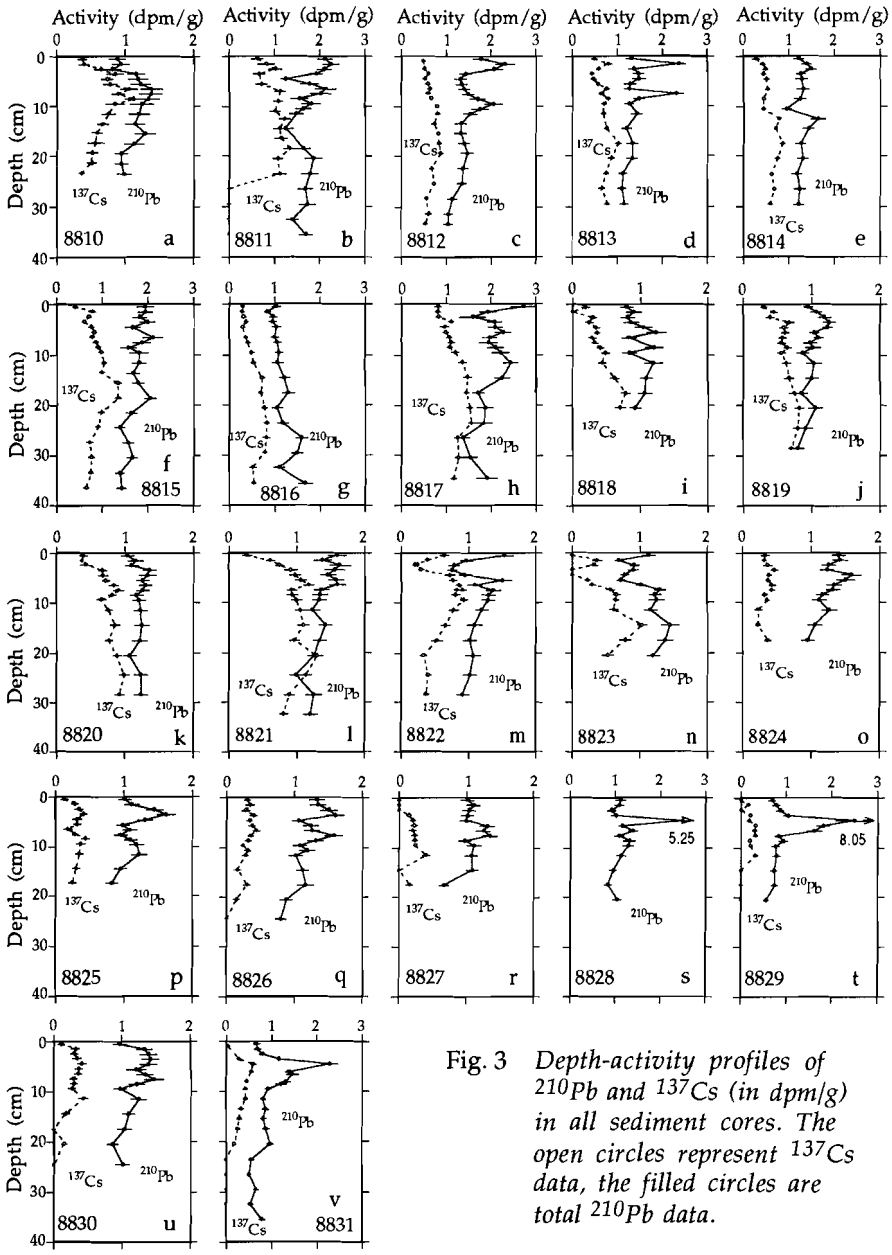

Fig. 3 *Depth-activity profiles of ^{210}Pb and ^{137}Cs (in dpm/g) in all sediment cores. The open circles represent ^{137}Cs data, the filled circles are total ^{210}Pb data.*

sulfidic conditions and thus, the mobility of ^{210}Pb is negligible under these conditions, indicating that the ^{210}Pb dating method is reliable. The ^{210}Pb subsurface maximum, therefore, must be produced by some other processes, such as biological processes.

^{137}Cs distribution

^{137}Cs profiles in some cores are remarkably similar in shape to the corresponding ^{210}Pb profiles (Fig. 3a, e, f, m, n, p, u, v) while in other cores, ^{137}Cs has relatively flat curves which are quite different from the corresponding ^{210}Pb profile (Fig 3c, d, h, i, o, q, r, t). This suggests that there must be some factors or processes which locally can affect the distribution of both nuclides. The most striking feature of ^{137}Cs distributions is that ^{137}Cs has a deep penetration down to the sampling depth in most of the cores, except in cores 8811, 8826-8831 (Fig. 3). Similar observations have been made in other previous studies (Davis et al., 1984; Anderson et al., 1987). One of the explanations proposed is that Cs is more soluble than Pb, and consequently there may be significant transport of ^{137}Cs dissolved in pore waters (Davis et al., 1984). Santschi et al. (1983) suggested that Cs introduced into the marine environment in a soluble form is considerably more mobile than other elements of Pu, Pb, Th, etc. The diffusion could also be responsible for the upward or downward shifting of the ^{137}Cs activity peak. Alternatively, release of ^{137}Cs in the bottom water or at the sediment-water interface coupled with its migration into sediments through a three dimensional network of relict burrows may provide a mechanism for introducing ^{137}Cs into sediments at depth (Aller, 1984). This mechanism may be especially important in perturbing the solid phase distribution produced by particle mixing alone since the fallout nuclides could be introduced in the sediment with zero or near-zero background levels (Cochran, 1985).

Inventories of ^{210}Pb and ^{137}Cs

Radionuclide inventories were calculated by summing the product of the isotope activity, the dry bulk density and section thickness for each increment over the core length. Interpolations between measured values were made for intervals in which ^{210}Pb and ^{137}Cs were not analyzed. In Table 1 the inventories of ^{210}Pb and ^{137}Cs and the isotope penetration depth for each core are tabulated. For cores in which $^{210}Pb_{xs}$ activities are present over the entire depth of the sediment column, the penetration

depth was set to account for 95% of the total inventory in the core. For ^{137}Cs, the penetration depth was overlain by 90% of the total ^{137}Cs inventory in that core.

Table 1: *Isotope inventories, inventory ratios and isotope penetration depths in sediments of the southern North Sea.*

Station	Penetration Depth (cm)*		Inventories (dpm/cm^2)		Inventory Ratio
	$^{210}Pb_{xs}$	^{137}Cs	$^{210}Pb_{xs}$	^{137}Cs	$^{210}Pb_{xs}/^{137}Cs$
8810	18	22	2.78±0.42	20.39±3.06	0.14
8811	36	26	>40.34±6.05	35.70±5.36	>1.13
8812	31	31	18.65±2.80	32.07±4.81	0.58
8813	25	27	12.70±1.91	30.28±4.54	0.42
8814	30	28	10.38±1.56	26.98±4.05	0.38
8815	34	33	31.19±4.68	44.50±6.68	0.70
8816	35	32	6.69±1.00	30.15±4.52	0.22
8817	33	32	38.56±5.78	57.35±8.60	0.67
8818	17	20	1.02±0.15	14.74±2.21	0.07
8819	5	27	0.56±0.08	28.89±4.33	0.02
8820	27	27	5.80±0.87	32.99±4.95	0.18
8821	23	29	10.82±1.62	44.78±6.72	0.24
8822	26	26	10.97±2.19	23.02±4.60	0.48
8823	20	19	10.08±2.02	15.96±3.19	0.63
8824	16	17	10.76±2.15	8.60±1.72	1.25
8825	18	17	8.23±1.65	8.58±1.72	0.96
8826	20	20	12.21±2.44	9.34±1.87	1.31
8827	16	16	6.92±1.38	4.30±0.86	1.61
8828	17	n.m.	14.38±2.88	n.m.	--
8829	9	12	15.49±3.10	4.25±0.85	3.64
8830	23	19	11.78±2.36	8.06±1.61	1.46
8831	22	22	3.84±0.77	12.62±2.52	0.30

* For cores in which the $^{210}Pb_{xs}$ activities present over the entire depth of the sediment, the penetration depth was set to account for 95% of the total inventory in the core. The ^{137}Cs penetration depth was overlain by 90% of the total ^{137}Cs inventory in that core.

We note that the penetration depths of both nuclides in the Outer Silver Pit are deeper than those in the German Bight, and the inventories of both $^{210}Pb_{xs}$ and ^{137}Cs show the same trend, that is, the Outer Silver Pit area has higher inventories than the German Bight (Table 1). The inventories of $^{210}Pb_{xs}$ in half of cores (7 in German Bight and 4 in Outer Silver Pit) are approximately in balance with the atmospheric supply (Table 1) which, at the study area, is estimated to be 13±3 dpm/cm^2, taking the ^{210}Pb flux to be 0.43±0.10 dpm/cm^2/yr (obtained from the

direct measurements over a two-year period, 1987-1988 in the northern Netherlands; Zuo et al., 1992). The ^{210}Pb inventories in cores 8811, 8815 and 8817 (Outer Silver Pit) are higher than this (range from 31.19 to > 40.34 dpm/cm^2), which is probably an effect of local sediment focussing. We believe that, the higher inventories and deeper penetrations of ^{210}Pb and ^{137}Cs in the Outer Silver Pit area suggest more effective sediment focussing and/or chemical scavenging.

6. PARTICLE MIXING RATE

Diffusion model

1) Mixing rates determined from ^{210}Pb.

Goldberg and Koide (1962) developed the first diffusive model to explain observed homogeneity in the ionium/thorium ratio in the upper portion of a pelagic sediment column. Since then, a large number of diffusion models have been used to explain the observed distributions of many radionuclides in sediments modified by biological mixing (Guinasso and Schink, 1975, Nozaki et al., 1977; Robbins, 1978; Cochran, 1985; Thomson et al., 1988). Clearly, the particles themselves do not diffuse, and neither the actions nor distribution of the organisms in sediments is random. However, the redistribution of solid particles by large numbers of small organisms and over a large number of individual transport events may be mathematically described by the diffusion analogy (Boudreau, 1986).

The general equation including the effects of particle mixing, sediment accumulation and radioactive decay can be written (Cochran, 1985):

$$\frac{\partial}{\partial t}\left[\rho A\right] = \frac{\partial}{\partial x}\left[\rho D_B \frac{\partial A}{\partial x}\right] - \frac{\partial}{\partial x}\left[\rho S A\right] - \lambda \rho A \qquad (1)$$

where
- t = time (yr)
- A = activity of radionuclide (dpm/g)
- D_B = particle mixing coefficient (cm^2/yr)
- x = depth in sediment column (cm)
- S = sediment accumulation rate (cm/yr)
- λ = decay constant for radionuclide (yr^{-1})
- ρ = dry bulk density (g dry sediment/cm^3 wet sediment)

Under steady-state conditions and assuming constant D_B in the mixed zone, constant ρ and employing the boundary conditions $A = A_0$ at $x=0$ and $A \rightarrow 0$ as $x \rightarrow \infty$, then the solution to eq. (1) is:

$$A(x) = A_0 \exp\{[(S - (S^2 + 4\lambda D_B)^{1/2})/2D_B]x\} \qquad (2)$$

Table 2: *Mixing rate coefficients (D_B) in sediments of the southern North Sea.*

Stations	$^{210}Pb_{xs}$		^{137}Cs	
	A_o[a] (dpm/g)	D_B[b] (cm^2/yr)	A_o[a] (dpm/g)	D_B[c] (cm^2/yr)
Outer Silver Pit				
8810	1.56	0.60	0.38	1.50 (2.50)
8811	2.57	1.20	0.63	3.32
8812	2.77	2.01	0.47	4.50
8813	2.99	1.02	0.49	2.87
8814	2.83	1.60	0.50	10.50
8815	7.75	2.47	0.79	8.03
8816	3.93	2.99	0.30	4.07
Markhams Hole				
8817	4.99	3.05	0.82	3.55
Botney Ground				
8818	3.33	0.34	0.30	1.66
8819	0.99	n.c.[d]	0.45	3.09
Western Mud Hole				
8820	0.80	3.45	0.39	1.80
New Zealand Ground				
8821	1.50	3.10	0.62	1.91
German Bight				
8822	1.20	3.81	0.64	6.50 (3.80)
8823	2.83	3.48	0.37	1.99
8824	3.81	0.87	0.33	1.41 (1.41)
8825	2.99	0.78	0.27	1.96
8826	3.15	1.21	0.31	1.81
8827	2.14	1.08	0.21	1.13
8828	6.46	0.60	n.m.[e]	-
8829	13.13	0.20	0.21	1.00
8830	2.40	1.81	0.33	2.11
8831	8.24	0.20	0.60	3.00 (2.50)

[a] A_o is the tracer concentration at the sediment-water interface. For excess ^{210}Pb, A_o was obtained by extrapolating the observed profile (below SML) to the x=0 interface from the $^{210}Pb_{xs}$ depth-activity profile. For ^{137}Cs, the observed concentration at (x=0) or near (x ranged 1-3 cm) the sediment-water interface was taken as A_o.

[b] Results derived from the diffusive model, see text.

[c] Results calculated from the pulse input model. Values in parentheses generated from the continuous input model, see text.

[d] n.c. = not calculated.

[e] n.m. = not measured.

For the sediments in the study area, assuming accumulation is negligible (S≈0), which is not unreasonable as sedimentological data indicate that the southern

North Sea is not a depositional area except for some local parts such as in the Frision Front area (Eisma, 1981; Eisma and Kalf, 1987), eq. (2) reduces to:

$$A(x) = A_0 \exp[-(\lambda/D_B)^{1/2}x] \quad (3)$$

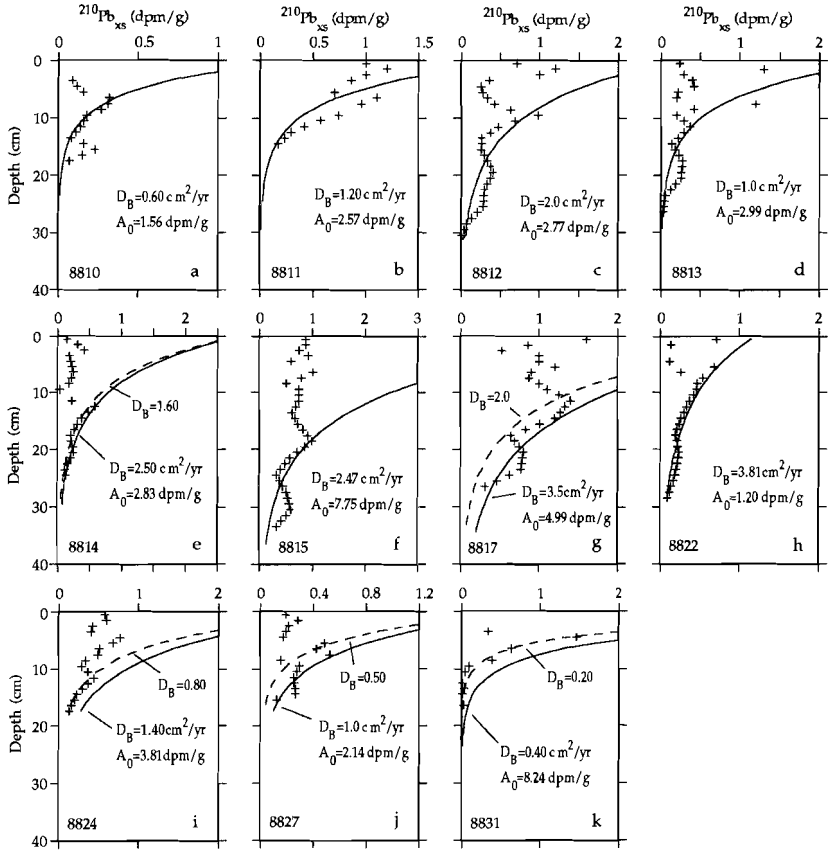

Fig. 4 *Excess ^{210}Pb vs. depth in sediments. Values of D_B corresponding to the best-fit line are shown in solid or dashed lines. Crosses are measured data points.*

Results of the mixing coefficient (D_B) and the best fit lines of deffusive model (eq. 3) are given in Table 2 and Figure 4. Obviously, only the lower part of the model-generated curve fits well with the measured data points, and the upper part of tracer distribution are poorly described by a diffusion analogue simulation. The values for D_B in the study area range from 0.20 to 3.81 cm^2/yr with an average value of 1.40 cm^2/yr (n=10) for the German Bight and 1.70 cm^2/yr (n=7) for the Outer Silver Pit (Table 2).

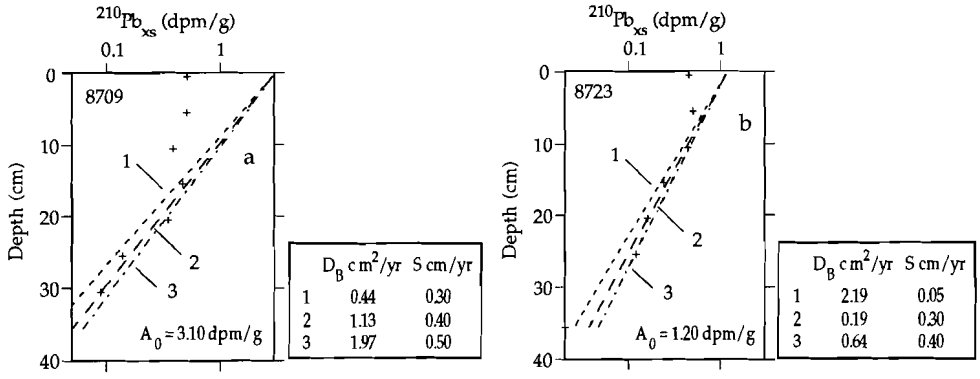

Fig. 5 *Excess ^{210}Pb vs. depth in cores 8709 and 8723 from the Oyster Ground (after Zuo et al., 1989). Calculated D_B and S values for the diffusion model are shown by fitted lines.*

However, for the Oyster Ground area (Fig. 1) where recent fine-grained deposits were found (Behre et al., 1984; Creutzberg 1985; Zuo et al., 1989), taking both biological reworking and accumulation into account, Figure 5 shows the distribution of excess ^{210}Pb and the model fits for D_B and S in cores 8709 and 8723. This was done by giving S a typical value range, based on previous sedimentation studies in the area (0.3-0.5 cm/yr for core 8709 and 0.05-0.4 cm/yr for core 8723; Creutzberg, 1985; Zuo et al., 1989), and varying the D_B value to get the best fit line for the data from eq. 2. The best fit curves give 1.13 cm^2/yr for D_B and 0.40 cm/yr for S for core 8709 (Fig. 5a) and 0.19 cm^2/yr and 0.30 cm/yr for D_B and S for core 8723 (Fig. 5b). The excess ^{210}Pb activities in both upper parts of the core (about 10 cm) have little gradients, indicating much intensive (bio)mixing in the top sediment layer. The data of total organic matter in sediments from both cores (Table 3) allow

an estimation of annual deposition of total organic matter in this muddy zone, which amounts to about 17 - 26 mg/cm^2/yr for the upper 35 cm of sediment column (Table 3). However, there is no clear relationship between mixing rate, excess ^{210}Pb concentration and total organic matter flux in the sediments in the Oyster Ground area. The sedimentation rates are smaller by a factor of 1.2 - 2.5 than those reported by Zuo et al. (1989) at the same sites, probably because the effect of bioturbation was not taken into account.

Table 3: *^{210}Pb data from the Oyster Ground (after Zuo et al., 1989).*

Station	Depth	^{210}Pb	^{210}Pb$_{xs}$	Total organic matter	
	cm	dpm/g		%	mg/cm^2/yr [a]
8709	0.5	1.01	0.51	4.12	22.7
	5.5	1.01	0.51	4.63	25.5
	10.5	0.89	0.39	5.00	27.5
	15.5	0.97	0.47	5.18	28.5
	20.5	0.85	0.35	4.55	25.0
	25.5	0.64	0.14	4.75	26.1
	30.5	0.59	0.09	4.68	25.7
	35.5	0.51	0.01	4.70	25.9
D_B = 1.13 cm^2/yr		S = 0.40 cm/yr	F[b] = 0.55 g/cm^2/yr		M[c] = 16.97dpm/cm^2
8723	0.5	1.05	0.45	4.22	17.3
	5.5	1.10	0.50	4.42	18.1
	10.5	1.04	0.44	4.34	17.8
	15.5	0.84	0.24	4.54	18.6
	20.5	0.76	0.16	4.67	19.1
	25.5	0.72	0.12	4.52	18.5
	30.5	0.61	0.01	4.51	18.5
	35.5	0.60	0.00	4.74	19.4
D_B = 0.19 cm^2/yr		S = 0.30 cm/yr	F = 0.41 g/cm^2/yr [b]		M = 13.25 dpm/cm^2

a Obtained by using water content = 25%, particle density ρ_S = 2.5 g/cm^3 and the calculated accumulation rate S (this table).

b F = the annual depositional flux of sediments.

c M = the inventory of excess ^{210}Pb in sediments.

2) Mixing rates determined from ^{137}Cs

The ^{137}Cs distribution cannot be assumed to be in steady-state because its input has taken place only since the early 1950's due to nuclear weapons testing. Global fallout patterns show maxima in 1963 corresponding to the year of

maximum fallout, and for purposes of modelling, we assume the peak input time of ^{137}Cs for the study area t = 25 years.

It is noteworthy that the weapons testing fall-out may not be the sole source of ^{137}Cs in this region, and effluent from the French reprocessing plant at Cap de la Hague and minor contribution from Sellafield will add to the ^{137}Cs inventory. Therefore, two extremes of input have been applied to eq. (1) for ^{137}Cs diffusive model: a pulse input of the tracer 25 years ago and a continuous deposition at a constant rate over 25 years. Assuming sediment deposition is negligible over the period of input, D_B and ρ are constant in the mixed zone and neglecting radioactive decay, eq. (1) becomes:

$$\frac{\partial A}{\partial t} = D_B \frac{\partial^2 A}{\partial x^2} \tag{4}$$

The solution to eq. (4) for pulse input is (Crank, 1975):

$$A = A_0 \exp(-x^2/4D_B t) \tag{5}$$

where A_0 = activity of tracer at sediment-water interface (= $M/(\pi D_B t)^{1/2}$ where M = total quantity of tracer deposited).

The solution to eq. (4) for a continuous input with a constant source over 25 years is:

$$A = A_0 \exp(-x^2/4D_B t) - \frac{A_0 x}{2} (\pi/D_B t)^{1/2} \operatorname{erfc}[x/2(D_B t)^{1/2}] \tag{6}$$

where $A_0 = 2q(t/D_B\pi)^{1/2}$ and q is the input flux (M = qdt; Carslaw and Jaeger, 1959; Duursma and Hoede, 1967; Cochran, 1985), and erfc is the error function complement.

The D_B values for all the sediment cores are listed in Table 2 and the model generated profiles of ^{137}Cs compared with the measured data points are shown in Figs 6 and 7. The mixing coefficients of ^{137}Cs vary from 1.0 to 10.5 cm^2/yr with an average of 4.97±3.17 cm^2/yr (n=7) for the Outer Silver Pit and 2.32±1.79 cm^2/yr (n=9) for the German Bight (Table 2). Evidently the model generated curves from the ^{137}Cs distribution (Figs 6 and 7) do not show better fits than the ^{210}Pb to the data. The fitting of the continuous input model differs even more than that of the pulse input model (Fig. 7), indicating that the pulse input model may be closer to reality. The magnitude of the mixing coefficients obtained from the distribution of ^{210}Pb and ^{137}Cs are compatible with many other works of the coastal and shelf sediments (Guinasso and Schink, 1975; Benninger et al., 1979; Carpenter et al. 1981). The discrepancy of mixing rates between ^{210}Pb and ^{137}Cs in the study area could probably be explained by size-dependent mixing or chemical mobilization.

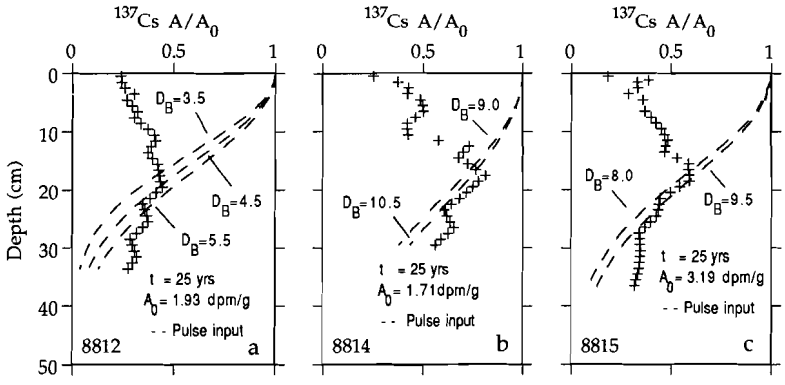

Fig. 6 *^{137}Cs activity-depth profiles (normalized to the A_0) in cores 8812, 8814 and 8815. Dashed lines show model generated curves with varied D_B values for the pulse input model. Crosses are measured data points. See text for discussion.*

Single event egestion model

In order to obtain a better understanding of the subsurface maximum of tracer activity in the sediment and obtain a better fit, we adopted the subsurface egestion model which was presented by Smith et al. (1986/1987). Their model examined two extremes: a single event model and a continuous subsurface egestion model. It was concluded that the former was closer to the character of a real subsurface egestion phenomenon for a particular surface deposit feeder (*Sipunculidae*) at their study site.

The assumptions for establishing a single-event model are:

1) the source of egested material may be sedimented material, located within a thin layer adjacent to the sediment-water interface;
2) a continuous background of constant biodiffusion in a finite layer of thickness L;
3) constant ρ in the mixed zone;
4) accumulation is negligible compared to biodiffusive transport over the period of interest (about 25 years).

At a given time, a sudden mixing event by a particular species of organism at a given locality disturbs the steady-state ^{210}Pb distribution and removes some of

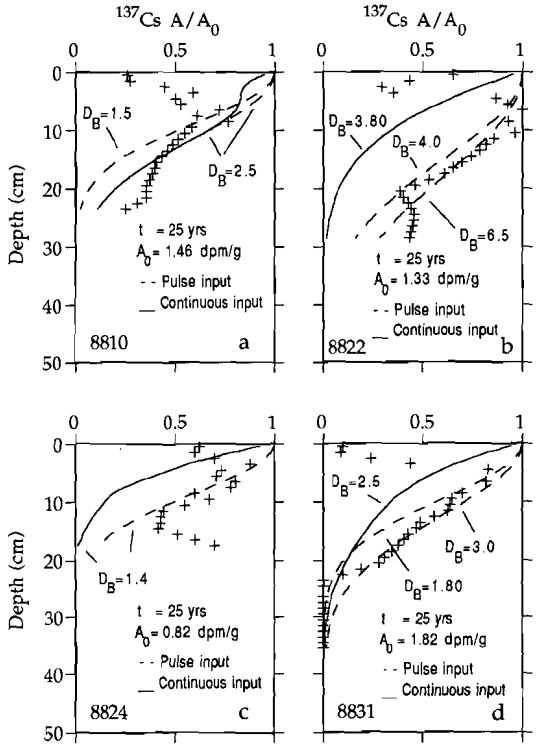

Fig. 7 *^{137}Cs activity-depth profiles (normalized to the A_0) in cores 8810, 8822, 8824 and 8831. Lines show model generated curves for the pulse input (dashed line) and the continuous input (solid line) models. Crosses are measured data points. See text for discussion.*

the tracer-bearing particles from a zone of thickness, l adjacent to the sediment-water interface, and injects it at depth. Biodiffusion and tracer delivery to the surface continue uninterrupted. The governing equation for ^{210}Pb in the mixed layer is (Smith et al., 1986/1987):

$$\frac{\partial A}{\partial t} = D_B \frac{\partial^2 A}{\partial x^2} - \lambda A \tag{7}$$

with boundary conditions:

$$-D_B \left(\frac{\partial A}{\partial x} \right)_{x=0} = f(t) \tag{8}$$

$$\left(\frac{\partial A}{\partial x} \right)_{x=L} = 0 \tag{9}$$

The equation for initial tracer distribution after the removal/egestion event is:

$$A(x,0) = A_S(x) - R(x)\, A_S(x) + E(x) \int_0^1 R(x)\, A_S(x)\, dx \tag{10}$$

where $f(t)$ = net tracer input, a constant for ^{210}Pb,

$A_s(x)$ = steady-state distribution of ^{210}Pb (before the injection event),

$R(x)$ = fraction removed from depth x within the zone $0 \le x \le 1$,

$E(x)$ = fraction of the total amount of ingested particles injected at x within the egestion zone.

To use the model $R(x)$ and $E(x)$ have the forms as following:

$$R(x) = \begin{cases} \varepsilon & 0 \le x \le 1 \\ 0 & 1 < x \end{cases} \tag{11}$$

$$E(x) = \begin{cases} (x_2 - x_1)^{-1} & x_1 \le x \le x_2 \\ 0 & x < x_1 \text{ or } x > x_2 \end{cases} \tag{12}$$

where x_1 and x_2 are the top and bottom of the egestion zone, respectively. ε is a prescribed constant.

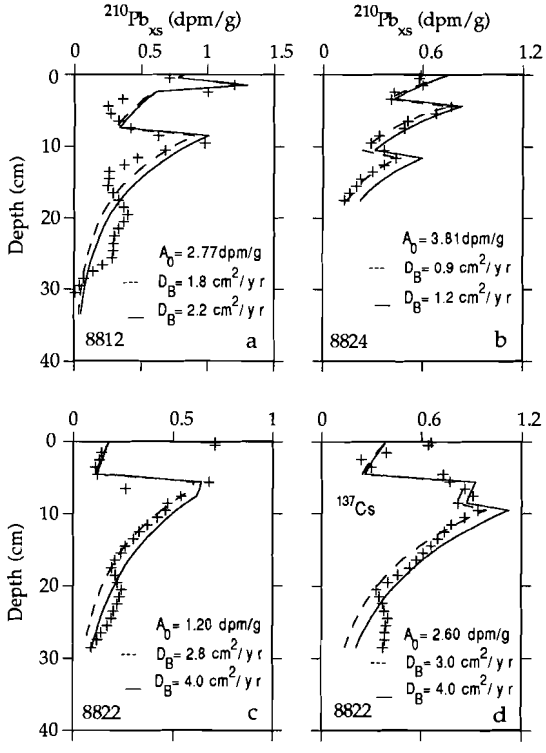

Fig. 8 *The distribution of ^{210}Pb in cores 8812 and 8824, and the ^{210}Pb and ^{137}Cs in core 8822. Solid and dashed lines are calculated best-fit curves for the subsurface egestion model. See text for discussion.*

Table 4: *Parameters of the subsurface egestion model for the southern North Sea area*[a].

Station	Tracer	A_0 dpm/g	L cm	x_1 cm	x_2 cm	D_B cm^2/yr	R(x)
8812	^{210}Pb	2.77	8	1.0	2.5	1.8, 2.5[b]	0.70
8822	^{210}Pb	1.20	7	5.0	7.0	2.8, 4.0	0.85
	^{137}Cs	2.60	9	5.0	9.0	3.0, 4.0	0.85
8824	^{210}Pb	3.81	11	4.0	5.0	0.9, 1.2	0.80 (0.55)[c]

a For model calculation, f(t) = 0.43 dpm/cm^2/yr (Zuo et al., 1992)

b Two different mixing coefficients were used in the model.

c R(x) = 0.80 for the depth of 0-5 cm; R(x) = 0.55 for the depth of 5-11 cm.

Figure 8 shows the best fit curves of the ^{210}Pb and ^{137}Cs distribution as calculated from the model and compared with the measured data points in cores 8812, 8822 and 8824. Obviously, the fitting is greatly improved and the subsurface maxima in the ^{210}Pb and ^{137}Cs profiles produced by the single event model subsurface model are in close agreement with the field data (Fig. 8). The parameters used for the model are listed in Table 4 which gives very reasonable mixing zone depths (7-11 cm) and the egestion/feeding zone depths (1-9 cm) for benthic organisms which are supported by the study of Duineveld et al. (1990). Based on their research of the macrobenthos composition and benthic ETS activity in the southern part of the North Sea, the macrobenthic fauna in the study area are controlled by the presence of four dominant benthic communities: an *Ophelia borealis* and *Echinocyamus pusillus* community in the southern Bight, a *Tellina fabula* community on the Dogger Bank proper and the northern part of the Southern Bight, an *Amphiura filiformis* community in the Oyster Ground and a different *A. filiformis* community in the deeper area of the Central North Sea, north of the Dogger Bank. In the German Bight, *Tellina fabula* and *Amphiura filiformis* were found to be the characteristic species which are surface deposit feeders and suspension feeders with a main feeding depth of 0-5 cm (Creutzberg et al., 1984). This corresponds with the depth of the observed and modelled subsurface maxima as shown in the Cores 8824 and 8822 (Fig. 7). The most abundant species of benthic organisms in the Outer Silver Pit area are the surface deposit feeders *Bathyporeia elegans* and *Spiophanes bombyx*, (living depth 0-5 cm), and a deep-burrowing specimen (*Magelona papillicornis*) with a much deeper living depth of 15 cm. Those two types of organism are possibly responsible for the two activity

peaks in the ^{210}Pb profile as found in Core 8812 (Fig. 7). Duineveld et al. (1990) also found that the Outer Silver Pit area has a higher population density (1900 individual/m^2) and a higher total biomass (15.0 g ADW/$m^{2)}$ than those in the German Bight, probably because the German Bight has relatively shallow water depth and stronger currents which limits the species density. This is also evident from both the diffusion and the subsurface egestion models, that biological mixing in the Outer Silver Pit is stronger than in the German Bight.

The D_B values derived from the single event model are in the order of 10-35% smaller than those obtained from the diffusion model. This suggests that applying the diffusion model to an area where post-depositional processes are dominated by bioadvection rather than random mixing could lead to overestimates of particle mixing rate (D_B).

7. CONCLUSIONS

The distribution of ^{210}Pb and ^{137}Cs in the sediments of the southern North Sea show the presence of strong sediment mixing. At least one subsurface maximum in ^{210}Pb profiles was found in most of the cores from the southern North Sea. Based on the eddy diffusion analogue model, particle mixing rates calculated from excess ^{210}Pb gradients range from 0.20 to 3.81 cm^2/yr, and are 1.0 to 10.5 cm^2/yr derived from ^{137}Cs distributions. The Outer Silver Pit area has higher mixing rates than those in the German Bight, probably because of the more active feeding habits of its resident benthic fauna. The deep penetration of ^{137}Cs in the study area may be linked to its release and migration as the carrier is decomposed, or may result from size-selective mixing, with ^{137}Cs associated with particles of different size as compared with ^{210}Pb.

The excess ^{210}Pb and ^{137}Cs activity profiles, generated from the single event subsurface egestion model, are in close agreement with the observed data. Thus, we believe that the subsurface maxima of excess ^{210}Pb in the sediments, to a great extent, are related to the non-diffusive biogenic mixing that may be one of the most dominant processes in sediment post-depositional systems of the southern North Sea. Other processes such as physical, chemical mixing and/or human activity, for example bottom trawling, may also be of some importance in the distribution of radionuclides in the sediments.

ACKNOWLEDGEMENTS--We are grateful to the captain and the crew of the R. V. *Aurelia* for their cooperation during the cruise and J. Kalf for his shipboard assistance of sample

collection. We thank G. W. Berger for his help with the laboratory techniques, E. Okkels, C. Fisher and R. Gieles for their assistance with the sample analyses and B. Verschuur for his help in the preparation of some of the figures. Our special acknowledgement goes to M. P. Bacon, J. K. Cochran and R. F. Anderson for their valuable and fruitful comments on this manuscript.

REFERENCES

Alexander C. R., D. J. DeMaster and C. A. Nittouer (1991) Sediment accumulation in a modern epicontinental-shelf setting: The Yellow Sea. *Marine Geol.*, **98**, 51-72.

Aller, R. C. (1984) The importance of relict burrow structures and burrow irrigation in controlling sedimentary solute distributions. *Geochim. Cosmochim. Acta*, **48**, 1928-1934.

Aller R. C. and D. J. DeMaster (1984) Estimates of particle flux and reworking at the deep-sea floor using $^{234}Th/^{238}U$ disequilibrium. *Earth Planet. Sci. Lett.*, **67**, 308-318.

Anderson R. F., S. L. Schiff and R. H. Hesslein (1987) Determining sediment accumulation and mixing rates using ^{210}Pb, ^{137}Cs and other tracers: Problems due to postdepositional mobility or coring artifacts. *Canad. J. Fish. Aquatic Sci.*, **44**, 231-250.

Anderson R.F., M.P. Bacon and P.G. Brewer (1983) Removal of ^{230}Th and ^{231}Pa from the open ocean. *Earth Planet. Sci. Lett.*, **62**, 7-23.

Appleby P. G., F. Oldfield, R. Thompson, P. Huttunen and K. Tolonen (1979) ^{210}Pb dating of annually laminated lake sediments from Finland. *Nature*, **208**, 53-55.

Behre K. J., Dörjes and G. Irion (1984) Ein datierter sedimentkern aus dem Holozän der südlichen Nord-see, Probleme der Kustenforschung im südlichen Nordseegebiet. *Verlag August Lax, Hildesheim*, **15**, 135-148.

Benninger L. K., R. C. Aller, J. K. Cochran and K. K. Turekian (1979) Effects of biological sediment mixing on the ^{210}Pb chronology and trace metal distribution in a Long Island Sound sediment core. *Earth Planet. Sci. Lett.*, **43**, 241-259.

Boudreau B. P. (1986) Mathematics of tracer mixing in sediments: I Spatially dependent, diffusive mixing. *Amer. J. Sci.*, **286**, 161-198.

Carpenter R. and T. M. Beasley (1981) Plutonium and americium in anoxic marine sediments: Evidence against remobilization. *Geochim. Cosmochim. Acta*, **45**, 1917-1930.

Carpenter R., J.T. Bennett and M.L. Peterson. (1981) ^{210}Pb activities in and fluxes to sediments of the Washington continental slope and shelf, *Geochim. Cosmochim. Acta*, **45**, 1155-1172.

Carslaw H. and J. C. Jaeger (1959) Conduction of heat in solids. Clarendon Press. Oxford.

Cochran J.K. (1985) Particle mixing rates in sediments of the eastern equatorial Pacific: Evidence from ^{210}Pb, $^{239+240}$Pu and ^{137}Cs distributions at MANOP sites. *Geochim. Cosmochim. Acta*, **49**, 1195-1210.

Crank J. (1975) The mathematics of diffusion. 2nd ed., Oxford Univ. Press, 414pp.

Creutzberg F. (1985) A persistent chlorophyll a maximum coinciding with an enriched benthic zone. In: P. E. Gibbs. Proceedings of the 19th European Marine Biology Symposium. Cambridge University Press: 97-108.

Creutzberg F., P. Wapenaar, G. Duineveld and N. L. Lopez (1984) Distribution and density of the benthic fauna in the southern North Sea in relation to bottom characteristics and hydrographic conditions. *Rapp. P.-v. Réun. Cons. int. Explor. Mer*, **183**, 101-110.

Crusius J. and R.F. Anderson (1990) ^{137}Cs mobility inferred from ^{210}Pb and $^{239+240}$ Pu analyses of laminated lake sediments. *EOS*, **71**, 72.

Crusius J. and R.F. Anderson (1991) Immobility of ^{210}Pb in Black Sea sediments. *Geochim. Cosmochim. Acta*, **55**, 327-333.

Davis M. B., C. T. Hess, S. A. Norton, D. W. Hanson, K. D. Hoagland and D. S. Anderson (1984) ^{137}Cs and ^{210}Pb dating of sediments from soft-water lakes in New England (U.S.A.) and Scandinavia, a failure of ^{137}Cs dating. *Chem. Geol.*, **44**, 151-185.

DeMaster D.J. and J.K. Cochran (1982) Particle mixing rates in deep-sea sediments determined from excess ^{210}Pb and ^{32}Si profiles. *Earth Planet. Sci. Lett.*, **61**, 257-261.

Dominik J., U. Förstner, A. Mangini and H.-E. Reineck (1978) ^{210}Pb and ^{137}Cs chronology of heavy metal pollution in a sediment core from the German Bight (North Sea). *Senckenbergiana Marit.*, **10** , 213-227.

Druffel E. R. M., P. M. Williams, H. D. Livingston and M. Koide (1984) Variability of natural and bomb-produced radionuclide distributions in abyssal red clay sediments. *Earth Planet. Sci. Lett.*, **71**, 205-214.

Duineveld G. C. A., P. A. W. J. De Wilde and A. Kok (1990) A synopsis of the macrobenthic assemblages and benthic ETS activity in the Dutch sector of the North Sea. Neth. *J. Sea Res.*, **26**, 125-138.

Duursma E. K. and C. Hoede (1967) Theoretical, experimental and field studies concerning molecular diffusion of radioisotopes in sediments and suspended solid particles of the sea. Part A: Theories and mathematical calculation. *Neth. J. Sea Res.*, **3**, 423-457.

Eisma D. (1981) Supply and deposition of suspended matter in the North Sea. *Spec. Publs int. Ass. Sediment.*, **5**, 415-428.

Eisma D. (1987) The North Sea: an overview. *Phil. Trans. R. Soc. Lond*, **B 316**, 461-485.

Eisma D. and J. Kalf (1987) Dispersal, concentration and deposition of suspended matter in the North Sea. *J. Geol. Society*, **144**, 161-178.

Gardner L. R., P. Sharma and W. S. Moore (1987) A regeneration model for the effect of bioturbation by fiddler crabs on ^{210}Pb profiles in salt marsh sediments. *J. Environ. Radioactivity*, **5**, 25-36.

Gerino M. (1990) The effects of bioturbation on particle redistribution in Mediterranean coastal sediment. Preliminary results. *Hydrobiologia*, **207**, 251-258.

Gobeil C. and N. Silverberg (1989) Early diagenesis of lead in Laurentian Trough sediments. *Geochim. Cosmochim. Acta*, **53**, 1889-1895.

Goldberg E.D. and M. Koide (1962) Geochronological studies of deep-sea sediments by the Ionium/Thorium method. *Geochim. Cosmochim. Acta*, **26**, 417-450.

Guinasso N. L., Jr. and D. R. Schink (1975) Quantitative estimates of biological mixing rates in abyssal sediments. *J. Geophys. Res.*, **80**, 3032-3043.

Koide M., K. W. Bruland and E. D. Goldberg (1973) Th-228/Th-232 and Pb-210 geochronologies in marine and lake sediments. *Geochim. Cosmochim. Acta*, **37**, 1171-1187.

McCave I. N. (1971) Wave effectiveness at the sea bed and its relationship to bedforms and deposition of mud. *J. Sedim. Petrol.*, **41**, 89-96.

Nozaki Y., J. K. Cochran, K. K. Turikian and G. Keller (1977) Radiocarbon and ^{210}Pb distribution in submersible-taken deep-sea cores from project FAMOUS. *Earth Planet. Sci. Lett.*, **34**, 167-173.

Rice D. L. (1986) Early diagenesis in bioadvective sediments: relationships between the diagenesis of Beryllium-7, sediment reworking rates, and the abundance of conveyor-belt deposit-feeders. *J. Marine Res.*, **44**, 149-184.

Rhoads D. C. (1974) Organism-sediment relations on the muddy sea floor. *Oceanogr. mar. Biol. Ann. Rev.*, **12**, 263-300.

Robbins J. A., P. L. McCall, J. B. Fisher and J. R. Krezoski (1979) Effect of deposit feeders on migration of ^{137}Cs in lake sediments. *Earth Planet. Sci. Lett.*, **42**, 277-287.

Santschi, P. H., Y.-H. Li, D. M. Adler, M. Amdurer, J. Bell and U. P. Nyffeler (1983) The relative mobility of natural (Th, Pb and Po) and fallout (Pu, Am, Cs) radionuclides in the coastal marine environment: results from model ecosystems (MERL) and Narragansett Bay. *Geochim. Cosmochim. Acta*, **47**, 201-210.

Shimmield G.B., J. W. Murray, J. Thomson, M. P. Bacon, R. F. Anderson and N. B. Price (1986) The distribution and behaviour of ^{230}Th and ^{231}Pa at an ocean margin, Baja California, Mexico. *Geochim. Cosmochim. Acta*, **50**, 2499-2507.

Smith J.N., B.P. Boudreau and V. Noshkin (1986/1987) Plutonium and ^{210}Pb distributions in northeast Atlantic sediments: subsurface anomalies caused by non-local mixing. *Earth Planet. Sci. Lett.*, **81**, 15-28.

Stordal M.C., J.W. Johnson, N.L. Guinasso and D.R. Schink (1985) Quantitative evaluation of bioturbation rates in deep ocean sediments. II. Comparison of rates determined by ^{210}Pb and $^{239,240}Pu$. *Marine Chem.*, **17**, 99-114.

Thomson J., S. Colley and P.P.E. Weaver (1988) Bioturbation into a recently emplaced deep-sea turbidite surface as revealed by ^{210}Pb excess, ^{230}Th excess and planktonic foraminifera distributions. *Earth Planet. Sci. Lett.*, **90**, 157-173.

Zuo Z., D. Eisma and G. W. Berger (1989) Recent sediment deposition rates in the Oyster Ground, North Sea. *Neth. J. Sea Res.*, **23**, 263-269.

Zuo Z., D. Eisma and G. W. Berger (1991) Determination of sediment accumulation and mixing rates in the Gulf of Lions, Mediterranean Sea. *Oceanol. Acta*, **14**, 253-262.

Zuo Z. and D. Eisma (1992) ^{210}Pb and ^{210}Po distributions and disequilibrium in the coastal and shelf waters of the southern North Sea. *Cont. Shelf Res.*, **12**, in press.

Appendix A: Concentrations of ^{137}Cs and ^{210}Pb in sediments from the southern North Sea. All activities are in dpm/g dry weight*.

Depth (cm)	Water Content	Porosity[a] Φ	Dry Bulk Density ρ[b]	^{137}Cs	^{210}Pb	$^{210}Pb_{xs}$[c]
Outer Silver Pit						
Core 8810: 54°00.14'N, 2°09.25'E; 80m, collected 4/25/88						
0-1	n.m.[d]	-	-	0.38±0.07	0.89±0.12	-0.18±0.02
1-2	n.m.	-	-	0.40±0.07	0.94±0.12	-0.13±0.02
2-3	n.m.	-	-	0.65±0.10	0.82±0.12	-0.25±0.04
3-4	n.m.	-	-	0.86±0.12	1.16±0.12	0.09±0.01
4-5	n.m.	-	-	0.73±0.08	1.19±0.14	0.12±0.01
5-6	n.m.	-	-	0.77±0.10	1.20±0.14	0.16±0.02
6-7	n.m.	-	-	1.05±0.12	1.39±0.16	0.32±0.04
7-8	n.m.	-	-	0.89±0.09	1.38±0.17	0.31±0.04
8-9	n.m.	-	-	1.12±0.12	1.34±0.16	0.27±0.03
9-10	n.m.	-	-	0.85±0.13	1.25±0.17	0.18±0.02
11-12	n.m.	-	-	0.75±0.10	1.21±0.15	0.14±0.02
13-14	n.m.	-	-	0.67±0.09	1.15±0.14	0.08±0.01
15-16	n.m.	-	-	0.57±0.08	1.30±0.15	0.23±0.03
17-18	n.m.	-	-	0.56±0.12	1.14±0.14	0.07±0.01
19-20	n.m.	-	-	0.52±0.09	0.95±0.10	-0.12±0.01
21-22	n.m.	-	-	0.52±0.06	0.95±0.09	-0.12±0.01
23-24	n.m.	-	-	0.37±0.05	0.99±0.10	-0.08±0.09
Inventory (dpm/cm^2)[e]				20.39±3.06[f]		2.78±0.42[f]
Core 8811: 54°04.18'N, 2°11.39'E; 82m, collected 4/25/88						
0-1	0.25	0.46	1.35	0.63±0.12	2.12±0.16	1.00±0.08
1-2	0.25	0.45	1.38	0.81±0.18	2.25±0.17	1.20±0.09
2-3	0.26	0.47	1.33	1.01±0.14	2.10±0.15	1.00±0.07
3-4	0.23	0.43	1.43	0.65±0.12	1.93±0.13	0.86±0.06
4-5	0.21	0.39	1.52	n.d.[g]	1.25±0.10	0.18±0.01
5-6	0.21	0.40	1.49	0.70±0.12	1.77±0.20	0.70±0.08
6-7	0.24	0.44	1.40	0.91±0.12	2.13±0.23	1.10±0.10
7-8	0.22	0.41	1.47	1.12±0.11	2.02±0.23	0.95±0.10
8-9	0.21	0.40	1.50	1.09±0.10	1.55±0.18	0.48±0.06
9-10	0.21	0.40	1.49	1.07±0.10	1.81±0.20	0.74±0.08
10-11	0.21	0.40	1.50	1.03±0.11	1.64±0.17	0.57±0.06
11-12	0.21	0.40	1.50	1.00±0.11	1.48±0.15	0.41±0.04
12-13	0.22	0.41	1.47	1.22±0.12	1.36±0.16	0.29±0.03
14-15	0.22	0.41	1.47	1.12±0.14	1.24±0.17	0.17±0.02
16-17	0.23	0.42	1.45	1.13±0.14	1.45±0.16	0.38±0.04
18-19	0.23	0.43	1.42	1.34±0.13	1.65±0.15	0.58±0.05
20-21	0.24	0.44	1.40	1.08±0.10	1.87±0.18	0.80±0.08
23-24	0.23	0.43	1.42	1.12±0.14	1.79±0.18	0.72±0.07
26-27	0.25	0.45	1.37	n.d.	1.68±0.16	0.61±0.06
29-30	0.23	0.43	1.43	n.d.	1.73±0.18	0.66±0.07
32-33	0.26	0.47	1.32	n.d.	1.39±0.13	0.32±0.03
35-36	0.23	0.42	1.44	n.d.	1.69±0.14	0.62±0.05
Inventory (dpm/cm^2)				35.70±5.36		>40.34±6.05

Appendix A: (continued)

Depth (cm)	Water Content	Porosity Φ	Dry Bulk Density ρ	^{137}Cs	^{210}Pb	$^{210}Pb_{xs}$
Core 8812: 54°04.77'N, 2°19.91'E; 71m, collected 4/25/88						
0-1	0.24	0.44	1.40	n.m.	1.78±0.16	0.71±0.06
1-2	0.23	0.43	1.42	0.47±0.04	2.31±0.21	1.20±0.10
2-3	0.23	0.42	1.44	0.50±0.05	2.07±0.19	1.00±0.09
3-4	0.20	0.38	1.54	0.59±0.03	1.43±0.13	0.36±0.03
4-5	0.18	0.36	1.61	0.52±0.04	1.32±0.13	0.25±0.02
5-6	0.18	0.36	1.61	0.57±0.05	1.34±0.13	0.27±0.03
6-7	0.18	0.36	1.60	0.62±0.05	1.40±0.13	0.33±0.03
7-8	0.19	0.36	1.59	0.59±0.05	1.49±0.13	0.42±0.04
8-9	0.18	0.36	1.60	0.65±0.04	1.70±0.16	0.63±0.06
9-10	0.19	0.37	1.57	0.72±0.04	2.05±0.20	0.98±0.10
10-11	0.19	0.37	1.57	0.78±0.04	1.75±0.18	0.68±0.07
11-12	0.19	0.37	1.58	0.79±0.05	1.54±0.15	0.47±0.05
13-14	0.19	0.37	1.58	0.72±0.05	1.33±0.13	0.26±0.03
15-16	0.19	0.37	1.59	0.81±0.05	1.32±0.13	0.25±0.02
17-18	0.19	0.37	1.57	0.83±0.04	1.40±0.13	0.33±0.03
19-20	0.20	0.38	1.55	0.86±0.05	1.47±0.14	0.40±0.04
22-23	0.20	0.38	1.55	0.67±0.05	1.37±0.12	0.30±0.03
25-26	0.20	0.38	1.54	0.72±0.05	1.35±0.11	0.28±0.02
28-29	0.19	0.36	1.59	0.55±0.04	1.14±0.10	0.07±0.01
31-32	0.18	0.36	1.61	0.61±0.06	1.05±0.09	-0.02±0.002
33-34	0.19	0.37	1.57	0.53±0.05	1.04±0.10	-0.03±0.003
Inventory (dpm/cm^2)				32.07±4.81		18.65±2.80
Core 8813: 54°07.97'N, 2°26.97'E; 65m, collected 4/25/88						
0-1	0.20	0.39	1.52	0.49±0.06	1.31±0.11	0.24±0.02
1-2	0.25	0.45	1.36	0.78±0.08	2.37±0.15	1.30±0.08
2-3	0.21	0.39	1.51	0.56±0.06	1.36±0.11	0.29±0.02
3-4	0.21	0.40	1.49	0.42±0.05	1.47±0.12	0.40±0.03
4-5	0.20	0.38	1.55	0.45±0.06	1.49±0.15	0.42±0.04
5-6	0.20	0.38	1.55	0.56±0.03	1.29±0.13	0.22±0.02
6-7	0.20	0.38	1.55	0.75±0.06	1.27±0.11	0.20±0.02
7-8	0.19	0.37	1.57	0.63±0.05	2.31±0.16	1.20±0.09
8-9	0.19	0.37	1.57	0.78±0.05	1.49±0.11	0.42±0.03
9-10	0.19	0.37	1.57	0.70±0.06	1.27±0.10	0.20±0.02
11-12	0.19	0.37	1.57	0.68±0.05	1.44±0.12	0.37±0.03
14-15	0.20	0.38	1.54	0.75±0.05	1.21±0.11	0.14±0.01
17-18	0.20	0.38	1.56	1.01±0.07	1.34±0.12	0.27±0.02
20-21	0.21	0.39	1.51	0.87±0.08	1.33±0.12	0.26±0.02
23-24	0.19	0.37	1.57	0.75±0.06	1.13±0.09	0.06±0.01
26-27	0.19	0.37	1.58	0.66±0.06	1.10±0.09	0.03±0.002
29-30	0.19	0.38	1.56	0.77±0.06	1.15±0.09	0.08±0.01
Inventory (dpm/cm^2)				30.28±4.54		12.70±1.91
Core 8814: 54°07.23'N, 2°34.88'E; 65m, collected 4/25/88						
0-1	0.21	0.40	1.51	0.28±0.07	1.22±0.10	0.15±0.01
1-2	0.21	0.39	1.52	0.42±0.05	1.39±0.10	0.32±0.02
2-3	0.21	0.40	1.50	0.49±0.05	1.49±0.11	0.42±0.03
3-4	0.18	0.35	1.61	0.45±0.05	1.26±0.09	0.19±0.01

Appendix A: (continued)

Depth (cm)	Water Content	Porosity Φ	Dry Bulk Density ρ	^{137}Cs	^{210}Pb	$^{210}Pb_{xs}$
4-5	0.18	0.35	1.63	0.51±0.06	1.28±0.13	0.21±0.02
6-7	0.18	0.36	1.60	0.54±0.05	1.32±0.13	0.25±0.02
8-9	0.18	0.36	1.61	0.45±0.04	1.25±0.13	0.18±0.02
10-11	0.18	0.35	1.63	0.45±0.05	0.95±0.10	-0.12±0.01
12-13	0.19	0.37	1.58	0.79±0.03	1.65±0.16	0.58±0.06
14-15	0.18	0.36	1.61	0.72±0.04	1.44±0.12	0.37±0.03
17-18	0.19	0.37	1.59	0.87±0.06	1.27±0.11	0.20±0.02
20-21	0.19	0.37	1.59	0.77±0.06	1.31±0.11	0.24±0.02
23-24	0.18	0.36	1.61	0.64±0.04	1.18±0.11	0.11±0.01
26-27	0.18	0.36	1.60	0.70±0.04	1.24±0.12	0.17±0.02
29-30	0.19	0.37	1.59	0.61±0.05	1.21±0.11	0.14±0.01
Inventory (dpm/cm^2)				26.98±4.05		10.38±1.56
Core 8815: 54°04.51'N, 2°28.26'E; 71m, collected 4/25/88						
0-1	0.22	0.42	1.45	0.40±0.05	1.94±0.18	0.87±0.08
1-2	0.26	0.46	1.34	0.79±0.07	1.94±0.15	0.87±0.07
2-3	0.21	0.40	1.50	0.71±0.05	1.82±0.15	0.75±0.06
3-4	0.21	0.40	1.51	0.61±0.04	1.99±0.16	0.92±0.07
4-5	0.21	0.40	1.51	0.76±0.05	1.66±0.16	0.59±0.06
5-6	0.21	0.40	1.50	0.83±0.05	n.m.	-
6-7	0.21	0.40	1.51	0.78±0.05	2.10±0.21	1.00±0.10
7-8	0.21	0.40	1.49	0.86±0.06	1.86±0.19	0.79±0.08
8-9	0.21	0.40	1.49	0.91±0.06	1.57±0.17	0.50±0.05
9-10	0.22	0.41	1.47	0.98±0.06	1.81±0.20	0.74±0.08
11-12	0.22	0.41	1.48	1.04±0.06	1.81±0.15	0.74±0.06
13-14	0.21	0.41	1.49	1.00±0.06	1.68±0.14	0.61±0.05
15-16	0.24	0.44	1.39	1.35±0.08	1.79±0.12	0.72±0.05
18-19	0.24	0.45	1.39	1.36±0.07	2.06±0.13	0.99±0.06
21-22	0.22	0.42	1.45	0.99±0.07	1.64±0.12	0.57±0.04
24-25	0.21	0.40	1.49	0.91±0.06	1.39±0.10	0.32±0.02
27-28	0.21	0.40	1.49	0.73±0.07	1.57±0.11	0.50±0.04
30-31	0.23	0.42	1.45	0.77±0.07	1.66±0.11	0.59±0.04
33-34	0.23	0.42	1.45	0.75±0.05	1.39±0.09	0.32±0.02
36-37	0.20	0.39	1.52	0.66±0.06	1.42±0.10	0.35±0.02
Inventory (dpm/cm^2)				44.50±6.68		31.19±4.68
Core 8816: 54°02.05'N, 2°27.68'E; 70m, collected 4/25/88						
0-1	0.19	0.37	1.59	0.30±0.03	1.04±0.09	-0.03±0.003
1-2	0.19	0.36	1.59	0.29±0.04	0.84±0.07	-0.23±0.02
2-3	0.20	0.39	1.52	0.32±0.04	0.97±0.08	-0.10±0.01
3-4	0.19	0.37	1.56	0.37±0.04	0.96±0.08	-0.11±0.01
4-5	0.19	0.37	1.57	0.30±0.04	1.04±0.09	-0.03±0.003
6-7	0.19	0.37	1.56	0.36±0.04	1.00±0.08	-0.07±0.01
7-8	0.19	0.37	1.56	0.41±0.05	1.06±0.08	-0.01±0.001
9-10	0.20	0.39	1.54	0.49±0.05	1.09±0.08	0.02±0.001
11-12	0.19	0.38	1.56	0.53±0.05	1.06±0.12	-0.01±0.001
14-15	0.21	0.40	1.49	0.72±0.05	1.21±0.11	0.14±0.01
17-18	0.19	0.37	1.57	0.70±0.05	1.30±0.13	0.23±0.02

Appendix A: (continued)

Depth (cm)	Water Content	Porosity Φ	Dry Bulk Density ρ	^{137}Cs	^{210}Pb	$^{210}Pb_{xs}$
20-21	0.20	0.39	1.53	0.77±0.06	1.06±0.11	-0.01±0.001
23-24	0.21	0.40	1.50	0.83±0.06	1.18±0.12	0.11±0.01
26-27	0.20	0.39	1.53	0.82±0.07	1.60±0.13	0.53±0.04
29-30	0.20	0.38	1.55	0.78±0.04	1.50±0.12	0.43±0.03
32-33	0.18	0.36	1.61	0.52±0.07	1.10±0.12	0.03±0.003
35-36	0.22	0.42	1.45	0.54±0.06	1.68±0.15	0.61±0.05
Inventory (dpm/cm^2)				30.15±4.52		6.69±1.00
Markhams Hole						
Core 8817: 53°50.78'N, 2°34.19'E; 71m, collected 4/25/88						
0-1	0.26	0.47	1.31	0.82±0.07	2.72±0.26	1.60±0.20
1-2	0.27	0.47	1.31	0.81±0.06	1.93±0.19	0.86±0.08
2-3	0.25	0.45	1.37	0.83±0.07	1.59±0.29	0.52±0.09
3-4	0.24	0.45	1.38	1.11±0.06	2.08±0.16	1.00±0.08
4-5	0.25	0.45	1.39	0.96±0.10	2.09±0.16	1.00±0.08
5-6	0.24	0.44	1.39	0.98±0.06	2.27±0.18	1.20±0.10
6-7	0.23	0.43	1.43	1.07±0.06	1.97±0.16	0.90±0.07
7-8	0.24	0.44	1.39	1.11±0.07	1.94±0.20	0.87±0.09
8-9	0.24	0.44	1.39	1.08±0.06	2.10±0.18	1.00±0.09
9-10	0.25	0.45	1.37	1.20±0.08	2.21±0.19	1.10±0.10
11-12	0.25	0.46	1.35	1.36±0.07	2.43±0.16	1.40±0.09
14-15	0.26	0.47	1.31	1.48±0.07	2.25±0.17	1.20±0.09
17-18	0.23	0.42	1.44	1.45±0.05	1.71±0.13	0.64±0.05
20-21	0.24	0.44	1.41	1.52±0.07	1.87±0.18	0.80±0.08
23-24	0.23	0.42	1.44	1.56±0.07	1.84±0.18	0.77±0.08
26-27	0.21	0.40	1.49	1.26±0.07	1.38±0.14	0.31±0.03
30-31	0.22	0.42	1.45	1.27±0.07	1.54±0.16	0.47±0.05
34-35	0.23	0.43	1.42	1.17±0.07	1.91±0.23	0.84±0.10
Inventory (dpm/cm^2)				57.35±8.60		38.56±5.78
Botney Ground						
Core 8818: 53°39.09'N, 2°52.13'E; 40m, collected 4/25/88						
0-1	0.16	0.32	1.69	0.19±0.06	0.80±0.09	-0.27±0.03
1-2	0.17	0.33	1.67	n.d.	0.90±0.11	-0.17±0.02
2-3	0.17	0.34	1.65	0.30±0.05	0.81±0.10	-0.26±0.03
3-4	0.18	0.35	1.63	0.24±0.06	0.86±0.11	-0.21±0.03
4-5	0.18	0.36	1.61	0.35±0.05	1.05±0.13	-0.02±0.002
5-6	0.18	0.35	1.63	0.36±0.04	1.24±0.14	0.17±0.02
6-7	0.17	0.34	1.65	0.29±0.06	0.83±0.11	-0.24±0.03
7-8	0.18	0.35	1.61	0.33±0.04	n.m.	-
8-9	0.18	0.36	1.61	0.41±0.05	1.21±0.13	0.14±0.02
9-10	0.18	0.36	1.61	0.49±0.06	0.84±0.10	-0.23±0.03
11-12	0.18	0.36	1.61	0.44±0.06	1.20±0.13	0.13±0.01
14-15	0.18	0.36	1.60	0.62±0.07	1.09±0.09	0.02±0.002
17-18	0.19	0.38	1.56	0.78±0.07	1.07±0.10	0.00
20-21	0.19	0.37	1.57	0.70±0.08	0.93±0.08	-0.14±0.01
Inventory (dpm/cm^2)				14.74±2.21		1.02±0.15

Appendix A: (continued)

Depth (cm)	Water Content	Porosity Φ	Dry Bulk Density ρ	^{137}Cs	^{210}Pb	$^{210}Pb_{xs}$
Core 8819: 53°38.87'N, 3°05.06'E; 40m, collected 4/25/88						
0-1	0.16	0.33	1.66	0.30±0.04	0.95±0.06	-0.12±0.01
1-2	0.16	0.33	1.67	0.45±0.05	1.07±0.08	0.00
2-3	0.18	0.35	1.64	0.40±0.06	1.19±0.09	0.12±0.01
3-4	0.18	0.36	1.60	0.68±0.07	1.26±0.09	0.19±0.01
4-5	0.18	0.35	1.62	0.60±0.06	1.23±0.07	0.16±0.01
5-6	0.18	0.35	1.62	0.62±0.06	1.04±0.07	-0.03±0.002
6-7	0.18	0.35	1.63	0.57±0.05	1.10±0.07	0.03±0.002
7-8	0.18	0.35	1.63	0.56±0.06	0.98±0.10	-0.09±0.01
8-9	0.18	0.35	1.63	0.65±0.05	1.02±0.11	-0.05±0.005
9-10	0.17	0.35	1.64	0.56±0.06	0.87±0.09	-0.20±0.02
11-12	0.18	0.35	1.63	0.63±0.06	1.04±0.11	-0.03±0.003
14-15	0.19	0.36	1.59	0.67±0.07	1.01±0.09	-0.06±0.005
17-18	0.18	0.36	1.60	0.76±0.08	0.86±0.08	-0.21±0.02
20-21	0.19	0.37	1.59	0.83±0.07	1.06±0.10	-0.01±0.001
24-25	0.19	0.36	1.59	0.80±0.07	0.92±0.09	-0.15±0.01
28-29	0.18	0.35	1.62	0.71±0.04	0.80±0.09	-0.27±0.03
Inventory (dpm/cm^2)				28.89±4.43		0.56±0.68
Western Mud Hole						
Core 8820: 53°37.94'N, 3°20.34'E; 41m, collected 4/25/88						
0-1	0.18	0.36	1.60	0.39±0.06	1.04±0.09	-0.03±0.003
1-2	0.18	0.36	1.61	0.38±0.005	1.16±0.11	0.09±0.01
2-3	0.18	0.35	1.63	0.44±0.08	1.10±0.10	0.03±0.003
3-4	0.19	0.37	1.59	0.68±0.06	1.36±0.09	0.29±0.02
4-5	0.19	0.37	1.58	0.68±0.07	1.33±0.12	0.26±0.02
5-6	0.19	0.37	1.57	0.73±0.05	1.26±0.09	0.19±0.01
6-7	0.19	0.37	1.57	0.84±0.06	1.30±0.09	0.23±0.02
7-8	0.19	0.37	1.57	0.91±0.07	1.26±0.09	0.19±0.01
8-9	0.19	0.36	1.59	0.82±0.06	1.17±0.09	0.10±0.01
9-10	0.18	0.36	1.61	0.66±0.06	1.21±0.09	0.14±0.01
11-12	0.18	0.36	1.60	0.77±0.06	1.23±0.10	0.16±0.01
14-15	0.20	0.38	1.54	0.86±0.07	1.25±0.10	0.18±0.01
17-18	0.20	0.38	1.55	0.77±0.06	1.22±0.11	0.15±0.01
20-21	0.20	0.38	1.55	0.89±0.06	1.07±0.09	0.00
24-25	0.21	0.40	1.50	1.00±0.07	1.24±0.10	0.17±0.01
28-29	0.20	0.39	1.52	0.92±0.06	1.24±0.10	0.17±0.01
Inventory (dpm/cm^2)				32.99±4.95		5.80±0.87
New Zealand Ground						
Core 8821: 53°36.08'N, 3°53.32'E; 39m, collected 4/25/88						
0-1	0.19	0.37	1.58	0.27±0.07	1.59±0.14	0.52±0.05
1-2	0.20	0.39	1.53	0.62±0.06	1.38±0.13	0.31±0.03
2-3	0.20	0.38	1.54	0.75±0.06	1.64±0.15	0.57±0.05
3-4	0.20	0.39	1.52	0.92±0.09	1.56±0.15	0.49±0.05
4-5	0.20	0.39	1.52	0.98±0.08	1.46±0.11	0.39±0.03
5-6	0.21	0.40	1.49	1.06±0.08	1.58±0.11	0.51±0.04
6-7	0.22	0.42	1.45	1.18±0.08	1.60±0.12	0.53±0.04

Appendix A: (continued)

Depth (cm)	Water Content	Porosity Φ	Dry Bulk Density ρ	^{137}Cs	^{210}Pb	$^{210}Pb_{xs}$
7-8	0.21	0.39	1.51	0.93±0.07	1.36±0.11	0.29±0.02
8-9	0.20	0.39	1.52	0.94±0.08	1.34±0.11	0.27±0.02
9-10	0.20	0.39	1.53	1.00±0.08	1.33±0.10	0.26±0.02
11-12	0.20	0.38	1.55	1.05±0.08	1.23±0.11	0.16±0.01
14-15	0.20	0.38	1.54	1.10±0.08	1.42±0.10	0.35±0.02
17-18	0.20	0.38	1.55	0.96±0.07	1.34±0.10	0.27±0.02
20-21	0.21	0.40	1.51	1.30±0.08	1.26±0.10	0.19±0.02
24-25	0.20	0.38	1.54	1.14±0.08	0.99±0.09	-0.08±0.01
28-29	0.20	0.38	1.55	0.89±0.07	1.25±0.12	0.18±0.02
32-33	0.19	0.36	1.59	0.81±0.06	1.20±0.10	0.13±0.01
Inventory (dpm/cm^2)				44.78±6.72		10.82±1.62
German Bight						
Core 8822: 55°01.89'N, 6°18.18'E; 46m, collected 4/26/88						
0-1	0.25	0.46	1.36	0.64±0.07	1.54±0.13	0.71±0.06
1-2	0.21	0.40	1.50	0.39±0.04	0.97±0.09	0.14±0.01
2-3	0.18	0.36	1.60	0.24±0.01	0.79±0.08	-0.04±0.004
3-4	0.18	0.35	1.61	0.30±0.03	0.76±0.07	-0.07±0.006
4-5	0.19	0.37	1.58	0.73±0.07	0.95±0.09	0.12±0.01
5-6	0.19	0.36	1.59	0.77±0.06	1.51±0.13	0.68±0.06
6-7	0.20	0.38	1.55	0.86±0.04	1.09±0.10	0.26±0.02
7-8	0.20	0.39	1.53	0.91±0.06	1.37±0.11	0.54±0.04
8-9	0.20	0.39	1.52	0.82±0.06	1.30±0.10	0.47±0.04
9-10	0.21	0.39	1.52	0.94±0.06	1.29±0.10	0.46±0.04
11-12	0.22	0.42	1.46	0.78±0.07	1.20±0.09	0.37±0.03
14-15	0.21	0.40	1.51	0.66±0.06	1.09±0.11	0.26±0.03
17-18	0.20	0.39	1.53	0.53±0.08	1.02±0.10	0.19±0.02
20-21	0.19	0.37	1.57	0.33±0.05	1.07±0.11	0.24±0.02
24-25	0.20	0.38	1.54	0.40±0.05	1.02±0.10	0.19±0.02
28-29	0.19	0.37	1.57	0.37±0.04	0.92±0.09	0.09±0.01
Inventory (dpm/cm^2)				23.02±4.60		10.97±2.19
Core 8823: 54°52.50'N, 6°29.07'E; 43m, collected 4/26/88						
0-1	0.19	0.37	1.57	n.d.	1.13±0.09	0.30±0.02
1-2	0.19	0.37	1.57	0.37±0.06	0.69±0.06	-0.14±0.01
2-3	0.20	0.38	1.55	0.32±0.06	0.92±0.07	0.09±0.01
3-4	0.19	0.36	1.59	n.d.	0.90±0.07	0.07±0.05
4-5	0.17	0.34	1.65	n.d.	0.78±0.06	-0.05±0.004
5-6	0.17	0.35	1.64	0.24±0.04	0.72±0.06	-0.11±0.01
6-7	0.19	0.37	1.57	0.30±0.05	1.02±0.07	0.19±0.01
7-8	0.19	0.37	1.58	0.57±0.06	1.30±0.08	0.47±0.03
8-9	0.19	0.36	1.59	0.66±0.05	1.23±0.08	0.40±0.03
9-10	0.19	0.36	1.59	0.65±0.05	1.25±0.11	0.42±0.04
11-12	0.19	0.37	1.58	0.62±0.06	1.16±0.10	0.33±0.03
14-15	0.21	0.41	1.48	1.03±0.07	1.45±0.13	0.62±0.06
17-18	0.20	0.39	1.53	0.79±0.08	1.38±0.11	0.55±0.04
20-21	0.20	0.39	1.53	0.52±0.08	1.20±0.09	0.37±0.03
Inventory (dpm/cm^2)				15.96±3.19		10.08±2.02

Appendix A: (continued)

Depth (cm)	Water Content	Porosity Φ	Dry Bulk Density ρ	^{137}Cs	^{210}Pb	$^{210}Pb_{xs}$
Core 8824: 54°41.17'N, 6°43.29'E; 41m, collected 4/26/88						
0-1	0.20	0.38	1.54	0.33±0.06	1.41±0.10	0.58±0.04
1-2	0.20	0.38	1.54	0.32±0.03	1.43±0.11	0.60±0.05
2-3	0.20	0.38	1.55	0.37±0.07	1.26±0.10	0.43±0.03
3-4	0.20	0.38	1.54	0.47±0.05	1.24±0.10	0.41±0.03
4-5	0.20	0.38	1.54	0.39±0.03	1.60±0.14	0.77±0.07
5-6	0.20	0.38	1.55	0.37±0.03	1.51±0.13	0.68±0.06
6-7	0.20	0.39	1.53	0.43±0.05	1.34±0.11	0.51±0.04
7-8	0.21	0.40	1.51	0.43±0.04	1.32±0.10	0.49±0.04
8-9	0.20	0.39	1.52	0.32±0.04	1.17±0.09	0.34±0.03
9-10	0.20	0.39	1.53	0.36±0.03	1.12±0.10	0.29±0.03
11-12	0.20	0.39	1.54	0.23±0.06	1.27±0.11	0.44±0.04
14-15	0.20	0.38	1.54	0.22±0.04	1.06±0.10	0.23±0.02
17-18	0.20	0.38	1.54	0.37±0.05	0.96±0.09	0.13±0.01
Inventory (dpm/cm^2)				8.60±1.72		10.76±2.15
Core 8825: 54°37.96'N, 6°59.75'E; 42m, collected 4/26/88						
0-1	0.16	0.32	1.70	0.13±0.05	1.02±0.09	0.19±0.02
1-2	0.17	0.34	1.64	0.27±0.05	1.12±0.10	0.29±0.03
2-3	0.18	0.36	1.60	0.34±0.06	1.45±0.12	0.62±0.05
3-4	0.20	0.38	1.54	0.42±0.05	1.62±0.13	0.79±0.06
4-5	0.20	0.38	1.54	0.32±0.07	1.31±0.11	0.48±0.04
5-6	0.18	0.36	1.60	0.32±0.05	0.99±0.09	0.16±0.01
6-7	0.17	0.34	1.64	0.19±0.06	1.09±0.10	0.26±0.02
7-8	0.18	0.35	1.63	0.29±0.05	0.96±0.09	0.13±0.01
8-9	0.18	0.35	1.62	0.45±0.05	1.10±0.09	0.27±0.02
9-10	0.18	0.35	1.62	0.37±0.06	1.19±0.10	0.36±0.03
11-12	0.17	0.35	1.64	0.35±0.06	1.23±0.11	0.40±0.04
14-15	0.17	0.34	1.64	0.30±0.06	0.96±0.09	0.13±0.01
17-18	0.18	0.35	1.62	0.25±0.05	0.83±0.09	0.00
Inventory (dpm/cm^2)				8.58±1.72		8.23±1.65
Core 8826: 54°34.10'N, 6°52.13'E; 39m, collected 4/26/88						
0-1	0.19	0.37	1.57	0.31±0.04	1.33±0.11	0.50±0.04
1-2	0.18	0.36	1.61	0.35±0.06	1.35±0.11	0.52±0.04
2-3	0.19	0.37	1.58	0.28±0.06	1.51±0.12	0.68±0.05
3-4	0.19	0.37	1.59	0.40±0.05	1.60±0.13	0.77±0.06
4-5	0.18	0.36	1.60	0.34±0.04	1.06±0.09	0.23±0.02
5-6	0.19	0.37	1.58	0.38±0.05	1.24±0.11	0.41±0.04
6-7	0.19	0.36	1.59	0.44±0.05	1.26±0.11	0.43±0.04
7-8	0.19	0.37	1.58	0.36±0.04	1.58±0.13	0.75±0.06
8-9	0.18	0.35	1.61	0.32±0.05	1.31±0.11	0.48±0.04
9-10	0.18	0.35	1.63	0.25±0.03	1.08±0.10	0.25±0.02
10-11	0.18	0.35	1.62	0.31±0.04	1.19±0.11	0.36±0.03
11-12	0.18	0.35	1.63	0.28±0.04	1.02±0.10	0.19±0.02
14-15	0.19	0.36	1.59	0.17±0.05	1.12±0.09	0.29±0.02
17-18	0.19	0.37	1.57	0.31±0.06	1.16±0.12	0.33±0.03

Appendix A: (continued)

Depth (cm)	Water Content	Porosity Φ	Dry Bulk Density ρ	^{137}Cs	^{210}Pb	$^{210}Pb_{xs}$
20-21	0.19	0.37	1.58	0.15±0.04	0.88±0.09	0.05±0.005
24-25	0.18	0.36	1.60	n.d.	0.80±0.08	-0.03±0.003
Inventory (dpm/cm^2)				9.34±1.87		12.21±2.44
Core 8827: 54°28.61'N, 7°08.36'E; 40m, collected 4/26/88						
0-1	0.16	0.33	1.67	n.d.	1.02±0.10	0.19±0.02
1-2	0.17	0.34	1.64	n.d.	1.11±0.10	0.28±0.03
2-3	0.17	0.35	1.64	n.d.	1.04±0.10	0.21±0.02
3-4	0.19	0.36	1.59	0.15±0.03	1.02±0.09	0.19±0.02
4-5	0.18	0.36	1.61	0.21±0.04	1.00±0.09	0.17±0.02
5-6	0.19	0.36	1.59	0.23±0.05	1.31±0.11	0.48±0.04
6-7	0.19	0.37	1.58	0.20±0.05	1.25±0.10	0.42±0.03
7-8	0.19	0.36	1.59	0.23±0.04	1.35±0.11	0.52±0.04
8-9	0.18	0.36	1.60	0.24±0.04	0.98±0.09	0.15±0.01
9-10	0.18	0.36	1.60	0.25±0.03	1.12±0.10	0.29±0.03
11-12	0.18	0.36	1.60	0.41±0.06	1.08±0.09	0.25±0.02
14-15	0.18	0.36	1.61	n.d.	1.09±0.09	0.26±0.02
17-18	0.18	0.35	1.62	0.16±0.05	0.67±0.07	-0.16±0.02
Inventory (dpm/cm^2)				4.30±0.86		6.92±1.38
Core 8828: 54°18.19'N, 7°18.61'E; 43m, collected 4/26/88						
0-1	0.18	0.35	1.63	n.m.	1.12±0.11	0.29±0.03
1-2	0.17	0.34	1.65	n.m.	1.09±0.10	0.26±0.02
2-3	0.16	0.33	1.68	n.m.	0.92±0.09	0.09±0.01
3-4	0.17	0.33	1.67	n.m.	1.02±0.10	0.19±0.02
4-5	0.17	0.34	1.65	n.m.	5.25±0.24	4.40±0.20
5-6	0.17	0.35	1.64	n.m.	1.16±0.08	0.33±0.02
6-7	0.18	0.36	1.60	n.m.	1.40±0.10	0.57±0.04
7-8	0.18	0.35	1.63	n.m.	1.09±0.10	0.26±0.02
8-9	0.17	0.34	1.65	n.m.	1.32±0.13	0.49±0.05
9-10	0.17	0.34	1.65	n.m.	1.29±0.12	0.46±0.04
11-12	0.18	0.35	1.63	n.m.	1.14±0.10	0.31±0.03
14-15	0.17	0.34	1.65	n.m.	0.96±0.08	0.13±0.01
17-18	0.17	0.34	1.64	n.m.	0.84±0.08	0.01±0.001
20-21	0.18	0.35	1.62	n.m.	1.05±0.09	0.22±0.02
Inventory (dpm/cm^2)				-		14.38±2.88
Core 8829: 54°17.14'N, 7°26.83'E; 43m, collected 4/26/88						
0-1	0.15	0.30	1.76	n.d.	0.69±0.07	-0.14±0.01
1-2	0.15	0.30	1.75	0.15±0.04	0.78±0.07	-0.05±0.004
2-3	0.16	0.32	1.69	n.d.	0.87±0.08	0.04±0.004
3-4	0.16	0.32	1.70	0.21±0.04	1.04±0.10	0.21±0.02
4-5	0.16	0.32	1.70	0.18±0.04	8.05±0.41	7.20±0.40
5-6	0.16	0.32	1.70	0.32±0.04	1.81±0.14	0.98±0.08
6-7	0.16	0.33	1.69	0.30±0.04	1.61±0.16	0.78±0.08
7-8	0.16	0.33	1.68	0.32±0.04	0.83±0.08	0.00
8-9	0.15	0.31	1.72	0.20±0.04	0.93±0.09	0.10±0.01
9-10	0.15	0.31	1.72	0.21±0.03	0.76±0.08	-0.07±0.007

Appendix A: (continued)

Depth (cm)	Water Content	Porosity Φ	Dry Bulk Density ρ	^{137}Cs	^{210}Pb	$^{210}Pb_{xs}$
11-12	0.16	0.32	1.70	0.33±0.06	0.78±0.08	-0.05±0.005
14-15	0.17	0.34	1.66	n.d.	0.73±0.07	-0.10±0.01
17-18	0.17	0.34	1.65	n.d.	0.74±0.07	-0.09±0.01
20-21	0.16	0.32	1.69	n.d.	0.56±0.06	-0.27±0.03
Inventory (dpm/cm^2)				4.25±0.85		15.49±3.10
Core 8830: 54°10.76'N, 7°40.23'E; 40m, collected 4/26/88						
0-1	0.15	0.30	1.75	0.12±0.04	0.97±0.09	0.14±0.01
1-2	0.16	0.32	1.70	0.33±0.06	1.33±0.11	0.50±0.04
2-3	0.16	0.33	1.67	0.31±0.05	1.39±0.12	0.56±0.05
3-4	0.17	0.34	1.65	0.35±0.06	1.42±0.12	0.59±0.05
4-5	0.18	0.35	1.62	0.42±0.06	1.39±0.12	0.56±0.05
5-6	0.18	0.35	1.61	0.37±0.05	1.21±0.14	0.38±0.04
6-7	0.18	0.36	1.60	0.37±0.05	1.34±0.12	0.51±0.05
7-8	0.18	0.35	1.62	0.30±0.04	1.47±0.14	0.64±0.06
8-9	0.17	0.34	1.65	0.30±0.05	1.22±0.11	0.39±0.04
9-10	0.18	0.35	1.62	0.27±0.05	0.98±0.09	0.15±0.01
11-12	0.18	0.36	1.60	0.44±0.07	1.25±0.11	0.42±0.04
14-15	0.19	0.37	1.56	0.18±0.06	1.10±0.09	0.27±0.02
17-18	0.18	0.36	1.60	n.d.	1.04±0.10	0.21±0.02
20-21	0.18	0.35	1.62	0.16±0.04	0.87±0.08	0.04±0.004
24-25	0.18	0.36	1.60	n.d.	1.02±0.10	0.19±0.02
Inventory (dpm/cm^2)				8.06±1.61		11.78±2.36
Core 8831: 54°05.54'N, 7°49.97'E; 44m, collected 4/26/88						
0-1	0.15	0.30	1.75	n.m.	0.67±0.07	-0.16±0.02
1-2	0.13	0.27	1.83	0.05±0.02	0.69±0.07	-0.14±0.01
2-3	0.14	0.29	1.78	n.d.	0.80±0.07	-0.03±0.003
3-4	0.20	0.38	1.55	0.28±0.05	1.17±0.07	0.34±0.02
4-5	0.24	0.44	1.39	0.60±0.06	2.29±0.17	1.50±0.10
5-6	0.25	0.45	1.37	n.m.	1.39±0.08	0.56±0.03
6-7	0.22	0.41	1.46	0.56±0.04	1.46±0.13	0.63±0.06
7-8	0.20	0.38	1.54	n.m.	1.32±0.09	0.49±0.03
8-9	0.19	0.37	1.57	0.45±0.03	1.21±0.12	0.38±0.04
9-10	0.19	0.37	1.57	0.42±0.04	0.92±0.07	0.09±0.007
11-12	0.22	0.41	1.48	0.43±0.05	0.81±0.06	-0.02±0.001
13-14	0.21	0.40	1.50	0.33±0.04	0.86±0.07	0.03±0.002
15-16	0.20	0.38	1.55	0.28±0.05	0.82±0.06	-0.01±0.001
17-18	0.21	0.40	1.49	0.26±0.05	0.87±0.07	0.04±0.003
20-21	0.21	0.41	1.49	0.19±0.04	0.97±0.07	0.14±0.01
23-24	0.18	0.36	1.61	n.d.	0.55±0.06	-0.28±0.03
26-27	0.20	0.38	1.55	n.d.	0.50±0.04	-0.33±0.03
29-30	0.21	0.41	1.48	n.d.	0.66±0.05	-0.17±0.01
32-33	0.21	0.40	1.50	n.d.	0.54±0.05	-0.29±0.03
35-36	0.21	0.40	1.50	n.d.	0.79±0.06	-0.04±0.003
Inventory (dpm/cm^2)				12.62±2.52		3.84±0.77

* Reported activities are not decay corrected. Uncertainties are standard errors based on counting statistics

a Porosity $\Phi = w\%/[\ w\%+(1-w\%)/\rho_S\ ]$, where w% = the measured percent water content by weight; ρ_S = particle density (assumed to be 2.5 g/cm^3 here).

b Dry bulk density ρ (g dry sediment/cm^3 wet sediment) = $\rho_S (1-\Phi)$ (Cochran, 1985).

c The ^{210}Pb concentrations in deeper sections of the sediments have been taken as an index of ^{226}Ra for the calculations of the excess ^{210}Pb. For cores from the Outer Silver Pit and the adjacent areas (cores 8810-8821), a value of 1.07±0.16 dpm/g (n=24, at depth ≥15 cm) was taken as the mean activity of ^{226}Ra; for cores from the German Bight (cores 8822-8831), the mean value of ^{226}Ra was assumed to be 0.83±0.17 dpm/g (n=28, at depth ≥ 15 cm).

d n.m. = not measured.

e Inventory = $\sum_{1}^{n} {}^{210}Pb_{xs}$ (or ^{137}Cs) x dry bulk density x sample thickness (Thomson et al., 1988).

Interpolations between measured values were made for intervals in which ^{210}Pb or ^{137}Cs was not analyzed. The ^{137}Cs inventories were integrated to a depth accounting for 90% of the total inventory in that core.

f A value of 24% was taken as the mean water content for the inventory calculation in core 8810 since there were no data available.

g n.d. = not detectable.

CHAPTER 4

^{210}PB AND ^{210}PO DISTRIBUTIONS AND DISEQUILIBRIUM IN THE COASTAL AND SHELF WATERS OF THE SOUTHERN NORTH SEA

ABSTRACT--Concentration profiles of ^{210}Pb and ^{210}Po were measured at 10 stations in the coastal and shelf areas of the southern North Sea. Scavenging processes in this study area are revealed by ^{210}Po/^{210}Pb disequilibrium and their distributions in the water column. Results for ^{210}Po show strong excess, relative to ^{210}Pb, in both dissolved and particulate forms, indicating an additional flux of ^{210}Po from the coastal and shelf sediment. A significant maximum of the dissolved ^{210}Po and ^{210}Pb over the fine grained depositional area (Oyster Ground) was observed to correspond with resuspension of the underlying muddy sediments. The relative greater uptake rate of dissolved ^{210}Po, derived from a box model calculation of mass balance, suggests that the ^{210}Po is more preferentially scavenged from the water column than ^{210}Pb, probably due to its higher activity and its high recycling efficiency. The low concentration of ^{210}Pb in the study area is related to the low atmospheric input of ^{210}Pb, the high concentration of suspended matter and the high sediment resuspension rates. A comparison of the data between the water and sediment columns shows that the excess of ^{210}Po, found in the water body, could be balanced by only a small amount of deficit of ^{210}Po in the sediment, due to the characteristics of this continental shelf area.

1. INTRODUCTION

The natural radioactive nuclides ^{210}Pb ($t_{1/2}$ = 22.3 years) and ^{210}Po ($t_{1/2}$ = 138.4 days) have been used intensively as key tracers to study processes of chemical scavenging, particle transport and sediment deposition in marine environments due to their suitable half lives (Rama et al.,1961; Craig et al., 1973; Bacon et al., 1976; Thomson and Turekian, 1976; Spencer et al., 1981; Cochran et al., 1983; Chung, 1987; Cochran et al., 1990). ^{210}Pb is principally produced within the water column, following the decay of ^{226}Ra, and is also introduced into the sea surface from the atmosphere via the decay of ^{222}Rn and in the coastal area through river inputs.. Being a granddaughter nuclide of ^{210}Pb, ^{210}Po in seawater is mostly formed *in situ* through decay. However, sediment resuspension, chemical diffusion and river input can also play important roles in supplying ^{210}Po to the water column.

The distribution of ^{210}Pb and ^{210}Po in continental shelf water has been studied by several authors (Benninger, 1978; Nozaki et al., 1980; Spencer et al., 1980;

Bacon et al., 1988). It has been noted that continental shelf water appears to be strongly depleted in ^{210}Pb, relative to ^{226}Ra. The residence times of ^{210}Pb in coastal waters are only a few months which is much shorter than those in open ocean waters (in the order of a few years). The ratios of $^{210}Po/^{210}Pb$ in many coastal waters are in excess of 1.

To study the distribution and disequilibrium of ^{210}Pb and ^{210}Po in the southern North Sea in order to understand the processes controlling supply, transfer and deposition of fine grained suspended sediment, the concentrations of ^{210}Pb and ^{210}Po in both particulate and dissolved phases were measured at 10 stations in an area off northern Holland between *ca* 53 and 55^{0}N (Fig. 1; Table 1). In this area, the water depth gradually increases northward to a maximum of about 50 m. The bottom is moderately steep with a general slope of 0.4 $x10^{-3}$, the slope between 30 and 40 m depth locally reaches $1.2x10^{-3}$. The water masses in the area are mainly controlled by the presence of relatively fresh coastal water along the Dutch coast, and more saline Central North Sea water and Channel water which are all moving in a generally eastward direction. Somewhat less saline English coastal water is at times drawn in between the latter two (Van Haren, 1990). The tidal currents decrease in amplitude towards the north (from 80 to 40 cm/sec, maximum speed of the surface tidal current in spring tides, Otto et al., 1990); the major axis is aligned with the isobaths. The water column, north of 53°30 N is thermally stratified from spring till autumn with a transition zone or a mixing front located between the 30 and 40 m isobaths (van Aken, 1986), while the southern part is vertically well-mixed throughout the year. Van Haren (1990) reported that the monthly mean along-isobath current component is always directed towards the east and that it is about three times larger than the, generally offshore directed, cross-isobath component.

2. SAMPLE COLLECTION AND ANALYTICAL METHODS

Water samples were collected at 10 stations with the R.V. *Aurelia* on 20-21 November 1989. About 20 l seawater was taken for each sample with 30 l PVC Niskin bottles and at times with a 150 l zinc water-box which is coated with polyurethane and equipped with a pressure-gauge to trigger the cover lock at the required water depth. The locations of the sampling stations are shown in Fig. 1. Each sample was filtered on board the ship through a 0.45 μm poresize, 142 mm diameter Millipore filter for collecting the suspended particulate matter. The filtered water was stored in a pre-cleaned polyethylene cubitainer and acidified to

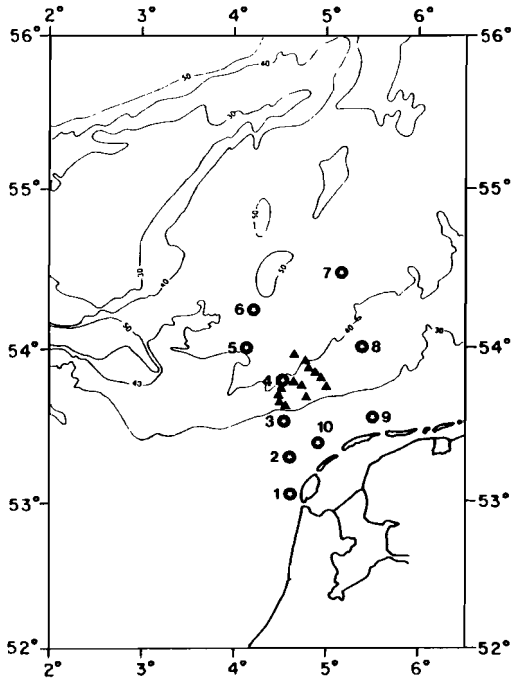

Fig. 1 *Station locations sampled for ^{210}Pb and ^{210}Po measurements (circles filled with star symbol), R. V. Aurelia cruise, 20-21 November 1989, and positions of the studied bottom sediment cores (triangles, Zuo et al., 1989).*

pH=2 with HCl, spiked with known amounts of ^{208}Po (purchased from Amershaw, U.K.) and stable Pb and stored for processing ashore. The filtration was completed within 1-3 h immediately after sample collection. The procedure for extracting ^{210}Pb and ^{210}Po from seawater is based on a method described by Fleer and Bacon (1984). The ^{210}Pb and ^{210}Po were coprecipitated with Co - APDC chelate by adding $Co(NO_3)_2$ solution (0.5 mg Co/l) and APDC solution (50 mg APDC/l seawater). The Co-APDC chelate was filtered onto 0.45 μm Millipore filters and returned to the laboratory for dissolved ^{210}Pb and ^{210}Po analysis. In the laboratory, the filters containing the particulate matter were dissolved in a mixture of HCl, HNO_3 and $HClO_4$ and spiked with ^{208}Po and Pb carrier for particulate ^{210}Pb and ^{210}Po analysis. Finally, both nuclides were spontaneously plated on silver discs and measured by alpha-spectrometry. The error of the activities was estimated on the basis of the statistical counting only.

The sample solutions were then stored for at least 6 months during which ^{210}Po was regenerated by decay of ^{210}Pb. A second portion of ^{208}Po tracer was added,

Table 1: *Station locations of North Sea Cruise, 20-21 November 1989.*

Station	Location		Water	Sampling
	Latitude	Longitude	Depth(m)	Date
1	53°03.40' N	4°37.10' E	19	Nov. 20 1989
2	53°17.00' N	4°36.00' E	30	Nov. 20 1989
3	53°31.00' N	4°33.00' E	28	Nov. 20 1989
4	53°47.00' N	4°32.00' E	41	Nov. 20 1989
5	53°59.00' N	4°08.00' E	45	Nov. 20 1989
6	54°14.00' N	4°13.00' E	50	Nov. 20 1989
7	54°28.00' N	5°11.70' E	42	Nov. 21 1989
8	54°00.00' N	5°23.00' E	39	Nov. 21 1989
9	53°32.23' N	5°30.13' E	20	Nov. 21 1989
10	53°23.00' N	4°55.20' E	21	Nov. 21 1989

and the samples were again plated and counted. Determination of this newly produced ^{210}Po gave a concentration of ^{210}Pb present in the sample. For analysis of stable lead, the sample solutions were diluted to a standard volume and measured by atomic absorption spectrophotometry. Recovery was determined by comparison with standards of Pb carrier diluted to the same volume in a matrix consisting of the same reagents as added to the samples. Sample and standard readings were alternated to correct for drifts in sensitivity and the results were based on duplicate readings. A correction for radioactive growth and decay and for losses during co-precipitation was made for all the data according to the method of Fleer and Bacon (1984) to obtain the accurate activities of ^{210}Po and ^{210}Pb at the time of sample collection.

Table 2: *Blank measurements.*

	Type	Number measured	^{208}Po dpm	^{210}Pb dpm
replating	sed. part. diss.	8	0.0026±0.0013	0.0015±0.0009
bottles	part.	3	0.0154±0.0105	0.0022±0.0013
	diss.	2	0.0017±0.0011	0.0016±0.0011

sed. = sediment; part. = particulate; diss. = dissolved.

A summary of blank measurements is given in Table 2. The ^{210}Po plating efficiency was checked periodically by replating the sample solutions immediately after previous 3 h plating and the counting results (Table 2) indicate that the plating efficiencies are better than 99%. The polyethylene bottles for storing the sample solutions were checked to examine whether there is any carryover ^{208}Po and possible ^{210}Pb loss by adsorption which would decrease the concentration of ^{210}Pb. This is performed by filling 6N HCl into the empty bottle after the storage, rinsing the bottle a few times more with acid and then replating the solution. Results (Table 2) show no appreciable carryover and loss for ^{208}Po and ^{210}Pb, and the concentrations that have left in the bottle do not exceed a few per cent for either ^{208}Po (<1%) or ^{210}Pb (<2%). In order to assess the accuracy of our method of ^{210}Pb, measurements were made on ^{210}Pb sediment standard samples, kindly provided by the Marine Sciences Research Center, Stony Brook State university of New York, U.S.A. The results agree to the standard value well with a deviation of less than 4%.

Table 3: *Blanks of Nuclepore filter and Aluminium discs in ashing method. Weight units are in mg.*

Sample	Before		After	Excess
	filter	Al disc	filter + Al disc	
177	13.70	386.78	386.79	+0.01
178	14.32	382.94	382.98	+0.04
179	14.34	393.66	393.76	+0.10
180	14.40	388.88	388.95	+0.07
181	14.45	387.61	387.59	-0.02
183	14.66	390.91	390.84	-0.07
184	15.31	387.43	387.50	+0.07
b13	–	388.45	388.44	-0.01
b22	–	384.42	384.44	+0.02
b32	–	379.16	379.23	+0.07
d42	–	391.13	391.12	-0.01

Samples for measurement of total suspended matter (TSM) were collected by filtering *ca* 0.5-1 l sea water using vacuum filtration, onto a pre-weighed, 0.4 μm

pore size, 47 mm diameter Nuclepore filter. The filters were rinsed with distilled water three times and then dried and weighed in the laboratory. The concentrations of total organic matter (TOM) were obtained by wrapping the filters into small Aluminium discs and ashing them at 550^{0}C for 8 h. Blanks of filter and Aluminium disc are listed in Table 3 which gives a mean background value of +0.02 mg. So for most samples the possible overestimates for the TOM data due to the residue of filter do not exceed 15%. For TSM, we estimate the error less than 10%. During the cruise, also CTD casts were taken with a Guildline CTD (model 8770) at each station.

3. THE DISTRIBUTION OF ^{210}PB AND ^{210}PO

The ten sampling stations were aligned along three transects (Fig. 1): transect 1 (from station 1-6, total distance *ca* 143.2 km) and transect 2 (from station 9 to 7, total distance *ca* 105.4 km) are approximately at right angles to the isobaths, while transect 3 (from station 2 to 9, total distance *ca* 66.4 km) is approximately parallel to the isobaths.

The concentrations of ^{210}Pb and ^{210}Po in dissolved and particulate form obtained from water sample measurements together with the total suspended matter concentration (TSM) and total organic matter concentration (TOM) are listed in Tables 4 and 5. The distribution of the hydrographic parameters (salinity, temperature and density) and the activities of ^{210}Pb and ^{210}Po, as well as TSM and TOM, are shown in Figs 2-5.

The detailed distribution sections of salinity, temperature and density excess (σ_t) running from south to north crossing the isobaths (transects 1 and 2, Fig. 2a-c; Fig. 3a-c) and running from west to east along the 20 m isobath (transect 3, Fig. 4a-c) show a relatively high salinity core (> 34.5‰) at the northernmost stations (ST 4-7, Fig. 2a, 3a) with the salinity decreasing gradually to the south and east. This reflects the mixing of the saline Central North Sea water with less saline coastal water. As can be seen from Figs 2-4, stations 1-3 and 10 are similar, being dominated by the fresher and colder coastal water (salinity ranging from 33.15 to 34.35‰; temperature 10.66 to 11.62°C; σ_t < 26.30 kg/m^3) and having relatively constant salinity and temperature over the entire depth. Station 9, which is located nearest to the coast, has the lowest salinity (< 33.8‰, Fig. 3a), temperature (< 9.7°C, Fig. 3b) and σ_t (< 25.43 kg/m^3, Fig. 4c) and shows a layer of coastal water along the surface. At stations 4-8 (Fig. 2a-c; Fig. 3a-c), north of the 30 m isobath, the water column is layered in the top 5 m with salinity decreasing upwards. Below this layer the water column is

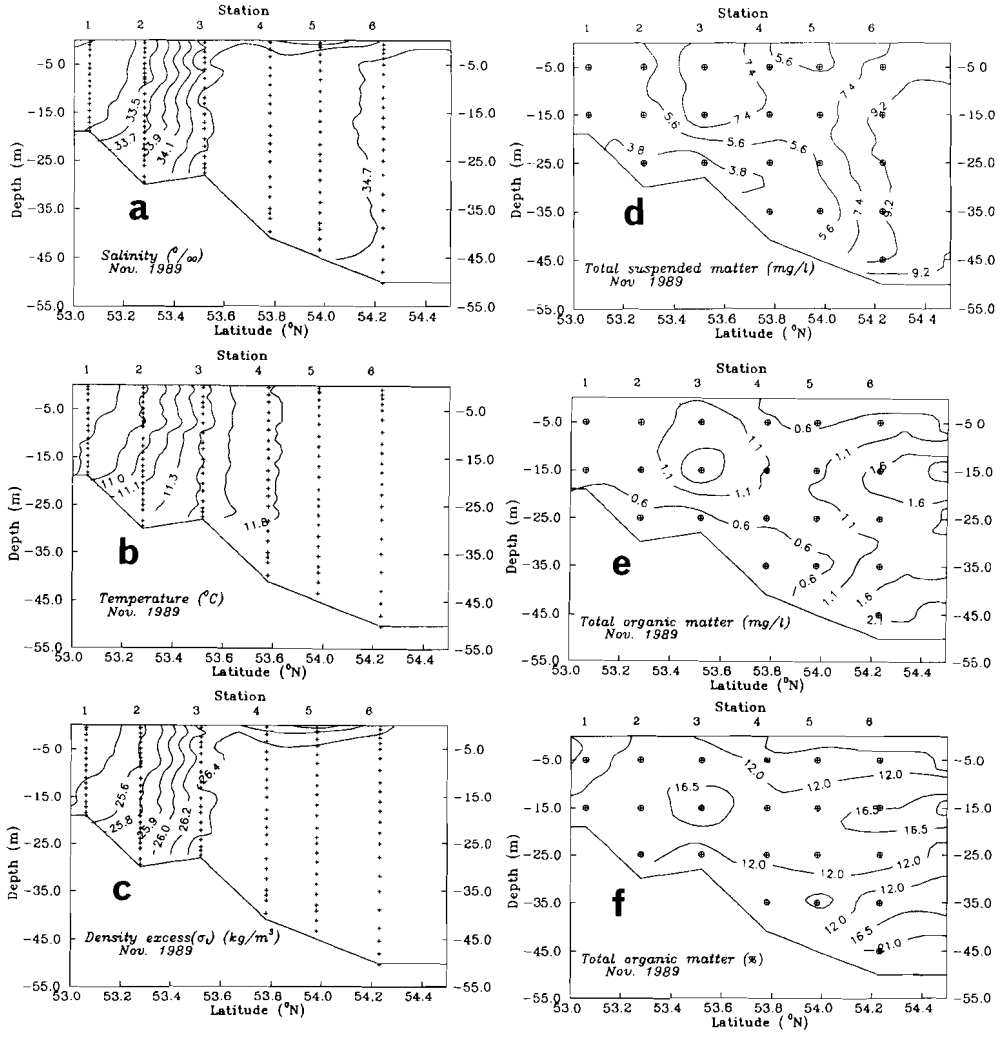

Fig. 2 *The hydrographic, ^{210}Pb and ^{210}Po together with suspended matter and total organic matter distributions in the transect 1 (from 53°03.4'N, 4°37.1'E to 54°14.0'N, 4°13.0'E, stations 1-6). Crosses and circled crosses represent data points. (a) salinity; (b) temperature; (c) density excess (σ_t); (d) suspended matter; (e) total organic matter; (f) the fraction of total organic matter (%); (g) dissolved ^{210}Po; (h) dissolved ^{210}Pb; (i) $^{210}Po/^{210}Pb$ in dissolved form; (j) particulate ^{210}Po; (k) particulate ^{210}Pb; (l) $^{210}Po/^{210}Pb$ in particulate form.*

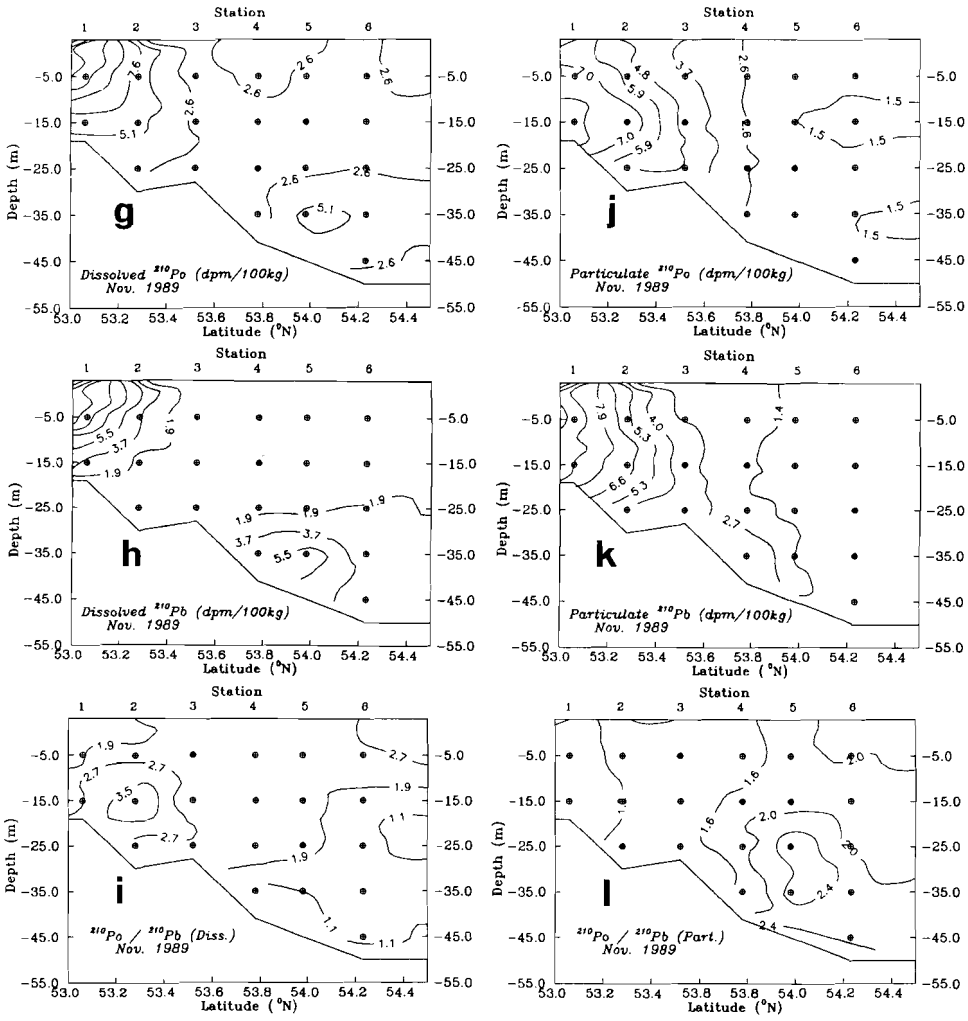

Fig. 2 *continued.*

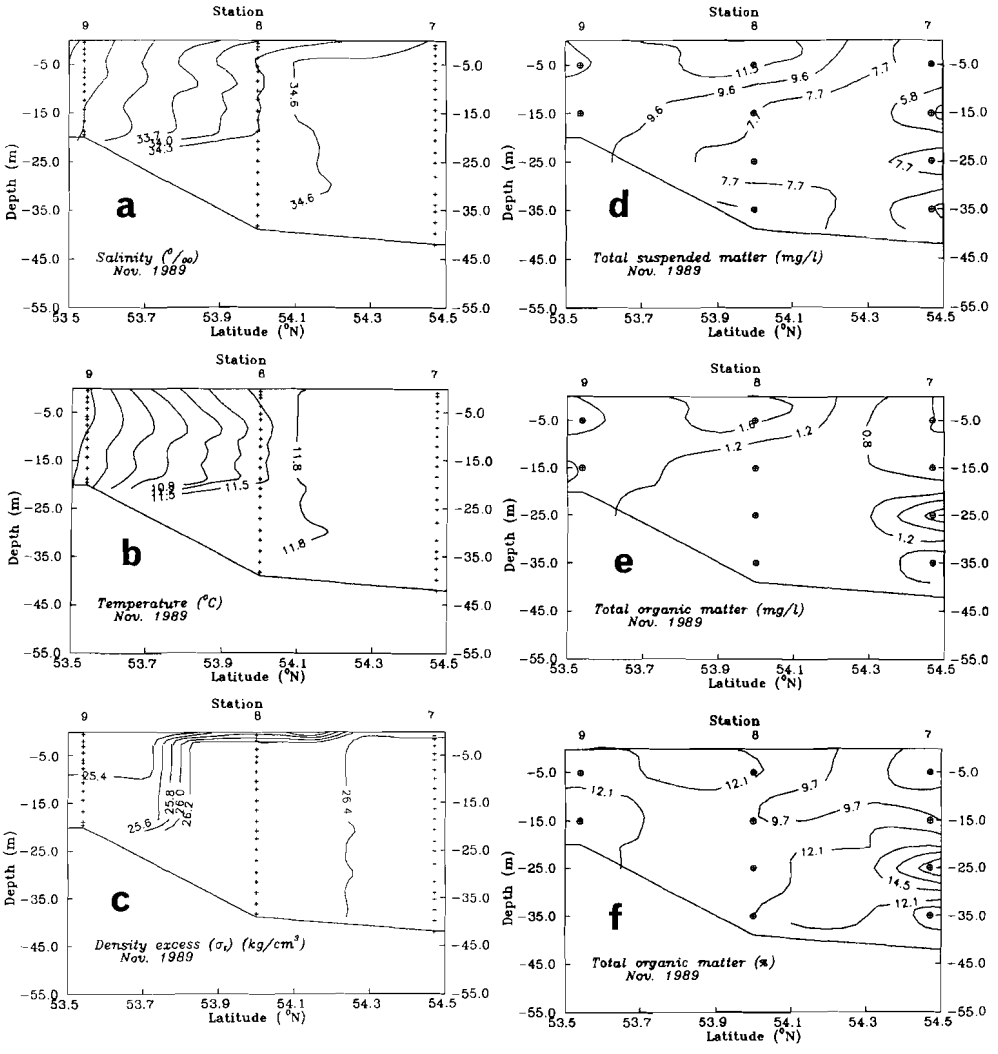

Fig. 3 *The hydrographic, ^{210}Pb and ^{210}Po together with suspended matter and total organic matter distributions in the transect 2 (from 53°32.2'N, 5°30.1'E to 54°28.0'N, 5°11.7'E, stations 9-7). For a detailed legend see Fig. 2.*

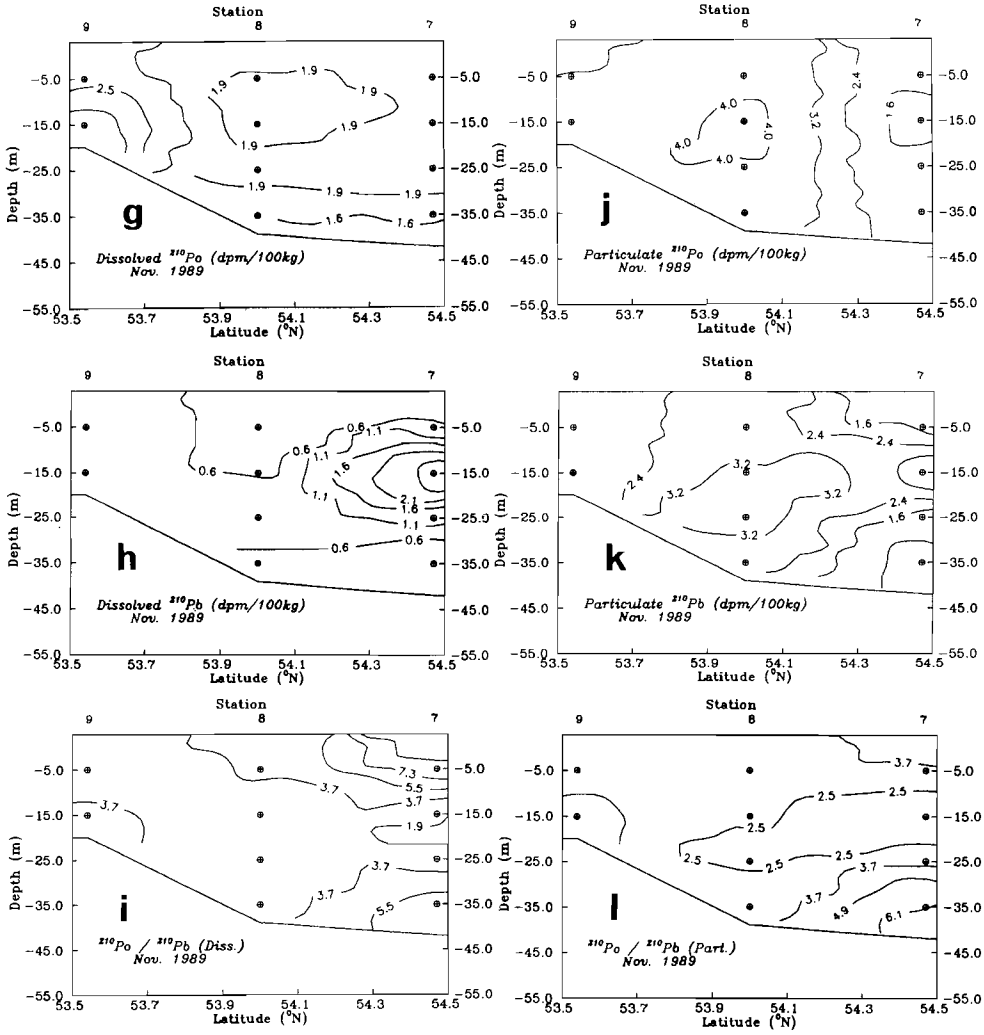

Fig. 3 *continued.*

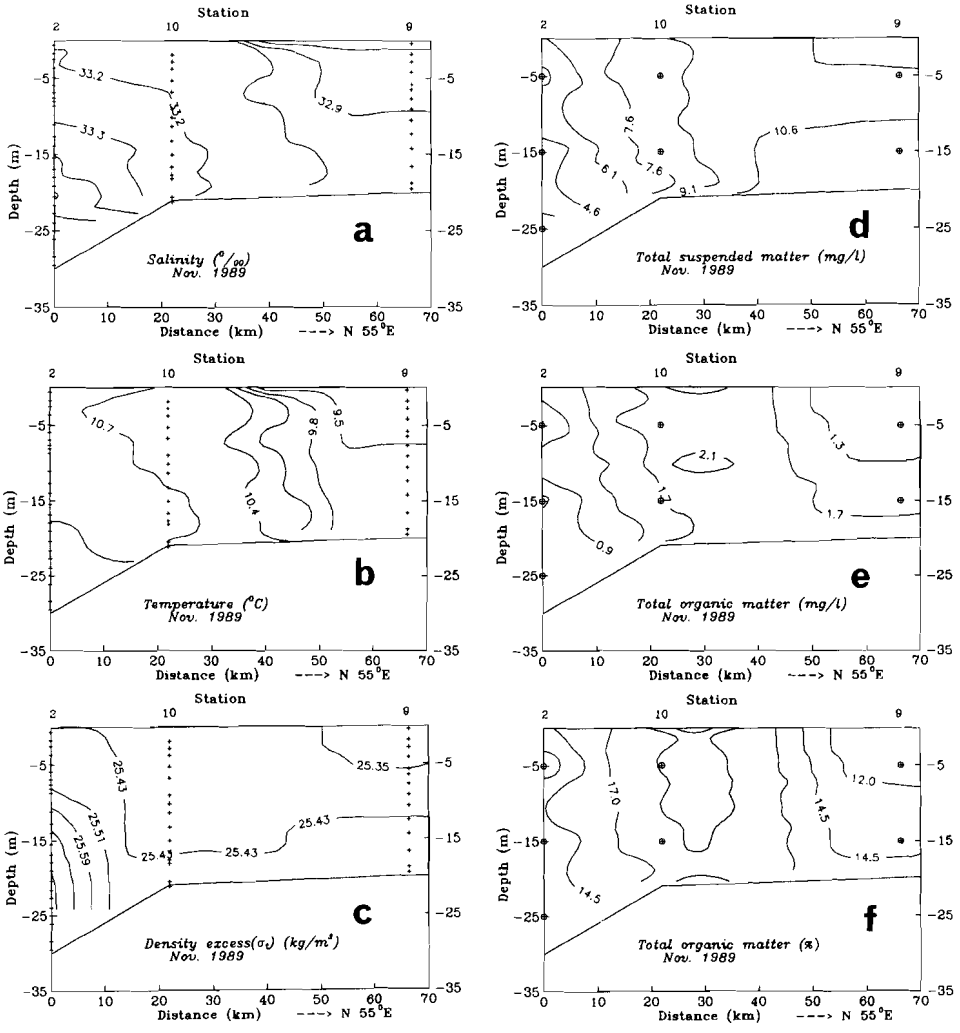

Fig. 4 *The hydrographic, ^{210}Pb and ^{210}Po together with suspended matter and total organic matter distributions in the transect 3 (from 53°17.0'N, 4°36.0'E to 53°32.2'N, 5°30.1'E, stations 2 to 9). For a detailed legend see Fig. 2.*

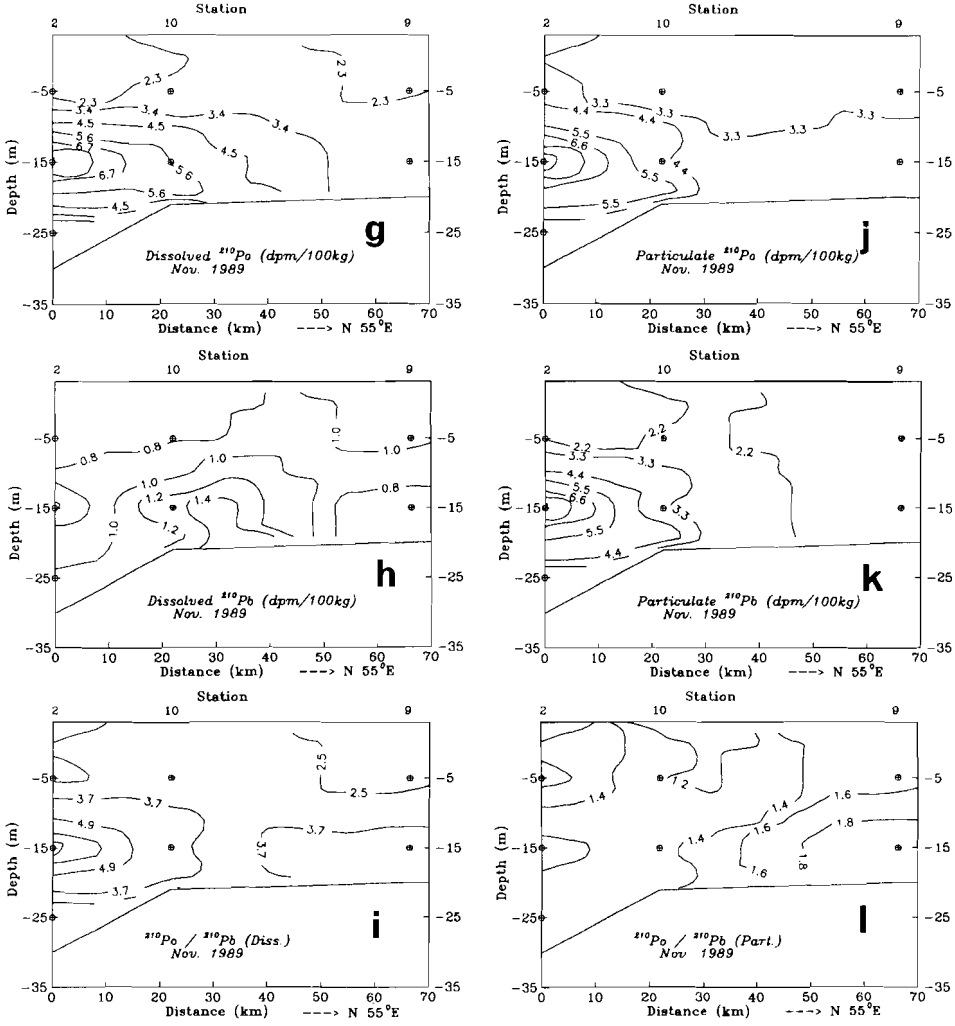

Fig. 4 *continued.*

relatively well mixed. The pattern of temperature in water column shows the same trends as salinity, being highest up north (11.85°C, ST 7) and decreasing to the south and east (the lowest value was found at station 9: 9.5°C). These features indicate that the colder less saline coastal water along the Dutch coast, during or sometime prior to the cruise time of 20-21 November 1989, driven by the wind and/or the offshore directed current, penetrated northward over the transition zone between the 30 and 40 m isobaths, where the mixing of the Central North Sea water with the coastal water takes place, which resulted in the gradients of salinity, temperature and density in the water column.

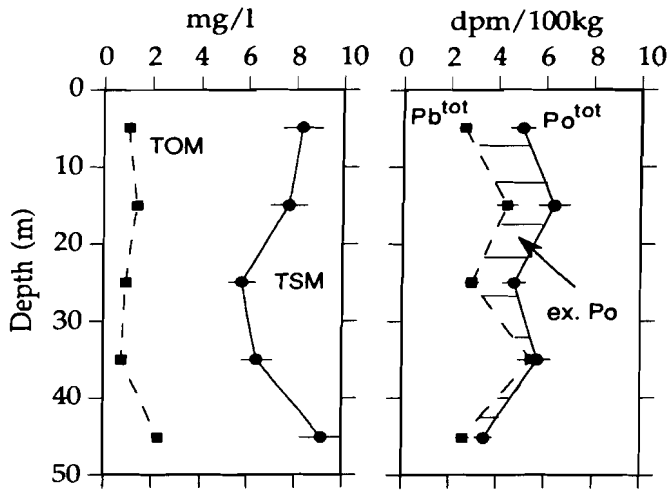

Fig. 5 *Vertical profiles of TSM, TOM, total ^{210}Po and total ^{210}Pb (mean values) in water column, clearly demonstrating a strong excess of ^{210}Po at all water depths.*

The concentration of total suspended matter (TSM) ranged from 1.36 to 15.76 mg/l with an average of 7.45±0.65 mg/l. The total organic matter (TOM) concentration varied from 0.03 to 2.84 mg/l with a mean value of 1.26±0.16 mg/l. The fraction of total organic matter in total suspended matter (> 0.4 μm) is about 2-26% (average 14%). These are in fair agreement with the values reported by Eisma (1981) and Eisma and Kalf (1987) (> 10 mg/l in the coastal waters and 1-5 mg/l in the remaining area of the southern North Sea for TSM; 1 mg/l in surface and

Table 4: *^{210}Pb and ^{210}Po data from North Sea Cruise, Nov. 20-21,1989. Activities are given in dpm/100kg sea water. Uncertainties are 1σ standard errors.*

	Depth (m)	TSM (mg/l)	TOM (mg/l)	Dissolved ^{210}Pb	Particulate ^{210}Pb	Dissolved ^{210}Po	Particulate ^{210}Pb
ST1							
	5	5.04	1.32	16.81±1.32	13.39±1.08	21.87±0.98	7.92±0.42
	15	5.64	0.76	1.35±0.24	9.04±0.73	1.56±0.16	8.80±0.47
ST 2							
	5	3.85	0.36	0.75±0.19	2.09±0.29	1.61±0.16	3.68±0.27
	15	2.97	0.35	0.48±0.23	9.47±1.20	9.32±1.60	9.85±0.78
	25	2.71	0.35	1.02±0.21	2.75±0.35	1.37±0.15	3.59±0.28
ST 3							
	5	10.77	1.66	0.65±0.16	2.59±0.33	1.19±0.12	3.87±0.29
	15	10.74	2.84	1.92±0.29	2.70±0.27	1.84±0.18	4.24±0.32
	25	2.70	0.18	0.72±0.16	3.29±0.34	1.89±0.25	5.08±0.37
ST 4							
	5	4.94	0.24	1.87±0.24	2.14±0.25	4.66±0.51	2.50±0.25
	15	8.56	1.30	0.63±0.13	1.62±0.21	1.59±0.24	2.57±0.22
	25	1.98	0.25	0.45±0.11	1.52±0.19	1.37±0.22	2.80±0.24
	35	5.94	0.71	5.33±0.59	6.09±0.68	0.82±0.14	2.78±0.23
ST 5							
	5	4.54	0.40	0.70±0.13	0.87±0.16	1.72±0.30	1.82±0.17
	15	6.42	0.98	0.86±0.17	0.62±0.13	1.66±0.25	1.12±0.13
	25	6.34	1.16	0.80±0.15	0.48±0.11	2.11±0.27	1.65±0.17
	35	1.36	0.03	8.11±0.59	0.49±0.10	7.78±0.58	1.53±0.16
ST 6							
	5	7.98	0.48	0.95±0.18	0.79±0.15	2.69±0.37	1.69±0.14
	15	10.96	2.42	1.74±0.26	0.79±0.16	2.47±0.30	1.32±0.13
	25	9.88	1.04	1.83±0.24	1.07±0.16	1.23±0.16	1.79±0.16
	35	10.62	1.50	2.85±0.32	0.68±0.14	5.27±0.49	1.43±0.15
	45	9.14	2.26	1.90±0.25	0.70±0.13	1.90±0.23	1.57±0.16
ST 7							
	5	7.60	0.36	0.20±0.06	0.86±0.16	1.93±0.36	1.71±0.16
	15	1.96	0.16	3.68±0.43	4.57±0.48	1.89±0.25	1.47±0.14
	25	11.02	2.72	0.95±0.14	1.02±0.17	2.34±0.26	1.75±0.18
	35	2.62	0.16	0.23±0.06	0.64±0.13	1.53±0.24	2.04±0.20
ST 8							
	5	15.76	2.48	0.49±0.11	2.53±0.29	1.94±0.25	3.78±0.29
	15	5.74	0.34	0.56±0.10	3.32±0.34	1.68±0.22	4.15±0.32
	25	5.64	0.70	0.86±0.14	3.82±0.40	2.15±0.25	3.97±0.31
	35	11.30	1.30	0.46±0.08	2.30±0.23	1.50±0.21	3.81±0.36
ST 9							
	5	8.76	0.94	1.03±0.14	2.05±0.23	2.29±0.24	3.13±0.31
	15	11.92	1.76	0.70±0.10	1.80±0.20	3.04±0.38	3.58±0.38
ST 10							
	5	10.36	2.44	0.78±0.12	2.23±0.26	2.56±0.31	2.58±0.22
	15	10.10	2.10	1.51±0.21	2.66±0.28	4.99±0.51	3.82±0.35

bottom water of the Dutch coastal area for TOM). Most of the suspended matter in the southern North Sea, as suggested by Eisma (1990), is supplied through the straits

of Dover, from rivers, the seafloor erosion and coastal erosion, and from the atmosphere (dust).

Table 5: *Summary of the ^{210}Pb and ^{210}Po concentrations in water column of the southern North Sea (Nov. 20-21,1989). Units are given in dpm/100kg sea water.*

Depth (m)	TSM (mg/l)	TOM	Diss. ^{210}Po	Part. ^{210}Po	Diss. ^{210}Pb	Part. ^{210}Pb	Total[a] ^{210}Po	Total[a] ^{210}Pb	$^{210}Po/^{210}Pb$ (total)
0-10 (n=9)[b]	8.28	1.04	2.29	2.75	0.82	1.79	5.04	2.61	1.93
10-20 (n=9)[b]	7.71	1.36	3.16	3.57	1.34	3.06	6.73	4.40	1.53
20-30 (n=7)	5.75	0.91	1.78	2.95	0.95	1.99	4.73	2.94	1.61
30-40 (n=5)	6.37	0.74	3.38	2.32	3.40	2.04	5.70	5.44	1.05
40-50 (n=1)	9.14	2.26	1.90	1.57	1.90	0.70	3.47	2.60	1.33

a. Total = Diss. + Part.
b. Station 1 was not taken into account due to its extreme values.

The activity distribution of ^{210}Pb and ^{210}Po shows considerable variation from one station to another which can be best seen in the iso-concentration contours along the three transects (Figs 2-4). The concentration of both nuclides, as shown in transect 1 (Fig. 2), decreases from south to north. The activity of the particulate ^{210}Pb and ^{210}Po, at most stations, shows a nearly constant vertical profile throughout the water column (Figs 2-4), while station 7 (Fig. 3j, k), station 10 (Fig. 4j, k), station 1 and 2 (Fig. 2j, k) have a mid-water maximum. Particulate ^{210}Pb is systematically lower compared to particulate ^{210}Po at all the stations by about 0.5-1.5 dpm/100kg (Figs 2-4l; Table 4) with exceptions at station 1, station 4 at 35 m depth (Fig. 2k) and station 7 between 10 and 20 m depth (Fig. 3k) ($^{210}Pb > ^{210}Po$). Dissolved ^{210}Pb has the same pattern as its particulate phase: being in excess with respect to dissolved ^{210}Pb at nearly all the stations (Fig. 2-4i). The regular excess of ^{210}Po in the dissolved phase is somewhat different from what was found by Spencer et al. (1980) in the northern North Sea water. They have observed strong surface water (< 50 m) depletion of dissolved ^{210}Po and excess of particulate ^{210}Po together with excesses of dissolved ^{210}Po in the thermocline region (60-130 m water depth) which was explained by the hypothesis of rapid uptake and recycling of ^{210}Po due to biological processes operating in the surface water. In their case, the excess of dissolved ^{210}Po

in deep water (60-130 m) is compensated by depletions of dissolved ^{210}Po in surface water. What we found is that strong excess of ^{210}Po present in almost entire water column, indicating an extra flux of ^{210}Po into the system besides the production from decay of ^{210}Pb. This point will be discussed further in later sections.

A pronounced maximum of both dissolved ^{210}Po and ^{210}Pb was found below a depth of 25 m at stations 4-6 (Fig. 2g, h). This is probably related to resuspension of underlying muddy sediments which are known for their rich benthic fauna (Oyster ground). An increase of TSM and TOM can be seen, indeed, below a depth of 30-35 m at station 6 (Fig. 2d-f). Similar situations were also observed at station 7 (at mid water depth, Fig. 3g, h) and station 10 (Fig. 4g, h) where relatively high concentrations of two dissolved elements coincided with high organic matter contents (Fig. 3 and 4e). The presence of a frontal zone in this area plays an important role in the deposition of organic matter produced in the Southern Bight, which forms the basis for a rich benthic fauna. The high concentrations of dissolved ^{210}Pb and ^{210}Po near the boundary layer can probably be explained as a result of remineralization or release of ^{210}Pb and ^{210}Po from organic matter. A strong correlation between the ^{210}Pb concentration and organic carbon content in trap sediments and in the water column has been reported by Biscaye et al. (1988) and Moore and Dymond (1988) and it was suggested that organic matter has a higher affinity for ^{210}Pb than the mineral phase has. A significant increase of particulate ^{210}Pb in the benthic boundary layer between station 4 and 5 (Fig. 2k) is consistent with the maximum observed in its dissolved phase (Fig. 2h). It is very likely that the resuspension of fine grained bottom sediments due to physical and biological effects is responsible for the increasing of ^{210}Pb in particles near the bottom boundary layer.

4. THE DISEQUILIBRIUM OF ^{210}PO AND ^{210}PB

The strong excess of ^{210}Po with respect to ^{210}Pb in the water column, as shown earlier in the transect contours (Figs 2-4i, l) and in the profile of the total ^{210}Po and ^{210}Pb (Fig. 5), indicates a strong depletion of ^{210}Pb with respect to ^{210}Po in the water column. A significant increase of the ^{210}Po/^{210}Pb ratio was observed where the coast and the sediment-water interface are approached (Fig. 2-4i), which was assumed to be a consequence of recycling and additional input of ^{210}Po. The excess of dissolved ^{210}Po, as conclude by Bacon et al. (1978), is maintained by release from particles settling from the surface water; results from a box-model of Bacon and coworkers indicated that the efficiency of this recycling is greater than 50%.

This was supported by the observation of ^{210}Po release from marine particles made by Heyraud et al. (1976) in which 41% of the ^{210}Po in fecal pellets was released in 5 days. The ratio of $^{210}Po/^{210}Pb$ in total, in study area, ranges from 1.05 to 1.93 (Table 5) and the ratio in suspended particles is mostly greater than 1 with a maximum of 3.5, which is compatible with a net uptake of ^{210}Po in the continental shelf and slope waters of south New England (Bacon et al., 1988). As Polonium is chemically more reactive it tends to be removed preferentially over Lead by sinking particles. A mid depth maximum of excess particulate ^{210}Po at stations 4-6 (Fig. 2l) is, therefore, possibly produced by this preferential uptake. The strong excess ^{210}Po in dissolved form with respect to ^{210}Pb and the fact that the standing crop of the total ^{210}Po in the water body is somewhat greater than that of the total ^{210}Pb (Fig. 5), as we believed, suggests a second source of ^{210}Po from the coastal and shelf sediments besides from decay of ^{210}Pb. Similar excess ^{210}Po has been reported by Schell (1977) for the Washington coastal area and Spencer et al. (1980) for the northern North Sea.

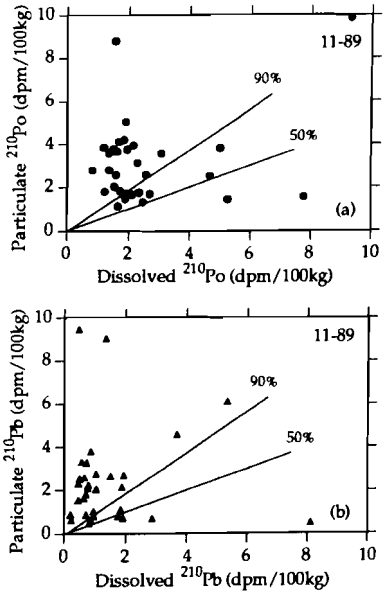

Fig. 6 *The particulate form versus the dissolved form plots for (a) ^{210}Po and (b) ^{210}Pb. Most of the data fall above the 50% line indicating that the particulate activities are more than 50% of the dissolved ones which reveals a strong scavenging of ^{210}Po and ^{210}Pb in the water column.Data points which fall below the 50% line are generally associated with the deeper water.*

Plots of the partition of ^{210}Po and ^{210}Pb between particulate and dissolved forms for all the stations are shown in Fig. 6. It is clear that most of the data fall

above the 50% line, indicating that activity of the particulate ^{210}Po and ^{210}Pb is more than 50% of activity of their dissolved phase. This implies that both elements in the water column are strongly removed by sinking particles; the scavenging is enhanced near the sediment-water interface because of increasing interaction between water and suspended/resuspended particles. A small fraction of ^{210}Po (Fig. 6a) and ^{210}Pb (Fig. 6b) in the particulate form(<50%) is generally associated with the relatively deeper water (> 40 m).

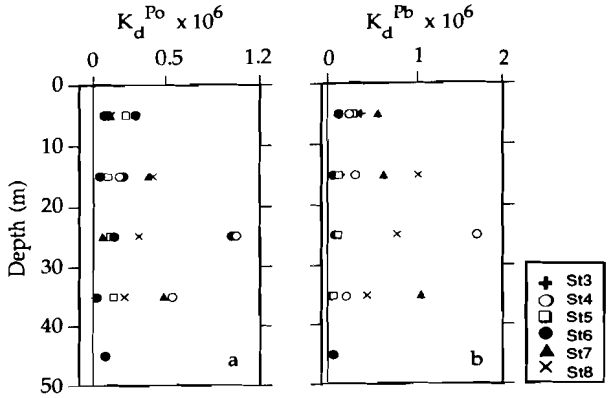

Fig. 7 *The vertical profiles of (a) ^{210}Po distribution coefficient, (b) ^{210}Pb distribution coefficient.*

Computing the empirical distribution coefficients (K_d) for the two nuclides could give more insight in their behaviours. The distribution coefficient K_d is given by (Bacon et al., 1988):

$$K_d = C^P / (C^d \cdot TSM) \quad (1)$$

where C^P and C^d are concentrations of the nuclides in particulate and dissolved phases (Table 4), and TSM is the total suspended matter concentration (Table 4). Results are plotted in Fig. 7. For ^{210}Po, the lowest distribution coefficients are found in the surface layer and maximum values in K_d^{Po} are found in the mid water depth (20-30 m) due to the strong uptake of ^{210}Po by suspended particles, and then the values decrease again downwards with a slight increase when the sea bed is approached (Fig. 7; st 5-7), which we believe is resulted from ^{210}Po regeneration due to destruction of the Po-bearing particles and resuspension of deposited sediments. For ^{210}Pb, on the other hand, the lowest K_d values are found near the sea floor (st. 7

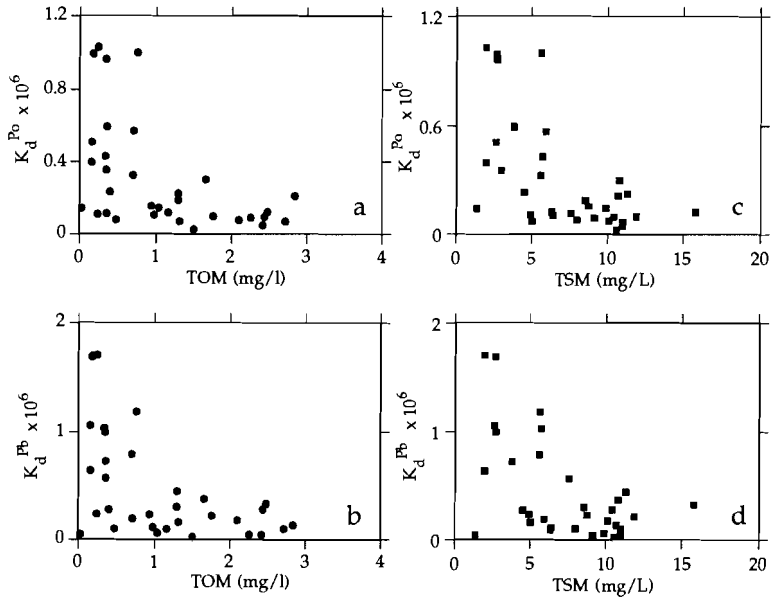

Fig. 8 *The relationship between distribution coefficient (K_d) of two tracers and (a), (b) total organic matter; (c), (d) total suspended matter.*

is an exception, Fig. 7), in support of the previous suggestion of sediment resuspension. The general greater values of K_d^{Pb} with respect to K_d^{Po} probably reflects the disequilibrium between two tracers in dissolved form. Figure 8 gives plots of K_d (Po, Pb) versus TOM (TSM) in all samples to examine the relationship among K_d and TOM, TSM. An apparent correlation between K_d and TSM was observed. The fact that K_d is inversely proportional to TSM can be explained by the scenario that the 'aged' particles are ejected from the seabed into the water body by intense winnowing due to bioturbation, storm, wave action and other biological and physical effects. Because of the radioactive decay on the particles during the time the particles were on the bottom, this leads only to a concentration increase of the suspended matter but not the particulate content of ^{210}Pb and ^{210}Po in the water column. Consequently, the K_d values decrease with an increasing content of suspended particles. There is also a significant correlation between K_d and total

organic matter (Fig. 8a, b). However, two clusters of data points can be identified from Fig. 8a and b, representing two types of organic material. The one with high concentrations of TOM (ranging from 1-3 mg/l) and low K_d values (<0.4) has probably originated from areas near the coast and the boundary layer where intensive resuspension occurs, producing large amount of 'old' organic particles to the water which only carry low amount of ^{210}Pb and ^{210}Po due to the prior decay. The one with low content of TOM (<1 mg/l) and high K_d values (up to 1.1-1.6; Fig. 8a, b), on the contrary, is probably formed in the shelf water: this 'fresh' and 'young' organic matter is more active in uptaking the nuclides from the solution compared to 'aged' organic particles. The differences in salinity, temperature and composition of organic matter between the coastal and the shelf waters may also play significant roles in controlling the distribution of particle-reactive nuclides in the water column.

5. MASS BALANCE ESTIMATES

For a general picture of the processes controlling the distribution of ^{210}Pb and ^{210}Po, meaningful results cannot be obtained by a simple treatment of data from individual stations, as there are considerable variations in the water column as well as non-steady-state processes. Therefore, a simple box model was used to examine material balances for ^{210}Pb, determined by the following parameters: (1) the atmospheric flux of ^{210}Pb; (2) the ^{210}Pb scavenging efficiency by particles; (3) the production of ^{210}Pb from its parent nuclide (^{226}Ra) by *in situ* decay; (4) the supply from resuspension of bottom sediment; (5) horizontal diffusion and advection; (6) vertical diffusion and advection; (7) the water depth.

The river input of ^{210}Pb and ^{210}Po

Although high concentrations of ^{210}Pb and ^{210}Po were found in the river mouths on the western Dutch coast south of the study area, supply of ^{210}Pb and ^{210}Po from this source is assumed to be unimportant because of rapid scavenging of ^{210}Pb by riverine sediment particles and efficient trapping of the sediment in estuaries and along the coast (Benninger et al., 1975). Indeed, as is confirmed by Berger and Eisma (1988), about 76% of the concentration of ^{210}Po and ^{210}Pb in the river mouth is removed by adsorption onto sediments already in the river and the remainder is mostly trapped in the estuary. The concentrations of ^{210}Po and ^{210}Pb at stations very near to the southern boundary of the study area are less than 10% of

our lowest data of ^{210}Po and ^{210}Pb (Table 4); (*ca* 0.008 dpm/100 kg for the total ^{210}Po, and the same value for the total ^{210}Pb; Berger and Eisma, 1988).

The atmospheric input of ^{210}Pb

The atmospheric input of ^{210}Pb has been extensively determined in many areas from both direct precipitation measurements and soil profiles (Fukuda and Tsunogai, 1975; Benninger, 1978; Turekian and Cochran, 1981; Turekian et al., 1983). Turekian et al. (1977) modelled the atmospheric flux of ^{210}Pb on the basis of estimated radon emanation rates from the continents, atmospheric circulation rates and aerosol mean residence times. Because of the prevailing west-to-east air circulation in mid-latitudes (15-55 ^{o}N) their model predicted that atmospheric flux of ^{210}Pb to the ocean surface should decrease from west to east across the Pacific and Atlantic Oceans. The predicted ^{210}Pb fluxes are 1-2 dpm/cm^2/yr in the North Pacific, 0.5-1 dpm/cm^2/yr in the North Atlantic and 0.2-0.5 dpm/cm^2/yr in the South Indian Ocean. From the direct measurements over a two-year period (1987 and 1988) in the northern Netherlands (Zuo et al., 1992), we have adopted a value of 0.43 ± 0.07 dpm/cm^2/yr ($x\pm\sigma$) as the deposition of ^{210}Pb to the southern North Sea for the present calculations. This number is consistent with the value predicted by Turekian's model (1977) for this area and is also very similar to the atmospheric flux of 0.51 dpm/cm^2/yr reported by Pierson et al. (1966) based on their ^{210}Pb study in rainwater at Milford Haven (England) in 1962-1964.

Deposition, resuspension rates and the total ^{210}Pb budget in sediments

It is realized that there must be strong interaction between the water body and bottom sediments in this study area due to the shallow water depth (30-50 m), the rich benthic fauna and especially in the winter period the frequent storm events. Therefore, it is important to take sediment resuspension into account for the mass balance calculation. To quantify the particle exchange at the water-sediment interface, we first consider the total ^{210}Pb balance in the mixed sediment box. Deposition of ^{210}Pb must be balanced by resuspension plus decay (Santschi et al., 1980; Bacon et al., 1991):

$$D\,C_{susp} = R\,C_{sed} + \lambda\,M \qquad (2)$$

where D is the particle deposition rate into the mixed sediment (g/cm^2/yr), R is the sediment resuspension rate (g/cm^2/yr), C_{susp} is the ^{210}Pb content (dpm/g RSM) of the suspended matter, and C_{sed} is the ^{210}Pb content of the surface sediment (dpm/g), λ is the decay constant (for ^{210}Pb, 0.031 yr^{-1}, for ^{210}Po 1.83 yr^{-1}), and M =

$_0\int^{\infty} \rho\ Pb_{ex}\ dz$ (dpm/cm^2), which is the excess ^{210}Pb inventory in sediment (ρ is the bulk sediment density, g/cm^3; Pb_{ex} is the ^{210}Pb activity of dry sediment, dpm/g; z is the sediment depth, cm). RSM is the refractory suspended matter (= TSM -TOM, Bacon et al., 1991), and for simplicity we ignore particle production and consumption and only consider the physical transport of the particles. From our measurements (Table 4 and 5), we adopt, over water depths of 0 - 50 m, an average of 7.45±0.65 mg/l for TSM (n=31) and 1.26±0.16 mg/l for TOM(n=31), which gives a RSM of 6.19±0.67 mg/l. And we take an average particulate ^{210}Pb concentration, from Tables 4 and 5 and over the same range of water depths, of 1.92±0.33 dpm/100 kg (n=31). The result of C_{susp} is a ^{210}Pb/RSM ratio of about 3.17±0.20 dpm/g. Uncertainties of the mean values assigned here and in the later part of the section are standard errors of the means.

The data of ^{210}Pb content from the sediment of the study area (Zuo et al., 1989; sediment core positions are shown by triangles in Fig. 1) can be used to estimate C_{sed}. The 13 sediment cores give a mean ^{210}Pb content of 0.91±0.09 dpm/g. Taking the total organic matter of 5% in sediment (Zuo and Eisma, 1992), this leads to C_{sed} = 0.96±0.09 dpm/g on a refractory sediment basis.

Table 6: *Inventories of ^{210}Pb in the sediment of the southern North Sea.*

Sediment thickness (cm)	^{210}Pb excess (dpm/cm^2)	^{210}Pb accumulation rate (dpm/cm^2/yr)
0 - 35	15.11±1.86[a] (n=13)	0.47±0.06 [b]

a. Assuming ρ = 2.50 g/cm^3, water content = 25% (Zuo et al., 1989).
b. see text.

To estimate the mean excess ^{210}Pb inventory (M), we believe that the available data from the Oyster Ground sediments (Zuo et al., 1989) are representative for this study area, and have adopted a value of 15.11±1.86 dpm/cm^2 as M (Table 6). Decay of this inventory would give a removal flux of 0.47±0.06 dpm/cm^2/yr at steady state, with respect to the ^{210}Pb mean life of 32.2 yrs, almost exactly in balance with the input of ^{210}Pb from the atmosphere (Table 6). The accumulation rate in the sediment was estimated to be in the range of 0.02 - 0.40 cm/yr (Zuo et al., 1989). For this calculation we take a mid value of 0.12 g/cm^2/yr (assuming w = 25%, particle density = 2.5 g/cm^3) as the accumulation flux (G).

Because there is no production or consumption of RSM in the water or sediment, deposition must be balanced by resuspension and accumulation:

$$D = R + G \quad (3)$$

From equations (2) and (3), substituting the estimated values above, we obtain R = 0.04±0.03 g/cm^2/yr and D = 0.16±0.03 g/cm^2/yr. If there is no net burial, then resuspension (R) and deposition (D) would be equal, which gives an upper limit of resuspension rate of 0.21±0.05 g/cm^2/yr. The resuspension rate that we have calculated can be considered as the integrated effect of sediment reworking by a number of processes, by physical as well as biological events.

The additional flux of ^{210}Po in the water column

The ratios of ^{210}Po/^{210}Pb have shown a strong excess of ^{210}Po in the water (previous section), suggesting an additional supply in dissolved ^{210}Po. We try to estimate this excess ^{210}Po flux by considering the total ^{210}Po budget in the water column. Deposition of ^{210}Po and decay loss should be balanced by production from decay of ^{210}Pb, resuspension and the additional flux:

$$DC_{susp} + \lambda C^{tot} = P_{Pb} + R\,C_{sed} + F \quad (4)$$

where C^{tot} is the total ^{210}Po content in the water (dpm/cm^2), P_{Pb} is the production rate of ^{210}Po (dpm/cm^2/yr), F is the additional flux of ^{210}Po (dpm/cm^2/yr) and the other terms are as previously defined. From Table 7 C^{tot} = 0.265±0.02 dpm/cm^2, P_{Pb} = 0.34±0.04 dpm/cm^2/yr, and from Tables 4 and 5, again using RSM = 6.19±0.67 mg/l, and mean particulate ^{210}Po concentration of 2.63±0.30 dpm/100 kg (n=31), C_{susp} = 4.38±0.16 dpm/g. For C_{sed} of ^{210}Po we use the same value of 0.96±0.09 dpm/g as for ^{210}Pb by assuming that ^{210}Po is in equilibrium with ^{210}Pb in sediments. Taking the previous calculated values of R= 0.04±0.03 g/cm^2/yr and D = 0.16±0.03 g/cm^2/yr, we obtain F = 0.81±0.14 dpm/cm^2/yr from eq (4). The uncertainty in terms of R, D and F contributes to the uncertainty in the final estimate of the mass balance.

Table 7: *Inventories of ^{226}Ra, ^{210}Pb and ^{210}Po of the water column in the southern North Sea. Units are dpm/cm^2.*

Reservoir thickness	C_{Ra}^{d}	C_{Po}^{d}	C_{Po}^{p}	C_{Pb}^{d}	C_{Pb}^{p}	C_{Po}^{tot}	C_{Pb}^{tot}
0-50 m	0.34[a]	0.129±0.017	0.136±0.015	0.087±0.015	0.099±0.017	0.265±0.023	0.186±0.020

a. Spencer et al, 1980; Berger and Eisma, 1988.

^{210}Pb and ^{210}Po mass balance in the water column

The inventories of ^{226}Ra, ^{210}Pb and ^{210}Po in the water column were summarized in Table 7 based on the data of Tables 4 and 5. Using a scavenging model to interpret the observed ^{210}Pb and ^{210}Po distributions, and assuming the effect of horizontal transport to be negligible, the steady state equations can be written as follows. For dissolved ^{210}Pb (C^d):

$$\frac{\partial C^d}{\partial t} = 0 = I + P_{Ra} - (\lambda + k)C^d \tag{5}$$

and for particulate ^{210}Pb (C^P):

$$\frac{\partial C^P}{\partial t} = 0 = RC_{sed} + kC^d - \lambda C^P - DC_{susp} \tag{6}$$

where C^d and C^P are the dissolved and particulate ^{210}Pb concentrations; I is the atmospheric input of ^{210}Pb; P_{Ra} is the production rate of ^{210}Pb from its parent nuclide ^{226}Ra; k is assumed to be the *in situ* first order scavenging rate constant of ^{210}Pb, referring to a transfer of dissolved ^{210}Pb to particulate ^{210}Pb and the other terms are as defined before. The residence time at the steady state is given by $\tau = 1/k$.

In equations (5) and (6) we have neglected the effect of diffusion and advection since we are only considering the water column as a well mixed single box, with the deposition of particulate matter determining the removal of ^{210}Pb from the water column.

Equation (5) gives the balance between production and atmospheric flux of dissolved ^{210}Pb and loss terms:

$$C^d = \frac{I + P}{\lambda + k} \tag{7}$$

Solving equation (7) by substitution of numeric values from Table 4 gives $k=5.03\pm1.35$ yr^{-1}, and the residence time of dissolved ^{210}Pb is $\tau_{Pb}{}^d = 1/k = 0.20\pm0.05$ yr.

For equation (6) at steady state, the resuspension and uptake of ^{210}Pb must balance the decay and removal of ^{210}Pb:

$$RC_{sed} + KC^d = \lambda C^P + DC_{susp} \tag{8}$$

which gives the average particle removal rate (DC_{susp}) of 0.51 ± 0.09 $dpm/cm^2/yr$ and the particulate ^{210}Pb residence time ($\tau_{Pb}{}^P = C^P/[DC_{susp}]$) of 0.19 ± 0.05 yr.

Constructing a material balance of ^{210}Po, we have for particulate ^{210}Po at the steady state:

$$\frac{\partial C^P}{\partial t} = 0 = P_{Pb}^P + RC_{sed} + k'C^d - \lambda C^P - DC_{susp} \tag{9}$$

and for dissolved ^{210}Po:

$$\frac{\partial C^d}{\partial t} = 0 = P^d_{Pb} + F - \lambda C^d - k'C^d \qquad (10)$$

where k' is the in situ adsorption rate constant of ^{210}Po, P^P_{Pb} and P^d_{Pb} are the production rates of ^{210}Po from decay of ^{210}Pb in particulate and dissolved phases, respectively.

The last term ($D\,C_{susp}$) in eq. (9) gives the mean removal rate for particulate ^{210}Po in the water column:

$$D\,C_{susp} = 0.70\pm0.12 \text{ dpm/cm}^2\text{/yr} \qquad (11)$$

and the residence time of particulate ^{210}Po ($\tau_{Po}{}^P = C^P/[DC_{susp}]$) is 0.19±0.04 yr. From eq. (10), using the measured data (Table 7), and F=0.81±0.14 dpm/cm^2/yr, we obtain K' = 5.68±1.37 yr^{-1} and the residence time of ^{210}Po in solution $\tau_{Po}{}^d$ = 0.18±0.04 yr.

Table 8: Summary of mass balance calculations for the southern North Sea.

Reservoir thickness		0 - 50 m
Atmospheric flux of ^{210}Pb		0.43±0.07 dpm/cm^2/yr
The removal rate in particulate form		
	^{210}Pb	0.51±0.09 dpm/cm^2/yr
	^{210}Po	0.70±0.12 dpm/cm^2/yr
The uptake rate from solution		
	^{210}Pb	0.44±0.12 dpm/cm^2/yr
	^{210}Po	0.73±0.20 dpm/cm^2/yr
Residence time		
	$\tau_{Pb}{}^d$	0.20±0.05 yr
	$\tau_{Po}{}^d$	0.18±0.04 yr
	$\tau_{Pb}{}^P$	0.19±0.05 yr
	$\tau_{Po}{}^P$	0.19±0.04 yr
Excess ^{210}Po flux from sediment		0.81±0.14 dpm/cm^2/yr
Sediment resuspension rate		0.04±0.03 g/cm^2/yr
Particle deposition rate		0.16±0.03 g/cm^2/yr

The results obtained from the above calculations are summarized in Table 8. The computed residence times for ^{210}Po and ^{210}Pb in both forms range from 66 to 80 days (0.18-0.20 yrs) which are not well constrained but consistent with those found by others in shallow water areas (Bacon et al., 1976; Santschi et al., 1979;

Eisma et al., 1989). The greater adsorption rate of dissolved ^{210}Po (0.73±0.20 dpm/cm^2/yr; Table 8) as compared with ^{210}Pb (0.44±0.12 dpm/cm^2/yr), indicates a preferential uptake and highly effective recycling of ^{210}Po in these coastal and shelf waters of the southern North Sea. But even so, because of the additional source of ^{210}Po from the underlying sediment, an excess of total ^{210}Po in the standing stock of the study area still remains. Based on this type of distribution of two elements, one would expect to find ^{210}Po deficiency in the sediments to balance the excess that we observed in the water column. Our measurements of ^{210}Pb and ^{210}Po in the sediment, unfortunately, did not show significant disequilibrium between those two, which appears to contradict the last statement. However, the mean excess of total ^{210}Po is about 0.08 dpm/cm^2 (Table 7) which would only account for less than 1% of the mean inventory of ^{210}Pb (15.11±1.86 dpm/cm^2, Table 6) in the sediment. This kind of deficit of ^{210}Po is within the error range of the measurements and is therefore too small to be identified. Thus, we conclude that only a small amount of deficiency of ^{210}Po (probably <0.1 dpm/cm^2) in the sediment would be enough to compensate the observed excess in the water body. It is important to note that the atmospheric input of ^{210}Pb in the study area is about a factor of two to three lower than it is around the North America where much of the previous data for the continental shelf have been collected (Benninger, 1978; Turekian et al., 1983), which, together with the facts of high concentration of suspended matter in the water and high rates of sediment resuspension, is probably responsible for the low ^{210}Pb concentrations that were found in the water and the low required deficit of ^{210}Po in the sediment.

Subtracting the sediment resuspension rate (0.04 g/cm^2/yr, Table 8) from the particle deposition rate (0.16 g/cm^2/yr, Table 8), leads to a net accumulation rate of 0.12 g/cm^2/yr. The depositional area of fine grained sediment in the study area was estimated to be about 1000 km^2, using the net accumulation rate of 0.12 g/cm^2/yr, we obtain the total amount of annual deposition of 1.2 x 10^9 kg in the muddy zone. This number is in the order of 50% less than what we estimated previously (Zuo et al., 1989), which was calculated without taking the effects of bioturbation into account.

It is also realized that the calculations based on the above simplified model were based on a first order irreversible scavenging process with the assumption that the changes due to diffusion and advection are small when compared with the production and loss terms. Bacon and Anderson (1982) and Nozaki (1986) have shown that scavenging may best be described by a reversible process for ^{210}Pb.

Unfortunately, we could not apply the reversible model for our calculations from the data available. Taking the reversible effect into account would increase uptake rates of dissolved ^{210}Pb and ^{210}Po and accordingly decrease the residence time of dissolved nuclides in solution. For better understanding of the scavenging processes of ^{210}Pb and ^{210}Po in the water column, a further study of multiple tracer distributions and ratios in the water and the sediment column is needed. In addition, horizontal and vertical transport of ^{210}Pb and ^{210}Po by eddy diffusion and advection in this coastal shallow water area also will be important for the removal of nuclides, which needs further investigation and evaluation.

6. CONCLUSIONS

The nearshore and shelf areas of the southern North Sea are effective sinks for ^{210}Pb and ^{210}Po. The distributions of ^{210}Pb and ^{210}Po in the water column show a strong excess of ^{210}Po in both dissolved and particulate forms, indicating an additional source of ^{210}Po from the bottom sediments. A significant maximum of both dissolved ^{210}Pb and ^{210}Po near the boundary layer at the northern stations of the study area is likely to be the result of resuspension of the underlying muddy sediments.

A budget for ^{210}Pb and ^{210}Po in the study area using a box model is presented, which allows the calculation of sediment resuspension and deposition rates at the water-sediment interface and residence times, uptake and removal rates in the water column for both radioactive nuclides. The quantitative conclusions that we have drawn here (listed in Table 8) are based on a limited data set, so that our estimates have rather large uncertainties. However, we have carefully assigned the uncertainties and therefore our major conclusions are essentially correct. The residence times for ^{210}Po and ^{210}Pb that we have obtained are in the order of 66-80 days which are consistent with those from other observations in the shallow coastal and shelf waters. The removal because of scavenging by sinking particles is strongly enhanced by resuspension and re-deposition. The K_d values are in inversely related to the concentration of total suspended matter which can be explained by resuspension of 'old' particles. The removal rate of ^{210}Pb is about equal to the flux from the atmosphere. River input of ^{210}Pb and ^{210}Po is not important. The low concentration of ^{210}Pb in the study area is related to the low atmospheric input of ^{210}Pb, the high concentration of suspended matter and the high sediment resuspension rates.

A comparison of the water and sediment data shows that only a small deficit of ^{210}Po in the sediment is enough to balance the excess of ^{210}Po that is present in the water column due to the characteristics that we discussed above of this continental shelf area. It is realized that lateral transport of ^{210}Pb and ^{210}Po, which we ignored in the calculations, can also be important in scavenging, recycling and deposition, and a reversible scavenging model would be more realistic in interpreting the processes in the water column.

ACKNOWLEDGEMENTS--We thank R. L. Groenewegen for his help with the CTD measurements; C. Fisher for his assistance in water sample collection and filtration; the captain and the crew of the R. V. *Aurelia* for their cooperation during the cruise; and B. R. Kuipers, H. Witte and H. J. Boekel for the use of water box. J. van der Plicht and H. Heijnis kindly provided the rain water samples and helpful discussions for this work; G. W. Berger supervised water sample collection and analyses; R. Gieles assisted with the stable Pb analyses; B. Verschuur helped in the preparation of some of the figures. Their efforts are particularly appreciated. Finally, we are especially grateful to M. P. Bacon, J. K. Cochran and R. F. Anderson for their fruitful discussions and valuable suggestions on this manuscript.

REFERENCES

Aken H. M. van (1986) The onset of seasonal stratification in the shelf seas due to differential advection in the presence of a salinity gradient. *Cont. Shelf Res.*, **5**, 475-485.

Bacon M. P., D. W. Spencer and P. G. Brewer (1976) $^{210}Pb/^{226}Ra$ and $^{210}Po/^{210}Pb$ disequilibria in seawater and suspended particulate matter. *Earth Planet. Sci. Lett.*, **32**, 277-296.

Bacon M. P., D. W. Spencer and P. G. Brewer (1978) Lead-210 and Polonium-210 as Marine geochemical tracers: review and discussion of results from the Labrador Sea. In: *Nature radiation environment III*, T. F. Gesell and W. F. Lowder, editors, Proceedings of a symposium held at Houston, Texas, U. S. A. No. 1, pp. 473-501.

Bacon M.P. and R.F. Anderson (1982) Distribution of thorium isotopes between dissolved and particulate forms in the deep sea. *J. Geophys. Res.*, **87**, 2045-2056.

Bacon M. P., R. A. Belastock, M. Tecotzky, K. K. Turekian and D. W. Spencer (1988) Lead-210 and polonium-210 in ocean water profiles of the continental shelf and slope south of New England. *Cont. Shelf Res.*, **8**, 841-853.

Bacon M. P., D. R. Belastock and M. H. Bothner (1991) Lead-210 balance and implications for particle transport on the continental shelf, Middle Atlantic Bight. Submitted.

Benninger L. K. (1978) ^{210}Pb balance in Long Island Sound. *Geochim.Cosmochim. Acta*, **42**, 1165-1174.

Benninger L. K., D. M. Lewis and K. K. Turekian (1975) The use of natural Pb-210 as a heavy metal tracer in the river-estuarine system. In: *Marine chemistry in the coastal environment*, T. M. Church, editor, ACS Symposium Series, No. 18, pp. 202-210.

Berger G.W. and D. Eisma (1988) Verslag van door het NIOZ uitgevoerde ^{210}Po en ^{210}Pb metingen in de Nederlandse kustwateren: de Nieuwe Waterweg, het Noordzeekanaal en de Westerschelde. NIOZ-rapport, **13**, 33 pp.

Biscaye P. E., R. F. Anderson and B. L. Deck (1988) Fluxes of particles and constituents to the eastern United States continental slope and rise: SEEP-I. *Cont. Shelf Res.*, **8**, 855-904.

Chung Y. (1987) ^{210}Po in the western Indian Ocean: distributions, disequilibria and partitioning between the dissolved and particulate phases. *Earth Planet. Sci. Lett.*, **85**, 28-40.

Cochran J. K., M. P. Bacon, S. Krishnaswami and K. K. Turekian (1983) ^{210}Po and ^{210}Pb distribution in the central and eastern Indian Ocean. *Earth Planet. Sci. Lett.*, **65**, 433-452.

Cochran J. K., T. McKibbin-Vaughan, M. M. Dornblaser, D. Hirschberg, H. D. Livingston and K. O. Buesseler (1990) ^{210}Pb scavenging in the North Atlantic and North Pacific Oceans. *Earth Planet. Sci. Lett.*, **97**, 332-352.

Craig H., S. Krishnaswami and B.L.K. Somayajulu (1973) ^{210}Pb- ^{226}Ra: radioactive disequilibrium in the deep sea. *Earth Planet. Sci. Lett.*, **17**, 295-305.

Eisma D. (1981) Supply and deposition of suspended matter in the North Sea. *Spec. Publs int. Ass. Sediment*, **5**, 415-428.

Eisma D. (1990) Transport and deposition of suspended matter in the North Sea and the relation to coastal siltation, pollution, and bottom fauna distribution. *Aquatic Sci.*, **3**, 181-216.

Eisma D. and J. Kalf (1987) Distribution, organic content and particle size of suspended matter in the North Sea. *Neth. J. Sea Res.*, **21**, 265-285.

Eisma D., G. W. Berger, W.-Y. Chen and J. Shen (1989) Pb-210 as a tracer for sediment transport and deposition in the Dutch-German Waddensea. In:

Coastal Lowlands, Geol. and Geotechnol., Proceedings KNGMG Symposium, 1987, pp. 237-253.

Fleer A. P. and M. P. Bacon (1984) Determination of ^{210}Pb and ^{210}Po in seawater and marine particulate matter. *Nucl. Instruments Meth. Phys. Res.,* **223**, 243-249.

Fukuda K. and S. Tsunogai (1975) Pb-210 in precipitation in Japan and its implication for the transport of continental aerosols across the ocean. *Tellus,* **27**, 514-521.

Heyraud M., S. W. Fowler, T. M. Beasley and R. D. Cherry (1976) Polonium-210 in Euphausiids: A detailed study. *Marine Biol.,* **34**, 127-136.

Moore W.S. and J. Dymond (1988) Correlation of ^{210}Pb removal with organic fluxes in the Pacific Ocean. *Nature,* **331**, 339-341.

Nozaki Y. (1986) ^{226}Ra- ^{222}Rn- ^{210}Pb systematics in seawater near the bottom of the ocean. *Earth Planet. Sci. Lett.* , **80**, 36-40.

Nozaki Y., K.K. Turekian and K. Von Damm (1980) ^{210}Pb in GEOSECS water profiles from the North Pacific. *Earth Planet. Sci. Lett.* , **49**, 393-400.

Otto L., J. T. F. Zimmerman, G. K. Furnes, M. Mork, R. Saetre and G. Becker (1990).Review of the physical oceanography of the North Sea. *Neth. J. Sea Res.,* **26**, 161-238.

Peirson D. H., R. S. Cambray and G. S. Spicer (1966) Lead-210 and polonium-210 in the atmosphere. *Tellus,* **18**, 427-433.

Rama, K. Minuro and E.D. Goldberg (1961) Lead-210 in natural waters. *Science,* **134**, 98-99.

Santschi P. H., Y.-H. Li and J. Bell (1979) Natural radionuclides in the water of Narragansett Bay. *Earth Planet. Sci. Lett.* , **45**, 201-213.

Santschi P. H., Y.-H. Li, J. Bell, R. M. Trier and K, Katwaluk (1980) Pu in coastal marine environments. *Earth Planet. Sci. Lett.* , **51**, 248-265.

Schell W. R. (1977) Concentrations, physico-chemical states and mean residence time of ^{210}Pb and ^{210}Po in marine and estuarine waters. *Geochim. Cosmochim. Acta,* **41**, 1019-1031.

Spencer D. W., M. P. Bacon and P.G. Brewer (1980) The distribution of ^{210}Pb and ^{210}Po in the North Sea. *Thalassia Jugoslavica,* **16**, 125-154.

Spencer D.W., Bacon, M.P. and P.G. Brewer (1981) Models of the distribution of ^{210}Pb in a section across the North Equatorial Atlantic Ocean. *J. Marine Res.,* **39**, 119-138.

Thomson J. and K. K. Turekian (1976) ^{210}Po and ^{210}Pb distributions in ocean water profiles from the eastern south Pacific. *Earth Planet. Sci. Lett.*, **32**, 297-303.

Turekian K. K., L. K. Benninger and E. P. Dion (1983) ^{7}Be and ^{210}Pb total deposition fluxes at New Haven, Connecticut and Bermuda. *J. Geophys. Res.*, **88**, 5411-5415.

Turekian K. K. and J. K. Cochran (1981) ^{210}Pb in surface air at Enewetak and the Asian dust flux to the Pacific. *Nature*, **292**, 522-525.

Turekian K. K.,Y. Nozaki and L. K. Benninger (1977) Geochemistry of atmospheric radon and radon products. *Annu. Rev. Earth Planet. Sci. Lett.*, **5**, 227-255.

Van Haren J. J. M. (1990) Observations on the structure of currents at tidal and sub-tidal frequencies in the central North Sea. Ph.D. dissertation, Utrecht University, The Netherlands, 102 pp.

Zuo Z. and D. Eisma (1992) Spatial distributions of ^{210}Pb and ^{137}Cs and mixing rates in sediments of the southern North Sea. *Cont. Shelf Res.*, Submitted.

Zuo Z., D. Eisma and G. W. Berger (1989) Recent sediment deposition rates in the Oyster Ground, North Sea. *Neth. J. Sea Res.*, **23**, 263-269.

Zuo Z., J. van der Plicht, H. Heijnis and D. Eisma (1992) Deposition fluxes of atmospheric ^{210}Pb in the Netherlands. *Earth Planet. Sci. Lett.*, Submitted.

CHAPTER 5

INFLUENCE OF SEASONAL FORCED SCAVENGING ON THE ^{210}PB AND ^{210}PO BEHAVIOURS IN THE DUTCH COASTAL AND SHELF SEAS

ABSTRACT--Seasonal influences on the distribution of ^{210}Pb and ^{210}Po in the water column was studied in the Dutch coastal zone. The concentration of dissolved ^{210}Pb and ^{210}Po was low during summer months, whereas the particulate content of ^{210}Pb and ^{210}Po was relatively high in spring and winter. The seasonal variation in concentration of the two radionuclides was attributed to high effective scavenging in summer and enhanced resuspension in winter. Seasonal variability of particle flux and particle composition contributes significantly to the seasonal variation of the ^{210}Pb and ^{210}Po distributions. A persistent excess of ^{210}Po with respect to ^{210}Pb in the water is related to the release of ^{210}Po from the coastal and shelf sediments. The residence time of the two nuclides indicates a preferential removal of ^{210}Po over ^{210}Pb from the water column and a highly effective scavenging in summer. An external horizontal influx of ^{210}Pb was indicated by calculations based on a scavenging model. A one-dimensional seasonal model was developed to account for the observed seasonal variation. The predicted time-variation of the total ^{210}Pb and ^{210}Po is in agreement with the field data. It is concluded that ^{210}Pb deposition at the sea surface plays a key role in controlling the distribution of ^{210}Pb and ^{210}Po in the study area; supply of suspended particulate matter and particle composition may also have some importance.

1. INTRODUCTION

Particle-reactive chemical species introduced into river and sea are removed from the water column by scavenging processes. Chemical adsorption onto particulate matter facilitates transport over vast distances before eventual deposition in the sediment. Though scavenging takes place throughout the ocean, it is particularly concentrated at the continental margins. The continental margin is a potential barrier for the transfer of material from land to the ocean basins, especially for those reactive species (suspended solids, trace metals, nutrient elements, etc.) which are likely to settle or change their speciation in the fresh water/salty water mixing zone. To quantify the fluxes of the chemical species by direct methods is not yet possible. However, by using natural radionuclides as tracers, it is possible to identify the mechanisms and time span of the processes

operating in the water and in the sediment, in order to predict the fate of these particle-reactive chemical substances.

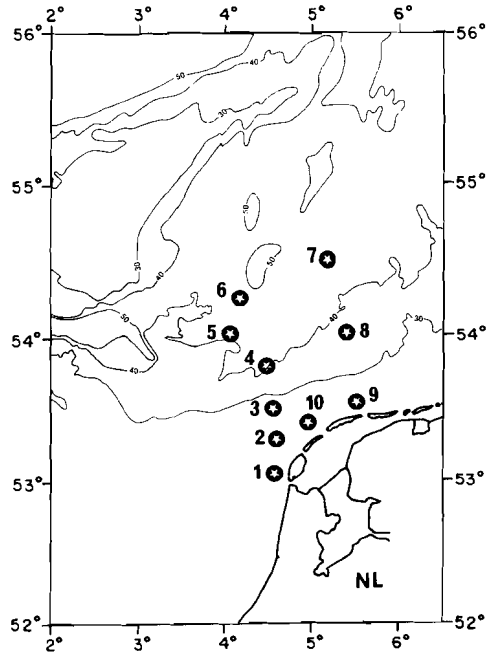

Fig. 1 *Location of seasonal sampling stations in the Dutch coastal and shelf seas (after Zuo and Eisma, 1992a).*

Members of the uranium decay series, particularly ^{210}Pb and ^{210}Po have proven to be useful in this pursuit because of their suitable half-lives and because their sources are well known (Koide et al., 1973; Guinasso and Schink, 1975; Bacon et al., 1978; Carpenter and Beasley, 1981; DeMaster and Cochran, 1982; Buesseler et al., 1985/1986; Bacon et al., 1988). The radioactive disequilibrium between ^{210}Po-^{210}Pb serves as a well-established tool for the measurements of scavenging rates, transport rates and particle mixing rates in nearshore waters and sediments: under steady-state conditions, the distribution of ^{210}Po and ^{210}Pb can be modelled by a

function of radioactive decay, production rate from their parents and transport processes.

Coastal waters often contain much less ^{210}Pb than open ocean surface waters and have a much shorter residence time of ^{210}Pb, which is believed to result from the higher concentrations of suspended matter in these waters (Krishnaswami et al., 1975; Schell, 1977; Spencer et al. 1980; Bacon et al., 1988). The concentrations of suspended particles in the water are very much influenced by the seasonal and short-term variations in water movement, waves conditions and primary productivity. This suggests that the biological and chemical scavenging processes which are dependent on the supply of particulate matter would also exhibit seasonal and short-term variability.

The aim of this study is to determine how the scavenging and transport of ^{210}Pb and ^{210}Po in the water column responds to the seasonal variations of the particle flux in order to gain a better understanding in processes governing sediment transport and deposition and, ultimately, of the fate of particle-reactive chemicals. This was done by carrying out ^{210}Pb and ^{210}Pb radiochemical analyses in both particulate and dissolved forms in the Dutch coastal and shelf seas during different seasons. An earlier preliminary part (the data of November 1989) of this study was published by Zuo and Eisma (1992).

2. SAMPLE COLLECTION.

The water samples used in this investigation were collected with 30l PVC Niskin bottles and at times with a 150l home-made water box at 10 stations located between *ca* 53-54°30'N and 4-5°30'E (Fig. 1). The stations were visited four times between November 1989 and January 1991 (Table 1). Gaps in the record of sampling were caused by rough weathers. Each sample was filtered on board through a 0.45 μm poresize, 142 mm diameter Millipore filter to collect the suspended particulate matter, and the sample for the measurement of dissolved ^{210}Pb and ^{210}Po was obtained by the Co-APDC coprecipitation method (Fleer and Bacon, 1984). At each occupation of the stations, samples of total suspended matter (TSM) were taken by filtration through a 0.40 μm poresize, 47 mm diameter Nucleopore filter. CTD data were obtained with a Guildline CTD (model 8770) during the cruises but not in April and August 1990 because of equipment failure or data loss. More details of sample collection and handling were given by Zuo and Eisma (1992a).

3. RADIOCHEMICAL PROCEDURES

The radiochemical analyses of ^{210}Pb and ^{210}Po were performed in the laboratory of the Institute (NIOZ). All samples for dissolved ^{210}Pb and ^{210}Po were subjected to total dissolution with mixtures of HNO_3, HCl, HF, $HClO_4$ in the presence of ^{208}Po and Pb carrier, added as a yield tracer and recovery indicator. Eventually both nuclides were spontaneously plated on silver discs and counted by alpha-spectrometry. The determination of ^{210}Pb is done by the measurement of ^{210}Po ingrowth after sample solution storage for at least six months. The uncertainties are standard errors based on counting statistics. The recovery was determined by measurement of stable Pb using atomic absorption spectrophotometry. The detailed method, calibration, blank correction and precision together with plating efficiency are described in Zuo and Eisma (1992a).

Table 1: *Location of the seasonal sampling stations in the Dutch coastal and shelf seas.*

Station	Location	Water depth	Sample collection			
		(m)	11/89	04/90	08/90	01/91
1	53°03.40' N 4°37.10' E	19	yes	yes	yes	yes
2	53°17.00' N 4°36.00' E	30	yes	yes	yes	yes
3	53°31.00' N 4°33.00' E	28	yes	yes	yes	yes
4	53°47.00' N 4°32.00' E	41	yes	yes	yes	yes
5	53°59.00' N 4°08.00' E	45	yes	yes	yes	yes
6	54°14.00' N 4°13.00' E	50	yes	yes	yes	yes
7	54°28.00' N 5°11.70' E	42	yes	no	yes	yes
8	54°00.00' N 5°23.00' E	39	yes	yes	yes	no
9	53°32.23' N 5°30.13' E	20	yes	yes	yes	no
10	53°23.00' N 4°55.20' E	21	yes	yes	yes	no

The concentration of ^{226}Ra (half life 1.622 yr) at four stations (station 3 to 6) for three sampling periods (except for January 1991) was determined indirectly by

measuring the activity of its radioactive daughter ^{222}Rn (half-life 3.82 d). The procedure for extraction is based on a method described by Glover and Reeburgh (1987) and van der Wijk (1987). The sample was suspended in approximately 300 ml of demineralized water in gas wash bottle. The overlying air, which may contain some ^{222}Rn, was replaced by helium to assure zero initial ^{222}Rn concentration. The bottle was closed and stored for about two weeks to allow the growth of ^{222}Rn. This ^{222}Rn was then stripped from the sample with a circulating helium stream and trapped on a cooled activated charcoal column. The radon was eventually transferred to an alpha scintillation counting cell, which was connected to a photomultiplier that registers an alpha particle by emission of a light pulse. From the number of light pulses the ^{226}Ra activity was calculated (Sarmiento et al. 1976; van der Wijk, 1987). The blank activity was determined by applying the extraction and transfer procedure to a wash bottle filled with demi-water and a correction was made accordingly. The overall efficiency was determined by measuring a ^{226}Ra standard sediment sample, kindly provided by the Marine Sciences Research Center (Stony Brook State University of New York, USA). The results showed that the overall efficiency of our system is about 85% for the counting cells used. For this percentage all the measured data were corrected.

4. SEASONAL INFLUENCES ON THE BEHAVIOURS OF ^{210}PB AND ^{210}PO

Table 2 lists the concentrations of total suspended matter (TSM), total organic matter (TOM), ^{226}Ra and dissolved and particulate ^{210}Pb and ^{210}Po. The sample collection covered approximately each season. ^{210}Pb and ^{210}Po, as well as TSM and TOM for station 1 to 6 (running from S to N crossing the isobaths) for the three seasons (April 90, Aug. 90 and Jan. 91) is shown in Fig. 2 to 4, the distributions for the season of November 1989 were given previously by Zuo and Eisma (1992). The hydrographic parameters (salinity, temperature and density) for the season of January 1991 are also shown in Fig. 4.

Temporal and spatial distributions

Inspection of the detailed distribution sections of salinity, temperature and density excess (Fig. 4j, k, l; Figs 2-4, Zuo and Eisma, 1992a) reveals that high salinity (> 34.5‰) and high temperature (>11.8 °C in 89; > 6.2 °C in Jan. 91) are generally located at the northernmost stations (stations 4-7, Fig. 1) with the salinity and temperature decreasing gradually to the south and east, which reflects the mixing of the saline Central North Sea water with less saline coastal water. In Jan. 1991, the

Table 2: *Seasonal ^{210}Pb , ^{210}Po and ^{226}Ra data from the southern North Sea. Concentrations are given in dpm/100kg sea water.*[a]

Depth (m)	TSM (mg/l)	TOM (mg/l)	Diss. ^{210}Pb	Part. ^{210}Pb	Diss. ^{210}Po	Part. ^{210}Po	^{226}Ra	Po/Pb Diss.	Po/Pb Part.
November 20-21, 1989[b]									
ST1									
5	5.04	1.32	16.81±1.32	13.39±1.08	21.87±0.98	7.92±0.42	n.m.[c]	1.30	0.59
15	5.64	0.76	1.35±0.24	9.04±0.73	1.56±0.16	8.80±0.47	n.m.	1.15	0.97
ST 2									
5	3.85	0.36	0.75±0.19	2.09±0.29	1.61±0.16	3.68±0.27	n.m.	2.15	1.76
15	2.97	0.35	0.48±0.23	9.47±1.20	9.32±1.60	9.85±0.78	n.m.	19.60	1.04
25	2.71	0.35	1.02±0.21	2.75±0.35	1.37±0.15	3.59±0.28	n.m.	1.34	1.31
ST 3									
5	10.77	1.66	0.65±0.16	2.59±0.33	1.19±0.12	3.87±0.29	2.72±0.58	1.81	1.49
15	10.74	2.84	1.92±0.29	2.70±0.27	1.84±0.18	4.24±0.32	2.92±0.12	0.96	1.57
25	2.70	0.18	0.72±0.16	3.29±0.34	1.89±0.25	5.08±0.37	3.47±0.08	2.61	1.54
ST 4									
5	4.94	0.24	1.87±0.24	2.14±0.25	4.66±0.51	2.50±0.25	1.56±0.18	2.49	1.17
15	8.56	1.30	0.63±0.13	1.62±0.21	1.59±0.24	2.57±0.22	2.89±0.12	2.54	1.59
25	1.98	0.25	0.45±0.11	1.52±0.19	1.37±0.22	2.80±0.24	2.49±0.01	3.07	1.84
35	5.94	0.71	5.33±0.59	6.09±0.68	0.82±0.14	2.78±0.23	2.19±0.01	0.15	0.46
ST 5									
5	4.54	0.40	0.70±0.13	0.87±0.16	1.72±0.30	1.82±0.17	3.54±0.33	2.44	2.10
15	6.42	0.98	0.86±0.17	0.62±0.13	1.66±0.25	1.12±0.13	2.40±0.04	1.92	1.80
25	6.34	1.16	0.80±0.15	0.48±0.11	2.11±0.27	1.65±0.17	2.02±0.15	2.65	3.43
35	1.36	0.03	8.11±0.59	0.49±0.10	7.78±0.58	1.53±0.16	2.44±0.12	0.96	3.13
ST 6									
5	7.98	0.48	0.95±0.18	0.79±0.15	2.69±0.37	1.69±0.14	5.36±0.09	2.82	2.13
15	10.96	2.42	1.74±0.26	0.79±0.16	2.47±0.30	1.32±0.13	2.18±0.53	1.41	1.66
25	9.88	1.04	1.83±0.24	1.07±0.16	1.23±0.16	1.79±0.16	2.14±0.34	0.67	1.68
35	10.62	1.50	2.85±0.32	0.68±0.14	5.27±0.49	1.43±0.15	2.04±0.09	1.85	2.11
45	9.14	2.26	1.90±0.25	0.70±0.13	1.90±0.23	1.57±0.16	3.94±0.82	1.00	2.25
ST 7									
5	7.60	0.36	0.20±0.06	0.86±0.16	1.93±0.36	1.71±0.16	n.m.	9.69	1.99
15	1.96	0.16	3.68±0.43	4.57±0.48	1.89±0.25	1.47±0.14	n.m.	0.51	0.32
25	11.02	2.72	0.95±0.14	1.02±0.17	2.34±0.26	1.75±0.18	n.m.	2.48	1.72
35	2.62	0.16	0.23±0.06	0.64±0.13	1.53±0.24	2.04±0.20	n.m.	6.68	3.20
ST 8									
5	15.76	2.48	0.49±0.11	2.53±0.29	1.94±0.25	3.78±0.29	n.m.	3.96	1.50
15	5.74	0.34	0.56±0.10	3.32±0.34	1.68±0.22	4.15±0.32	n.m.	3.00	1.25
25	5.64	0.70	0.86±0.14	3.82±0.40	2.15±0.25	3.97±0.31	n.m.	2.48	1.04
35	11.30	1.30	0.46±0.08	2.30±0.23	1.50±0.21	3.81±0.36	n.m.	3.27	1.66
ST 9									
5	8.76	0.94	1.03±0.14	2.05±0.23	2.29±0.24	3.13±0.31	n.m.	2.22	1.52
15	11.92	1.76	0.70±0.10	1.80±0.20	3.04±0.38	3.58±0.38	n.m.	4.36	1.99
ST 10									
5	10.36	2.44	0.78±0.12	2.23±0.26	2.56±0.31	2.58±0.22	n.m.	3.27	1.16
15	10.10	2.10	1.51±0.21	2.66±0.28	4.99±0.51	3.82±0.35	n.m.	3.30	1.44

water column was layered in the top 10 m with salinity and temperature decreasing upwards (Fig. 4j, k). Below this layer the water column was relatively well mixed.

Table 2: *continued.*

Depth (m)	TSM (mg/l)	TOM (mg/l)	Diss. ^{210}Pb	Part. ^{210}Pb	Diss. ^{210}Po	Part. ^{210}Po	^{226}Ra	Po/Pb Diss.	Po/Pb Part.
April 2-6, 1990									
ST1									
5	10.37	4.23	1.09±0.22	9.85±1.60	1.92±0.39	4.90±0.62	n.m.	1.76	0.50
15	11.95	3.28	0.99±0.17	7.76±0.98	2.19±0.24	8.09±0.60	n.m.	2.20	1.04
ST 2									
5	4.44	1.20	1.10±0.21	3.57±0.44	1.13±0.14	6.51±0.34	n.m.	1.03	1.82
15	4.63	1.12	0.82±0.14	4.05±0.48	0.98±0.13	4.27±0.27	n.m.	1.19	1.06
25	11.23	2.11	0.84±0.17	3.16±0.28	1.10±0.12	4.94±0.29	n.m.	1.30	1.56
ST 3									
0	2.76	1.27	2.51±0.28	3.88±0.48	1.56±0.18	3.13±0.20	3.52±0.58	0.62	0.81
5	5.92	1.34	0.66±0.11	2.55±0.37	0.71±0.10	3.55±0.19	3.20±0.11	1.07	1.39
15	11.40	2.36	0.54±0.10	3.66±0.42	1.17±0.13	4.13±0.24	2.53±0.16	2.17	1.13
25	16.80	2.70	0.69±0.14	8.64±0.76	0.88±0.11	8.98±0.34	2.93±0.53	1.29	1.04
ST 4									
0	1.57	1.03	0.89±0.15	1.84±0.29	0.80±0.10	1.56±0.11	n.m.	0.90	0.85
5	4.64	0.69	0.71±0.14	1.52±0.28	0.79±0.10	1.83±0.12	2.99±0.11	1.11	1.20
15	5.33	1.15	1.15±0.20	1.26±0.21	1.35±0.15	1.90±0.14	2.98±0.21	1.18	1.50
25	4.26	0.96	0.51±0.10	0.93±0.18	0.81±0.10	1.90±0.14	2.93±0.28	1.58	2.04
35	5.38	1.42	0.44±0.10	1.16±0.15	1.13±0.13	4.34±0.35	1.60±0.08	2.59	3.73
ST 5									
0	5.08	0.25	1.05±0.19	1.31±0.13	0.78±0.10	1.06±0.12	3.38±0.20	0.74	0.81
5	7.02	0.66	0.73±0.13	0.85±0.15	0.85±0.09	1.08±0.15	n.m.	1.16	1.27
15	4.64	0.68	0.66±0.15	0.74±0.13	0.43±0.08	1.02±0.12	4.67±0.44	0.65	1.37
25	2.02	0.72	2.95±0.32	1.01±0.15	2.32±0.19	1.01±0.10	4.15±0.73	0.79	1.00
35	7.64	2.26	0.59±0.10	1.07±0.14	0.58±0.07	1.27±0.14	2.22±0.36	0.99	1.19
ST 6									
0	8.51	1.13	0.54±0.10	2.11±0.20	0.73±0.09	1.90±0.15	3.39±0.19	1.36	0.90
5	3.23	0.48	0.57±0.11	1.28±0.19	0.71±0.09	1.15±0.11	n.m.	1.24	0.90
15	5.84	0.60	0.54±0.10	0.81±0.13	0.60±0.08	1.42±0.12	2.32±0.01	1.12	1.76
25	8.52	0.34	0.61±0.12	1.53±0.23	1.33±0.16	5.05±0.35	n.m.	2.14	3.31
35	0.42	0.02	1.28±0.22	1.48±0.20	0.35±0.05	1.24±0.11	1.73±0.36	0.28	0.84
45	2.44	0.28	2.26±0.30	1.07±0.14	1.91±0.23	1.47±0.13	2.80±0.06	0.85	1.37
ST 8									
0	5.56	0.42	1.62±0.25	2.40±0.24	3.61±0.32	3.30±0.24	n.m.	2.23	1.38
5	9.18	1.32	0.88±0.17	2.83±0.26	1.02±0.11	3.19±0.20	n.m.	1.16	1.13
15	4.82	1.00	0.82±0.14	2.78±0.25	0.93±0.11	3.15±0.24	n.m.	1.13	1.13
25	11.54	1.56	0.70±0.15	3.60±0.29	1.07±0.11	4.03±0.22	n.m.	1.52	1.12
35	10.28	1.30	0.60±.13	4.01±0.32	0.74±0.08	4.97±0.26	n.m.	1.23	1.24
ST 9									
0	10.32	2.86	1.29±0.25	2.70±0.25	1.03±0.15	3.73±0.21	n.m.	0.80	1.38
5	9.83	2.88	0.96±0.20	3.12±0.29	0.90±0.12	3.95±0.21	n.m.	0.94	1.27
15	12.97	3.77	2.02±0.43	4.43±0.45	2.71±0.45	4.96±0.31	n.m.	1.34	1.12
ST 10									
0	8.27	1.87	2.72±0.73	2.87±0.32	2.21±0.50	10.94±0.77	n.m.	0.81	3.81
5	5.26	1.97	0.91±0.19	4.25±0.33	0.74±0.12	4.74±0.30	n.m.	0.82	1.12
15	16.40	3.23	2.51±0.60	5.45±0.42	3.05±0.70	7.32±0.54	n.m.	1.22	1.34

The same situation was also observed in November 1989 at stations 4-8. This was explained by mixing Central North Sea water with the coastal water (Zuo and Eisma, 1992a). During or sometime prior to the sample collection, the colder and

Table 2: *continued*.

Depth (m)	TSM (mg/l)	TOM (mg/l)	Diss. ^{210}Pb	Part. ^{210}Pb	Diss. ^{210}Po	Part. ^{210}Po	^{226}Ra	Po/Pb Diss.	Po/Pb Part.
August 27-28, 1990.									
ST1									
0	5.58	2.80	1.97±0.29	2.36±0.28	1.71±0.16	7.96±1.01	n.m.	0.87	3.38
5	3.16	1.22	2.06±0.37	2.06±0.23	1.34±0.13	5.14±0.45	n.m.	0.65	2.49
15	5.40	2.40	1.20±0.26	2.94±0.31	2.06±0.16	4.88±0.42	n.m.	1.72	1.66
ST2									
0	7.23	1.93	0.55±0.11	1.27±0.21	1.71±0.14	6.94±0.85	n.m.	3.09	5.46
5	4.60	2.28	1.02±0.21	1.12±0.14	1.59±0.16	3.59±0.38	n.m.	1.56	3.20
15	5.58	2.40	1.35±0.18	0.62±0.12	2.32±0.20	2.46±0.22	n.m.	1.72	3.94
ST3									
0	6.68	3.42	0.68±0.14	0.77±0.11	2.19±0.28	3.23±0.29	2.81±0.44	3.20	4.18
5	3.14	1.58	1.19±0.24	0.75±0.10	2.16±0.24	3.18±0.33	3.29±0.16	1.82	4.23
15	1.72	1.16	1.38±0.25	1.03±0.14	1.73±0.15	3.07±0.27	3.88±0.09	1.26	2.97
25	2.13	1.31	1.06±0.22	1.00±0.12	1.52±0.13	3.52±0.28	3.29±0.46	1.43	3.50
ST4									
0	1.78	0.88	0.87±0.17	0.54±0.10	1.16±0.10	2.13±0.29	n.m.	1.33	3.97
5	1.73	0.84	1.01±0.22	0.74±0.10	0.93±0.09	2.22±0.23	3.06±0.09	0.92	3.01
15	1.76	0.20	0.42±0.10	0.31±0.05	1.52±0.20	1.49±0.18	2.89±0.35	3.62	4.75
25	1.20	0.59	0.61±0.13	0.54±0.09	1.31±0.12	1.50±0.17	3.95±0.45	2.15	2.76
35	10.19	2.10	1.55±0.35	1.35±0.20	1.06±0.16	3.05±0.44	3.29±0.18	0.68	2.27
ST5									
0	2.93	1.07	2.16±0.39	0.91±0.11	1.63±0.20	1.95±0.23	4.44±0.38	0.75	2.15
5	2.07	0.71	0.85±0.21	0.48±0.08	1.54±0.24	1.46±0.20	2.29±0.15	1.82	3.04
15	3.86	1.47	0.47±0.13	0.35±0.06	0.59±0.14	0.80±0.10	5.73±0.01	1.26	2.25
25	3.91	1.79	0.45±0.13	0.41±0.06	1.55±0.34	0.77±0.10	3.49±0.11	3.47	1.90
35	3.54	2.41	1.12±0.27	0.43±0.06	1.07±0.26	0.89±0.13	3.76±0.64	0.96	2.08
ST6									
0	1.16	0.60	0.78±0.10	0.65±0.09	0.56±0.09	1.69±0.15	2.73±0.18	0.71	2.61
5	2.30	0.91	0.65±0.15	0.38±0.06	0.47±0.10	1.40±0.15	2.95±0.08	0.72	3.68
15	3.96	1.36	1.05±0.23	0.55±0.09	0.81±0.14	1.57±0.25	3.60±0.25	0.77	2.84
25	3.90	0.80	0.61±0.09	0.60±0.10	1.35±0.17	1.02±0.18	3.39±0.31	2.22	1.70
35	4.60	1.87	0.54±0.11	0.72±0.11	0.65±0.10	1.28±0.21	3.38±0.32	1.20	1.78
45	4.15	1.19	0.84±0.20	0.94±0.11	0.37±0.07	0.78±0.15	4.18±0.21	0.44	0.82
ST7									
0	0.61	0.12	0.68±0.19	0.66±0.11	2.38±0.44	1.80±0.18	n.m.	3.51	2.74
5	0.94	0.20	0.45±0.13	0.56±0.10	0.42±0.09	1.76±0.21	n.m.	0.92	3.17
15	0.96	0.21	0.49±0.12	1.04±0.12	1.30±0.18	0.83±0.10	n.m.	2.62	0.80
25	1.04	0.44	0.63±0.18	3.73±0.22	0.88±0.19	0.21±0.03	n.m.	1.40	0.06
35	1.24	0.27	0.53±0.15	0.67±0.10	0.96±0.14	1.35±0.14	n.m.	1.82	2.01
ST8									
0	2.10	0.64	1.33±0.29	1.16±0.13	1.15±0.17	3.04±0.28	n.m.	0.86	2.62
5	1.50	0.60	0.78±0.13	1.26±0.16	1.38±0.16	3.01±0.28	n.m.	1.78	2.40
15	2.17	0.64	1.44±0.35	1.22±0.18	1.13±0.14	2.90±0.25	n.m.	0.79	2.38
25	3.75	0.92	0.59±0.11	1.27±0.18	1.65±0.17	2.96±0.33	n.m.	2.81	2.33
35	6.94	2.39	1.02±0.28	1.43±0.21	0.94±0.13	2.75±0.29	n.m.	0.92	1.92
ST9									
0	1.52	0.50	0.94±0.15	0.85±0.12	1.48±0.16	3.28±0.26	n.m.	1.57	3.88
5	1.88	0.60	0.85±0.29	0.75±0.14	1.12±0.12	2.94±0.24	n.m.	1.32	3.90
15	1.48	0.54	0.64±0.12	0.50±0.10	1.43±0.16	3.53±0.30	n.m.	2.22	7.00
ST10									
0	1.46	0.78	0.87±0.16	0.84±0.13	1.44±0.16	4.09±0.50	n.m.	1.66	4.86
5	1.10	0.80	1.25±0.16	0.43±0.08	1.78±0.19	2.62±0.32	n.m.	1.43	6.08
15	2.12	1.06	1.42±0.38	0.58±0.10	1.33±0.16	1.86±0.26	n.m.	0.94	3.19

Table 2: *continued.*

Depth (m)	TSM (mg/l)	TOM (mg/l)	Diss. ^{210}Pb	Part. ^{210}Pb	Diss. ^{210}Po	Part. ^{210}Po	^{226}Ra	Po/Pb Diss.	Po/Pb Part.
January 14-15, 1991									
ST1									
0	9.28	0.88	0.69±0.13	8.39±0.80	2.33±0.26	6.87±0.60	n.m.	3.36	0.82
5	13.48	1.84	0.88±0.15	4.43±0.80	1.50±0.17	6.98±1.02	n.m.	1.71	1.58
15	13.40	2.70	0.84±0.20	10.17±1.00	1.64±0.20	11.39±0.98	n.m.	1.97	1.12
ST2									
0	7.70	1.40	1.45±0.23	4.16±0.50	2.26±0.25	4.54±0.61	n.m.	1.56	1.09
5	4.48	0.18	1.44±0.24	2.72±0.41	1.55±0.16	4.12±0.42	n.m.	1.08	1.52
15	5.67	1.37	1.36±0.21	4.76±0.49	2.32±0.27	5.09±0.55	n.m.	1.71	1.07
25	8.63	1.37	1.27±0.20	6.29±0.57	1.52±0.16	7.54±0.65	n.m.	1.20	1.20
ST3									
0	9.22	1.52	2.99±0.27	7.38±0.73	3.10±0.23	6.23±0.49	n.m.	1.04	0.84
5	9.68	1.08	1.08±0.15	5.74±0.54	2.53±0.22	6.54±0.54	n.m.	2.34	1.14
15	10.29	1.05	1.69±0.19	4.86±0.54	2.50±0.23	6.66±0.59	n.m.	1.48	1.37
25	11.91	1.79	1.23±0.18	5.08±0.55	1.98±0.19	6.92±0.58	n.m.	1.61	1.36
ST4									
0	5.80	0.36	2.66±0.32	3.70±0.43	3.52±0.30	4.75±0.45	n.m.	1.33	1.28
5	6.24	0.95	0.71±0.11	2.91±0.37	3.11±0.36	4.16±0.39	n.m.	4.36	1.43
15	6.33	0.55	1.76±0.27	2.91±0.32	1.31±0.18	4.21±0.39	n.m.	0.75	1.45
25	7.01	0.85	1.60±0.21	3.22±0.37	2.00±0.24	4.06±0.41	n.m.	1.24	1.26
35	7.63	0.71	1.56±0.23	3.78±0.40	1.12±0.16	4.18±0.28	n.m.	0.72	1.11
ST5									
0	3.43	0.15	0.86±0.14	2.51±0.38	1.94±0.19	3.34±0.42	n.m.	2.26	1.33
5	5.35	0.48	0.97±0.14	2.40±0.23	2.37±0.29	3.21±0.27	n.m.	2.44	1.34
15	4.07	0.40	0.84±0.13	2.96±0.33	1.23±0.14	3.66±0.28	n.m.	1.47	1.23
25	4.39	0.73	0.71±0.10	2.01±0.22	1.45±0.13	2.61±0.22	n.m.	2.06	1.30
35	4.49	0.09	0.90±0.14	2.81±0.33	1.73±0.19	3.60±0.38	n.m.	1.93	1.28
ST6									
0	3.61	0.19	1.26±0.16	2.30±0.25	1.16±0.13	2.86±0.29	n.m.	0.92	1.25
5	4.55	0.95	0.93±0.13	1.78±0.23	1.58±0.18	3.20±0.32	n.m.	1.69	1.79
15	6.11	0.48	0.66±0.12	2.05±0.27	1.21±0.15	3.01±0.29	n.m.	1.82	1.47
25	4.40	0.87	2.49±0.27	2.16±0.30	3.14±0.31	2.77±0.25	n.m.	1.26	1.28
35	3.91	0.64	0.82±0.13	2.22±0.26	1.31±0.17	3.27±0.32	n.m.	1.58	1.47
45	5.47	0.72	1.31±0.15	2.33±0.28	1.26±0.17	3.24±0.26	n.m.	0.96	1.39
ST7									
0	9.15	1.24	1.31±0.21	4.53±0.63	2.61±0.26	5.42±0.57	n.m.	1.99	1.20
5	8.52	1.55	1.26±0.17	3.58±0.31	2.06±0.23	4.84±0.33	n.m.	1.63	1.35
15	11.36	1.32	1.70±0.19	4.47±0.38	1.88±0.20	5.19±0.39	n.m.	1.11	1.16
25	10.03	1.17	0.95±0.14	4.80±0.46	1.17±0.12	4.37±0.35	n.m.	1.23	0.91
35	10.29	1.83	1.55±0.17	4.73±0.39	1.41±0.15	5.40±0.38	n.m.	0.91	1.14

a. All data of isotopes are decay corrected to the sampling date. Uncertainties are 1 s standard errors based on counting statistics.
b. The November data set has been published previously (Zuo and Eisma, 1992a) except for the ^{226}Ra data.
c. n.m.= not measured.

fresher Dutch coastal water penetrated northward over the transition zone between the 30 and 40 m isobaths, which resulted in the gradients of salinity, temperature and density in the water column. Studies show that from spring till autumn the water column is thermally stratified north 53°30 N, with a transition zone between

the 30 and 40 m isobaths (van Aken, 1986), while the southern part is vertically well mixed throughout the year. The thermal stratification, however, is not stable, it will be destroyed during storm events (van Haren, 1990).

The sources of suspended material to the Dutch coastal zone are the English Channel, the Flemish Banks, the seafloor, the coasts erosion, the rivers and the atmosphere (Eisma, 1990; Visser et al., 1991). The transported water masses and suspended particle fluxes through the Strait of Dover into the the southern North Sea both reach a maximum in winter and are relatively small in spring and summer. Accordingly, the total amount of suspended matter present in the Dutch coastal zone shows seasonal fluctuation (Visser et al., 1991). The measurements of TSM in this study also reveal a seasonal variability; in the winter the concentrations were higher than in summer, both in the coastal and off-shore waters (Table 2). The average concentration of TSM (for each season) shows a maximum in November 1989 (7.45±0.65 mg/l, range 1.36-15.76) and minimum in August 1990 (2.95±0.33 mg/l, range 0.61 - 10.19). The average concentration of TOM varies from 0.90±0.09 (Jan. 91) to 1.38±0.16 (April 90) (Table 2). The average fraction of total TOM in suspended particulate matter (0.4 μm) is about 13% in November 89, 21% in April 90, 39% in August 90 and 12% in January 91, respectively. The higher values of the TOM fraction were found in spring and summer, which to a large extent reflects the impact of spring and summer phytoplankton blooms.

The distribution of ^{210}Pb and ^{210}Po activities show considerable seasonal variations (Figs 2-4). In April 1990, the concentration of ^{210}Pb and ^{210}Po in both forms showed generally a decrease in surface water from south to north (Fig 2a, b, d, e). A pronounced maximum of both dissolved nuclides was found below a depth of 25 m at stations 4, 5 and 6 (Fig. 2a, b), which is probably related to resuspension of underlying sediments. This is indicated by an increase of TSM (at stations 3-5, Fig. 2g) and TOM (at stations 3-5, Fig. 2h) concentrations near the sea floor. The ratio ^{210}Po/^{210}Pb is about 0.9 - 1.1 in most of the surface water (< 10 m) and in the deeper part of water (35-50 m) in station 6, while the rest of the water body has a ratio exceeding 1.0, indicating an excess of ^{210}Po in both the dissolved and particulate phases (Fig. 2c, f).

In August 1990, the patterns of the ^{210}Pb and ^{210}Po distributions reveal that the concentrations in particulate form were relatively low (Fig. 3d, e, Table 2) compared with the three other seasons, except the dissolved concentration during spring which is in the same range (0.7-2.0 dpm/100kg). The low particulate activity (in seawater) of two tracers is related to the concentration of TSM in the water body

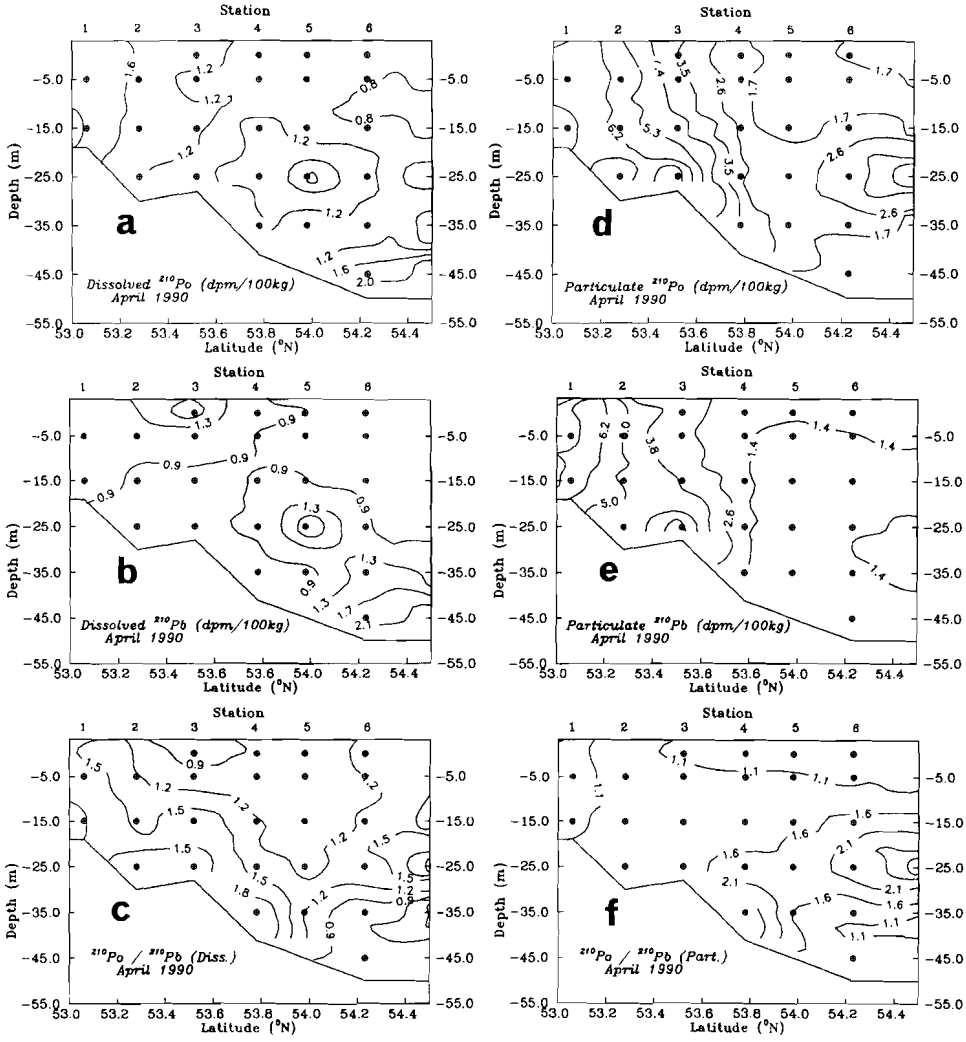

Fig. 2 *The distribution of ^{210}Pb, ^{210}Po, TSM and TOM (station 1 to 6, from 53°03.4'N,4°37.1'E to 54°14.0'N, 4°13.0'E) in April 2-6, 1990. Circled crosses are data points. (a) dissolved ^{210}Po; (b) dissolved $^{210}PbPb$; (c) $^{210}Po/^{210}Pb$ in dissolved form; (d) particulate ^{210}Po; (e) particulate ^{210}Pb; (f) $^{210}Po/^{210}Pb$ in particulate form; (g) TSM (total suspended matter); (h) TOM (total organic matter); (i) the fraction of total organic matter.*

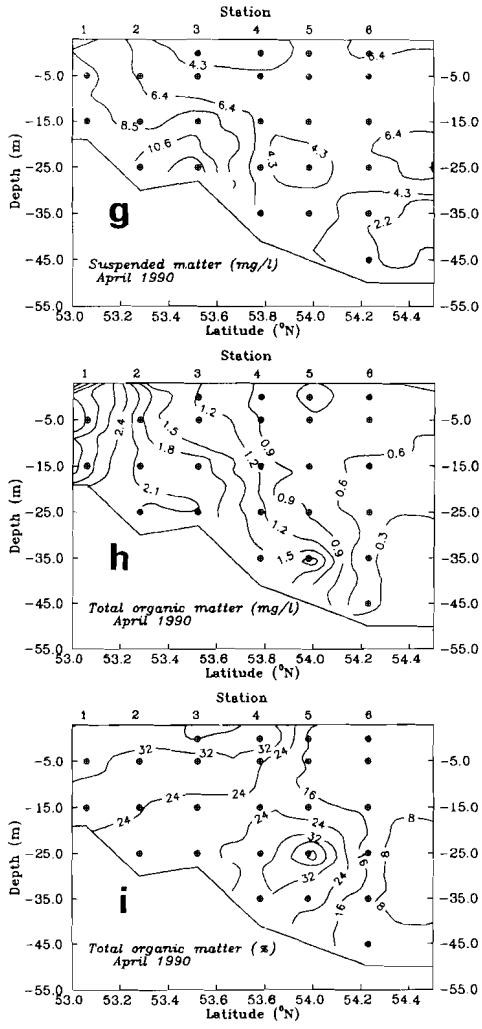

Fig. 2 *continued.*

in response to the seasonal variation of the suspended particle flux. The maximum of dissolved ^{210}Pb near the sea bed was again observed (Fig. 3b) which coincided with an increase of TSM and TOM at the same locations (Fig. 3g, h). However, bottom maximum of dissolved ^{210}Po was not found which may be explained by a strong uptake of ^{210}Po in the water of the summer bloom that produces 'young'

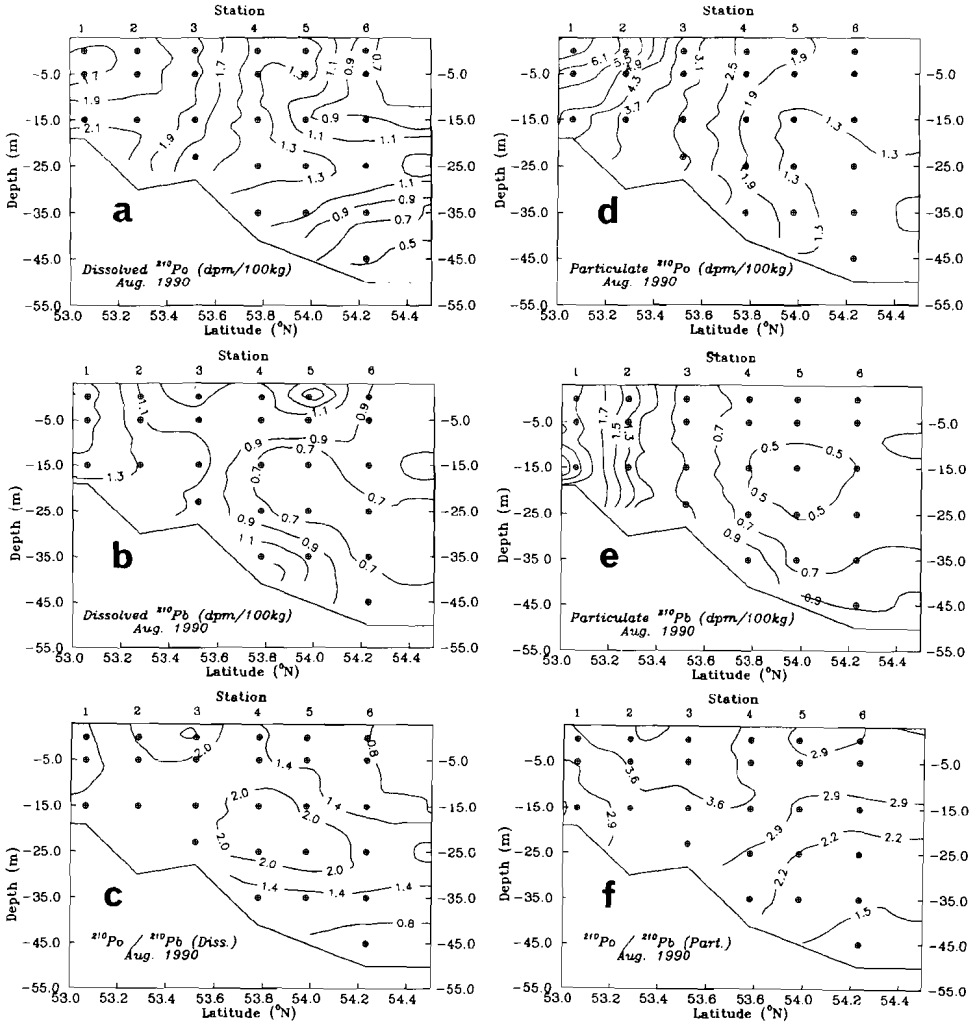

Fig. 3 *The distribution of ^{210}Pb, ^{210}Po, TSM and TOM (station 1 to 6, from 53°03.4'N, 4°37.1'E to 54°14.0'N, 4°13.0'E) in August 27-28, 1990. For a detailed legend see Fig.2.*

and 'fresher' organic particles that adsorp ^{210}Po more effectively. An excess of total ^{210}Po is present at almost all stations (Fig. 3c, f), indicating a strong depletion of ^{210}Pb with respect to ^{210}Po in the water column. It is worth to note that the ratio in

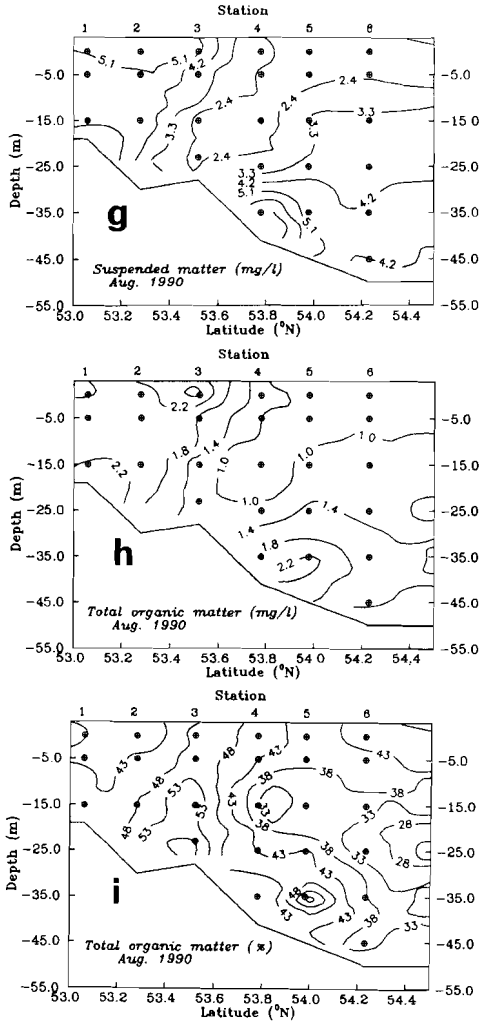

Fig. 3 *continued.*

particulate form reaches the highest range (0.82-7.00, Table 2) with an average of 3.04±0.22.

In January 1991, as shown in Fig. 4, two nuclides show relatively high concentrations with rather well mixed activity-depth profiles. Again, a net excess of total ^{210}Po is present at all the depth, which is consistent with the observation from all the other seasons.

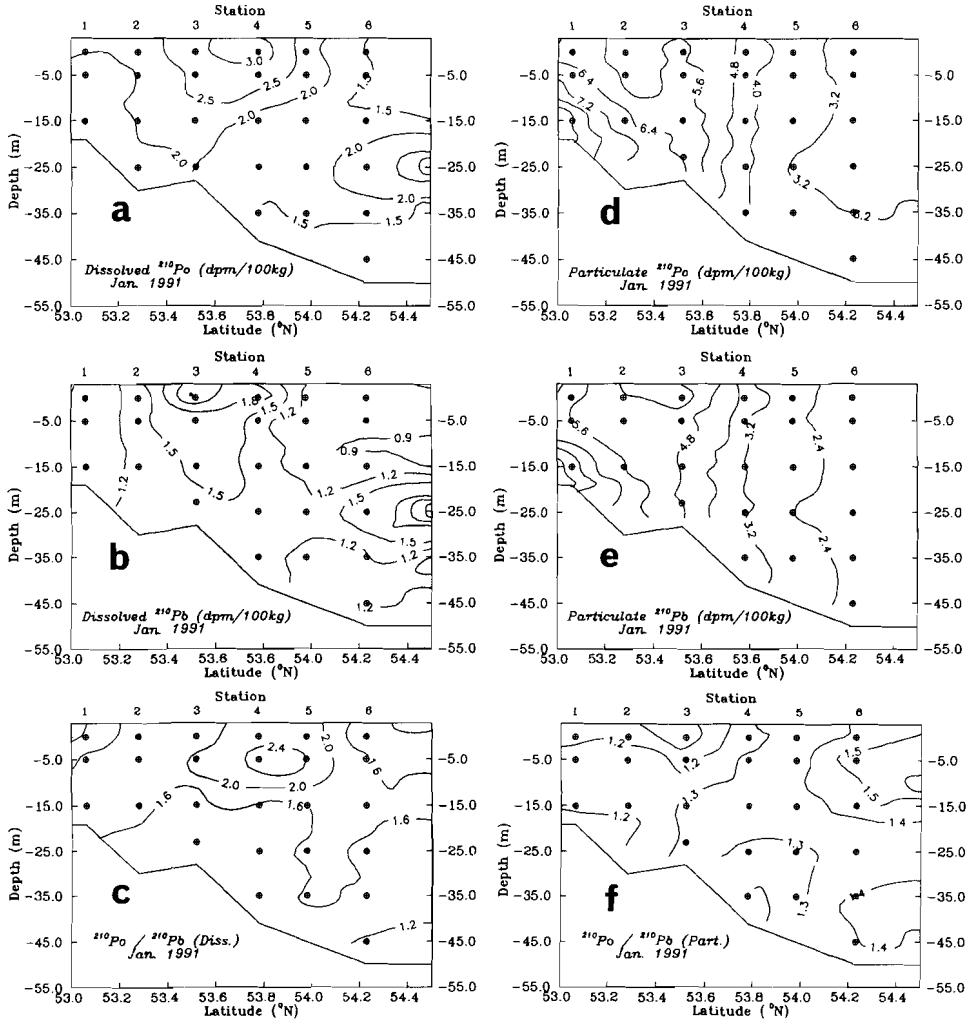

Fig. 4 *The distribution of ^{210}Pb, ^{210}Po, TSM and TOM (station 1 to 6, from 53°03.4'N, 4°37.1'E to 54°14.0'N, 4°13.0'E) in January 14-15,1991. From (a) to (i) for a detailed legend see Fig. 2. (j) salinity; (k) temperature; (l) density excess (σ_t).*

The distribution of ^{210}Pb and ^{210}Po in the period of November 1989 has been described in detail earlier by Zuo and Eisma (1992), and is characterized by relative high concentration of ^{210}Pb and ^{210}Po in both phases, a high resuspension

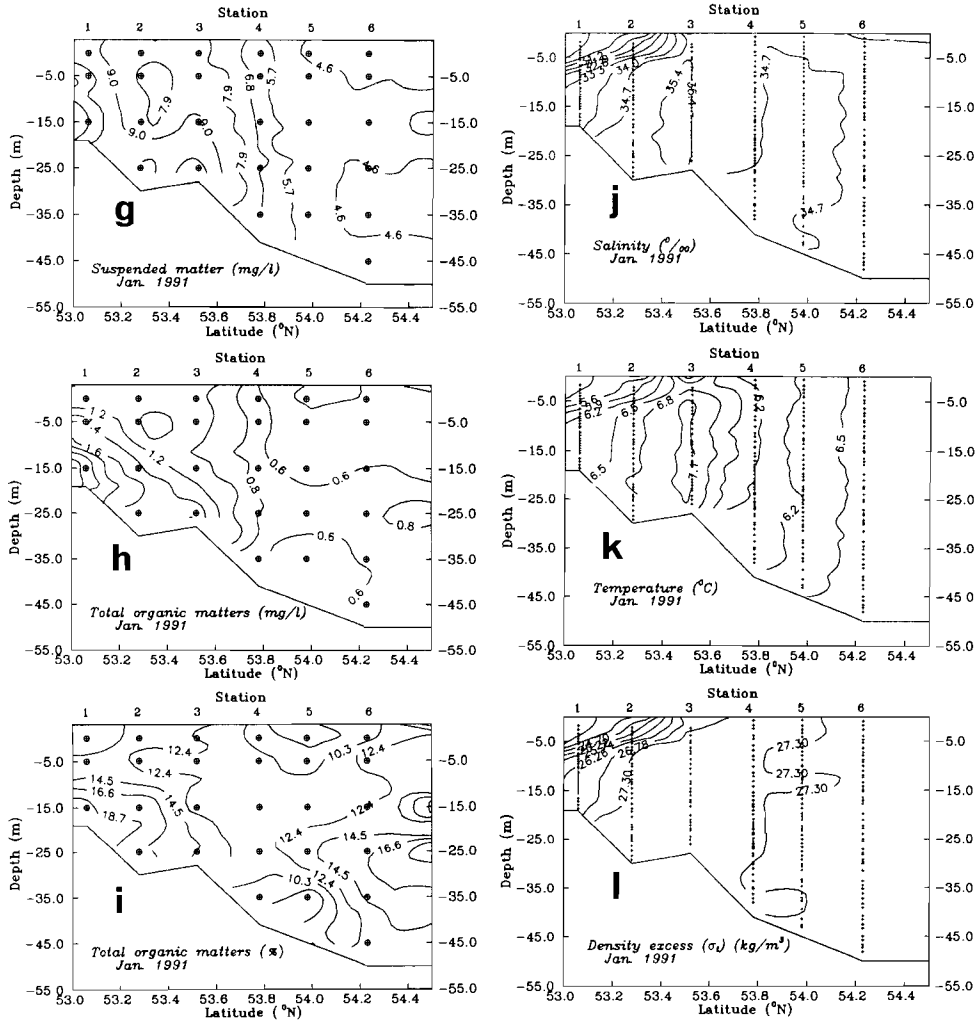

Fig. 4 *continued.*

rate and strong excess of ^{210}Po in the water column. The systematic excess of ^{210}Po with respect to ^{210}Pb and the fact that the standing crop of the total ^{210}Po in the water is greater, was believed to result from an additional input of ^{210}Po from the coastal and shelf sediments (Bacon et al., 1978; Zuo and Eisma, 1992a). Similar excess ^{210}Po has been observed elsewhere by Schell (1977, the Washington area) and

by Spencer et al. (1980, the northern North Sea). It is realized that this phenomenon could be a common feature in coastal and shelf waters.

Seasonal variation and partition

The above data demonstrate that the distribution of ^{210}Pb and ^{210}Po in the water column of the Dutch coastal and shelf areas is highly variable. There are large differences between the individual patterns which are influenced by boundary conditions (wind, location and activity of sources) and by the circulation in the study area. For a general picture of the processes controlling the distribution of the two radioactive tracers, it is difficult to obtain meaningful ideas by a simple data treatment from individual stations due to its variable nature of the processes involved. Thus, we consider the study area as a well mixed water box in order to get better understanding in behaviours of ^{210}Pb and ^{210}Po in the water column. Figure 5 shows the time series of the concentration variation on ^{210}Pb and ^{210}Po, ^{226}Ra as well as TSM and TOM. Each data point in the plots is a mean of the data set from corresponding sample collection and uncertainties were determined from standard deviations of the means which will later be carried through the whole computations to give a rough idea of the uncertainty in the derived results. The data of station 1 were not taken into account because of the extremity of values. An example of an activity depth profile at an individual station (station 6) is also given in Figure 6.

The total concentrations of both radionuclides illustrate seasonal variations which are follow the variations in suspended particulate concentrations (Fig. 5a, c), suggesting that processes removing those nuclides from the water column respond at least to some extent to fluctuations in supply of particulate matter in the study area. The dissolved nuclides show the highest activities in winter (Oct. - Mar.)and fall and lower ones in summer (April-Sep.) (Fig. 5b), implying that the scavenging is stronger in spring and summer than in winter. This is not surprising because in spring and summer the phytoplankton blooms take place which increases the content of ' fresh' organic matter in the water column. The total organic matter content, indeed, as seen in Figure 5a, exhibits a slight increase in spring and summer. The apparent seasonal variation of TOM content, however, appears to be small, which suggests that although the TOM content does not vary much, the origin and composition of organic material may vary. This can explain the different behaviour of organic particles in the uptake of radionuclides from the seawater. Studies by Eisma (1981) and Owens et al. (1990) pointed out that the increase of

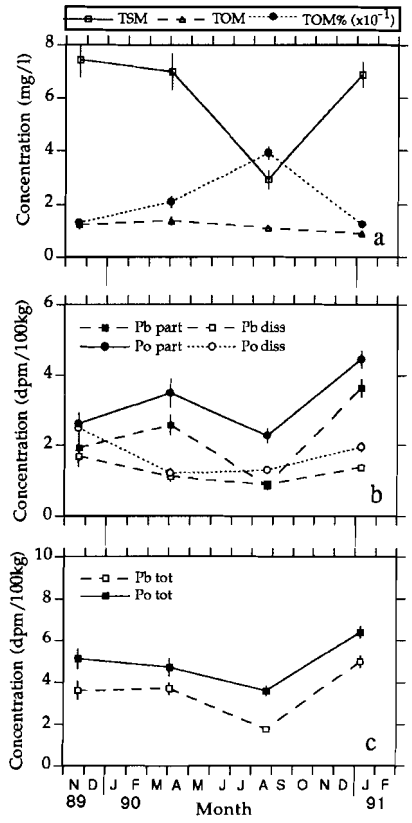

Fig. 5 *Time series of average concentrations of (a) TSM and TOM; (b) particulate and dissolved ^{210}Pb and ^{210}Pb; (c) total ^{210}Pb and ^{210}Po during the period Nov. 1989 - Jan. 1991. The data points are averages of all data of an exception (station 1).*

organic matter content during the warm seasons (spring and summer) is related to the primary production. During the winter, the suspended organic matter most likely has a mixed origin: being derived from the bottom sediments, coastal sediments, river supply, primary production and bottom-dwelling organisms. Later

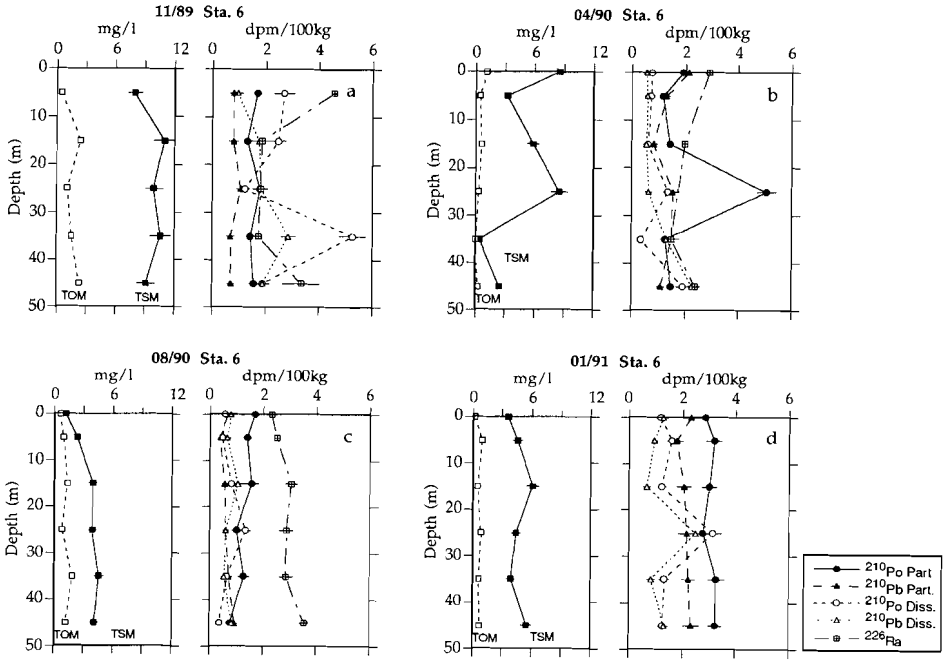

Fig. 6 *Activity-depth profile of ^{210}Pb, ^{210}Po and ^{226}Ra of station 6.*

work indicated that a dominant portion of the organic matter in water may be supplied by the bottom fauna through the formation of faeces and pseudo faeces that subsequently fall apart into aggregates (Eisma et al., 1983; Eisma, 1986). The particulate nuclides show two concentration maxima: in spring and in winter (Fig. 5b). The spring peak reflects an increase of scavenging rate due to the high efficiency of tracer adsorption onto newly formed particles, while the winter increase is probably caused by the combined impact of a high rate of resuspension and more supply of suspended particulate matter. The minimum of both elements in summer (Fig. 5b) is considered to be an influence of low content of total suspended matter (Fig. 5a) which is due to a small supply of suspended material in summer (Visser et al., 1991) and the formation of thermal stratification (Owens et al., 1990). It

is interesting to see that the particulate ^{210}Po profiles have the tendency to approach equilibrium with ^{210}Pb near the sea bed (Fig. 6b, c, d), reflecting in part the admixture of old sediment resuspended from the sea bottom. A disequilibrium between ^{226}Ra and ^{210}Pb was observed in the profiles of almost all seasons (Fig. 6), as was agreed by many investigators (Rama et al., 1961; Thomson and Turekian, 1976; Nozaki, 1986). The disequilibrium is caused by the preferential removal of ^{210}Pb from the water.

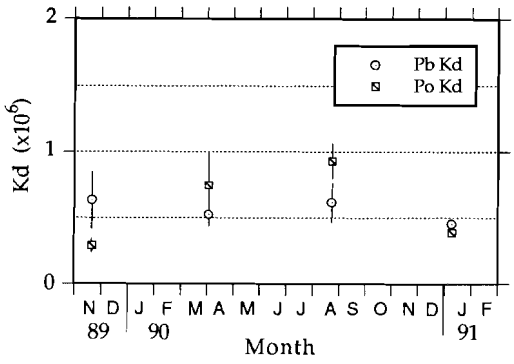

Fig. 7 *Seasonal variation of distribution coefficient (K_d) of two tracers from Nov. 1989 to Jan. 1991.*

For both nuclides, we computed the empirical distribution coefficients (K_d) according to Bacon et al.'s method (1988):

$$K_d = C^p / \left(C^d \, TSM \right) \quad (1)$$

where C^P and C^d are the concentrations of the tracers in the particulate and dissolved phases. The results are plotted in Figure 7. The average K_d values are lower in winter and high in summer (Fig. 7), in support of the previous suggestion of high sediment resuspension in winter and stronger scavenging in spring and summer (Fig. 8). Figure 8 gives plots of K_d (Pb, Po) versus TSM and TOM. To a certain extent there is an inverse correlation between the K_d value and total suspended matter (Fig. 8a) which can be explained by resuspension of 'old' particles that carry low concentration of both two nuclides because of prior decay. There is

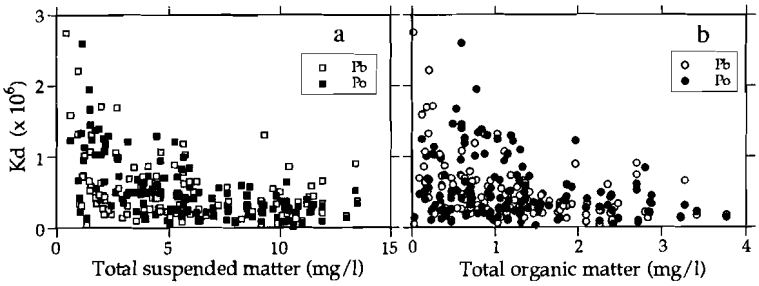

Fig. 8 *The relationship between distribution coefficient (K_d) of ^{210}Pb and ^{210}Po and (a) total suspended matter; (b) total organic matter*

also a correlation between K_d and total organic matter (Fig. 8b). We believe that the group with high content of TOM and low K_d values was originated by resuspension of 'aged' organic particles from the sea bed; the one with relatively low content of TOM and high Kd values, on the other hand, consists of 'young' and 'new' organic particles that are related to primary production (Zuo and Eisma, 1992a). Apparently, the two groups of organic material behave in different ways in uptaking nuclides in the water column.

5. COMPUTATION OF MASS BALANCE

As pointed out previously, we consider the study area as a well mixed single box to examine the material balance for ^{210}Pb and ^{210}Po. The supply of ^{210}Pb to the sea water is governed by the following factors: the atmospheric input of ^{210}Pb, the scavenging efficiency of ^{210}Pb by sinking particles, the production rate of ^{210}Pb from *in situ* decay of its parent nuclide ^{226}Ra, the supply from resuspension of bottom sediments and the lateral transport. The input of ^{210}Po to the water, on the other hand, is almost entirely due to ^{210}Pb decay in the water column. Atmospheric ^{210}Po deposition is only about 10% of the ^{210}Pb flux because of the low ratio of $^{210}Po/^{210}Pb$ in air and in precipitation (Burton and Stewart, 1960; Poet et al., 1972). The data set of this study has shown a pronounced systematic excess of ^{210}Po in the water

column. For this reason we believe that there is an additional supply in dissolved ^{210}Po from the sediments of the Dutch coastal zone. Supply of ^{210}Pb and ^{210}Po by rivers is considered to be less important because these nuclides are rapidly scavenged by the sediment particles and efficiently trapped by estuaries and along the coast (Rama et al., 1961; Benninger et al., 1975; Lewis, 1977; Zuo and Eisma, 1992a).

With the above consideration in mind, we developed a scavenging model to interpret the observed ^{210}Pb and ^{210}Po distributions. We assume a steady state and a negligible horizontal transport, the mass balance of ^{210}Pb and ^{210}Po can be expressed as follows.

For dissolved ^{210}Pb (C^d):

$$\frac{\partial C^d}{\partial t} = 0 = I + P_{Ra} - (\lambda + k) C^d \quad (2)$$

and for particulate ^{210}Pb (C^P):

$$\frac{\partial C^P}{\partial t} = 0 = RC_s + kC^d - \lambda C^P DC_w \quad (3)$$

For dissolved ^{210}Po (C^d):

$$\frac{\partial C^d}{\partial t} = 0 = P^d_{Pb} + F - \lambda C^d - k'C^d \quad (4)$$

and for particulate ^{210}Po (C^P):

$$\frac{\partial C^P}{\partial t} = 0 = P^P_{Pb} + RC_s + k'C^d - \lambda C^P DC_w \quad (5)$$

where C^d and C^P are the dissolved and particulate ^{210}Pb and ^{210}Po concentrations (dpm/cm^2); I is the atmospheric input of ^{210}Pb (dpm/cm^2/yr); P_{Ra} is the production rate of ^{210}Pb from its parent nuclide ^{226}Ra (dpm/cm^2/yr); k and k' are the *in situ* first order scavenging rate constants of ^{210}Pb and ^{210}Po respectively, referring to a transfer of dissolved ^{210}Pb to particulate ^{210}Pb (yr^{-1}); P^P_{Pb} and P^d_{Pb} are the production rates of ^{210}Po from decay of ^{210}Pb in particulate and dissolved phases (dpm/cm^2/yr), respectively; D is the particle deposition rate into the mixed sediment (g/cm^2/yr); R is the sediment resuspension rate (g/cm^2/yr); F is the additional flux of ^{210}Po (dpm/cm^2/yr); C_W is the ^{210}Pb and ^{210}Po concentration of the suspended matter (dpm/g RSM); C_S is the ^{210}Pb and ^{210}Po activity of the surface sediment (dpm/g) and λ is the decay constant (for ^{210}Pb 0.031 yr^{-1}; for ^{210}Po, 1.83 yr^{-1}). The residence time at the steady state is given by $\tau = 1/k$ (yr). RSM is the refractory suspended matter (=TSM - TOM, Bacon et al, 1991) that is taken for simplicity to exclude particle production and consumption and only consider the physical transport of the particles.

Table 3: *Inventories of ^{226}Ra, ^{210}Pb and ^{210}Po of the water column in the southern North Sea[a]. Units are dpm/cm^2.[b]*

Sample collection	C_{Ra}^{d}	C_{Po}^{d}	C_{Po}^{p}	C_{Pb}^{d}	C_{Pb}^{p}	C_{Po}^{tot}	C_{Pb}^{tot}
11-89	0.14±0.01	0.13±0.02	0.14±0.02	0.09±0.01	0.10±0.02	0.27±0.02	0.19±0.02
04-90	0.15±0.01	0.06±0.01	0.18±0.02	0.06±0.01	0.13±0.01	0.24±0.02	0.19±0.02
08-90	0.18±0.01	0.07±0.004	0.12±0.01	0.05±0.003	0.04±0.005	0.19±0.01	0.09±0.01
01-91	n.m.	0.10±0.01	0.23±0.01	0.07±0.005	0.19±0.01	0.33±0.01	0.26±0.01

a. Reservoir thickness was taken to be 50 m.
b. Using the water density σ_ω= 1.0267 kg/l (S= 34-35 ‰, T= 6-12°C) for the calculation of the inventories.
c. n.m.= not measured.

The inventories of ^{226}Ra, ^{210}Pb and ^{210}Po in all the seasons are summarized in Table 3, based on the data set of Table 2. For the atmospheric flux of ^{210}Pb I, we have adopted averages of the data from a rain-collection station at Texel, The Netherlands. These were collected over the same period for each season (Zuo et al., 1992), and varied from 0.14±0.02 to 0.46±0.09 dpm/cm^2/yr (Table 4). These values are consistent with the figure predicted by Turekian's model (1977) for this region (±0.5 dpm/cm^2/yr) and is about two to five times lower than around North America where continental shelf data have been collected (Benninger, 1978; Turekian et al., 1983).

To quantify the particle deposition rate D, the sediment resuspension R and the additional flux of ^{210}Po F, we try to consider the total ^{210}Pb budget in the mixed sediment box and the total ^{210}Po balance in the water column. That is, the deposition of ^{210}Pb must be balanced by the resuspension and decay (Santschi et al, 1980; Bacon et al., 1991):

$$DC_w = RC_s + \lambda M \quad (6)$$

and the deposition and decay loss of ^{210}Po should be balanced by the production from decay of ^{210}Pb, the resuspension and the additional flux:

$$DC_w + \lambda C^{tot} = P_{Pb} + RC_s + F \quad (7)$$

where M is the excess ^{210}Pb inventory in sediment (dpm/cm^2); C^{tot} is the total ^{210}Po content in the water (dpm/cm^2), P_{Pb} is the production rate of ^{210}Po (dpm/cm^2/yr). Because there is no production or consumption of RSM in the water or sediment, deposition must be balanced by resuspension and accumulation:

$$D = R + G \quad (8)$$

where G is accumulation flux in sediments (g/cm^2/yr).

In this model, we have adopted the following values from the existing data in the study area in Zuo et al. (1989) and Zuo and Eisma (1992b): M = 15.11±1.86 dpm/cm^2; Cs = 0.96±0.36 dpm/g; the accumulation rate G was taken to be in a range of 0.06 - 0.12 g/cm^2/yr. The value of C_w for the two nuclides was calculated based on the measured data (Table 2) and listed in Table 4. The detailed method for the model computations were described earlier by Zuo and Eisma (1992). The results of the model calculations are summarized in Table 4 and shown in Figure 9. For the convenience of plotting and table-listing, we define J as the removal rate of particulate nuclides (dpm/cm^2/yr; = DC_w) and A as the adsorption (uptake) rate of dissolved nuclides onto the suspended particles (dpm/cm^2/yr; = KC^d or $K'C^d$).

It is important to mention that the budget calculations for dissolved ^{210}Pb using eq. (2) leads to an imbalance between the input and output. The input concentration is systematically lower than the loss. This suggests that an additional term is needed to sustain the mass balance of dissolved ^{210}Pb in the water column. It is unlikely that this additional ^{210}Pb is introduced into the system from the coastal and shelf sediments, because many investigators have agreed that ^{210}Pb is generally immobile (Appleby et al., 1979; Crusius and Anderson, 1990; 1991) and ^{210}Pb will be rapidly transported from the sea surface to the bottom without any important release in the water column (Bacon et al., 1978). Our interpretation of the imbalance is that, during most of the time, a lateral influx of dissolved ^{210}Pb exists. We envision that an external flux of dissolved ^{210}Pb is brought into the system by horizontal transport of water masses from the Southern North Sea. This external flux was defined as E and calculated for each season in the study area (Table 4). We believe that the external flux can also account for dissolved ^{210}Po, as one would expect, which has already been taken into account in the additional flux. Therefore, the term E should be added in eq. (2) as part of supply flux for the computation of dissolved ^{210}Pb mass budget.

The computed residence times for the two tracers range from 0.09 to 0.38 yr (33-139 days) for the dissolved phase and from 0.05 to 0.18 yr (18-66 days) for the particulate phase, which are consistent with other findings in shallow water systems (Santschi et al, 1979; Eisma et al., 1989). As shown in Fig. 9 and Table 4, the deposition flux D does not differ significantly during the year. The resuspension flux R is relatively low in spring and high in November, indicating a significant contribution to the total suspended matter distribution in the water column. The additional flux F is generally constant in most of seasons but with a sharp increase in summer time, while the external flux E increases from November 1989 to

Table 4: *Summary of the mass balance calculation in the Dutch coastal and shelf seas.*

		Nov-89	Apr-90	Aug-90	Jan-91
INPUT[a]					
TSM	mg/l	7.45±0.65	7.00±0.67	2.95±0.33	6.89±0.46
TOM	mg/l	1.26±0.16	1.38±0.16	1.12±0.12	0.90±0.09
RSM	mg/l	6.19±0.67	5.62±0.69	1.83±0.35	5.99±0.47
C_w^{Pb}	dpm/g	3.18±0.20	4.73±0.16	4.82±0.22	6.22±0.11
C_w^{Po}	dpm/g	4.36±0.16	6.39±0.17	12.79±0.21	7.63±0.10
I[b]	dpm/cm^2/yr	0.46±0.09	0.36±0.09	0.33±0.07	0.14±0.02
G[c]	dpm/cm^2/yr	0.12	0.09	0.08	0.06
OUTPUT					
R	g/cm^2/yr	0.040±0.03	0.012±0.02	0.022±0.02	0.018±0.01
D	g/cm^2/yr	0.160±0.03	0.102±0.02	0.102±0.02	0.078±0.01
E	dpm/cm^2/yr	0.012±0.03	0.112±0.02	0.138±0.02	0.334±0.02
F	dpm/cm^2/yr	0.80±0.14	0.73±0.12	1.45±0.20	0.71±0.09
k	yr^{-1}	5.48±2.61	8.32±3.06	10.20±3.20	6.81±2.15
k'	yr^{-1}	5.65±1.38	11.66±2.27	21.19±3.30	6.60±1.06
J_{Pb}	dpm/cm^2/yr	0.51±0.09	0.48±0.08	0.49±0.08	0.49±0.07
J_{Po}	dpm/cm^2/yr	0.70±0.12	0.65±0.10	1.30±0.20	0.60±0.09
A_{Pb}	dpm/cm^2/yr	0.47±0.24	0.47±0.18	0.47±0.15	0.48±0.15
A_{Po}	dpm/cm^2/yr	0.73±0.20	0.73±0.16	1.42±0.24	0.66±0.11
τ_{Pb}^{p}	yr	0.19±0.05	0.28±0.05	0.09±0.02	0.38±0.06
τ_{Po}^{p}	yr	0.19±0.04	0.28±0.05	0.09±0.02	0.38±0.06
τ_{Pb}^{d}	yr	0.18±0.09	0.12±0.04	0.10±0.03	0.15±0.05
τ_{Po}^{d}	yr	0.18±0.04	0.09±0.02	0.05±0.01	0.15±0.02

a. The value of each period is a mean of the whole data set excluding station 1. Uncertainties are standard errors. See text.
b. Zuo et al., 1992.
c. Based on our previous study (Zuo et al., 1989).

January 1991 by a factor two to ten (Table 4). We do not understand yet completely the actual exchange mechanisms of the dissolved nuclides between sediment and water and between the reservoir and the surrounding systems. ^{210}Po, as shown in figure 9b, is much stronger removed from the system by sinking particles than ^{210}Pb, with a peak level in the summer which supports the previous suggestions of high affinity of ^{210}Po to rich-organic particles (Zuo and Eisma, 1992a). The removal of ^{210}Pb from the water column is almost constant despite the seasonal variation of

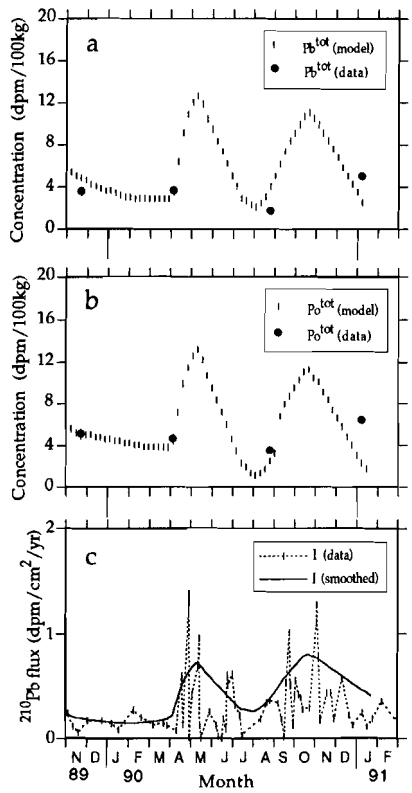

Fig. 9 *Seasonal variability of (a) resuspension R (g/cm^2/yr), deposition D (g/cm^2/yr), ^{210}Po flux F (dpm/cm^2/yr) and ^{210}Pb flux E (dpm/cm^2/yr); (b) removal rate J and adsorption rate A; (c) residence time t, derived from the mass balance calculations for the period Nov.1989 - Jan. 1991.*

particle supply in the system, indicating a remarkably stable radiochemical composition of the settling particles throughout the annual cycle. A similar behaviour was also found by Bacon et al. (1985) for Th isotopes in the Sargasso Sea. Their interpretation of the phenomenon is that there exists a relative stable reservoir of particulate material in the water column which consists of two classes

of particles: the fine suspended matter and the large aggregates. The reservoir is thought to be tapped in quantities that are seasonally variable. The fine particles control the adsorption of radio nuclides with a high content, large turnover times and negligible settling velocities, whereas the second class is responsible for the removal and deposition. It is the two classes of particles that work together through interaction of adsorption, desorption, aggregation and disaggregation to bring the downward transport of radionuclides (Lal, 1980; Bacon et al., 1985). The overall result of above gives the difference in residence time of ^{210}Pb and ^{210}Po in both phases. It is clear that the dissolved ^{210}Pb has a relatively longer residence time than the dissolved ^{210}Po (Fig. 9c) due to the preferential adsorption of ^{210}Po by particles. Shorter residence time in both dissolved nuclides occur in summer in response to the high scavenging activity processes. The residence time of particulate nuclides is relatively long in spring and winter with a minimum in summer months (Fig. 9c). This is a combined effect of seasonal variations of particle supply, more stormy weather causing more resuspension, and a constant rate of tracer removal as discussed above.

6. SEASONAL MODEL

In order to get more insight of the seasonal variability of the processes that control scavenging, deposition and particle transport on-going in the study area, we tried to develop a seasonal scavenging model for the system. We have chosen a model that is one-dimensional and is time-dependent (Fig. 10). The symbols used in Figure 10 are as defined in the previous sections. The upper water box represents the reservoir in the study area with a water depth of 50 m (which is about the maximum water depth in the study area). It is assumed that the concentrations of dissolved and particulate radionuclides are homogeneously distributed within the box. The change of the total concentration of nuclides is determined by the following factors: (1) atmospheric input of ^{210}Pb I; (2) in situ production of ^{210}Pb by ^{226}Ra decay P; (3) particle deposition flux D; (4) sediment resuspension flux R; (5) radioactive decay λC; (6) additional flux of ^{210}Po F; (7) external flux of ^{210}Pb E. Moreover, we have assumed that the nuclides are taken up by sinking particles and removed out of the system by deposition. No diffusive transport is considered.

In our model, the time dependence of the atmospheric flux of ^{210}Pb is taken from the observations made at a station of Texel (Zuo et al., 1992). In addition, the production rates of ^{210}Pb and the ^{210}Pb content in the bottom sediment are taken to be known and constant with time. At a given time, the total concentration of ^{210}Pb

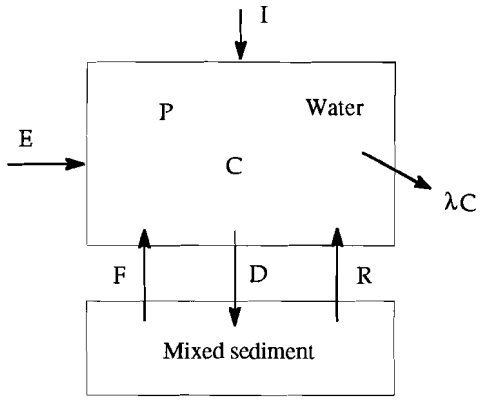

Fig. 10 *Seasonal scavenging model for the Dutch coastal and shelf seas. For symbols, see text.*

is determined by the atmospheric input, the production rate, the resuspension and deposition rate, the decay and the lateral flux. The governing equation for ^{210}Pb in the water column can be written as:

$$\frac{\partial C^{Pb}}{\partial t} = I(t) + E(t) + P + C_s R(t) - \lambda C^{Pb}(t) - D(t) C_w(t) \qquad (9)$$

where C^{Pb} is the total concentration of ^{210}Pb in dpm/cm^2.

Constructing the governing equation for the total concentration of ^{210}Po, we have:

$$\frac{\partial C^{Po}}{\partial t} = \lambda C^{Pb}(t) + C_s R(t) + F(t) - \lambda C^{Po}(t) - D(t) C_w(t) \qquad (10$$

where C^{Po} is the total amount of ^{210}Po in the water column.

The boundary conditions for eq. (9) and eq. (10) are:

At t=0,

$$C^{Pb} = C_0^{Pb} \qquad (11)$$

$$C^{Po} = C_0^{Po} \qquad (12)$$

We have assumed that the external flux, the deposition and resuspension rates are constant with time, and an average of the data for E, D and R (Table 4) for the four seasons was taken for the calculation. The term $C_w(t)$ in (9) and (10) can be determined from the measured data as follows:

$$C_w^{Pb}(t) = 3.24 + 2.46\,t \tag{13}$$

$$C_w^{Po}(t) = 2.45 + 20.64\,t - 13.26\,t^2 \tag{14}$$

Table 5: *Parameters of the seasonal model calculations for the Dutch coastal and shelf seas.*

	Δt	I_0	C_0	C_{Ra}	C_{w0}	C_s	D	R	E	F^a
	day	dpm/cm2/yr	dpm/cm2		dpm/g		g/cm2/yr		dpm/cm2/yr	
^{210}Pb	7	0.25	0.185	0.158	3.18	0.96	0.11	0.023	0.149	-
^{210}Po	7	-	0.264	0.158	4.36	0.96	0.11	0.023	-	0.75(0.90)

a. Two different values were used for F in the model: $F = 0.75$, at $0 \le t \le 300$; $F = 0.90$, at $t > 300$. See text.

Equation (13) is a linear fit using least squares regression (R=0.93) and equation (14) is a second order polynomial fit (R=1.0), both obtained from the measured data. The additional flux F was considered as variable only between two time intervals and kept constant within each time period. The input flux I(t) was smoothed based on the field data to minimize the variations between individual data points. The model computation is started at 1 November 1989 with a time step of 7 days. The model parameters, used in the computation are listed in Table 5, the computed time-variation of total ^{210}Pb and ^{210}Po together with the input ^{210}Pb data are shown in Figure 11.

The derived ^{210}Pb and ^{210}Po concentrations show clearly two peak values in spring months and winter months (Fig. 11a, b) which coincide with the peak values of the atmospheric flux of ^{210}Pb (Fig. 11: c). Except for the ^{210}Pb data in January 1991, the model reproduces the observed values very closely. It is remarkable to see that the variation of two nuclide contents in the water column respond strongly to the variation of the ^{210}Pb flux from the atmosphere, which suggests that the

atmospheric supply of ^{210}Pb plays a dominant role in controlling the distribution of ^{210}Pb and ^{210}Po in the Dutch coastal and shelf seas.

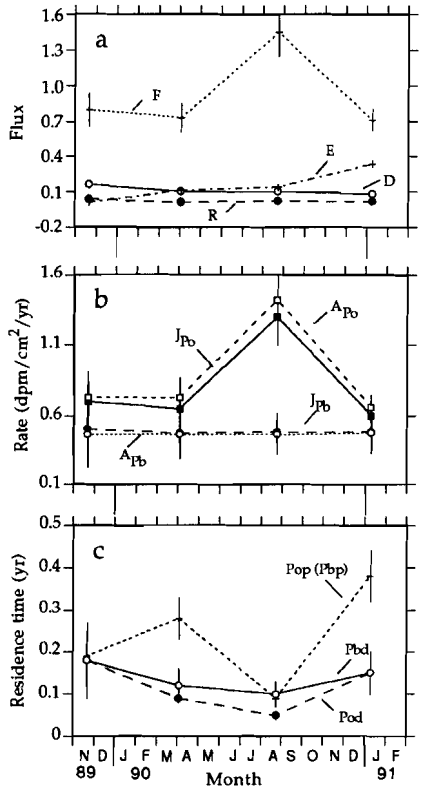

Fig. 11 *Predicted time-variation of (a) total ^{210}Pb and (b) ^{210}Po from the seasonal model. The filled circles represent the observed data points in the period of Nov.1989 -Jan. 1991. The bar curves represent the best model fits. (c) ^{210}Pb deposition according to Zuo et al. (1992).*

The continuous solution to the non-steady-state model shows that, with frequent enough sampling, it is possible to observe the effect of the seasonally

pulsed input of ^{210}Pb. Unfortunately the sampling periods did not catch the concentration peaks, so the data are not a sufficient test of the model. It is also realized that the results derived from the seasonal model are only based on a limited data set and the effects of seasonal variation in resuspension and deposition as well as in the dissolved flux exchange between the system and the boundaries were not taken into account, which is probably the reason for the deviation between model values and the data points. Therefore, further investigation is needed.

7. CONCLUSIONS

During the period between November 1989 and January 1991, the distribution of ^{210}Pb and ^{210}Po in the Dutch coastal and shelf seas were examined. The data show that the concentrations of dissolved ^{210}Pb and ^{210}Po were low during summer months, whereas the concentrations of the particulate radionuclides were relatively high during these periods. The observed concentrations in the summer are attributed mainly to scavenging, particle composition and atmospheric ^{210}Pb. The winter concentrations, on the other hand, are attributed to sediment resuspension, ^{210}Pb deposition and suspended matter supply.

A mass balance for ^{210}Pb and ^{210}Po in the study area is constructed by use of a scavenging model which gives the quantities of scavenging, removal and residence time of two nuclides in the water and resuspension and deposition at the water-sediment interface. The derived residence time of ^{210}Pb and ^{210}Po indicates that ^{210}Po is preferentially removed from the water column by settling particles, the scavenging process takes place more actively in the summer months. An additional flux of dissolved ^{210}Po suggested by a persistent excess of ^{210}Po with respect to ^{210}Pb was concluded to result from the release of ^{210}Po from coastal and shelf sediments. An external flux of dissolved ^{210}Pb was also found through the box model calculation, and is believed to be an effect of lateral transport of ^{210}Pb. The rates of resuspension and deposition in the study area range from 0.01 to 0.04 $g/cm^2/yr$ and from 0.08 to 0.16 $g/cm^2/yr$, respectively, with a less important variations throughout the year.

A one-dimensional seasonal model has been developed to account for the observed seasonal variation. The activity variations of the radionuclides in the coastal zone are simulated by atmospheric supply and vertical particle transport. The predicted time-variation of the total ^{210}Pb and ^{210}Po is in agreement with the observed data and follows the seasonally pulsed input of ^{210}Pb. It is concluded that

the atmospheric deposition of ^{210}Pb plays a key role in controlling distribution of ^{210}Pb and ^{210}Po in the Dutch coastal and shelf sea. Supply of suspended particulate matter and particle composition may also be of importance.

ACKNOWLEDGEMENTS--We are grateful to the captain and the crew of the R. V. *Aurelia* for their pleasant cooperation during the cruises. We thank R. L. Groenewegen for his help with the CTD measurements; C. Fisher, R. Gieles, J. Beks for their shipboard assistance in water sample collection and filtration; and B. R. Kuipers, H. Witte, H. J. Boekel for the use of the water box. We thank R. Gieles for carrying out some water sample measurements and the stable Pb analyses. We also like to thank W. Helder and R. Nolting for allowing us to use their atomic absorption spectrophotometer, J. de Jong has been very helpful in the techniques of machine uses. The standard ^{210}Pb and ^{226}Ra sediment samples were kindly provided by J. K. Cochran (the Marine Sciences Research Center, Stony Brook State University, USA). We are much indebted to M. P. Bacon, J. K. Cochran, R. F. Anderson and J. H. F. Jansen for their valuable discussions and constructive comments on this manuscript.

REFERENCES

Appleby P. G., F. Oldfield, R. Thompson, P. Huttunen and K. Tolonen (1979) ^{210}Pb dating of annually laminated lake sediments from Finland. *Nature*, **208**, 53-55.

Aken H. M. van (1986) The onset of seasonal stratification in the shelf seas due to differential advection in the presence of a salinity gradient. *Cont. Shelf Res.*, **5**, 475-485.

Bacon M. P., D. W. Spencer and P. G. Brewer (1978) Lead-210 and Polonium-210 as Marine geochemical tracers: review and discussion of results from the Labrador Sea. In: *Nature radiation environment III*, T. F. Gesell and W. F. Lowder, editors, Proceedings of a symposium held at Houston, Texas, U. S. A. No. 1, pp. 473-501.

Bacon M. P., C.-A. Huh, A. P. Fleer and W. G. Deuser (1985) Seasonality in the flux of natural radionuclides and plutonium in the deep Sargasso Sea. *Deep-Sea Res.*, **32**, 273-286.

Bacon M. P., R. A. Belastock, M. Tecotzky, K. K. Turekian and D. W. Spencer (1988) Lead-210 and polonium-210 in ocean water profiles of the continental shelf and slope south of New England. *Cont. Shelf Res.*, **8**, 841-853.

Bacon M. P., D. R. Belastock and M. H. Bothner (1991) Lead-210 balance and implications for particle transport on the continental shelf, Middle Atlantic Bight. Submitted.

Benninger L. K. (1978) ^{210}Pb balance in Long Island Sound. *Geochim. Cosmochim. Acta*, **42**, 1165-1174.

Benninger L. K., D. M. Lewis and K. K. Turekian (1975) The use of natural Pb-210 as a heavy metal tracer in the river-estuarine system. In: *Marine chemistry in the coastal environment*, T. M. Church, editor, ACS Symposium Series, No. 18, 202-210 pp.

Buesseler K. O., H. D. Livingston and E. R. Sholkovitz (1985/86) ^{239,240}Pu and excess ^{210}Pb inventories along the shelf and slope of the northeast U.S.A.*Earth Planet. Sci. Lett.*, **76**, 10-22.

Burton W. M. and N. G. Stewart (1960) Use of long-lived natural radioactivity as an atmospheric tracer. *Nature*, **186**, 584-589.

Carpenter R. and T. M. Beasley (1981) Plutonium and americium in anoxic marine sediments: Evidence against remobilization. *Geochim. Cosmochim. Acta*, **45**, 1917-1930.

Crusius J. and R.F. Anderson (1990) ^{137}Cs mobility inferred from ^{210}Pb and $^{239+240}$Pu analyses of laminated lake sediments. *EOS*, **71**, 72.

Crusius J. and R.F. Anderson (1991) Immobility of ^{210}Pb in Black Sea sediments. *Geochim. Cosmochim. Acta*, **55**, 327-333.

DeMaster D.J. and J.K. Cochran (1982) Particle mixing rates in deep-sea sediments determined from excess ^{210}Pb and ^{32}Si profiles. *Earth Planet. Sci. Lett.*, **61**, 257-261.

Eisma D. (1981) Supply and deposition of suspended matter in the North Sea. *Spec. Publs int. Ass. Sediment.*, **5**, 415-428.

Eisma D. (1986) Flocculation and deflocculation in estuaries.*Neth. J. Sea Res.*, **20**, 183-199.

Eisma D. (1990) Transport and deposition of suspended matter in the North Sea and the relation to coastal siltation, pollution, and bottom fauna distribution. *Aquatic Sci.*, **3**, 181-216.

Eisma D., J. Boon, R. Groenewegen, V. Ittekkot, J. Kalf and W. G. Mook (1983) Observation on macro-aggregates, particle size and organic composition of suspended matter in the Ems estuary. *Mitt. Paläont. Inst. Univ. Hamburg*, SCOPE/UNEP Sonderband, **55**, 295-314.

Eisma D., G. W. Berger, W.-Y. Chen and J. Shen (1989) Pb-210 as a tracer for sediment transport and deposition in the Dutch-German Waddensea. In: *Coastal Lowlands, Geol. Geotechnol.,* Proceedings KNGMG Symposium, 1987, 237-253 pp.

Fleer A. P. and M. P. Bacon (1984) Determination of ^{210}Pb and ^{210}Po in seawater and marine particulate matter. *Nucl. Instruments Meth. Phys. Res.*, **223**, 243-249.

Glover D. V. and W. S. Reeburgh (1987) Radon-222 and radium-226 in southeastern Bering Sea shelf waters and sediment. *Cont. Shelf Res.*, **7**, 433-456.

Guinasso N. L., Jr. and D. R. Schink (1975) Quantitative estimates of biological mixing rates in abyssal sediments. *J. Geophys. Res.*, **80**, 3032-3043.

Koide M., K. W. Bruland and E. D. Goldberg (1973) Th-228/Th-232 and Pb-210 geochronologies in marine and lake sediments. *Geochim. Cosmochim. Acta*, **37**, 1171-1187.

Krishnaswami S., B. L. K. Somayajulu and Y. Chung (1975) ^{210}Pb/^{226}Ra disequilibrium in the Santa Barbara Basin. *Earth Planet. Sci. Lett.*, **27**, 338-392.

Lal D. (1980) Comments on some aspects of particulate transport in the oceans. *Earth Planet. Sci. Lett.*, **49**, 520-527.

Lewis D. M. (1977) The use of ^{210}Pb as a heavy metal tracer in the Susquehanna river system. *Geochim. Cosmochim. Acta*, **41**, 1557-1564.

Nozaki Y. (1986) ^{226}Ra- ^{222}Rn- ^{210}Pb systematics in seawater near the bottom of the ocean. *Earth Planet. Sci. Lett.*, **80**, 36-40.

Owens N. G. H. P., E. M. S. Woodward, J. Aiken, I. E. Bellan and A. P. Rees (1990) Primary production and nitrogen assimilation in the North Sea during July 1987. *Neth. J. Sea Res.*, **25**, 143-154.

Poet S. E., H. E Moore and E. A. Martell (1972) Lead-210, Bismuth-210 and Polonium-210 in the atmosphere: Accurate ratio measurements and application to aerosol residence time determination. *J. Geophys. Res.*, **77**, 6515-6527.

Rama, K. Minuro and E.D. Goldberg (1961) Lead-210 in natural waters. *Science*, **134**, 98-99.

Santschi P. H., Y.-H. Li and J. Bell (1979) Natural radionuclides in the water of Narragansett Bay. *Earth Planet. Sci. Lett.*, **45**, 201-213.

Santschi P. H., Y.-H. Li, J. Bell, R. M. Trier and K, Katwaluk (1980) Pu in coastal marine environments. *Earth Planet. Sci. Lett.*, **51**, 248-265.

Sarmiento J. L., D. E. Hammond and W. S. Broecker (1976) The calculation of the statistical counting error for Rn-222 scintillation counting.*Earth Planet. Sci. Lett.*, **32**, 351-356.

Schell W. R. (1977) Concentrations, physico-chemical states and mean residence time of ^{210}Pb and ^{210}Po in marine and estuarine waters. *Geochim. Cosmochim. Acta*, **41**, 1019-1031.

Spencer D. W., M. P. Bacon and P. G. Brewer (1980) The distribution of ^{210}Pb and ^{210}Po in the North Sea. *Thalassia Jugoslavica*, **16**, 125-154.

Thomson J. and K. K. Turekian (1976) ^{210}Po and ^{210}Pb distributions in ocean water profiles from the eastern south Pacific. *Earth Planet. Sci. Lett.*, **32**, 297- 303.

Turekian K. K.,Y. Nozaki and L. K. Benninger (1977) Geochemistry of atmospheric radon and radon products. *Annu. Rev. Earth Planet. Sci. Lett.*, **5**, 227-255.

Turekian K. K., L. K. Benninger and E. P. Dion (1983) ^{7}Be and ^{210}Pb total deposition fluxes at New Haven, Connecticut and Bermuda. *J. Geophys. Res.*, **88**, 5411-5415.

Van Haren J. J. M. (1990) Observations on the structure of currents at tidal and sub-tidal frequencies in the central North Sea. *Ph.D. dissertation, Utrecht University, The Netherlands*, 102 pp.

Visser M., W. P. M. de Ruijter and L. Postma (1991) The distribution of suspended matter in the Dutch coastal zone.*Neth J. Sea Res.*, **27**, 127-143.

Wijk A. van der (1987) Radiometric dating by alpha spectrometry on Uranium series nuclides. Ph.D Thesis, State University of Groningen, The Netherlands, 168 pp.

Zuo Z., D. Eisma and G. W. Berger (1989) Recent sediment deposition rates in the Oyster Ground, North Sea. *Neth J. Sea Res.*, **23**, 263-269.

Zuo Z.and D. Eisma (1992a) ^{210}Pb and ^{210}Po distributions and disequilibrium in the coastal and shelf waters of the southern North Sea. *Cont. Shelf Res.*, **12**, In press.

Zuo Z. and D. Eisma (1992b) Spatial distributions of ^{210}Pb and ^{137}Cs and mixing rates in sediments of the southern North Sea. *Cont. Shelf Res.*, Submitted.

Zuo Z., J. van der Plicht, H. Heijnis and D. Eisma (1992) Deposition fluxes of atmospheric ^{210}Pb in the Netherlands. *Earth Planet. Sci. Lett.*, Submitted.

CHAPTER 6

DEPOSITION FLUXES OF ATMOSPHERIC ^{210}PB IN THE NETHERLANDS

ABSTRACT--The deposition flux of atmospheric ^{210}Pb was determined at three sites in the Netherlands during the periods of 1987-1988 and 1990-1991. The daily deposition rate of ^{210}Pb showed strong seasonal variations at all the stations. The observed annual supply of the total ^{210}Pb, however, does not differ significantly from year to year. A good correlation between the daily ^{210}Pb deposition and the precipitation was found, indicating the presence of a seasonal effect between the summer months and the winter periods: the deposition rate of atmospheric ^{210}Pb is higher in summer than in winter. The mean deposition velocity of the total ^{210}Pb was estimated to be 0.89±0.29 cm/s which is consistent with the results found along other continental margin areas. The deposition flux of the dry fallout, derived from the relation of the total ^{210}Pb deposition with the rainfall, is about 16-38% of the total flux of ^{210}Pb. This suggests that the contribution of dry fallout is of much importance with respect to the atmospheric supply of ^{210}Pb.

1. INTRODUCTION

^{210}Pb (half-life 22.3 yrs) is a radioactive nuclide produced in the atmosphere by decay of gaseous ^{222}Rn (halflife 3.8 d) emanating from continental soils. Decay of ^{222}Rn in the atmosphere proceeds through a series of short-lived, involatile daughter radionuclides to ^{210}Pb. The decay half-lives of the intervening nuclides are short relative to the mean residence time (a few days) of the atmospheric aerosol, so that almost all atoms emitted as ^{222}Rn are re-deposited as ^{210}Pb. As ^{210}Pb is produced, it is removed by precipitation and dry fallout processes, and its mean life with respect to scavenging from the atmosphere is about 5 days (Turekian et al., 1977). The transport of this ^{210}Pb from the continent to the ocean is chiefly controlled by the wind system and the fall velocity of the aerosols in the atmosphere.

Direct atmospheric deposition is thus one important source of excess ^{210}Pb to the sea surface (Benninger, 1978), therefore an important oceanographic tracer. However, there are few good observations available that allow us to place limits on its deposition flux to the ocean waters. In this paper, we have tried to determine the atmospheric deposition fluxes of ^{210}Pb at three sites in the Netherlands over the time periods of 1987-1988 and 1990-1991. Such a data set is very useful in radionuclide geochemical studies for the Dutch coastal zone and the north Atlantic

region, in helping to understand the dynamical behaviour of radionuclides as well as other chemical substances in the water column and coastal sediments.

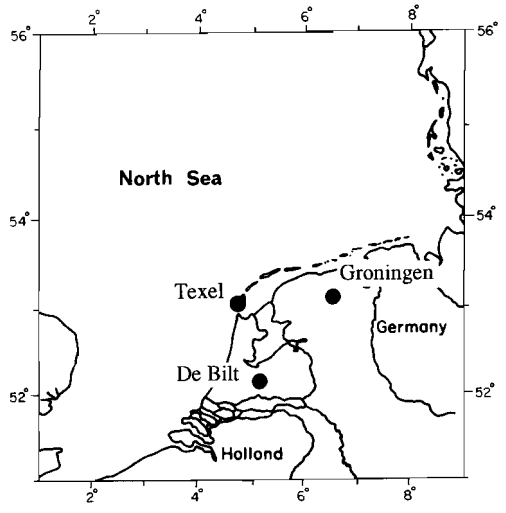

Fig. 1 *Sampling locations in the Netherlands.*

2. SAMPLE COLLECTION AND ANALYTICAL METHODS

Atmospheric aerosols, as mentioned earlier, may be removed either by precipitation - scavenging or by dry fallout settling. It is difficult to assess the relative importance of the two mechanisms on a universal basis. For any site and sampling period, however, for which dry deposition contributes appreciably to the total atmospheric ^{210}Pb, estimates of deposition based solely on episodic collections of wet precipitation, no matter how complete, will be too low (Turekian et al., 1977). Continuously exposed integrated samples (total deposition = dry + wet) may be expected to be more representative of the true ^{210}Pb deposition.

Our sampling was based on such total deposition. Three sampling sites were chosen (Fig. 1). The Groningen station is located in the northeast of the Netherlands; De Bilt station is located in the central part of the country and Texel station is on Texel island along the northwest Dutch coast. The collector was a plastic funnel that emptied via a short narrow-diameter tube, to suppress

evaporation, into a polyethylene bottle containing nitric acid to prevent sorptive loss of ^{210}Pb. Plastic isolation foil was also used around the bottle at De Bilt and Texel stations, in order to minimize the effect of evaporation. The surface area of the collector is 314 cm^2 at Groningen station and 1963 cm^2 at the two other stations. Samples were taken at approximately weekly intervals determined by the amount of water collected. Precipitation was estimated from the amount of water in the bottle, assuming no evaporation.

The sampling for ^{210}Pb at Groningen began in January 1987 and terminated in December 1988; the Texel sampling started in March 1990 and terminated in July 1991, whereas the collection in De Bilt started in April 1990 and stopped one year later.

The rain samples were stored for at least six months to one year to allow radioactive growth of ^{210}Po. Subsequently the ^{210}Po activities were determined using the method as described in Benninger (1978) and van der Wijk (1987). In the laboratory, ^{208}Po tracer, Pb carrier and Fe carrier were added to water samples and, after at least 24 hrs, iron hydroxide was precipitated at pH 7-8 using ammonium hydroxide. The precipitate was concentrated by settling and centrifugation, then treated with hydrochloric acid to achieve complete dissolution in 1N HCl for ^{210}Po analysis. After Po plating (Fleer and Bacon, 1984), Pb recovery was determined with an atomic absorption method (Zuo and Eisma, 1992). The overall yield for ^{210}Pb was about 80% (range 55 - 95%). The ^{210}Pb activities were calculated by extrapolation from zero initial ^{210}Po activity. This assumption is justified based on the fact that the short residence time of ^{210}Pb in the aerosol (a few days), primarily produced by decay of atmospheric radon, precludes the presence of much ^{210}Po (halflife 138 d) in the atmosphere. This is, indeed, evident from a number of earlier studies of radionuclides in air and in rain water (Burton and Stewart, 1960; Peirson et al., 1966; Poet et al., 1972; Turekian and Cochran, 1981).

3. RESULTS AND DISCUSSION

Patterns of ^{210}Pb deposition flux

Results obtained from measurements of the total ^{210}Pb deposition at three sites are listed in Tables 1-3. A summary of replicates and blanks is given in Table 4. Uncertainties are standard errors based on counting statistics. The concentration in the blanks, determined by analysis of demineralized water through routine procedure, showed an insignificant contribution from contamination and does not exceed a few percent of the total ^{210}Pb concentration.

Table 1: *The data of ^{210}Pb flux at Texel, The Netherlands.*

Sample number	Collection date (m d y)	Flux (μBq/cm2/d)	Conc. (dpm/l)	Rainfall (mm/d)
9001	3/21/90-3/26/90	6.61±0.39	6.96±0.42	0.57
9002	3/26/90-4/08/90	5.78±0.44	5.49±0.42	0.63
9003	4/08/90-4/16/90	3.50±0.22	8.56±0.60	0.24
9004	4/16/90-4/18/90	27.56±1.17	7.21±0.31	2.29
9005	4/18/90-4/26/90	6.17±0.33	22.50±1.20	0.16
9006	4/26/90-4/27/90	63.11±2.67	8.28±0.35	4.57
9007	4/27/90-5/01/90	0.56±0.06	26.20±3.60	0.01
9008	5/01/90-5/09/90	19.11±0.83	26.60±1.10	0.43
9009	5/09/90-5/11/90	31.28±1.06	8.82±0.30	2.13
9010	5/11/90-5/12/90	43.89±3.17	2.59±0.19	10.20
9011	5/12/90-5/14/90	5.67±0.44	2.08±0.16	1.63
9012	5/14/90-5/26/90	0.33±0.06	24.80±2.30	0.01
9013	5/26/90-6/05/90	11.67±0.67	6.86±0.39	1.02
9014	6/05/90-6/08/90	5.67±0.33	4.47±0.26	0.76
9015	6/08/90-6/13/90	0.89±0.06	8.61±0.71	0.06
9016	6/13/90-6/15/90	0.33±0.06	18.90±3.20	0.01
9017	6/15/90-6/19/90	8.83±0.44	21.50±1.10	0.25
9018	6/19/90-6/21/90	4.06±0.28	10.10±0.69	0.24
9019	6/21/90-6/22/90	27.89±3.17	3.64±0.42	4.59
9020	6/22/90-6/28/90	23.22±1.78	8.65±0.66	1.61
9021	6/28/90-7/02/90	28.50±1.83	6.92±0.44	2.47
9022	7/02/90-7/09/90	14.39±1.17	11.90±0.94	0.73
9023	7/09/90-7/12/90	10.17±0.68	10.40±1.00	0.59
9024	7/12/90-8/08/90	1.56±0.11	4.65±0.37	0.20
9025	8/08/90-8/17/90	8.56±0.56	6.64±0.44	0.78
9026	8/17/90-8/21/90	15.61±1.33	3.65±0.31	2.57
9027	8/21/90-9/02/90	16.50±0.91	18.30±1.10	0.54
9028	9/02/90-9/07/90	15.44±1.22	4.48±0.35	2.07
9029	9/07/90-9/11/90	8.33±0.89	2.98±0.32	1.68
9030	9/11/90-9/14/90	0.72±0.11	12.70±2.10	0.03
9031	9/14/90-9/19/90	24.56±2.06	7.13±0.60	2.07
9032	9/19/90-9/20/90	46.22±4.61	5.19±0.52	5.35
9033	9/20/90-9/24/90	23.44±2.22	5.47±0.52	2.57
9034	9/24/90-9/26/90	5.83±0.50	16.20±1.40	0.22
9035	9/26/90-9/28/90	18.33±1.37	11.20±0.63	0.98
9036	9/28/90-10/2/90	25.33±1.89	5.95±0.44	2.56
9037	10/02/90-10/05/90	18.89±1.39	6.02±0.45	1.88
9038	10/05/90-10/08/90	17.83±1.50	4.27±0.36	2.51
9039	10/08/90-10/18/90	12.56±0.89	17.90±1.30	0.42
9040	10/18/90-10/28/90	13.28±1.11	3.89±0.33	2.05
9041	10/28/90-10/29/90	50.39±3.89	4.37±0.34	6.93
9042	10/29/90-10/31/90	58.72±5.11	6.80±0.59	5.18

Figures 2 and 3 show the daily deposition flux of ^{210}Pb observed at the three sites as well as the amount of precipitation. The distribution of the wind direction for every 10 day period (in percentages) at Texel and De Bilt during March 1990 - April 1991 is also shown in Figure 2. It is clear that the depostion flux of ^{210}Pb

Table 1: *Continued.*

Sample number	Collection date (m d y)	Flux (μBq/cm2/d)	Conc. (dpm/l)	Rainfall (mm/d)
9043	10/31/90-11/03/90	36.11±2.89	7.38±0.59	2.94
9044	11/03/90-11/12/90	7.67±0.72	3.99±0.37	1.15
9045	11/12/90-11/18/90	19.67±1.28	6.91±0.45	1.71
9046	11/18/90-11/23/90	20.11±2.39	4.67±0.55	3.97
9047	11/23/90-12/04/90	8.28±0.56	5.33±0.37	0.93
9048	12/04/90-12/15/90	27.06±2.67	8.11±0.50	0.96
9049	12/15/90-12/20/90	10.06±0.56	22.30±1.20	0.27
9050	12/20/90-1/03/91	5.72±0.44	4.56±0.34	0.76
9101	1/03/91-1/10/91	11.11±0.97	4.42±0.41	1.51
9102	1/10/91-1/18/91	5.33±0.61	2.44±0.28	1.32
9103	1/18/91-1/31/91	8.78±0.83	4.84±0.61	0.32
9104	1/31/91-2/21/91	16.22±1.50	9.54±0.92	0.49
9105	2/21/91-3/07/91	7.61±0.61	6.08±0.47	0.75
9106	3/07/91-3/17/91	6.44±0.61	20.05±1.80	0.19
9107	3/17/91-4/07/91	3.83±0.39	4.53±0.49	0.50
9108	4/07/91-4/19/91	12.33±0.78	8.60±0.53	0.86
9109	4/19/91-5/06/91	9.28±0.61	9.03±0.61	0.62
9110	5/06/91-5/23/91	6.00±0.44	5.82±0.44	0.62
9111	5/23/91-6/04/91	8.72±0.83	5.88±0.58	0.89
9112	6/04/91-6/10/91	2.44±0.28	3.63±0.38	0.41
9113	6/10/91-6/19/91	8.94±0.78	4.56±0.39	1.18
9114	6/19/91-6/27/91	12.94±1.33	4.24±0.40	1.32
9115	6/27/91-7/08/91	8.72±0.72	5.42±0.44	0.96
9116	7/08/91-7/14/91	12.22±1.11	5.96±0.54	1.23
Mean		15.26±1.69	8.76±0.77	1.54

shows a considerable variation at each station. As seen in Figure 2, two remarkable peaks among the daily deposition rate of ^{210}Pb are found in spring and later fall at both the Texel and De Bilt stations. Minimum values of ^{210}Pb flux occur in the summer and winter months. This seasonal variation is apparently related to the seasonal tendency of local climate conditions, as is evident from the fluctuation of precipitation during the same time period (Fig. 2). The May maximum of the ^{210}Pb flux at Texel appears to be due to precipitation (i. e., Coincides with unusually intense rainfall; Fig. 2a). With substantially lower precipitation the April event gave a higher ^{210}Pb flux, which is probably due to predominantly northeast winds (off the continent) prior to the April event (Fig. 2a). A similar pattern can be observed in the May 90 flux at De Bilt (Fig. 2b). So far as NE winds are concerned, this pattern cannot be expected in winter precipitation, due to frozen ground upwind. A similar seasonal variation of ^{210}Pb concentration in surface air was reported earlier at Chilton, England in 1961 - 1965 by Peirson et al (1966), which was interpreted as a result of the varying rates of radon exhalation under different

Table 2: *The data of ^{210}Pb flux at De Bilt,The Netherlands.*

Sample number	Collection date (m d y)	Flux (μBq/cm2/d)	Conc. (dpm/l)	Rainfall (mm/d)
9001	4/11/90-4/16/90	13.67±0.72	3.98±0.21	2.11
9002	4/16/90-4/19/90	9.72±0.44	6.21±0.27	0.94
9003	4/19/90-4/24/90	12.44±0.50	11.20±0.45	0.66
9004	4/24/90-5/01/90	14.39±0.52	13.60±0.49	0.64
9005	5/01/90-5/08/90	0.11±0.02	109.26±17.89	0.0007
9006	5/08/90-5/09/90	73.06±14.10	31.40±6.04	1.40
9007	5/09/90-5/16/90	27.39±2.61	11.50±1.10	1.43
9008	5/16/90-5/24/90	0.72±0.11	5.66±0.65	0.08
9009	5/24/90-5/29/90	-	-	-
9010	5/29/90-6/05/90	14.39±1.28	5.70±0.51	1.51
9011	6/05/90-6/11/90	12.61±1.17	4.32±0.39	1.75
9012	6/11/90-6/15/90	-	-	-
9013	6/15/90-6/19/90	-	-	-
9014	6/19/90-6/20/90	127.20±10.06	7.93±0.63	9.63
9015	6/20/90-6/26/90	5.01±0.44	4.41±0.39	0.68
9016	6/26/90-6/29/90	6.89±0.39	48.90±2.80	0.08
9017	6/29/90-7/05/90	13.39±0.94	4.57±0.32	1.76
9018	7/05/90-7/10/90	11.33±0.83	4.10±0.30	1.66
9019	7/10/90-7/14/90	-	-	-
9020	7/14/90-8/06/90	6.28±0.39	14.00±0.91	0.27
9021	8/06/90-8/14/90	2.44±0.17	104.04±7.10	0.01
9022	8/14/90-8/23/90	11.17±0.89	5.75±0.47	1.16
9023	8/23/90-9/05/90	10.83±0.72	8.01±0.54	0.81
9024	9/5/90-9/15/90	7.50±0.56	4.27±0.32	1.06
9025	9/15/90-9/29/90	5.56±0.50	4.44±0.40	0.75
9026	9/29/90-10/8/90	17.22±1.11	8.74±0.56	1.18
9027	10/8/90-10/18/90	14.06±0.78	10.50±0.60	0.80
9028	10/18/90-10/31/90	5.72±0.44	4.27±0.33	0.81
9029	10/31/90-11/5/90	18.94±1.28	5.50±0.37	2.06
9030	11/5/90-11/12/90	12.11±1.06	4.81±0.42	1.51
9031	11/12/90-11/14/90	18.83±1.50	2.80±0.23	4.04
9032	11/14/90-11/19/90	26.50±1.56	7.51±0.44	2.12
9033	11/19/90-11/21/90	31.78±2.44	3.68±0.28	5.18
9034	11/21/90-11/26/90	8.39±0.67	6.60±0.54	0.76
9035	11/26/90-12/05/90	4.44±0.33	5.21±0.37	0.51
9036	12/05/90-12/14/90	14.56±1.22	7.67±0.65	1.14
9037	12/14/90-12/21/90	9.72±0.83	3.90±0.33	1.50
9038	12/21/90-12/28/90	6.39±0.56	2.62±0.22	1.47
9039	12/28/90-1/02/91	9.72±0.94	2.56±0.26	2.11
9101	1/02/91-1/07/91	9.56±0.83	3.16±0.27	1.81
9102	1/07/91-1/13/91	8.78±0.72	3.10±0.26	1.70
9103	1/13/91-1/17/91	-	-	-
9104	1/17/91-1/22/91	8.22±0.61	5.62±0.43	0.88
9105	1/22/91-2/19/91	5.56±0.39	9.06±0.60	0.37
9106	2/19/91-3/18/91	6.72±0.50	10.57±0.82	0.38
9107	3/18/91-3/25/91	15.94±1.17	6.51±0.47	1.47
9108	3/25/91-4/01/91	-	-	-
9109	4/01/91-4/16/91	5.33±0.28	11.50±0.63	0.28
Mean		15.34±3.27	12.84±3.51	1.44

Table 3: *The data of ^{210}Pb flux at Groningen, The Netherlands.*

Sample number	Collection date (m d y)	Flux (μBq/cm2/d)	Conc. (dpm/l)	Rainfall (mm/d)
8701	12/26/86-1/07/87	8.21±0.70	3.81±0.32	1.27
8702	1/07/87-1/29/87	9.14±0.57	12.58±0.78	0.43
8703	1/29/87-2/12/87	6.38±0.58	3.46±0.31	1.09
8704	2/12/87-2/25/87	4.66±0.40	11.27±0.98	0.24
8705	2/25/87-3/05/87	12.12±0.86	4.32±0.31	1.66
8706	3/05/87-3/18/87	6.12±0.48	4.26±0.33	0.85
8707	3/18/87-3/25/87	7.84±0.71	2.12±0.19	2.18
8708	3/25/87-4/01/87	4.35±0.50	2.55±0.29	1.01
8709	4/01/87-4/08/87	15.00±1.50	13.94±1.39	0.64
8710	4/08/87-4/16/87	3.77±0.53	1.99±0.28	1.12
8711	4/16/87-4/22/87	4.72±0.69	5.01±0.74	0.56
8712	4/22/87-5/06/87	11.20±0.96	6.21±0.53	1.07
8713	5/06/87-5/13/87	14.42±1.16	3.73±0.30	2.29
8714	5/13/87-5/19/87	20.46±1.70	4.70±0.39	2.57
8715	5/19/87-6/03/87	10.51±0.79	5.82±0.43	1.07
8716	6/03/87-6/10/87	15.99±1.26	4.17±0.33	2.27
8717	6/10/87-6/16/87	15.36±1.31	3.47±0.30	2.62
8718	6/16/87-6/24/87	17.41±1.25	5.14±0.37	2.00
8719	6/24/87-7/01/87	13.96±1.12	3.60±0.29	2.29
8720	7/01/87-7/15/87	5.51±0.67	14.35±1.75	0.23
8721	7/15/87-7/22/87	44.63±3.86	11.66±1.01	2.27
8722	7/22/87-7/23/87	230.56±21.63	4.67±0.46	30.30
8723	7/23/87-7/29/87	17.08±1.94	3.85±0.44	2.62
8724	7/29/87-8/05/87	14.90±1.65	4.40±0.49	2.00
8725	8/05/87-8/12/87	20.94±1.90	5.38±0.49	2.30
8726	8/12/87-8/19/87	25.23±1.71	9.72±0.66	1.54
8727	8/19/87-8/26/87	30.92±2.89	8.02±0.75	2.28
8728	8/26/87-9/02/87	10.09±1.05	5.04±0.53	1.18
8729	9/02/87-9/09/87	36.55±2.93	9.48±0.76	2.28
8730	9/09/87-9/16/87	20.20±1.53	5.29±0.40	2.26
8731	9/16/87-9/23/87	58.39±3.24	15.30±0.85	2.26
8732	9/23/87-10/07/87	10.81±1.19	5.72±0.63	1.12
8733	10/07/87-10/15/87	12.69±1.38	3.78±0.41	1.98
8734	10/15/87-10/21/87	3.54±0.48	1.95±0.26	1.07
8735	10/21/87-10/28/87	4.22±0.56	4.18±0.56	0.60
8736	10/28/87-11/04/87	30.66±2.73	24.17±2.15	0.75
8737	11/04/87-11/11/87	21.07±1.80	21.93±1.87	0.57
8738	11/11/87-11/18/87	8.64±0.91	2.28±0.24	2.25
8739	11/18/87-11/25/87	7.66±0.92	2.01±0.24	2.26
8740	11/25/87-12/02/87	26.47±1.56	9.99±0.59	1.57
8741	12/02/87-12/17/87	9.74±0.83	6.50±0.55	0.89
8742	12/17/87-12/22/87	16.28±1.44	3.29±0.29	2.93
8743	12/22/87-12/30/87	16.88±1.97	5.83±0.68	1.71
8801	1/02/88-1/06/88	19.22±2.12	2.85±0.31	3.99
8802	1/06/88-1/13/88	16.04±1.49	4.21±0.39	2.26
8803	1/13/88-1/27/88	18.56±1.66	9.82±0.88	1.12
8804	1/27/88-2/20/88	10.85±1.09	2.44±0.24	2.63
8805	2/02/88-2/10/88	8.76±1.08	2.58±0.32	2.01
8806	2/10/88-2/24/88	10.23±0.94	5.32±0.49	1.14
8807	2/24/88-3/09/88	32.23±2.10	17.29±1.12	1.10

Table 3: *Continued.*

Sample number	Collection date (m d y)	Flux (μBq/cm2/d)	Conc. (dpm/l)	Rainfall (mm/d)
8808	3/09/88-3/16/88	22.69±2.24	5.92±0.58	2.27
8809	3/16/88-3/23/88	22.24±2.09	5.68±0.53	2.32
8810	3/23/88-3/30/88	22.67±2.29	5.93±0.60	2.26
8811	3/30/88-4/06/88	5.46±0.61	8.87±0.99	0.36
8812	4/06/88-4/20/88	4.43±0.42	6.23±0.59	0.42
8813	4/20/88-5/11/88	7.93±0.63	15.24±1.21	0.31
8814	5/11/88-5/26/88	21.97±1.36	26.97±1.67	0.48
8815	5/26/88-6/01/88	24.73±2.37	5.51±0.53	2.66
8816	6/01/88-6/07/88	29.07±2.19	6.42±0.48	2.68
8817	6/07/88-6/22/88	8.07±0.64	26.15±2.06	0.18
8818	6/22/88-6/29/88	11.70±0.99	11.27±0.96	0.61
8819	6/29/88-7/06/88	32.29±3.05	8.42±0.79	2.27
8820	7/06/88-7/13/88	20.83±1.64	5.34±0.42	2.31
8821	7/13/88-7/20/88	32.91±2.77	8.64±0.73	2.25
8822	7/20/88-7/27/88	31.72±2.28	8.18±0.59	2.29
8823	7/27/88-8/11/88	13.28±1.04	15.80±1.24	0.50
8824	8/11/88-8/22/88	19.29±1.32	8.03±0.55	1.42
8825	8/22/88-8/31/88	19.02±1.68	6.55±0.58	1.72
8826	8/31/88-9/07/88	32.42±2.82	7.99±0.70	2.40
8827	9/07/88-9/14/88	16.41±1.35	4.31±0.35	2.25
8828	9/14/88-9/28/88	22.99±1.82	11.84±0.94	1.15
8829	9/28/88-10/05/88	4.40±0.56	4.03±0.52	0.65
8830	10/05/88-10/12/88	20.49±1.65	5.42±0.44	2.24
8831	10/12/88-11/02/88	12.79±0.88	20.23±1.40	0.37
8832	11/02/88-11/16/88	12.89±1.10	6.76±0.57	1.13
8833	11/16/88-11/22/88	26.43±2.36	5.93±0.53	2.64
8834	11/22/88-11/30/88	14.49±1.22	11.60±0.98	0.74
8835	11/30/88-12/06/88	35.69±2.61	7.70±0.59	2.67
Mean		19.87±2.98	7.77±0.63	1.98

condition of soil, viz. the variation of temperature, moisture content and wind velocity near ground level.

The deposition flux of ^{210}Pb at Groningen during 1987-1988 illustrates a different pattern. A pronounced maximum was observed in early summer in 1987, whereas no apparent peak value was found throughout the year 1988 (Fig. 3). It is obvious that the fluctuations in the ^{210}Pb flux are closely correlated with the amount of precipitation (Fig. 3). Comparison between the existing data collected in 1983-1984, 1986 at the same site (Groningen station) (van der Wijk, 1987) and the data of this study, indicates a regional uniformity in the atmospheric ^{210}Pb deposition, characterized by a maximum deposition of ^{210}Pb in early summer (June - July). However the year 1988 is an exception. The systematic increase of ^{210}Pb deposition at Groningen in early summer or late spring is probably related to a local

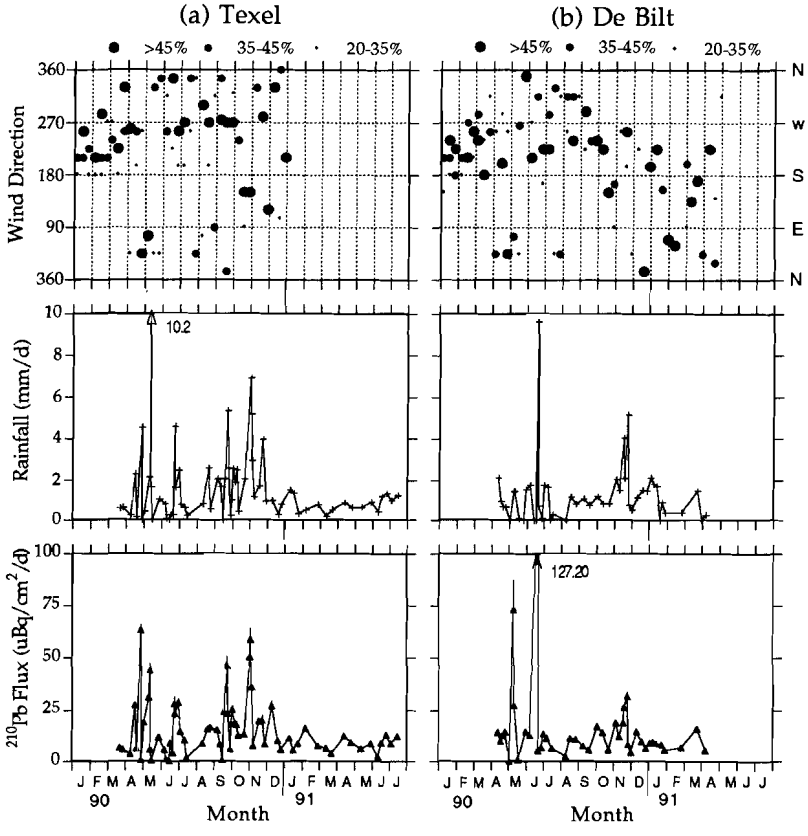

Fig. 2 *Daily atmospheric deposition of ^{210}Pb together with wind direction and precipitation in (a) Texel; (b) de Bilt, Mar. 1990 - July 1991. Full circles in different size represent fraction of the wind direction occurred during each 10-day period.*

enhanced radon exhalation, or a lateral transport of radon-rich air masses from elsewhere. Fukuda and Tsunogai (1975) reported the presence of a strong seasonal effect in ^{210}Pb concentration in precipitation in Japan; a winter maximum in their data was concluded to result from direct transport of continental aerosols over the Japan Islands by the winter north-west monsoon.

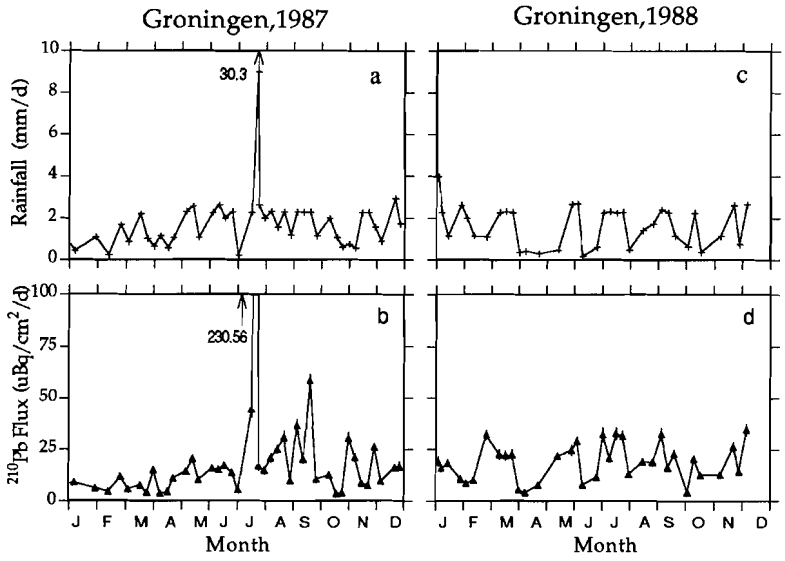

Fig. 3 *Daily atmospheric deposition of ^{210}Pb and precipitation in Groningen in the period of (a) and (b) Jan. 1987-Dec. 1987; (c) and (d) Jan. 1988-Dec. 1988.*

Table 4: *Measurement of replicates and blanks.*

Sample	^{210}Pb	
number	dpm/cm^2/mon	dpm/l
9002	0.0104±0.0008	5.49±0.42
(rain)	0.0108±0.0008	5.71±0.41
	0.0101±0.0006	5.36±0.31
9104	-	2.43±0.39
(snow)	-	2.67±0.25
	-	2.50±0.32
	-	2.33±0.22
blk1	-	0.12±0.04
blk2	-	0.08±0.01

Total ^{210}Pb deposition and its relation to the precipitation

The ^{210}Pb concentration in a sample representing a single precipitation event will clearly depend on complex array of variables, including the history of the air mass and the particular characteristics of the storm (intensity, duration, height of cloud cover, etc.). It is therefore not surprising that ^{210}Pb concentrations in rainfall vary considerably.

During the period March 1990 to July 1991, the daily ^{210}Pb flux at Texel varied from 0.33 to 63.11 $\mu Bq/cm^2/d$ with an annual average ^{210}Pb deposition of 0.32±0.04 $dpm/cm^2/yr$ (5.33±0.67$mBq/cm^2/yr$) (x±σ); the average of ^{210}Pb concentration in rain was 8.76±0.77 dpm/l (Table 1). The range of daily ^{210}Pb flux in De Bilt is 0.11-127.20 $\mu Bq/cm^2/d$ with an annual ^{210}Pb flux of 0.34±0.07 dpm/cm2/yr (5.67±0.66 $mBq/cm^2/yr$). The ^{210}Pb concentration in precipitation shows a relatively broad range (Table 2) with an average of 12.84±3.51 dpm/l. It is interesting to note that, though, there was more rainfall at Texel (562.10 mm/yr) than at De Bilt (525.60 mm/yr) during the sampling period (Fig. 2), the annual deposition flux of ^{210}Pb at the two sites was the same. We consider the observation as a result of regional variability. The relative high annual deposition flux of ^{210}Pb at De Bilt was contributed significantly by a heavy precipitation event that occurred in mid June of 1990 which, probably resulted from the convective weather system (local effect), somehow carried much more ^{210}Pb (Fig. 2b). In the year 1987-1988, the average annual deposition of ^{210}Pb at the northern station, Groningen, was 0.43±0.07 $dpm/cm^2/yr$ (7.25±1.53 $mBq/cm^2/yr$) with an average ^{210}Pb content of 7.77±0.63 dpm/l in precipitation (Table 3). The observed annual deposition flux of total ^{210}Pb at Groningen station is compatible with the previous result of 0.52 $dpm/cm^2/yr$ (8.8 $mBq/cm^2/yr$) based on the rain sample measurements in 1983-1984 (van der Wijk, 1987), suggesting relatively constant supply of total ^{210}Pb from the atmosphere on a yearly basis. In general, the annual deposition flux of ^{210}Pb does not differ significantly from site to site.

Turekian et al. (1977) have proposed a model for the atmospheric ^{210}Pb flux based on the large-scale atmospheric circulation and on aerosol residence times. The model considers one-dimensional transport by the west-to-east air circulation in latitude band 15 to 55° and predicts significant longitudinal variation in the ^{210}Pb flux. According to the model, the total ^{210}Pb deposition flux decreases from west to east across the Pacific and Atlantic oceans. The ^{210}Pb flux at the Netherlands by this model would be 0.5-1 $dpm/cm^2/yr$, which is about equal (lower limit) to the flux at Groningen and greater by a factor 1.5 to 3 than the fluxes at Texel and De Bilt. A

lower flux of ^{210}Pb compared with the model value was also reported by Turekian et al. (1983) at New Haven, and their explanation is that, during the summer the 'Bermuda high' is sufficiently developed to block passage of air coming directly off the North American continent. The reason in our case is probably related to the similar fact that the local air circulation somehow blocked transport pathways of Radon-rich air mass during some periods of the summer and winter, resulting in low ^{210}Pb deposition. In other words, the local climate condition of the Netherlands in some periods of the summer and winter was mainly controlled by the high pressure systems with generally little or no rain that block the route of a Radon-rich air mass, coming from the east; consequently ^{210}Pb deposition became less.

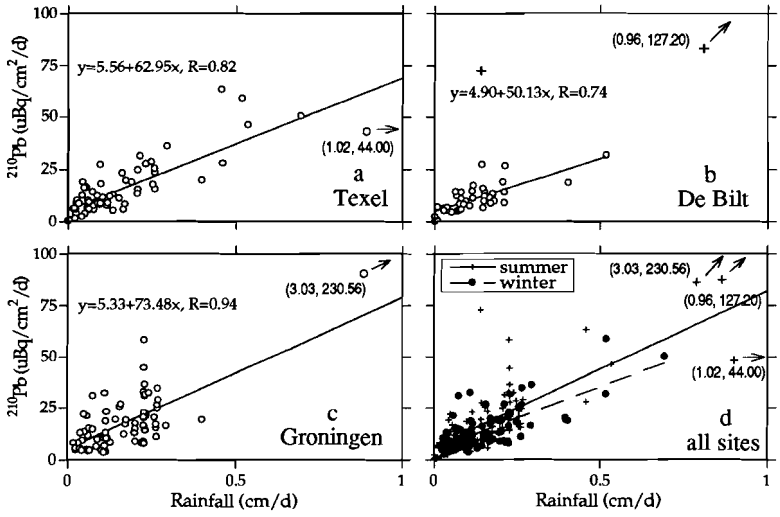

Fig. 4 *Daily ^{210}Pb total deposition plotted against daily precipitation in the Netherlands.*

Figure 4 shows a positive correlation between the daily deposition rate of ^{210}Pb and the amount of precipitation at all sites (R=0.94 at Groningen, 0.83 at Texel and 0.74 at De Bilt; Fig. 4a, b, c). The positive correlation coefficient in summer months (April to Sep.; y =5.47+76.36x. R=0.91) is higher than in winter months (Oct. - Mar.; y=4.69+60.60x, R=0.72) (Fig. 4d). Fukuda and Tsunogai (1975) observed the

inverse effect in Japan which they considered to be an influence of the north-west monsoon. Our observation may be explained by the fact that in winter the soil is occasionally frozen which prevents radon emanation.

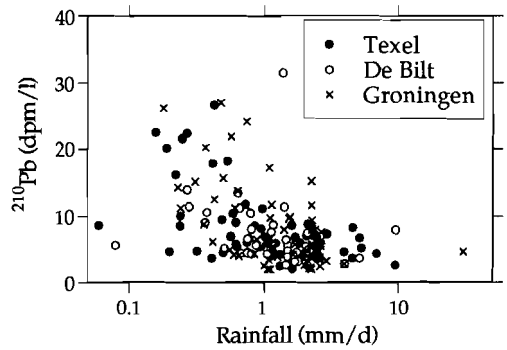

Fig. 5 *Scattergram showing inversely correlation of ^{210}Pb concentration in precipitation with average rainfall.*

As pointed out by Turekian et al. (1977) previously, in the idealized linear model for ^{210}Pb deposition vs. precipitation, the intercept at zero precipitation for a regression line can be used as an estimate of dry deposition (fallout). Based on highly correlated relation of ^{210}Pb flux to precipitation in our data (Fig. 4), the estimation of annual dry fallout at three sampling site was made and shown in Table 5. The result indicates that annual dry deposition of ^{210}Pb is about 16-38% of the total flux. The contribution of dry fallout, therefore, is an important part of the atmospheric supply of ^{210}Pb. The calculation for the dry deposition of ^{210}Pb at De Bilt did not take two extreme values (data numbers 9006 and 9014; Table 2) into account. With all data included, the dry deposition flux would be 0.003 dpm/cm^2/yr (R=0.81), less than 1% of the total ^{210}Pb deposition, which is an exceptionally low relative amount of dry deposition in the Netherlands.

Figure 5 is a plot of the ^{210}Pb concentration in rain against the amount of rainfall for all the stations. There is an inverse correlation between two components, suggesting that light rains tend to have higher concentrations of ^{210}Pb than heavy rains. A relation of the ^{210}Pb total deposition with the frequency of wind direction was also examined by plotting one against another (Fig. 6). As

shown in Figure 6a, there appears to be some correlation between the ^{210}Pb flux and wind direction at Texel; the ^{210}Pb deposition flux increases when the wind direction changes from NW to NE. This may be explained by a regional effect, with the ^{210}Pb concentration in the air enriched by a NE wind that crosses the European land mass and carries more Radon. The plot for ^{210}Pb flux and wind direction at De Bilt also shows similar trend (Fig. 6b). However, these measurements cover only a short timespan, so a meaningful conclusion cannot be drawn. For a better understanding of the behaviour of atmospheric ^{210}Pb, long term measurements are required.

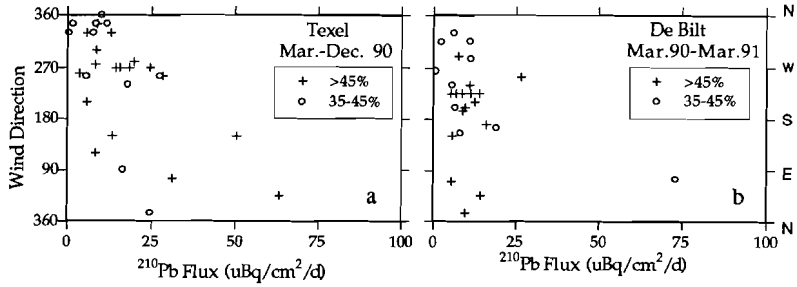

Fig. 6 *Plot of ^{210}Pb total flux versus wind direction at (a) Texel; and (b) de Bilt during Mar. 1990 - Mar. 1991. Wind directions are expressed as fractions in the 10 day period time.*

Total deposition velocity of ^{210}Pb

The deposition velocity concept has been extended to relate the surface-air concentration of ^{210}Pb (and other nuclides) to total fluxes, including deposition by all processes. This is not a strictly accurate transformation. The total deposition velocity, v, of a nuclide is calculated by the ratio (Turekian et al., 1983):

$$v = \frac{F}{C} \qquad (1)$$

where F is the total flux to the earth's surface (wet + dry); C is the concentration in air at some reference level. Here we are concerned with concentrations measured in surface air (reference = ground level). A number of studies have been carried out on the determination of ^{210}Pb concentration in the atmosphere (Lockhart, 1964; Peirson et al., 1966; Jaworoski, 1969; Turekian and Cochran, 1981; Samuelsson et al.,

1986). For ^{210}Pb in surface air in the Netherlands, we have adopted a value 5.02 x10^{-3} pCi/kg (0.013 dpm/m^3) measured at Chilton (England) by Peirson et al. (1966) in 1964 since we have no measured data available. Combining the value of ^{210}Pb concentration in air with our monthly ^{210}Pb deposition fluxes at three stations gives a mean total deposition velocity of 0.89±0.29 cm/s (n=192) in the Netherlands (Table 5). Furthermore, using the seasonal ^{210}Pb deposition flux for calculation we obtain the total ^{210}Pb deposition velocity of 1.02±0.15 cm/s for summer months and 0.76±0.07 cm/s for winter period (Table 5). The results derived here are in fair agreement with those found along other continental margin areas (Japan, Fukuda and Tsunogai, 1975; US, Turekian et al., 1983).

Table 5: *Estimation of annual total deposition and dry fallout of ^{210}Pb in the Netherlands.*

		^{210}Pb deposition (dpm/cm^2/yr)			Depos. velocity
	n	total	dry	dry/total	cm/s
De Bilt	46	0.34±0.07	0.11±0.02*	0.16±0.03*	0.83±0.17
Groningen	78	0.43±0.07	0.12±0.02	0.28±0.05	1.05±0.17
Texel	66	0.32±0.04	0.12±0.02	0.38±0.05	0.78±0.10
All sites (average)					
Summer (Apr.- Sep.)		0.42±0.06	0.12±0.02	0.29±0.06	1.02±0.15
Winter (Oct.- Mar.)		0.31±0.03	0.10±0.01	0.32±0.04	0.76±0.07

* Excluding the two extreme data points at De Bilt. With all data points included, the dry deposition would be 0.003 dpm/cm^2/yr, 0.7% of the total ^{210}Pb deposition (R=0.81).

4. CONCLUSIONS

The rate of atmospheric deposition of ^{210}Pb in the Netherlands is subjected to strong variations on a short time scale (a few days to a few weeks). The average annual deposition, however, appears to be rather constant on a year basis.

The observed annual deposition flux of ^{210}Pb varies from 0.32 to 0.43 dpm/cm^2/yr (5.33-7.25 mBq/cm^2/yr) at different locations in the Netherlands, which is about a factor of two to three lower than around North America. The

average total deposition velocity of ^{210}Pb is about 0.89 cm/s, which is compatible with other observations.

There is a good correlation between the daily ^{210}Pb deposition and the precipitation, which indicates the presence of a strong seasonal effect between summer periods and winter months: the deposition flux is higher in summer than in winter. The dry fallout flux, estimated from the relation of ^{210}Pb flux with precipitation, is about 16-38% of the total deposition of ^{210}Pb. It is concluded that total deposition data are of greater value in assessing atmospheric ^{210}Pb deposition at a given locality than are data on individual precipitation events since dry deposition is included. Furthermore, for a good representation of the flux, measurements on a long time scale are required to overcome the influence of strong seasonal variation and regional variability.

ACKNOWLEDGEMENTS--We wish to thank R. Gieles and C. Fisher for their assistance of sample measurements. We thank H. J. Boekel and his group for making the rain collectors. Dr. A. G. M. Driedonks and Dr. J. W. Schaap (KNMI) made the rain collection possible at De Bilt and provided many useful meteorological data; Q. Liu kindly collected all the samples at the De Bilt station; their help is highly appreciated.

REFERENCES

Benninger L. K. (1978) ^{210}Pb balance in Long Island Sound. *Geochim. Cosmochim. Acta*, **42**, 1165-1174.

Burton W. M. and N. G. Stewart (1960) Use of long-lived natural radioactivity as an atmospheric tracer. *Nature*, **186**, 584-589.

Fleer A. P. and M. P. Bacon (1984) Determination of ^{210}Pb and ^{210}Po in seawater and marine particulate matter. *Nucl. Instruments Meth. Phys. Res.*, **223**, 243-249.

Fukuda K. and S. Tsunogai (1975) Pb-210 in precipitation in Japan and its implication for the transport of continental aerosols across the ocean. *Tellus*, **27**, 514-521.

Jaworoski, Z. (1969) Radioactive lead in the environment and in the human body. *Atomic Energy Rev.*, **7**, 3-45.

Lockhart, L. B. Jr. (1962) Natural radioactive isotopes in the atmosphere at Kodiak and Wales, Alaska. *Tellus*, **14**, 350-355.

Peirson D. H., R. S. Cambray and G. S. Spicer (1966) Lead-210 and Polonium-210 in the atmosphere. *Tellus.*, **18**, 427-433.

Poet S. E., H. E Moore and E. A. Martell (1972) Lead-210, Bismuth-210 and Polonium-210 in the atmosphere: Accurate ratio measurements and application to aerosol residence time determination. *J. Geophys. Res*, **77**, 6515-6527.

Samuelsson C., L. Hallstadius, B. Persson, R. Hedvall, E. Holm and B. Forkman (1986) ^{222}Rn and ^{210}Pb in the Arctic summer air. *J. Environ. Radioactivity*, **3**, 35-54.

Turekian K.K.,Y. Nozaki and L.K. Benninger (1977) Geochemistry of atmospheric radon and radon products. *Annu. Rev. Earth Planet. Sci. Lett.*, **5**, 227-255.

Turekian K.K. and J.K. Cochran. (1981) 210Pb in surface air at Enewetok and the Asian dust flux to the Pacific. *Nature*, **292**, 522-525.

Turekian K. K., L. K. Benninger and E. P. Dion (1983) ^{7}Be and ^{210}Pb total deposition fluxes at New Haven, Connecticut and Bermuda. *J. Geophys. Res.*, **88**, 5411-5415.

Wijk A. van der (1987) Radiometric dating by alpha spectrometry on Uranium series nuclides. Ph.D Thesis, State University of Groningen, The Netherlands, 168 pp.

Zuo Z. and D. Eisma (1992) Spatial distributions of ^{210}Pb and ^{137}Cs and mixing rates in sediments of the southern North Sea. *Cont. Shelf Res.*, Submitted.

CHAPTER 7

DETERMINATION OF SEDIMENT ACCUMULATION AND MIXING RATES IN THE GULF OF LIONS, THE MEDITERRANEAN SEA

ABSTRACT

Sediment mixing and accumulation rates in the Gulf of Lions were determined, applying the ^{210}Pb and ^{137}Cs dating methods to a total of 20 boxcores taken in 1987, 1988 and 1989.

The distribution of excess ^{210}Pb profiles indicated the presence of surface mixed layers in the nearshore sediment cores which ranged from 3 to 15 cm. The apparent ^{210}Pb accumulation rates varied from 0.02 to 0.63 cm.yr^{-1} in this study area. Rates were highest near the river mouth of the Rhône and decreased with increasing water depth and increasing distance from the river mouth.

Observed depths of ^{137}Cs penetration within the sediments were compared with depths predicted from the surface mixed layer thickness and the ^{210}Pb accumulation rate. These showed a general agreement but one station suggests that there are some effects of relatively deep mixing below the intensely mixed surface layer. However, the agreement of ^{210}Pb and ^{137}Cs data of most stations indicates a general absence of deep mixing in the Gulf of Lions. Therefore, the apparent accumulation rates calculated from the ^{210}Pb profiles (below the surface mixed layer) generally reflect the true sedimentation rates.

From the sedimentation distribution, the annual amount of sediment deposited in this study area was estimated to be 10.1×10^9 kg. yr^{-1}, of which 30 % is biogenic and at least 20 % is contributed by atmospheric input. It is concluded that most of the sediment supplied by the Rhône river was deposited near the river mouth, and the remainder on the continental shelf and the upper slope, only a small amount being transported to the deep-sea basin.

INTRODUCTION

The Gulf of Lions is an important feature of the Mediterranean coastline of France (Fig. 1). The deposit of sediment in this area is governed not only by the intricate topography of the sea bed but also by the terrigenous input and water circulation. The steep continental slope is indented by a large number of submarine canyons which constitute about 50 % of the slope surface. This margin is characterized by relatively low annual sediment inputs, irregularly discharged over the years due to the Mediterranean climatic conditions (Courp and Monaco, 1990). The Rhone river is the dominant (80 %) source of sediment for the continental shelf of the Gulf of Lions. Pauc (1970), Blanc (1977) and Leveau and Coste (1987) have suggested that the annual discharge by the Rhone river is 3-5 x 10^9 kg.yr^{-1}. Water circulation is mainly controlled by the Liguro-Provencal current (Monaco *et al.*, 1987; Millot, 1987), a NE-SW flow, on which the outflow plume of the Rhone river is superposed. Besides a direct feeding of material from the continent by the Rhone river and other less important coastal rivers, atmospheric input from the Sahara desert dust and biogenic (carbonate, organirc matter, opal, *etc.*) production that are produced in the surface water also play important roles in the depositional system of the Gulf of lions. Applying ^{210}Pb and ^{137}Cs dating method measurements to a total of 20 boxcores, this paper discusses quantitative analyses of accumulation, mixing and distribution of bottom sediments in the Gulf of Lions. Preliminary results of this work were published in the proceedings of the EROS-2000 meeting in Paris in 1989 (Water Pollution Research Report 13, Zuo *et al.*, 1989 *b*).

SAMPLING AND MATERIAL

In 1987, 12 boxcores were collected by the Nehterlands research vessel *Tyro* in the area of the Gulf of Lions. A year later, seven other boxcores were taken during a cruise with the English research vessel *Discovery*. An additional eight boxcores were obtained in 1989 during a cruise of the Italian research vessel *Bannock*. Out of the twelve cores collected in 1987, four were not used for dating beeause two were very sandy and two others were duplicates. Also the core taken at station 8908 in 1989 was not analysed because its location was close to that of the core taken at station 8917, but all cores collected in 1988 were used for geochronological dating. Not taken into account is core RT2 from the river mouth area, because it did not penetrate the top mixing layer. Figure 1 shows the location of the boxcores which are the subject of this paper.

The boxcores were subsampled with PVC pipe (6 cm Ø), and were stored upright to avoid mixing of the soft top layer during transportation. The sediment cores were split, described and an X-ray radiograph was made for each core. The subsampling was made at 1-3 cm intervals for ^{210}Pb and ^{137}Cs dating. The determination of water content in the sediment was done to calculate sediment porosities (Ø) according to Anderson *et al.* (1987):

$$\text{Ø} = \frac{\%W}{\%W + (1 - \%W) / p_s} \qquad (1)$$

where %W is the measured water percentage by weight and p_s is the dry density of the sediments, which was assumed to be 1.60 g.cm^{-3} for this study area. The carbonate content is 25-30 % in the nearshore coastal sediments and 40-50 % in the offshore sediments (Nolting, 1989).
The sediments cores, according to both X-ray radiographs and observation, showed distinct differences between the nearshore cores (< 1000 m) and the offshore cores (Fig. 1). Clay or silty clay were dominant in the former, together with a disturbed top layer. Cores showed numerous small burrows and tubes ranging from 1-5 mm in diameter. Though in cores ME1 and 8725 a mottled structure with many shell and shell fragments was present, X-ray radiographs showed little burrowing below the surface mixed layer (SML). The foraminifera and many other

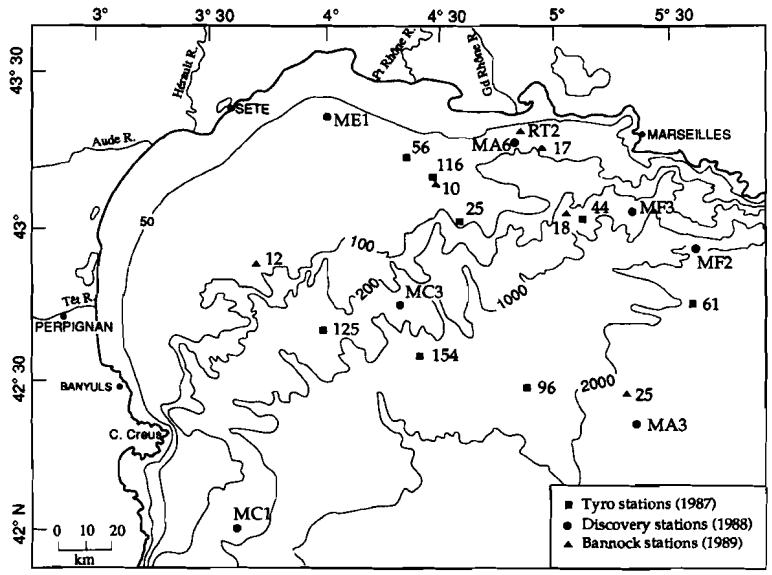

Figure 1

General map of Gulf of Lions, Mediterranean Sea, showing the location of boxcores collected in 1987, 1988 and 1989.

elements of the indigeous meiofaunal community are generally confined to the uppermost centimetre of the sediment due to their feeding habits (Smith and Schafer, 1984), which indicates that the bioturbation processes were mainly restricted in the surface zone, ranging in this area from a few centimetres to about 15 cm. In cores taken from areas deeper than 1000 m, grey or brown grey clay with uniform or weakly layered structure were observed. The X-ray radiographs exhibited faint beddings in the sediment, which suggests that the deep water area might be an inhospitable environment for burrowing macrofauna.

DATING METHODS AND MIXING

The use of the natural radionuclide ^{210}Pb to determine marine and freshwater sedimentation is now a well established technique (El-Daoushy, 1978; Chanton *et al.*, 1983; Binford and Brenner, 1986; Berger *et al.*, 1987; Eisma *et al.*, 1989). Its half-life of 22.3 years makes ^{210}Pb a powerful tool in relating sedimentation to oceanic processes which have occurred during the past 100 years or so. ^{210}Pb is brought into the sediment both by *in situ* production through radioactive decay of ^{226}Ra (supported ^{210}Pb) as well as by deposition of the decay product of ^{222}Rn (excess ^{210}Pb) which is produced in the atmosphere and in the water column. Being a beta emitting nuclide, ^{210}Pb cannot directly be measured by alpha spectrometry. Therefore, the ^{210}Pb activity is determined indirectly by measuring its alpha emitting granddaughter ^{210}Po (half-life 138 days). Secular equilibrium between these two nuclides is reached in approximately two years so that in older natural systems the ^{210}Po activity equals the ^{210}Pb activity, provided that the sediments acts as a closed system with respect to lead and polonium (Van der Wijk, 1987).

If we assume that the deposition of ^{210}Pb is at steady state, then the ^{210}Pb profile can be used to calculate the accumulation rate (S) using the following relationship (Robbins and Edgington, 1975; Goldberg *et al.*, 1977; Anderson *et al.*, 1987):

$$S = \frac{\lambda Z}{\ln (A_0/A_z)} \qquad (2)$$

where:

A_0 = excess ^{210}Pb activity at the sediment surface (dpm.g^{-1});

A_z = excess ^{210}Pb activity at depth z (dpm.g^{-1}) below level of A_0;

λ = decay constant of ^{210}Pb (= 0.03114 yr^{-1}) and

Z = depth.

Seldom is sediment accumulation a simple burial of particles. In marine environments, sedimentation can undergo significant change on time scales of 100 years. Typical accumulation rates on continental margins are millimetres to centimentres per year (Nittrouer *et al.*, 1983/1984), therefore the last 100 years of accumulation are represented

by the upper metre or so of the seabed. This is also the region reworked by mixing processes, especially by benthic organisms, which complicate the mechanism of sediment accumulation and the interpretation of ^{210}Pb profiles. The biological mixing process modelled as a diffusion process (Guinasso and Schink, 1975; Nittrouer *et al.*, 1983/1984; DeMaster *et al.*, 1985) is given by the advec-

$$D_B \frac{\partial^2 A}{\partial Z^2} - S \frac{\partial A}{\partial Z} - \lambda A = 0 \quad (3)$$

tion-diffusion equation:
where D_B is the particle mixing coefficient ($cm^2.yr^{-1}$); the other terms are as defined above. The solution to this equa-

$$S = \frac{\lambda Z}{\ln (A_0/A_z)} - \frac{D_B}{Z} [\ln.A_0/A_z)] \quad (4)$$

tion can be rearranged for calculation of accumulation rate
If mixing is negligible ($D_B = 0$), equation 4 simplifies to equation 2. However, if mixing is present, equation 4 demonstrates that consideration of only accumulation and radioactive decay provides an apparent accumulation rate which overestimates the true accumulation rate. In equation 4, there are two unknown parameters (D_B and S). To solve this, ^{137}Cs measurement was used in conjunction with ^{210}Pb dating method (Robbins and Edgington, 1975). In some cores (MA3, 8925, 8796 and 8761) fine undisturbed bedding with at most a few small burrows indicated that D_B is 0 or very nearly 0.

The particle-reactive isotope ^{137}Cs (half-life 30 years) is a fission product initially introduced into the environment as a result of nuclear weapons testing. Significant amounts of ^{137}Cs deposition began to occur in about 1953 and the maximum ^{137}Cs concentration in the sediment corresponds to the 1963 maximum in atmospheric ^{137}Cs fall out. This approach presumes that: 1) the time between atmospheric production and ^{137}Cs arrival at the seabed is short; 2) there is no intensely mixed surface layer. Under these conditions, the depth of ^{137}Cs penetration into the seabed can be measured and related to the mixing and accumulation rates by incorporating the dispersion-advection equation (Guinasso and Schink, 1975):

$$H = (2D_B t)^{1/2} + St \quad (5)$$

where H is the depth of penetration (cm) for particles with ^{137}Cs activity, and t is the elapsed time (yr) since ^{137}Cs activity reached the seabed. ^{134}Cs is also a man-made radionuclide with a much shorter half-life of two years. In our study area it is strongly related to the river input because of the release from the power plants located upstream on the Rhône river. However, it is possible to use Cs isotopes as the best potential tool to check ^{210}Pb accumulation rates (Robbins *et al.*, 1978; Von Gunten *et al.*, 1987; Wan *et al.*, 1987).

For ^{210}Pb dating, samples of 0.5 g (dry weight) were spiked with a known amount of ^{208}Po as a yield tracer and leached with HF, $HClO_4$, HNO_3 and HCl solutions. The Po-isotopes were plated on silver discs at 85°C after reduction of Fe^{3+} with ascorbic acid and analysed using a-spectroscopy. The supported ^{210}Pb activity was obtained by measuring the ^{226}Ra concentration and assuming secular equilibrium with ^{210}Pb, or by measuring ^{210}Pb in sediments old enough to accept that all the unsupported ^{210}Pb has decayed and assuming that supported ^{210}Pb is constant.

For cesium dating, about 20 g of dried sediment was taken for each sample at intervals of 1-3 cm. The concentration of cesium was measured nondestructively in a high-resolution Germanium detector for about 24 hours to obtain enough counts. Activity of ^{137}Cs was calculated by integrating the counts under the peak at 662 KeV and activity ^{134}Cs was determined by integrating counts under the peaks at 604 and 795 KeV.

RESULTS AND DISCUSSION

Lead- 210 distribution and apparent accumulation rate

Table 1 lists surface mixed layer depth (L), the apparent accumulation rate (S) and the sediment flux (R) derived from the excess ^{210}Pb activity-depth profiles in twenty cores.

Table 1

Sedimentation rates (S), fluxes (R), surface mixed layer depth (L, from ^{210}PB profiles) and water content (W, in upper 20cm) in 20 sediment cores.

Station	Mixing depth on X-radiograph (cm)	Surface mixed layer L (cm)	Water depth (m)	Accumulation S (cm.yr-1)	Accumulation R (g. cm-2 yr-1)	Water content W (%)
*** 1987**						
8725	n.b.	6	100	0.15	0.12	39
8744	n.b.	2	420	0.13	0.11	35
8756	1	3	68	0.14	0.10	44
8761	≈0		2250	0.04	0.02	49
8796	≈0		1701	0.05	0.04	35
87116	n.b.		69	0.15	0.12	39
87125	n.b.		728	0.11	0.07	47
87154	n.b.		1270	0.11	0.08	41
***1988**						
MA3	≈0		2230	0.02	0.02	36
MA6	n.b.	15	73	0.63	0.47	41
MC1	6		780	0.05	0.04	37
ME1	n.b.	8	49	0.18	0.17	30
MF2	n.b.	4	1100	0.08	0.05	47
MF3	n.b.	6	560	0.09	0.06	48
MC3	n.b.	5	260	0.17	0.13	40
***1989**						
8910	n.b.	8	79	0.12**	0.09	40
8912	n.b.	3	98	0.15	0.14	30
8917	n.b.	8	90	0.20	0.16	39
8918	n.b.		390	0.12	0.09	42
8925	≈0		2160	0.03	0.03	35

n.b. = no bedding.
* the year in wich the boxcores were taken.
** calculated from ^{137}Cs profile (^{210}Pb not measured).

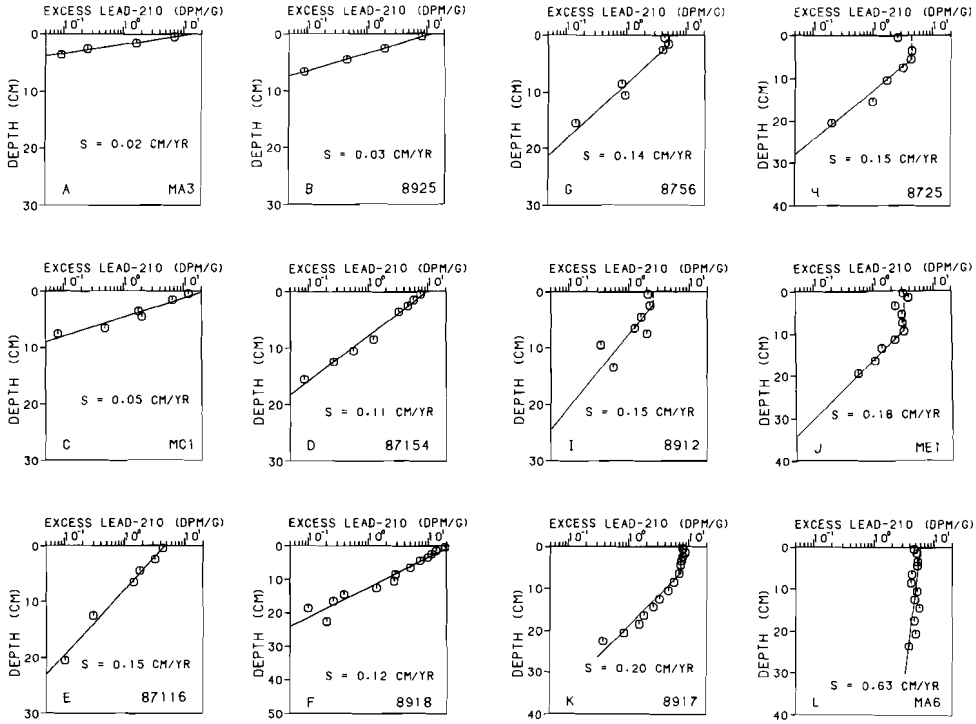

Figure 2

Semi-logarithmic profiles of excess ^{210}Pb activity against sediment depth

The sediment flux (R) was calculated according to the following equation

$$R = S (1 - \emptyset) p_s \quad (6)$$

Near to the sediment-water interface, the ^{210}Pb activities ranged from 2.08 to 18.92 dpm.g^{-1}, which is higher than that in the sediments of the North Sea (0.7 to 1.2 dpm.g^{-1}; Zuo *et al.*, 1989 *a*). The values of ^{210}Pb background varied from 0.54 to 1.44 dpm.g^{-1}.

Two types of excess ^{210}Pb distribution were observed (Fig. 2):

1) the excess ^{210}Pb activities decrease exponentially downward the sediment-water interface with a constant gradient (MA3, 8925, 8761, 87154, 87116, 8918, MC1 and 87125; Fig. 2: A, B, C, D, E, F). In cores MA3, 8925, 8761 and 8796 this corresponds with the evidence from X- ray radiographs which show fine layerings in the top layers. MC1 in top layer of 6 cm shows some signs of bioturbation but is not very clear. All other cores of this group have no bedding and show signs of burrowing. Therefore, mixing is negligible in four cores and the ^{210}Pb apparent accumulation rates in these cores are representatives of the true accumulation rate. The cores belonging to this type were collected from the offshore area with relatively deep water (100- 2250 m);

2) Most of the cores in this type had uniform ^{210}Pb activities in the upper few centimetres, below which the excess ^{210}Pb activities decreased exponentially with depth (cores 8756, 8725, 8912, ME1, 8917, MA6, MF2, 8744, 8756 and MC3; Fig. 2: G, H, I, J, K, L). The surface mixed layer ranged from 3 to 15 cm. X-radiographic evidence of burrowing intersecting the top 15 cm interval indicates that the ^{210}Pb subsurface maximum was caused by rapid mixing of surface sediments possibly due to biological processes. The accumulation rates from those cores calculated below the mixed surface zone are maximum accumulatiuon rates because the effects of deep mixing below the surface mixed layer are not known.

The apparent sediment rates of twenty cores were ranged from 0.02 to 0.63 cm.yr^{-1} or 0.02 to 0.47 g.cm^{-2}.yr^{-1}. The highest rate (0.63 cm.yr^{-1}) was found at over 73 m depth, just off the Rhône river mouth (station MA6), while the lowest (0.02 cm.yr^{-1}) was found about 2000 m water depth (station MA3), far from the continental shelf and upper slope, which indicates a significant decrease of

deposition rate with increasing water depth.

Cesium-137 distribution and penetration

Table 2 shows the concentrations of cesium isotope in the sediment of nine cores obtained from gamma spectrum measurements. The activities of ^{137}Cs ranged from 5 to 309 $Bq.kg^{-1}$, while the activities of ^{134}Cs were from 0.5 to 16.5 $Bq.kg^{-1}$.

Table 2

Concentrations of cesium isotopes in sediment cores.

Station	^{137}Cs ($Bq.kg^{-1}$)		^{134}Cs ($Bq.kg^{-1}$)		$^{134}Cs/^{137}Cs$ (%)	
	Range	Average	Range	Average	Surface	Average
MA6	81.9-141	118.9	0.5-16.5	8.2	12.5	6.9
ME1	7.8-66.6	45	0.0	-	-	-
8725	5-126	52.6	0.0	-	-	-
8910	32.2-241	170.9	0.0	-	-	-
8918	94.7-207	123.3	0.0	-	-	-
8917	31.7-309	148.1	0.0	-	-	-
MA3	5.4	(0-1.5 cm)	0.0	-	-	-
8 925	84.4	(0-1.5 cm)	0.0	-	-	-
MC1	14.2	(0-2 cm)	0.0	-	-	-

Figure 3 shows the activity-depth profile of radiocesium in nine sediment cores. Significant amounts of ^{134}Cs were only found in station MA6 (Fig. 3 *A*) just off the river mouth, and were accompanied by relatively high concentrations of ^{137}Cs.

Nittrouer *et al.* (1983/1984) have concluded that in a two-layer model (*i.e.* negligible mixing below the surface layer), the observed ^{137}Cs penetration should be the sum of mixed layer thickness plus sediment accumulation since ^{137}Cs emplacement (about 1953 for this study area). It is important to recognize that mixing below the surface layer will cause deeper penetration of particles (and ^{137}Cs) than is predicted by the ^{210}Pb accumulation rate, which was confirmed to be true from the ^{137}Cs activity profiles by Nittrouer *et al.* (1983/1984). A corollary is that if the observed and predicted depths of ^{137}Cs penetration agree, the effect of deep mixing on the ^{210}Pb accumulation rate is negligible. Table 3 compares the depths of ^{137}Cs predicted (H_p) from ^{210}Pb profiles and those actually observed (H_o) from Figure 3. Except for one core (station 8725), in gene-

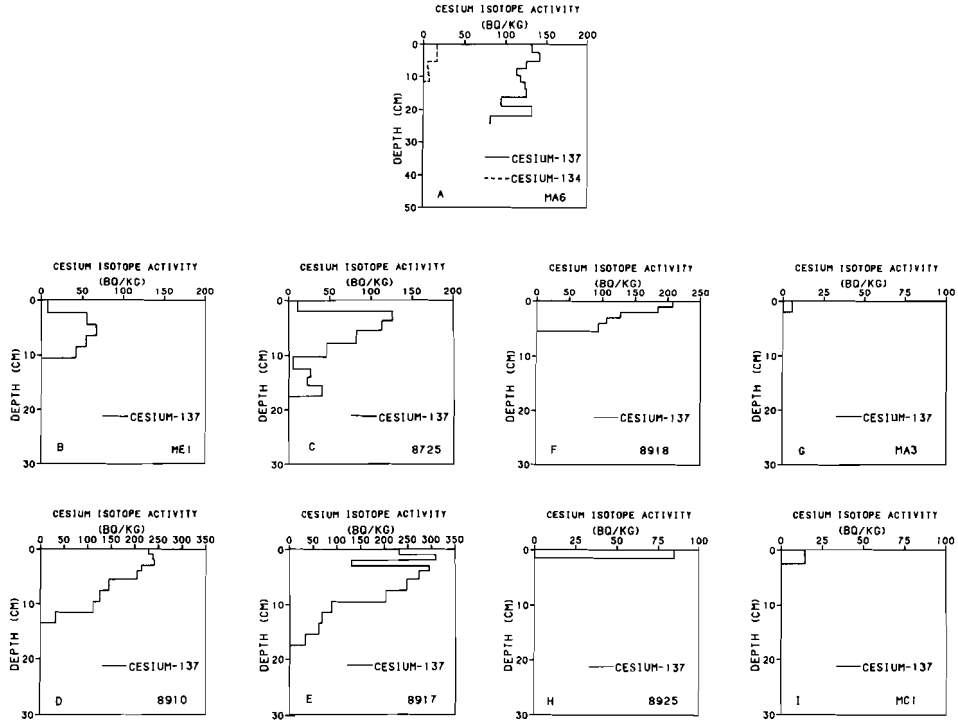

Figure 3

The activity-depth profiles of radiocesium isotopes in nine sediment cores.

ral, the agreement between H_p and H_o is good. Hence, deep mixing is not a common occurrence and ^{210}Pb accumulation rates calculated with the assumption of no deep mixing are accurate for most of the Gulf of Lions. This is true especially for the relatively deep water area because the observed depth of ^{137}Cs penetration in cores 8918, MA3, 8925 and MC1 (Fig. 3) would give independently very similar accumulation rates since the significant amount of ^{137}Cs occurred after 1952. Anderson *et al.* (1987) and Robbins and Edgington (1975) revealed that mixing and winnowing of sediments could cause redistribution of ^{137}Cs peak either downward or upward which was also observed in our ^{137}Cs profiles, while Davis *et al.* (1984) suggested that the shifting of the ^{137}Cs peak in sediments could be the result of transport of ^{137}Cs dissolved in pore waters.

From equation 5 (*see* above), using the observed ^{137}Cs penetration depth, H_p, and the ^{210}Pb accumulation rate, S, the mixing coefficient, D_B, can be estimated by rearranging equation 5:

$$D_B = (H_O - St)^2/2t \quad (7)$$

The values of D_B in our cores ranged from 0.0001 to 2.08 $cm^2.yr^{-1}$ (Tab. 3) which are rather low figures. Guinasso and Schinck (1975) described a dimensionless parameter G, which is equal to the mixing rate (D_B/L) divided by the accumulation rate S. When G is high (>10), mixing dominates the effects of accumulation; while G is low (<1), the accumulation term dominates. In our sediment cores, G is generally low (Tab. 3) and except for station 8725, the values of G confirm that the ^{210}Pb apparent accumulation rates reflect the true rates of sedimentation in the Gulf of Lions. The relatively high figures of D_B (2.08 $cm^2.yr^{-1}$) and G (2.31) in core 8725 indicate that in this core there are some effects of relatively deep mixing compared to the other sediment cores.

The ^{134}Cs to ^{137}Cs isotope ratio in core MA6 is shown in Figure 4. The ratio (0.04-0.13) in the core MA6 decrease with depth to zero at a depth of 12 cm, which is similar to those found by Martin and Thomas (1990, 0.12-0.24) in the same area. In fact, the higher the ratio, the higher is the contribution of the most recent input. The activity of ^{137}Cs in our cores is clearly related to the distance from the river mouth and to the water depth. This distribution supports the hypothesis that in the area of river mouth the direct input from the atmosphere is less significant than the contribution from the river.

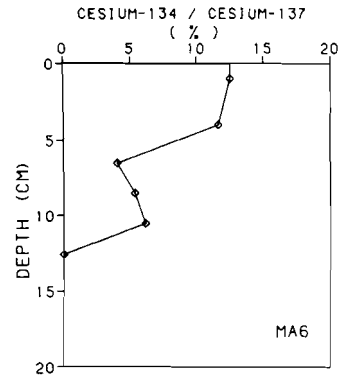

Figure 4

Variation profile of the isotope ratio (^{134}Cs to ^{137}Cs) at different sediment depths in core MA6.

Table 3

Comparison of predicted (Hp) and observed (Ho) ^{137}Cs penetration depth, mixing coefficients (Db) and the parametre G in the sediments.

Station	Collection date	^{210}Pb data		^{137}Cs penetration		Db	G
		Surface mixed layer L (cm)	Accumulation rate S (cm.yr^{-1})	Hp (cm)	Ho (cm)	($cm^2.yr^{-1}$)	
MA6	1988	15	0,63	37	26•	0.22	0.02
ME1	1988	8	0,18	14	11	0.33	0.25
8725	1987	6	0.15	11	17	2.08	2.31
8910	1989	8	not measured		12		
8917	1989	8	0.20	15	17	1.33	0.83
8918	1989		0.12	4	5	0.006	
MA3	1988		0.02	1	1.5	0.009	
8 925	1989		0.03	1	1	0.0001	
MC1	1988		0.05	2	2	0.001	

• The core did not penetrate the ^{137}Cs layer due its limited length.

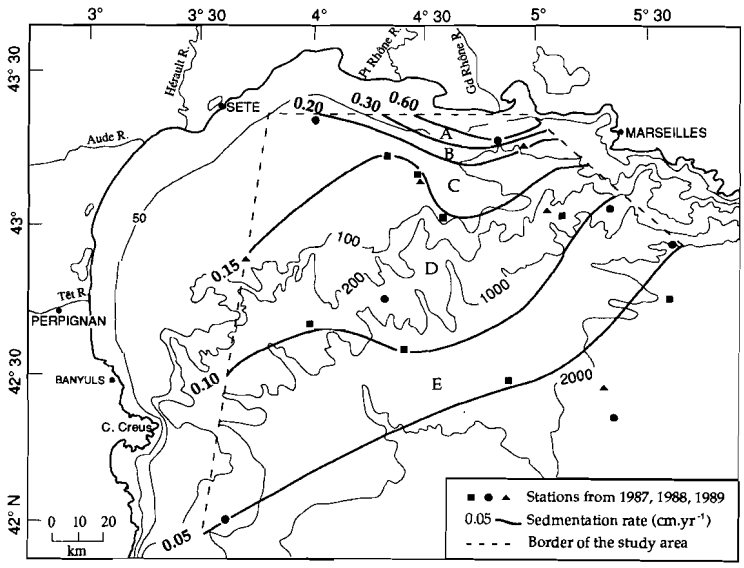

Figure 5

Spatial distribution of accumulation rates in the Gulf of Lions.

Sedimentation distribution

Figure 5 indicates a rough-like spatial distribution of ^{210}Pb apparent accumulation rates with a seaward decreasing gradient in the Gulf of Lions, which divides the studied area into five zones (A to E) by the isolines of sedimentation rate. Combining all isoline values and the corresponding isoline distances to the point of the highest isoline (0.6; Fig. 5) on a two-dimensional plot (Fig. 6), it is very clear that the distribution is nonlinear: the sedimentation rate drops sharply within the nearshore zone while the value decreases slowly further offshore. So the mean sedimentation rate (S_i) for each zone was calculated (Tab. 4), using an inverse square root (ISR) transformation to get a best fit of the curve by linearization according to the following formula

$$S_i = 1/\{[\sum_{i}^{i+1} (1/\sqrt{x_i})]/2\}^2 \quad (8)$$

where x_i = the sedimentation rate at isoline i (i = 1). This transformation prevents the overestimation of the mean sedimentation rate as compared to using simply the mean between two isolines. Taking this as a base together with an average sediment water content of 40 %, the maximum annual amount of the deposited sediment in each zone was estimated (Tab. 4).

In our study area, four depositional environments were observed:

1)- The Rhône prodeltaic area (zones A and B, Fig. 5) which is characterized by a strong contribution of the Rhone river. Sediment accumulation here is about 1.4 x 10^9 kg.yr^{-1}. Very near to river mouth, only one core (RT2) is available, with a limited length which is not considered representative for the estuarine area.

2)- The continental shelf area (zone C) in which erosion and resuspension often occur, fluxes being only indicative (Monaco *et al.*, 1990). Therefore, the figure of 2.8 x 10^9 kg.yr^{-1} is too high and is probably in reality much lower (in the order of 50 %).

3)- The continental slope area (zone D): in this region the depositional system is governed by both erosion and rapid transfer across the shelf and the upper canyon, and accumulation in the canyons (Courp and Monaco, 1990). The upper canyons in this area account for about 50 % of the slope surface which leads to a sedimentation of 2.9 x 10^9 kg.yr^{-1}.

4)- The upper fan area (zone E) dominated by accumulation with little sediment reworking processes.

Finally the total annual deposited amount of sediment in our study area becomes about 10.1 x 10^9 kg.yr^{-1} which

Table 4

Mean accumulation rate (S_i) for each zone and maximum deposited amount of sediments in the Gulf of Lions.

Site	Zone	Surface area (km^2)	S_i (ISR) ($cm.yr^{-1}$)	R ($g.cm^{-2}.yr^{-1}$)	Sediment accumulation 10^9 ($kg.yr^{-1}$)
Rhône prodelta					
	A (0.60-0.30)	240	0.41	0.31	0.7
	B (0.30-0.20)	400	0.24	0.18	0.7
shelf					
	C (0.20-0.15)	2,200	0.17	0.13	2.8
slope					
	D (0.15-0.10)	6,500*	0.12	0.09	2.9
upper fan					
	E (0.10-0.05)	6,000	0.07	0.05	3.0
TOTAL		15,340			10.1

* only 50% of this area was taken into account, see text.

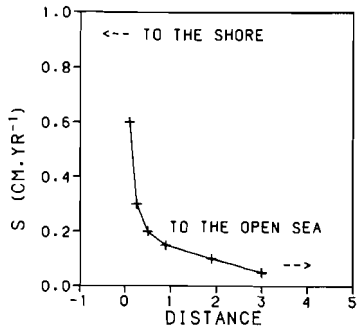

Figure 6

Variation curve of the isoline value (S) against the corresponding isoline distance to the position of the highest isoline (0.6), see Fig. 5.

Table 5

Estimations for sediment accumulation in the Gulf of Lions.

	Flux	Accumulation	
	g. $cm^{-2}.yr^{-1}$	10^9 $kg.yr^{-1}$	%
The study area: 15.340 km^2			
River input (Rhone)		3-5*	30-50
Biogenic deposit	0.02**	3.1	30
Atmospheric deposit		2-4	20-40
Total deposition	0.05-0.31	10.1	

* *Pauc (1970); Blanc (1977) and Leveau and Coste (1987).*
** *Courp (1990) and Monaco* et al *(1990), see* text.

also includes the accumulation of biogenic production. Monaco *et al.* (1990) suggested that in the surface water there are two periods of maximum fluxes for biogenic constituents: one in summer with a strong contribution of organic carbon, carbonate and opal on both shelf and slope; and one in spring for opal which characterizes the fluxes over the slope. Their study of mass fluxes with a sediment trap in the western part of the Gulf of Lions (1990) indicated that the annual fecal pellet flux could become as high as 20 % of the total particle mass at the base of a 600 m water column, with an average flux of biogenic constituents of about 1100 $mg.m^{-2}.d^{-1}$ which amounts to 0.04 $g.cm^{-2}.yr^{-1}$.

However, fluxes increase up to a factor of 6 from east to west in the Gulf of Lions (Courp, 1990). Therefore, we took the value of 0.02 $g.cm^{-2}.yr^{-1}$ (50 % of the biogenic flux of the western part of the Gulf of Lions, Monaco *et al.*, 1990) which we consider as representative for the study area.The annual biogenic accumulation, assuming that no degradation or consumption ocurred, would become about 3.1 x 10^9 $kg.yr^{-1}$ in the Gulf of Lions, leaving the deposit of about 2-4 x 10^9 $kg.yr^{-1}$ to the atmospheric contribution which is in agreement with the number (4 x 10^9 $kg.yr^{-1}$) suggested by Martin *et al.* (1989), due to the annual discharge of the Rhone river (3-5 x 10^9 kg, Pauc, 1970; Blanc, 1977; Leveau and Coste, 1987; Tab. 5).

CONCLUSIONS

The ^{210}Pb analyses demonstrated the presence of surface mixed layers in the sediments of the nearshore area in the Gulf of Lions. Accumulation rates were determined by using the ^{210}Pb and ^{137}Cs dating methods. The agreement of ^{210}Pb and ^{137}Cs data indicates a general absence of deep mixing in the Gulf of Lions. Therefore, the apparent accumulation rates calculated from ^{210}Pb profiles (below the intensely surface mixed layer) generally reflect the true sedimentation rates.

The spatial distribution of deposition rates shows a seaward decrease in value, which suggests that a significant amount (30-45 %) of sediment supplied by the Rhône river is deposited on the river prodeltaic area and the remainder on the continental shelf and the slope in the study area.

The distribution of radiocesium activity confirms a strong contribution of sediment discharge by the Rhône river in the nearshore area. The annual deposited amount of sediment in this study area was estimated to be about 10.1 x 10^9 kg, of which some 3.1 x 10^9 $kg.yr^{-1}$ is biogenic and where atmospheric input accounts for at least 20 % of the

total amount of deposition. It can be concluded that in the last 100 years about 60 cm of sediment, or more, have been deposited in the shallow part of the Gulf of Lions with less than 100 m water depth, 10-15 cm on the shelf and the slope areas, and only 2-5 cm in the deeper part (> 2000 m) of the area.

Acknowledgements

This work was supported by the EEC as part of the EROS- 2000 programme. We are much indebted to the captains and crews of the R/V *Tyro*, the R/V *Discovery* and the R/V *Bannock*, and to our colleagues from the EROS-2000 programme who participated in the cruises, for their friendly and efficient cooperation. We also wish to thank Mr. B. Verschuur for making some of the drawings. Finally we gratefully acknowledge helpful comments and criticisms by two anonymous referees.

REFERENCES

Anderson R.F., R.L. Schiff and R.H. Hesslein (1987). Determining sediment accumulation and mixing rates using ^{210}Pb, ^{137}Cs, and other tracers: problems due to postpositional mobility or coring artifacts. *Can. J. Fish. aquat. Sci.*, **44**, 231-250.

Berger G.W., D. Eisma and A.J. van Bennekom (1987). ^{210}Pb derived sedimentation rate in the Vlieter, a recently filled-in tidal channel in the Wadden Sea. *Neth. J. Sea Res.*, **21**, 287-294.

Binford M.W. and M. Brenner (1986). Dilution of ^{210}Pb by organic sedimentation in lakes of different trophic states, and applications to studies of sediment-water interactions. *Limnol. Oceanogr.*, **31**, 584-595.

Blanc J. (1977). Recherches de sédimentologie appliquée au littoral du delta du Rhône de Fos au Grau du Roi. Publications CNEXO, 75/1, 193, 69 pp.

Chanton J.-P., C.S. Martens and G.W. Kipphut (1983). Lead-210 sediment geochronology in a changing coastal environment. *Geochim. cosmochim. Acta*, 47, 1791-1804.

Courp T. and A. Monaco (1990). Sediment dispersal and accumulation on the continental margin of the Gulf of Lions: sedimentary budget. *Continent. Shelf Res.*, **10**, 1063-1087.

Courp T. (1990). Flux et bilans de matière dans un environnement de marge continentale : la marge nord-occidentale méditerranéenne. *Ph. D. Thesis, University of Perpignan, France*, 212 pp.

Davis R.B., C.T. Hess, S.A. Norton, D.W. Hanbson, K.D. Hoagland and D.S. Andson (1984). ^{137}Cs and ^{210}Pb dating sediment from soft-water lakes in New England (USA) and Scandinavia, a failure of ^{137}Cs dating. *Chem. Geol.*, **44**, 151-185.

Eisma D., G.W. Berger, W.Y. Chen and J. Shen (1989). ^{210}Pb as a racer for sediment transport and deposition in the Dutch-German Wadden Sea. *Proceedings KNGMG Symposium on coastal lowlands, Den Haag, 1987*, 237-253.

El-Daoushy F. (1978). The determination of ^{210}Pb and ^{226}Ra in lake sediments and dating applications. UUIP 979, 45 pp.

Goldberg E.D., E. Gamble, J.J. Griffin and M. Koide (1977). Pollution history of Narragansett Bay as recorded in its sediments. *Estuar. coast. mar. Sci.*, **5**, 549-561.

Guinasso N.L. and D.R. Schink (1975). Quantitative estimates of biological mixing rates in abyssal sediments. *J. geophys. Res.*, **80**, 3032-3043.

Leveau M. and B. Coste (1987). Impact des apports rhodaniens sur le milieu pélagique du Golfe du Lion. *Bull. Écol.*, **18**, 119-122.

Martin J.-M., F. Elbaz-Poulichet, C. Guieu, M.D. Loÿe-Pilot and G. Han (1989). River *versus* atmospheric input of material to the Mediterranean Sea: an overview. *Mar. Chem.*, **28**, 159-182.

Martin J.-M. and A.J. Thomas (1991). Origins, concentrations and distributions of artificial radionuclides discharged by the Rhone river to the Mediterranean Sea. *J. environ. Radioactivity*, **11**, 105-139.

DeMaster D.J., B.A. McKee, C.A. Nittrouer, J.C. Qian and G.D. Cheng (1985). Rates of sediment accumulation and particle reworking based on radiochemical measurements from continental shelf deposits in the East China Sea. *Continent. Shelf Res.*, **4**, 143-158.

Millot C. (1987). Circulation in the western Mediterranean Sea. *Oceanologica Acta*, **10**, 2, 143-149.

Monaco A., S. Heussner, T. Courp, R. Buscail and J. Carbonne (1987). Particulate matter transport on the Gulf of Lions margin: process and quantification. *Colloque international d'Océanologie, Perpignan, CIESM*, 47.

Monaco A., T. Courp, S. Heussner, J. Carbonne, S.W. Fowler and B. Deniaux (1990). Seasonality and composition of particulate fluxes during Exomarge-I in the Western Gulf of Lions. *Continent. Shelf Res.*, **10**,959-987.

Nittrouer C.A., D.J. DeMaster, B.A. McKee, N.H. Cutshall and I.L. Larsen (1983/1984). The effect of sediment mixing on ^{210}Pb accumulation rates for the Washington continental shelf. *Mar. Geol.*, **54**, 201-221.

Nolting R.F. (1989). Preliminary results about dissolved and particulate trace metals in sediments of the Gulf of Lions, in: *Water Pollution Research, Report 13*, J.-M. Martin and H. Barth, editors, Paris, 314-340.

Pauc H. (1970). Contribution à l'étude dynamique et structurale des suspensions solides au large du grand-Rhône (Grau de Roustan), *Ph. D. Thesis, University of Montpellier-Perpignan, France*, 126 pp.

Robbins J. and D.N. Edgington (1975). Determination of recent sedimentation rates in Lake Michigan using ^{210}Pb and ^{137}Cs. *Geochim. cosmochim. Acta*, **39**, 285-301.

Robbins J., D.N. Edgington and A.L.W. Kemp (1978). Comparative ^{210}Pb, ^{137}Cs, and pollen geochronologies of sediments from Lakes Ontario and Erie. *Quat. Res.*, **10**, 256-278.

Smith J.N. and C.T. Schafer (1984). Bioturbation processes in continental slope and rise sediments delineated by ^{210}Pb, microfossil and textural indicators. *J. mar. Res.*, **42**, 1117-1145.

Van der Wijk A. (1987). Radiometric dating by alpha spectrometry on uranium series nuclides. *Ph. D. Thesis, State University of Groningen, The Netherlands*, 168 pp.

Von Gunten H.R., M. Sturm, H.N. Erten, E. Rössler and F. Wegmüller (1987). Sedimentation rates in the central Lake Constance determined with ^{210}Pb and ^{137}Cs. *Schweiz. Z. Hydrol.*, **49**. 3, 275-283.

Wan G.J., P.H. Santschi, M. Sturm, K. Farrenkothen, A. Lueck, E. Werth and C. Schuler (1987). Natural (^{210}Pb, ^{7}Be) and fallout (^{137}Cs, $^{239\ 240}Pu$, ^{90}Sr) radionuclides as geochemical tracers of sedimentation in Greifensee, Switzerland. *Chem. Geol.*, **63**, 181-196.

Zuo Z., D. Eisma and G.W. Berger (1989 *a*). Recent sedimentation deposition rates in the Oyster Ground, North Sea. *Neth. J. Sea Res.*, **23**, 3, 263-269.

Zuo Z., D. Eisma and G.W. Berger (1989 *b*). Recent sediment accumulation in the Gulf of Lions. in: *Water Pollution Research, Report 13*, J.-M. Martin and H. Barth, editors, Paris, 298-313.

But I must continue on the path I have taken now;
If I do nothing, if I don't study, if I stop searching,
then I am lost, in misery. That is how I see things,
persevere, persevere, that is what I must do.
But what is your final goal, you may ask.

Borinage, July 1880.

CURRICULUM VITAE

Zhizheng Zuo received her B.S. degree in hydrogeology and engineering geology from the Nanjing University in January 1982. After graduation she worked for three years in the department of limnological sedimentology and Geochemistry at Nanjing Institute of Limnology and Geography, Academia Sinica and received her M.S. degree in July 1985. Then she worked as Research Assistant at the same Institute for two years to build up the radioactive isotope laboratory for geochronological and geochemical studies. In December 1987, she succeeded in obtaining a Ph.D. position in the Netherlands Institute For Sea Research and went to Europe working on the subject "Dynamic behaviours of ^{210}Pb, ^{210}Po and ^{137}Cs in coastal and shelf environments" in the southern North Sea and in the Northwestern Mediterranean.

ERRATUM

Following a compilation error the figures (excluding the Figure captions) on page 118 and page 122 have to be switched.